PROCEEDINGS

of the

HEALTH PHYSICS SOCIETY

First Annual Meeting

June 25-27, 1956

University of Michigan

Ann Arbor, Michigan

Distributed by

THE HEALTH PHYSICS SOCIETY
C. C. Palmiter
Radiation Control Service
University of Michigan
Ann Arbor, Michigan
Price: $3.00

PROCEEDINGS

of the

HEALTH PHYSICS SOCIETY

FIRST ANNUAL MEETING

JUNE 25-27, 1957

Sponsored By:

THE RADIATION CONTROL SERVICE AND
THE NUCLEAR ENGINEERING COMMITTEE
of the
UNIVERSITY OF MICHIGAN
ANN ARBOR, MICHIGAN

OFFICERS OF THE HEALTH PHYSICS SOCIETY

President
K. Z. Morgan

President-Elect
F. P. Cowan

Secretary
E. E. Anderson (2 years)

Treasurer
R. G. Gallaghar (1 year)

BOARD OF DIRECTORS

One Year Term	Two Year Term	Three Year Term
J. W. Healy	E. C. Barnes	W. D. Claus
H. Mermagen	W. H. Langham	G. W. C. Tait
W. E. Nolan	C. M. Patterson	L. S. Taylor

PROGRAM COMMITTEE

F. P. Cowan, Chairman
L. J. Deal
W. A. McAdams
D. D. Meyer
G. W. Morgan
J. V. Nehemias
J. F. O'Brien
H. W. Patterson

ACKNOWLEDGEMENTS

The Editorial Board and the Health Physics Society wish to acknowledge the assistance of the Continued Education Service of the School of Public Health, University of Michigan, in supervising preparation of the material for publication of this Proceedings. We are grateful to Mr. H. E. Miller, the Director, for this assistance and especially to Miss Ann Murphy of that group for her enthusiastic and skillful editorial service. To Mrs. Louise Schiller we express our appreciation for her cooperation and general assistance in the preparation of the Proceedings.

FOREWORD

Health physics, as known today, began its existence at the Metallurgical Laboratory of the University of Chicago in the fall of 1942, about the time of the start-up of the first nuclear reactor on December 2, 1942. It had its initial meeting as a group of professional associates last year (1955) at Ohio State University. At that meeting the health physicists voted almost unanimously to form a society, and this year at the University of Michigan, with the adoption of a Constitution and Bylaws, the election of officers, and the selection of a name, the Health Physics Society had its birth.

It is of the greatest significance that this is not exclusively an American organization. Although most of the 748 charter members are from the United States and Canada, it is hoped that ultimately the Society will have members from all countries of the world. Truly health physics is a sphere of activity in which all people of the world have a vested interest and in which they should be vitally concerned, and the exchange of information on problems of protection from ionizing radiation must not be hampered by secrecy restrictions or by national and political limitations.

Many new problems in applied health physics are being introduced as a result of the rapidly expanding peacetime uses of radioactive materials, the prospect of atomic energy becoming an important source of electrical power, and the establishment of state, federal, and international control of radiation hazards. Likewise, there are many new research opportunities in health physics; e.g., methods of radioactive waste disposal must be developed, methods which are safe, economical, and compatible with a large atomic energy power industry. Hence, the Health Physics Society includes members who are engaged in both applied and research activities relating to radiation protection.

The papers given at this Health Physics Conference at the University of Michigan do not cover more than a random sampling of the many health physics activities. They are sufficient, however, to indicate that health physics is very broad in its scope, supplying structure and stature in the great voids between the conventional interests of the well established sciences of physics, biology, chemistry, medicine, and engineering. This is only the beginning of an organization dedicated to the advancement of the peacetime application of atomic energy and directed in a manner that is intended to bring a maximum of benefit and a minimum of suffering to all mankind. The health physicists are, in no small measure, responsible for making the atomic energy industry one of the safest major industries in the world today in spite of its immense potential for radiation hazards. So long as men continue to dedicate their lives to the problems of health physics, just so long can we expect this freedom from radiation injury to continue in the atomic energy industry.

K. Z. Morgan
President, Health Physics Society

TABLE OF CONTENTS

ABSTRACTS

INTRODUCTORY REMARKS

F. J. Hodges, M. D.

Department of Radiology
University of Michigan
Ann Arbor, Michigan

It is unfortunate that Dean Ralph Sawyer, who was scheduled to open this scientific session, could not be here in person for, as a physicist of outstanding reputation, as director of instrumentation at the Bikini bomb tests, and as Director of the Michigan Memorial Phoenix Project, his grasp of your interests and problems is well suited to the occasion. In his behalf, as a member of the Executive Committee of the Phoenix Project rather than as a medical radiologist, I welcome you to the Michigan campus and applaud the motives which have banded you together.

My first encounter with the term "health physics" took place in 1940, when I was on leave from this University as a research associate in Dr. Ernest O. Lawrence's radiation laboratory on the Berkeley campus. I had gone there to complete some experiments begun by my associate, Dr. Lampe, requiring the neutron output of a cyclotron, and soon became deeply engrossed in the thrilling activities which centered around the Crocker Laboratory. To that mecca had been attracted a remarkable army of researchers in physics, chemistry, physiology, tissue culture, and many other fields, all seeking the expansion of knowledge promised by the new agency of nuclear disintegration - the term "atomic energy" was still to be invented.

Among the throng of investigators who daily were making thrilling discoveries, there were men, designated as "Health Physicists," whose responsibilities were confined to the detection and control of potentially dangerous radiations. Their chief work appeared to be decontamination of used materials and apparatus. It was difficult to believe that such endeavors would long hold the interest of trained physicists or of persons whose education had been in the biological field.

One day, toward the end of my stay, an incident occurred which abruptly changed my concept of health physics. For many weeks, in addition to completing some experiments on rabbits begun by my associate Dr. Lampe with the Michigan cyclotron and continued on the Crocker Laboratory instrument, I had been exploring the effect of parenteral P-32 on the growth of mouse lymphomas. Ordinarily, ashed samples of tissues from the mice were sent by messenger to the basement laboratory in the nearby physics building for radiation assay by the health physics group. This particular day I delivered the material in person, and was watching the assay procedure with interest when I was asked if I would please step out of the building because the electroscope being used was recording an annoyingly high background. Moderately insulted by the implication that through careless technique I had brought hands soiled with invisible radioactivity into the measurements room, I was quickly convinced, and at once my estimate of the importance of health physics in the age of expanding nuclear physics grew in respect.

Some years later, during a visit to the Argonne Laboratory, Dr. Lampe and I were greatly impressed with the scope and potentialities of health physics. The array of testing instruments, the standardizing methods employed for those instruments, and the special shop for construction and repairs were impressive, but over and beyond those items, we were thrilled with the original experimentation being conducted by the health physics staff. When a necessary service operation requiring broad technical knowledge and ability expands and develops its own peculiar sphere of

productive research, it becomes a respected and attractive basis for an academic career and is certain to attract able and devoted students and scholars.

The founding of your Society is the natural and prudent outgrowth of this recent development of special interest in a promising field which has moved ahead so rapidly in the past decade. Much should be accomplished by the exchange of ideas concerning useful instruments for the detection and measurement of all types of radiation and the results of physical and biological research.

In years past, medical radiology, starkly needing instrumentation "know-how" in the successful operation of high-energy X-ray generators, lured youthful physicists into positions of limited opportunity for life-long achievement, paying well as a rule for humdrum, repetitive services. Today the introduction of so many new forms of useful radiation accentuates the need for physicists in medical radiology, and it is now possible and highly desirable for those staff members to progress steadily within a recognized and respected division without sacrificing their identity as physicists. That is a desirable state of affairs for all concerned.

It is to be hoped that during the period of your meetings you will find opportunity to visit some of the centers of radiation activity on this campus. Here in Ann Arbor virtually all divisions of the University have found common interest in the peacetime uses of atomic energy as participants in the Michigan Memorial Phoenix Project, which is dedicated to continuing research in that broad field as a lasting memorial to University students and faculty who were lost in World War II. Our health physicists, steadily increasing in numbers, have been highly instrumental in the successful development and the continuing operation of the Phoenix Project.

The University welcomes you and extends its sincere wish that your meeting on this campus may be interesting and of lasting value.

A FAST NEUTRON INSENSITIVE GAMMA DOSIMETER

J. A. Auxier and G. S. Hurst

Health Physics Division
Oak Ridge National Laboratory
Oak Ridge, Tennessee

One of the most difficult problems in radiation dosimetry is the accurate determination of gamma dose in the presence of a high flux of fast neutrons. All ionization chambers suitable for gamma dosimetry have some response to neutrons. Chambers having walls and gas of low atomic weight, the best gamma dosimeters, absorb a significant amount of energy from neutrons by elastic scattering. As the atomic number increases, the usefulness of the ionization chamber in gamma radiation dosimetry decreases and the neutron energy absorbed as a result of inelastic scattering generally increases.

A technique which promises to decrease considerably the problems of mixed radiation dosimetry is now being tested. It involves the use of a miniature cavity with walls and gas of materials having atomic numbers of 6 to 16 inclusive (Figure 1). The dimensions and gas pressure are sufficiently small to make the probability much less than 1 that a 30 kev electron will form an ion pair in crossing the cavity. If a single ion pair can be detected, and if secondary electrons only rarely produce more than 1 ion pair in the cavity, a summation of counts is tantamount to a summation of energy absorbed, or dose, when the volume and energy required to form an ion pair are known.

The specific ionization produced by recoil nuclei is hundreds to thousands of times greater than that produced by secondary electrons of over 30 kev. The single count resulting when a recoil nucleus traverses the cavity, however, gives no more weight to the recoil nucleus than it would to a secondary electron, even though it represents only a small fraction of the energy expended by the recoil nucleus. In addition, 1 rep of fast neutrons deposits only approximately 10 percent as much energy in these materials as in tissue. The result is a weighting against neutrons by a factor of at least a thousand.

Ideally, this device would be a Geiger counter, but the size and pressure are prohibitively small. It is used instead as a "semi" proportional counter in which gas amplification extends out into the cavity and perhaps to the walls. When the wall thickness satisfies the Bragg-Gray conditions, there is no detectable quality dependence for cerium-144, cesium-137, and cobalt-60, a range of 130 kev to 1.2 Mev. Lower energies also will be used as well as further intermediate ones. For the proper voltage and gain, the pulse height distribution produced by a Po-Be neutron source was the same shape as for a pure gamma emitter, as indicated in Figure 2. Since the average pulse heights generated by recoil nuclei must be higher than those generated by electrons, this would seem to indicate that the neutron sensitivity of the counter is negligible. This is further demonstrated in Figure 3. For the same dose rate and gain, pulse height distributions are plotted as a function of the counter voltage. The upper curve represents the same voltage gain conditions shown in Figure 2, and coincides in shape with the curves obtained with a Po-Be source. For lower voltages, even though the system is still quality independent, the influence of occasional recoil nuclei tends to decrease the slope slightly. The counter is therefore used at as high a voltage as stability will permit.

If this counter could be operated as a proportional counter with good resolution, there should be a well defined pulse height structure with an initial plateau, then a sharp decrease in

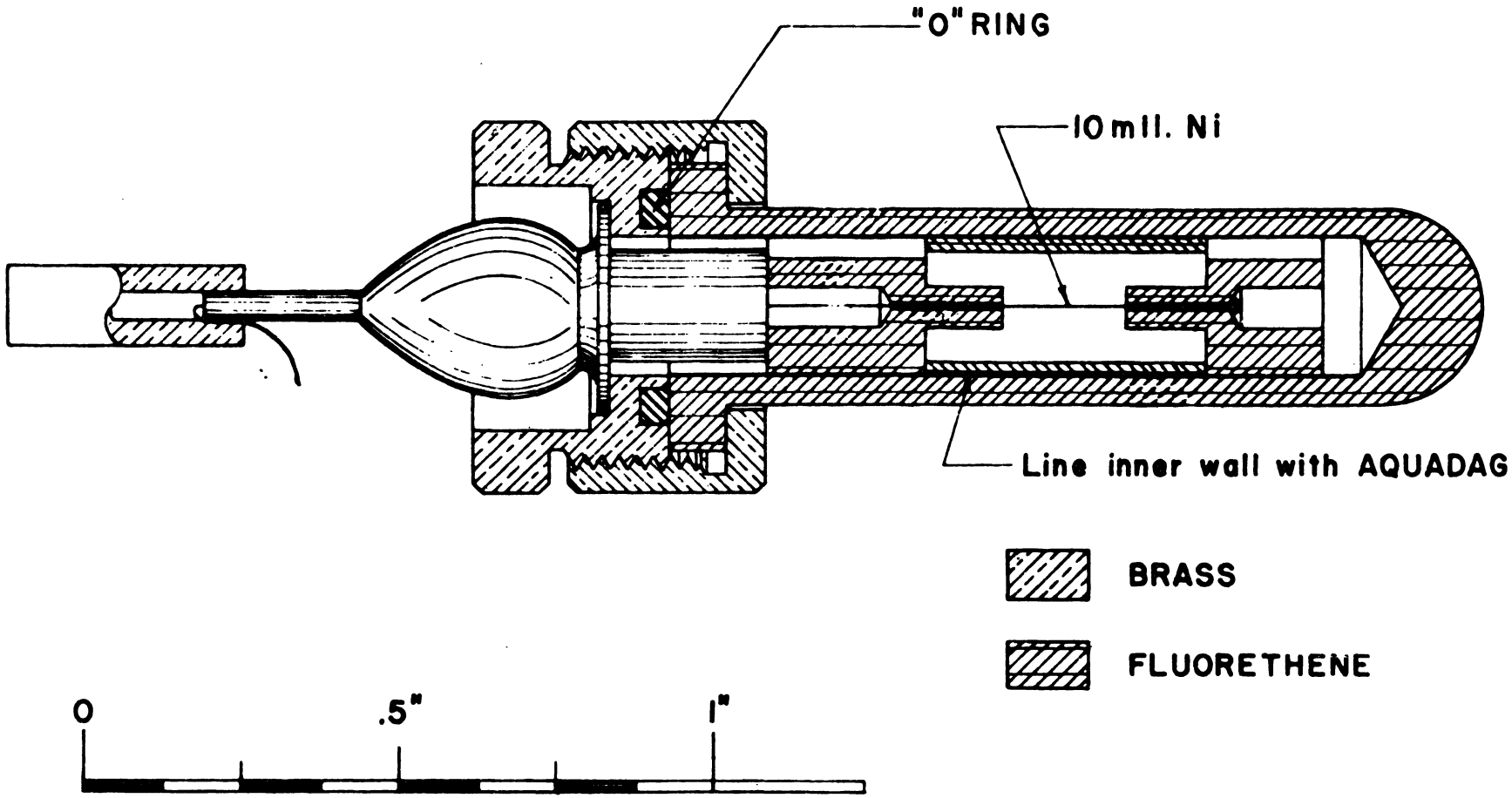

Figure 1. GAMMA DOSIMETER

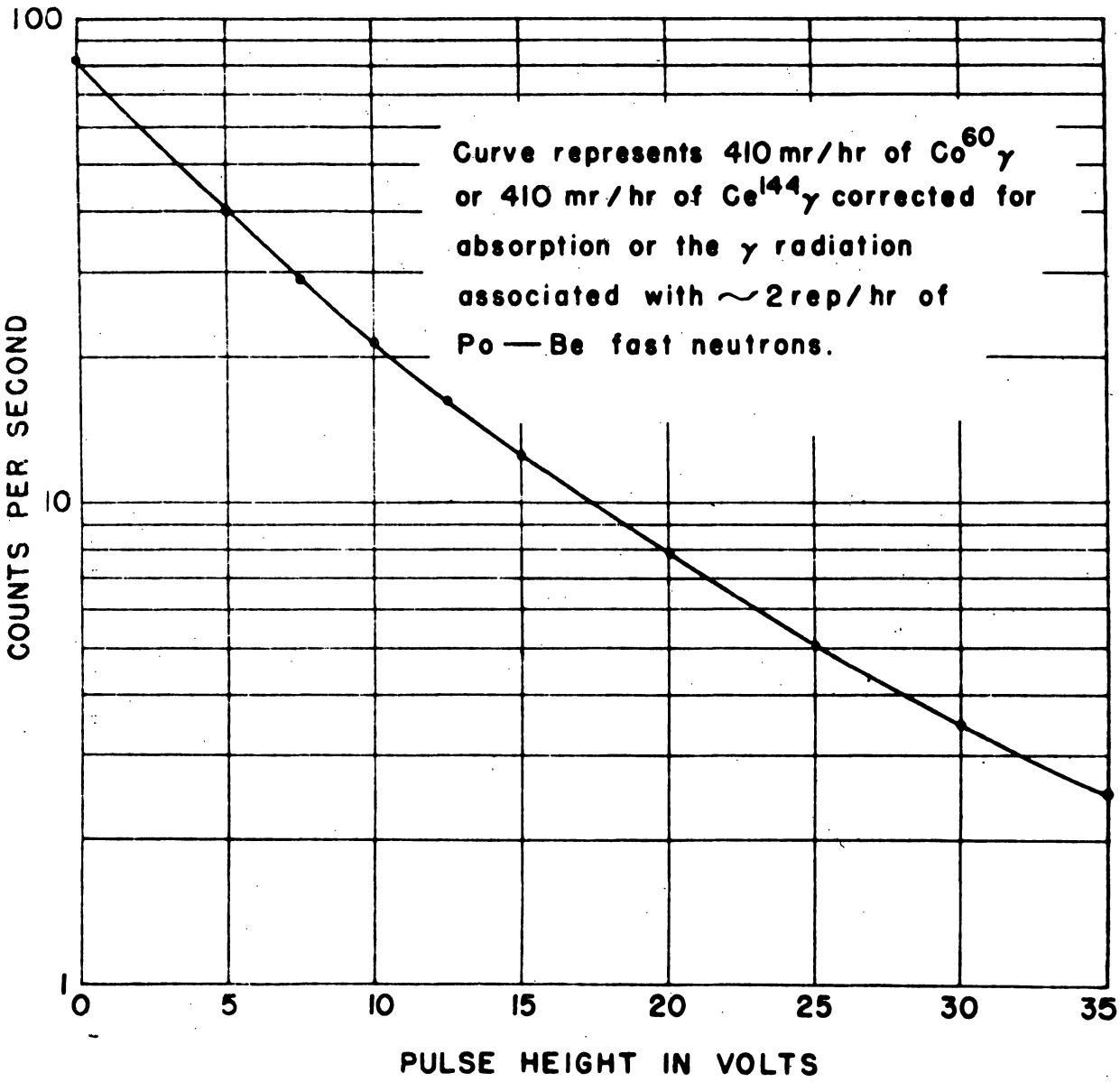

Figure 2. TYPICAL PULSE HEIGHT DISTRIBUTION

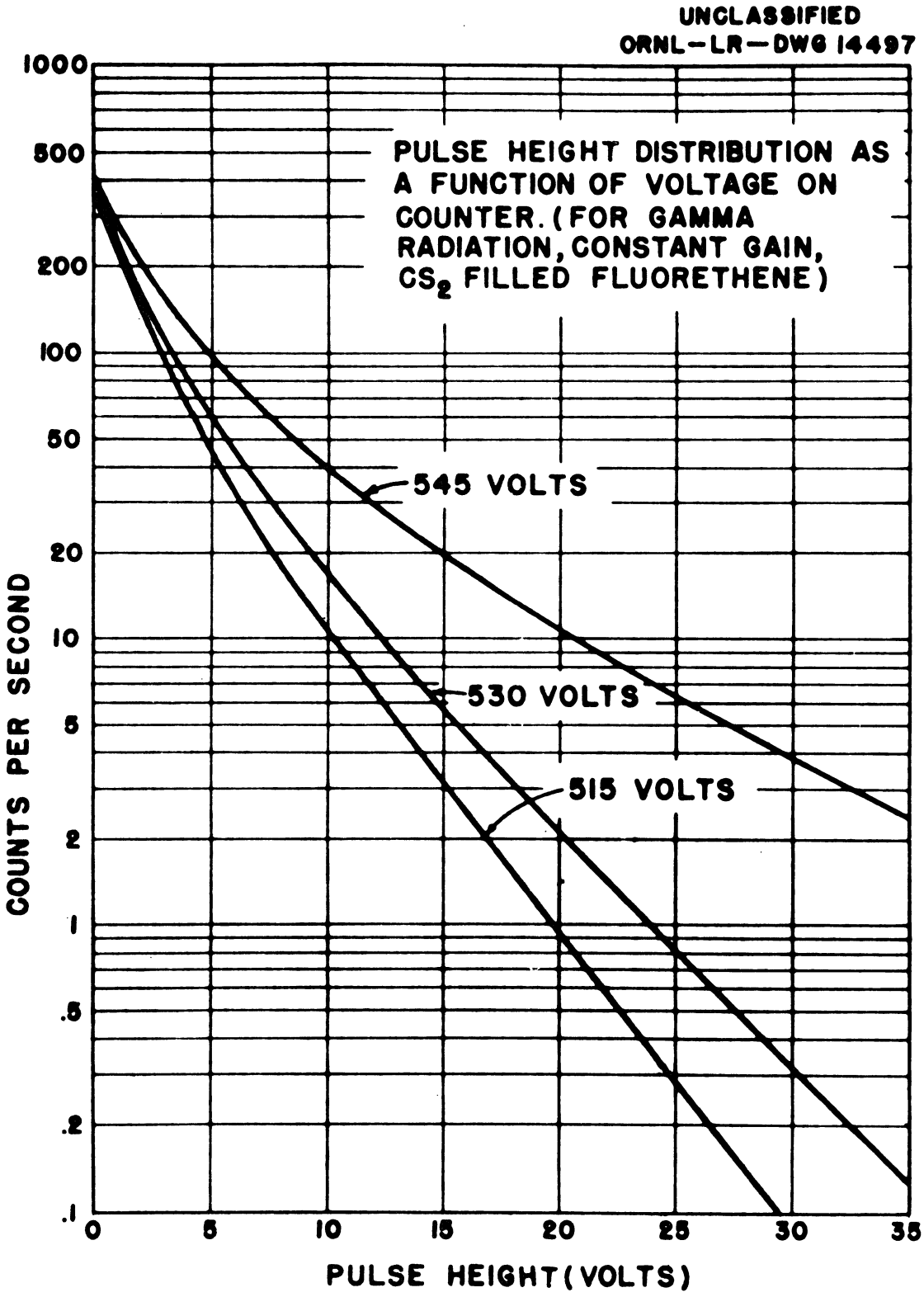
UNCLASSIFIED
ORNL-LR-DWG 14497
PULSE HEIGHT DISTRIBUTION AS A FUNCTION OF VOLTAGE ON COUNTER. (FOR GAMMA RADIATION, CONSTANT GAIN, CS_2 FILLED FLUORETHENE)
545 VOLTS
530 VOLTS
515 VOLTS
COUNTS PER SECOND
1000
500
200
100
50
20
10
5
2
1
.5
.2
.1
0
5
10
15
20
25
30
35
PULSE HEIGHT (VOLTS)

Figure 3

count rate evident at the point representing cut-off for pulses generated by 1 ion pair, then a plateau representing pulses generated by 2 ion pairs, etc. Such resolution could not be obtained. The pulse height distribution, however, should extrapolate to the height of the "1 electron" plateau at zero pulse height setting. This has been verified by extrapolating to zero and comparing the result with the calculated number of ion pairs formed. Agreement has always been within about 5 percent.

A PORTABLE THULIUM-170 X-RAY UNIT

E. W. Coleman

Fission Products Laboratory
University of Michigan
Ann Arbor, Michigan

Of the readily available radioactive isotopes, thulium-170 has found widest application in isotopic devices for human diagnostic radiography.[1,2,3] The accepted decay scheme of thulium-170 would indicate that shielding problems with thulium sources should be small, since the most penetrating decay radiation is an 84 kev gamma ray, as shown in Figure 1.

As early as 1952, radiographs had been produced with the radiations of thulium-170.[1] The source then used consisted of a few millicuries of thulium oxide evaporated from solution to produce a point source. Radiographic exposure times of several hours were required to produce radiographs of diagnostic quality. Based on work with this early source, a fairly accurate prediction of the source strength required to reduce exposure times to the order of seconds was made. Predictions of shielding requirements for these larger sources, however, were grossly inadequate.

Recognizing the possible utilization of thulium-170 as a radiographic source for industry and medicine, Liden and Starfelt undertook an intensive study of the electromagnetic spectra from thulium sources.[5] Their work indicated the extent of bremsstrahlen and X-ray production for sources from zero to 1 gm/cm^2 of Tm. The spectral distribution was found to be strongly dependent upon source thickness. For a source of about 10 mg/cm^2, the spectrum was roughly divided into 37 percent gamma rays, 52 percent X rays, and 11 percent bremsstrahlen. The bremsstrahlen of energies greater than 85 kev accounted for only 3.3 percent of the total. For a source of 1 gm/cm^2, the spectral composition was found to be 10 percent gamma rays, 47 percent X rays, and 43 percent bremsstrahlen. Of the total output, bremsstrahlen of energies greater than 85 kev accounted for 31 percent.

Although the production of bremsstrahlung was anticipated in this work, the magnitude of the resulting shielding problem was unknown. To evaluate problems relative to exposure times, radiographic quality, shielding requirements, and biological effectiveness of thulium-170 radiations from multicurie sources, a pilot model was constructed and tested.

The pilot model is shown in Figure 2. The operating characteristics and constructional features are discussed elsewhere.[3] The main shielding component is a lead sphere 5 inches in diameter. It was originally assumed this sphere would provide sufficient shielding for a 30-curie source. Initial results were somewhat dismaying, since the surface dose rate on the sphere was 120 mr/hr. The possibility was presented that the thulium metal had become contaminated with tantalum during its manufacture. On neutron activation of the source, 115-day Ta-182 would then be produced, yielding a maximum gamma energy of about 1.2 Mev on decay. Spectral analysis by lead absorption of the radiations passing through the sphere confirmed the presence of 1.2 Mev gamma photons. Lead absorption measurements were taken for the total spectrum, and after subtracting the 1.2 Mev gammas, the major shielding problem was found to be photons with a mass

---

The work reported here was conducted for the Office of the Surgeon General, U. S. Army, by the Army Medical Research Laboratory, Fort Knox, Kentucky.

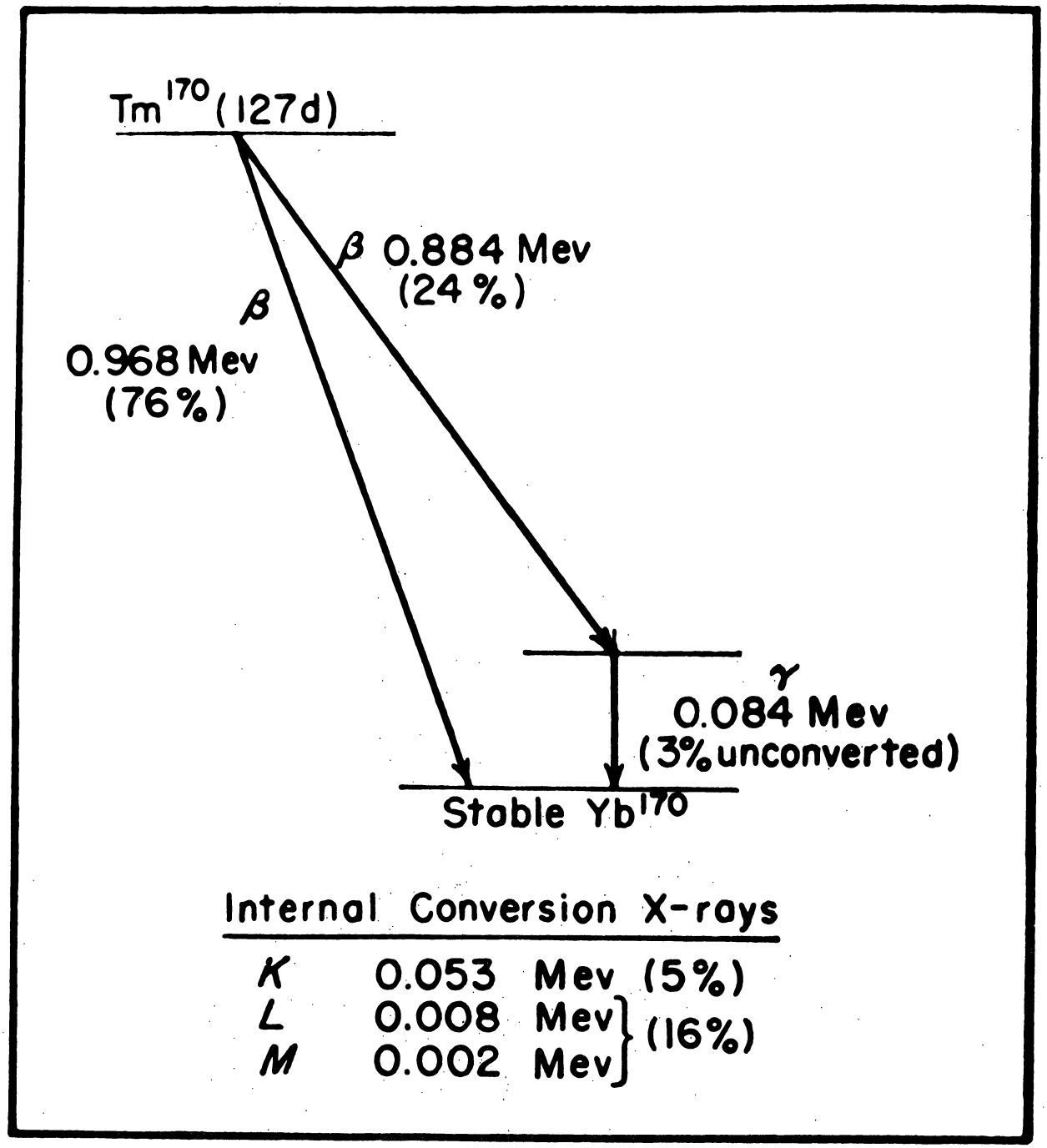

Decay scheme for Tm^{170}

Figure 1

absorption coefficient of 0.195 cm^2/gm for lead. Using the work of Fano[6], the energy is 0.42 Mev. Subtraction of these photons indicated an energy component with a mass absorption coefficient of 0.940 cm^2/gm for lead. This coefficient corresponds to an energy of 0.205 Mev. It is interesting to note that some of the early investigators of the thulium decay scheme reported 0.2 and 0.44 Mev gamma rays.[7] It is now believed these apparently discrete energies are associated with bremsstrahlung photons. Whether they are "discrete" energies or not is unimportant to this work. It is of importance to note, however, that if lead is to be used for shielding thulium sources, calculations of shielding thickness must be based upon 0.42 Mev photon energy, with intensity varying with source thickness.

The biological effectiveness of thulium-170 radiation in producing splenic atrophy in mice has been determined. The effectiveness relative to 200 KVP X rays was found to be 0.54 for the conditions of the study. The dose rate was considerably lower in the case of thulium-170 radiation than in the case of X radiation. Although fractionation of X-ray dose was used, there was no assurance that compensation was complete. In general, low dose rates are less effective than high dose rates in producing biological effects. The thulium-170 radiation contained a considerable amount of "soft" radiation, which was more or less attenuated by the tissue lying between the source and the spleen. Finally, the high energy bremsstrahlung component and the Ta-182 contaminant radiation would be expected to have a relatively low biological effectiveness. In view of these considerations, a value of about 0.5 for RBE appears very reasonable. It is concluded that the biological effectiveness of thulium-170 radiations does not differ significantly from that of conventional X radiation.[8]

With the benefit of information gained in the design, construction, and operation of the pilot model, a field model was produced. The unit is shown in Figure 3. The pilot model and field model are compared in Table 1.

TABLE 1

COMPARISON OF THE PILOT MODEL AND FIELD MODEL

	Pilot	Field
Source		
mass	about 0.4 gm	0.399 gm
diameter	about 4 mm	4.3 mm
height	about 4 mm	3.2 mm
strength	about 30 curies	120 ± 20 curies
contaminants	tantalum-182	none
Unit		
weight	48 pounds	22 pounds
shielding	2 1/4 to 3 inches Pb	1 3/4 inches Pb
carrying method	back harness	belt pouch

The shape of the field unit resulted from the design method. To achieve minimum shielding weight, the necessary source seals, shuttering mechanisms, etc., were first designed as compactly as possible. Then radial lines were drawn from the position of the source. The outer surface of the shielding lead was chosen so that each radial line passed through a total lead thickness of 1 3/4 inches. This thickness was estimated to yield a surface dose rate of 5 mr/hr. Actual measurements later showed the surface dose to be 10 mr/hr. This discrepancy is believed to be caused by neglect of build-up factor in the shielding calculations. Considering the available build-up factor information for lead with a point isotropic source[9], a build-up factor of 2 does not seem unreasonable for the configuration used.

The source capsule used in this unit contained about 400 mg of thulium metal, obtained from the Rare Earths Loan Collection of Ames Laboratory, Iowa State College. The metal was welded in a 2S aluminum capsule and irradiated in the MTR. The specific activity of thulium-170



was rated at 300 ± 50 curies/gm, giving a source strength of 120 ± 20 curies. Periodic smears of the source capsule have indicated no leakage of thulium. (Thulium metal is gradually converted to the oxide on exposure to air. The oxide is quite easily air-borne, and is extremely difficult to remove from lead surfaces by usual decontamination procedures.)

The problems involved in the design of a suitable aperture and shutter system for a portable radiographic unit are manifold. The most important considerations are (1) minimum dose to patient, (2) minimum space requirements within the shielding, and (3) uniform exposure of film to an unattenuated beam. The difficulties involved in removing the lead aperture plug in the uniform manner required for radiographic quality were overcome by utilizing 2 shutters, a safety shutter and a radiographic shutter.

It was experimentally determined that less than 0.050 inch of gold was required to protect radiographic film from fogging radiation for at least 2 minutes. The radiographic shutter was therefore constructed of brass with a gold inlay over the source. This compact shutter is easily opened with the aid of a cable extending through the shielding. A 40^{o} conic aperture with axis common to the source is used to provide full-area exposure of a 10 by 12 inch film at 19 inches source-to-film distance. The aperture is closed at the source end by a thin aluminum disc to prevent foreign bodies from entering the shutter mechanism. Since the apex of the aperture lies behind the source, no step is required in the safety shutter closing the aperture. The safety shutter is lead, cast in a thin brass jacket. It provides a minimum shielding thickness of 1 3/4 inches of lead. This plug is hinged to the main shielding component by means of a sliding hinge mechanism. The safety shutter opens to slight pressure on the top of the hinge. To prevent accidental or unauthorized opening of the safety shutter, a slot in the hinge receives a hasp which provides a lock when rotated 90^{o} with respect to the slot. The hasp may be locked in this position by a small padlock.

The tripod for supporting the unit during exposure has telescoping legs, thus permitting the exposure distance to be varied between 19 and 36 inches. The tripod legs are located outside the primary radiation cone in order to minimize scattered radiation. A slot in the tripod head permits the use of the unit in the horizontal as well as vertical position.

During the operation of the unit, the operator's hands do not approach the primary cone, since all manipulations are confined to the upper half of the shielding. The cable allows the operator to stand approximately 4 feet from the unit while opening and closing the radiographic shutter. Scattered radiation dose rate to the body is less than 5 mr/hr.

The dose rate at 19 inches during exposure was found to be 3.12 r/hr, as measured by Victoreen r-meter. This is an unattenuated film dose rate of less than 1 mr/sec. At 11 inches, the closest approach of the patient in 19-inch radiography of the extremities, the dose rate was approximately 2.6 mr/sec. Since normal exposure times range from 10 to 30 seconds, the limits of radiation dose to the patient are from 10 to 78 mr/radiograph.

Although radiographs obtained with isotopic units are inferior in general to those obtained with electronic machines, they are capable of indicating gross fractures and foreign bodies. The pilot model and field models discussed here are certainly subject to further improvements. Improved sources and units may be expected, with a resulting improvement in radiographic quality. However, unless radically new films and/or intensifying methods are developed, exposure times will remain of the order of seconds.

Perhaps the most important contribution of human isotopic radiography will be to serve as a stimulus to develop new electronic X-ray devices based upon new and as yet untried theories. In any event, truly portable X-ray units are in the offing.

BIBLIOGRAPHY

1. Mayneord, W. V. "Radiography of the Human Body with Radioactive Isotopes." Brit. J. Radiol., 25:517-525, 1952.

2. Untermeyer, S., F. H. Spedding, A. H. Daane, J. E. Powell, and R. J. Hasterlik. "Portable Thulium X-Ray Unit." Nucleonics 12, No. 5:35, 1954.

3. Carpenter, A. W., R. R. Heer, Jr., L. H. Krohn, E. W. Coleman, and F. J. Boyer. "Preliminary Report on a Complete Portable X-Ray Unit." AMRL Report No. 168, 1954.

4. Graham, R. L., J. L. Wolfson, and R. E. Bell. "The Disintegration of Tm^{170}." Can. J. Physics, 30:459, 1952.

5. Liden, K. and N. Starfelt. "Gamma-rays, X-rays and Bremsstrahlung from Tm^{170} Sources." Arkiv Fysik 7, No. 9:109-166, 1953.

6. Fano, U. "Gamma-ray Attenuation. Part I." Nucleonics 11, No. 8:10, 1953.

7. Grant, P. J. and R. Richmond. "Decay of Thulium-170 and Rhenium-186." Nature, 163:840, 1949.

8. Storer, J. B., L. H. Krohn, and H. Simonsen. "Relative Biological Effectiveness of Thulium-170 Radiation as Measured by Splenic Atrophy in Mice." AMRL Report No. 169, 1954.

9. Goldstein, H. J., E. Wilkins, Jr., and S. Preiser. "Interim Report on the NDA-NBS Calculations of Gamma-Ray Penetration." NDA Memo 15C-20, Sept., 1953.

DESIGN AND USE OF A UNIFORM HIGH INTENSITY COBALT-60 IRRADIATION CHAMBER

E. Nielsen

Radiation Laboratory
University of California
Berkeley, California

This irradiation unit was designed and built for Dr. Tolbert and his group of the University of California's Donner Laboratory for use in chemical and biochemical irradiation studies. Their specifications were for:

1. As high a radiation field as possible from approximately 100 curies of Co-60. Exposures of 10^7 to 10^9 roentgens desired.
2. As uniform a field as possible.
3. Immediate use for small samples.
4. Possible later use for larger samples.
5. Ability to handle multiple samples.

These criteria, coupled with the safety requirement and supplemented by 2 additional requirements, became the basis for planning. The 2 additional requirements were (1) provision for cobalt-60 replacement when radioactive decay so dictated, and (2) provisions to cover an expectation that, before long, it would be desired to increase the cobalt-60 content by a factor of 10. Planning was initiated early enough to permit specifying the optimum dimensions for the cobalt-60 that would be required.

Consideration evolved early towards a cylindrical arrangement of cobalt-60, with the volume inside the cylinder being the irradiation space. To provide the necessary versatility, it was proposed to form the walls of the cylinder as a ring of line sources, that could be moved radially to form various size cylinders. From calculations as to the volume in which there would be a reasonably uniform field, it was decided to have 16 such line sources, each 1 1/2 inches long, each line source to consist of 6 cobalt-60 pellets 1/4 inch long by 1/8 inch in diameter, with each pellet being approximately 1 curie.

Figure 1 illustrates this arrangement incorporated in its final shielding assembly. Two of the source holders are shown attached to control rods that penetrate the shielding of the irradiation chamber. The control rods terminate at a scroll plate. Rotation of the scroll plate establishes the radial location of the source holders. The irradiation chamber can be rolled by means of rack and pinion gears so as to be either above the sample preparation chamber or retracted over the shielding slab, exposing the sample preparation chamber. Interlocks prohibit movement of the irradiation chamber when the sample table is in the raised position.

With the irradiation chamber retracted, materials to be irradiated are placed on the sample table in holders so designed as to locate their position accurately with respect to the axis of the irradiation chamber and the median plane of the line sources. The irradiation chamber is rolled over the sample preparation chamber. The sample table is raised into position and the line sources are then moved to the desired radius for a given irradiation. Rotation of the sample table permits some averaging of variations in the radiation flux. Two types of sample holders have been used - one holding a single sample or collection of samples on the center axis of the irradiation chamber,

Figure 1

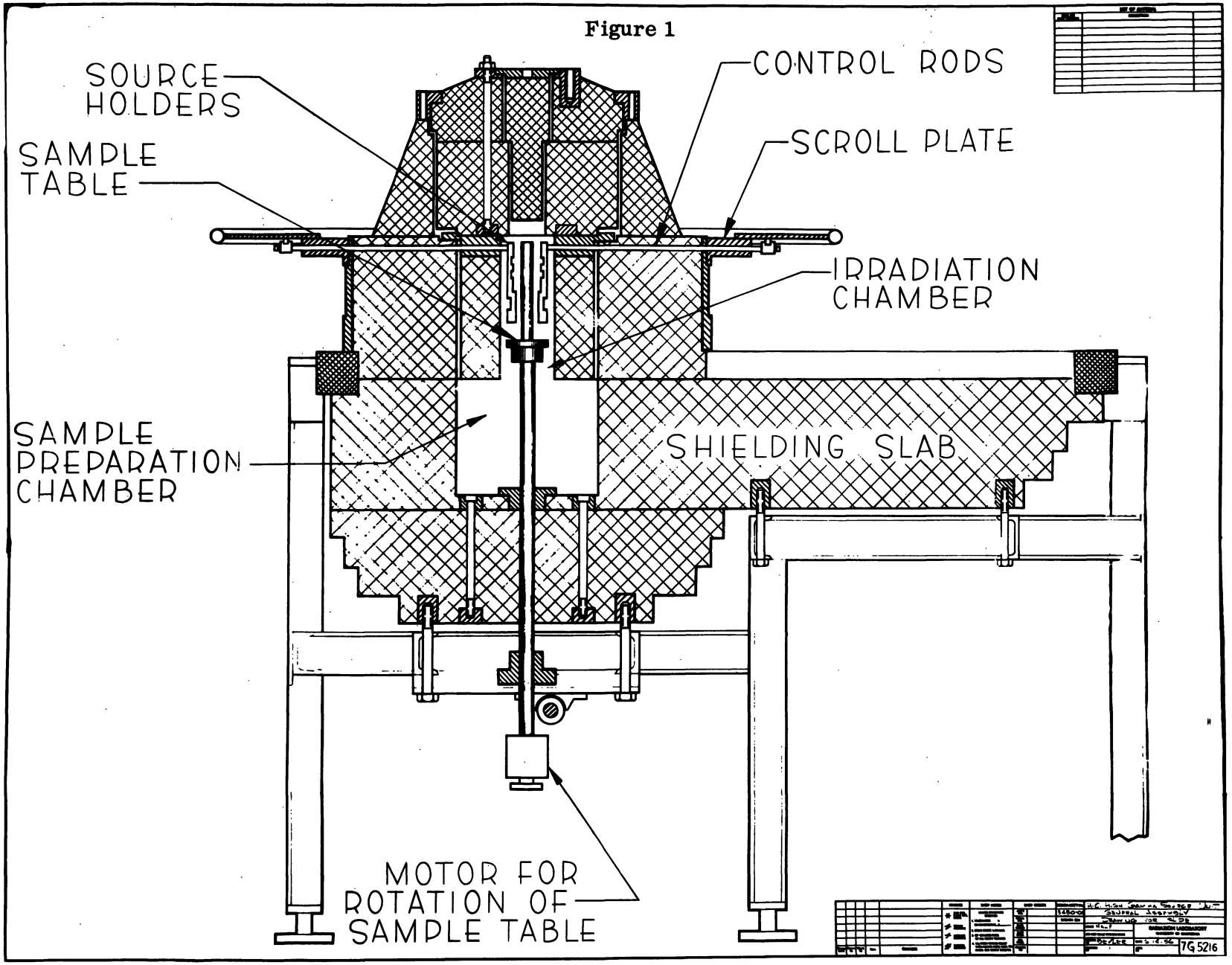
SOURCE HOLDERS
CONTROL RODS
SAMPLE TABLE
SCROLL PLATE
IRRADIATION CHAMBER
SAMPLE PREPARATION CHAMBER
SHIELDING SLAB
MOTOR FOR ROTATION OF SAMPLE TABLE
7G 5216

the other holding in addition 4 samples located symmetrically off the axis of the irradiation chamber. In the latter case, rotation of each individual sample as well as of the sample table can be made. Several openings were provided from the exterior into the sample preparation chamber should the introduction of electrical leads be desired.

The irradiation chamber measures 4 inches in diameter by 10 inches high. The shielding surrounding the irradiation chamber consists of several parts. A section immediately surrounding the irradiation chamber can be removed should it be desired to increase the diameter of the irradiation chamber. The lead section immediately above the irradiation chamber is removable and contains in addition a removable lead plug. This section served as a transfer case for transporting a source holder to this unit from a lead cave where the preparation of the cobalt-60 pellets and the placing of the pellets in each source holder took place.

More details of the irradiation chamber area are shown in Figure 2. The central section shows a source holder being disconnected from the transfer case holder for joining to a control rod. The tube section holding the 1/8 inch diameter pellets can be seen. The closure on each end of this tube section was specified to be dust-tight (against cobalt oxide) but not necessarily gas-tight. This type of removable end closures was chosen in order to permit replacement of the cobalt pellets with higher specific activity material when so desired. To the right in Figure 2 is a plan view of the source holders showing them in their maximum and minimum diameter position.

Figure 3 is a photograph of this machine showing the irradiation chamber in the retracted position, revealing the sample preparation chamber and material to be irradiated in place on the sample table.

Measurements made by Dr. Tolbert and his group of the maximum radiation field at the center position, when the line sources are at their minimum diameter of 0.882 inch, showed a radiation intensity of 400,000 r/hr. With the line sources at a diameter of 1.750 inches, another measurement was taken of the radiation at the center position and at a radial position 7/16 of an inch from the center. The 4-sample rotating table was used for this measurement. The intensity at the center was 148,000 r/hr, while that at the radial position was 157,000 r/hr. This latter measurement indicates less variation in the radiation intensity in this region than was predicted from the calculations.

It is believed that a major value of such a presentation as this is a discussion of the things that one would or would not duplicate in constructing another such machine. The curie content of this machine will not be increased. Instead, a new machine containing 2,500 curies of cobalt-60 will be used to supplement it. Such a new machine is presently under construction.

The diameter of the cobalt-60 pellets, the length of the line sources, and the radial movement of the line sources remain the same. The scroll plate for simultaneous setting of the radial position of all line sources has been replaced with a simpler mechanism.

The location of the control rods has been changed. They will enter near the bottom of the irradiation chamber rather than at the top. This, together with the change in construction of the control rods and the source holders, is expected to ensure better alignment of the individual source holders, as well as to protect against injury or misalignment from improper operation of the sample table.

The individual source holders, fastened to their control rods, will be initially introduced through the control rod openings. They can later be removed in the same manner.

In order to take full advantage of the space in the irradiation chamber, there will be 2 sample preparation chambers. One will operate from below the irradiation chamber, as in the existing machine, for insertion of samples in the space inside the line sources. The other will operate from above the irradiation chamber for insertion of samples in the space outside the line sources. Insertion from either sample chamber can be accomplished without interfering with the

Figure 2

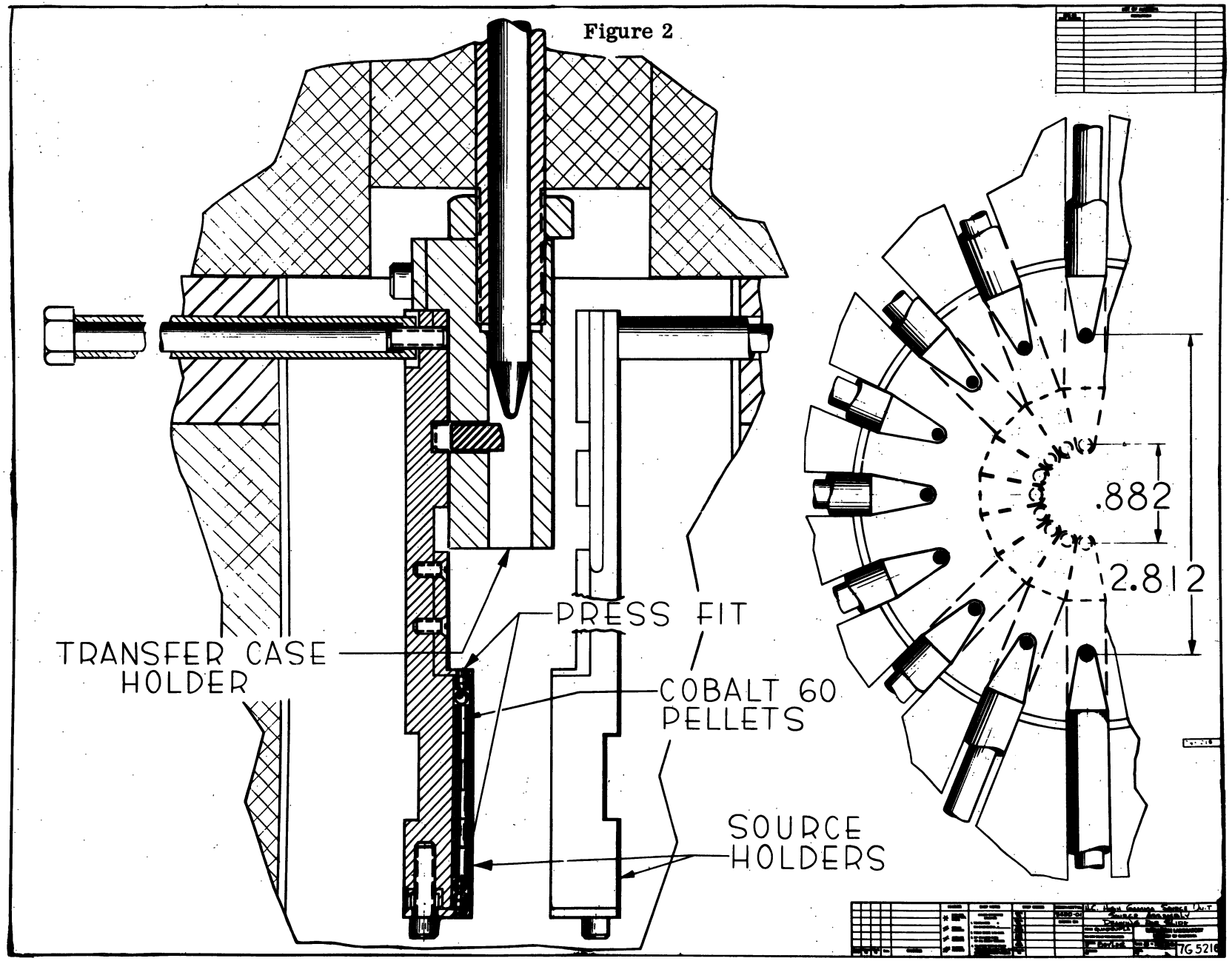
TRANSFER CASE
HOLDER
PRESS FIT
COBALT 60
PELLETS
SOURCE
HOLDERS
.882
2.812

samples from the other chamber. It is planned to use the outer chamber for radiation damage studies on plastics, paints, and other materials used in radiochemical operations.

The closure on the tube containing the cobalt-60 pellets will be soldered. After about 2 years of operation, a slight but measurable amount of cobalt oxide has been detected coming through the closures used on the existing machine. With the soldered closure, any future change of cobalt-60 pellets will require replacement of the entire source holder. Some of the changes in design outlined for the new machine will make this operation simpler.

In general, the existing machine has been found to perform quite satisfactorily in accordance with the expectations and to provide considerable versatility in the studies for which it was designed.

THE STATUS OF BIOASSAY TECHNIQUES FOR EVALUATION OF INTERNAL EXPOSURES FROM RADIOACTIVE ISOTOPES

J. W. Healy

Hanford Atomic Products Operation
General Electric Company
Richland, Washington

INTRODUCTION

Control of the intake of radioisotopes by an individual is based on the control of the materials in his environment and by good work habits to avoid accidents. A final check on these control measures is useful, not only to indicate the efficiency of the control techniques but also to indicate possible curtailment of an individual's exposure if a significant body burden has been accumulated. Thus the estimation of the body burden of radioactive materials becomes an important step in the over-all control practices of a nuclear installation.

The first radioisotope of concern in human exposure was radium. In this case primary reliance was placed on the measurements of the exhaled radon, although measurements of the total gamma radiation from the body were also used. With the increased production of potentially toxic radioactive materials in the nuclear reactor and the increased exposure of workers to these materials, a method for estimation of the body burden became of importance. Since the bulk of these artificially radioactive materials do not liberate a noble gas adequate for measurement in breath samples, the analysis of urine samples was used. The term "bioassay" was chosen to describe this type of analysis and now has the connotation in radiation protection work of the analysis of excreta for the estimation of body burden, although Webster defines the word in terms of the estimation of the strength of a drug by use of a living organism.

This paper reviews some of the concepts involved in the estimation of the body burden from the results of analyses of excreta. Emphasis is placed on the theory rather than on the constants for particular isotopes, although several of the isotopes which have been investigated in humans are used as illustrations.

EXCRETION PATHS

Isotopes taken into the body may be excreted by any of the normal routes by which the body eliminates waste materials, i.e., urine, feces, exhaled air, or perspiration. The particular path involved in a given case will depend upon the chemical and/or physical properties of the isotope and upon the method by which it gains entry to the body. The excreta chosen for measurement will depend to some extent on these features, although in practice the choice may be dictated by the ease of sampling. Thus most bioassay measurements are obtained from urine samples, with feces required in special cases.

In order to estimate the body burden, a reference standard such as the average excretion rate from a group of individuals who contain a known quantity of the isotope is needed. The standard implies that the behavior of the accidentally administered isotope in the body matches the behavior of the material administered to obtain the standard curve. Since the excretion curves used

This paper is based on work performed for the AEC under Contract #W-31-109-Eng-52.

for such comparisons are usually obtained from the results of intravenous administrations of a particular compound, an exact correspondence between the exposed individual and the standard curve is rarely obtained. This leads to the first assumption necessary for interpretation of results: The excretion rate of a radioisotope reaching the bloodstream will be the same regardless of the route by which it arrives there. Thus the excretion rate will be assumed to be the same for materials absorbed through the GI tract, lung alveoli, or skin.

If this assumption is accepted, the comparison to the standard curves (as well as the establishment of the curve) must be on the basis of the time of administration to the bloodstream. An intramuscular or intraperitoneal administration may result in a deposition of the isotope in a relatively insoluble form, so the rate of movement to the blood is slow. Such a condition must be interpreted as a chronic administration, although the actual intake to the body is acute.

The accuracy of estimation is limited by the biological variations. These may be variations from period to period in the same individual, variations between individuals of the same species, and interspecies variations. Individual variations limit the accuracy with which the rate of excretion may be established and may require a number of samples to establish the average rate. Variations between individuals of the same species make application of a curve derived by measurements from a number of individuals uncertain, since it is possible that the subject is different from the average. For this reason, the estimate made for any one person can be regarded only as the most probable value. The probability of significant deviation can be established by examination of a large number of individuals with a known body burden. Interspecies variation is troublesome in the establishment of a standard curve since human data for a particular isotope are usually meager and it is necessary to use excretion rates obtained from animals. Although animal data must be used if human data are not available, the practice is risky and results should be regarded as tentative.

EXCRETION PATTERNS FOLLOWING ACUTE INTAKE

The type of excretion curve for a particular isotope depends upon the metabolic features of the element. The description of retention using the half-life or exponential function implies that all of the isotope in the body is available for excretion, regardless of the time since administration or the degree of "fixation" in the body. This concept appears to be valid for those isotopes which are reduced in concentration in the body through dilution by the incoming element and excretion of the resulting mixture. An example of this type of material is tritium oxide, which is excreted in the same fraction per unit time as the body water. Even this case is complicated, however, by the interchange of the tritium in the water with the hydrogen of the organic compounds in the body.[1] This "bound tritium" fraction is more tightly held in the body, so the rate of elimination is slower than that for water.

Several authors have noted that the excretion rates of isotopes such as strontium-90[2, 3] follow closely to a straight line if the data are plotted as logarithms. Langham[4] used this relationship to correlate the data from the intravenous administration of plutonium to humans, and recently the studies of radium metabolism by Norris, et al.[5] have indicated the same type of function for the retention of radium in the human. Although such a relationship may be written as the sum of a series of exponential functions, it has generally been found more satisfactory to use a single empirical correlation in which the excretion rate is expressed as a power function of time.

If the retention of a particular isotope is represented by

$$(1) \quad R = At^{-n}$$

where A and n are constants for a particular species and isotope, then the total excretion rate is given by

$$(2) \quad E = -\frac{dR}{dt} = An\, t^{-(n+1)}$$

or

$$(3) \quad E = Bt^{-m}$$

In these equations E and R are expressed as fractions of the administered dose per unit time and apply only to the biological elimination or retention. Norris, et al.[5] have pointed out that the excretion rate of the retained quantity may be obtained from the ratio of E/R.

$$(4) \quad E/R = nt^{-1}$$

The rate of excretion of the retained quantity is thus inversely proportional to the time since administration.

Following an acute administration, there is a rise in the excretion rate as the material is absorbed and distributed in the body. This increase usually occurs over the first few hours, or in some cases the first few days. A maximum is eventually reached and the excretion rate approaches the power function. Thus there is a period immediately following administration for which these relations do not hold. The interpretation of samples taken during this period is difficult since the elimination of wastes from the body is a discontinuous function and the exact time represented by a given sample is difficult to interpret. If feces samples are involved, the time of passage through the GI tract becomes of importance.

If the time at which the isotope is taken into the body is known, a measurement of the excretion rate will permit estimation of the body burden from equation (1). If the time of administration is not known, it can be estimated theoretically from measurement of 2 samples taken sufficiently far apart in time that a significant difference between the 2 results is available. The interval necessary depends upon the time since administration, as the fraction excreted per unit time changes with time. Thus if D_1 is the quantity excreted at an unknown time T after intake, and D_2 is the quantity excreted after a time interval ΔT, a simultaneous solution of equation (3) at these 2 times leads to

$$(5) \quad T = \frac{\Delta T}{(D_1/D_2)^{1/n} - 1}$$

This time between exposure and the first sample may then be used to estimate the body burden from equation (3). In practice, the application of this type of analysis is difficult because of the variations obtained between individual samples and the possible influence of the unknown method of administration. In many cases, a series of measurements will indicate the approximate time since exposure by the average rate of change.

The lack of human data for most isotopes makes the practical interpretation of excreta analyses difficult. Comparison to published data for experimental animals may be necessary in many cases, but results obtained in this manner are poor estimates. The best data available at this time are for plutonium and radium. Langham[4] has correlated the excretion data for the human following intravenous administration.

$$(6) \quad E_u = 0.002\, t^{-0.74} \text{ (urine)}$$

$$(7) \quad E_f = 0.0063\, t^{-1.09} \text{ (feces)}$$

$$(8) \quad E_{u+f} = 0.0079\, t^{-0.94} \text{ (urine plus feces)}$$

where E is the fraction of the administered plutonium excreted per day. These equations have been shown to apply to at least 5 years after administration.

The studies of Norris, et al.[5] of the metabolism of radium in the human have resulted in a description of the retention by

$$(9) \quad R = 0.54\, t^{-0.52}$$

From this the total excretion rate is

$$(10) \quad E = 0.36\, t^{-1.52}$$

Data for other isotopes are practically unavailable. Some of the information for various animals for Sr-90 is given in Table 1 to indicate the amount of interspecies dependency.

TABLE 1

SR-90 EXCRETION

	Urine	Feces	Total
Humans*	$Kt^{-1.3}$	-	-
Dogs[3]	$0.077\, t^{-1.65}$	$0.22\, t^{-1.75}$	-
Goats[7]	$Kt^{-1.8}$	$Kt^{-2.4}$	-
Mice[2]	-	-	$0.092\, t^{-1.17}$
Rats[2]	$0.04\, t^{-1.3}$	-	$0.093\, t^{-1.16}$
Rabbits[2]	$0.14\, t^{-1.85}$	-	$0.14\, t^{-1.44}$

* from accident cases[6]

There is considerable variation between species. Since a number of investigators were involved, a portion of this variation may be caused by differences in compounds used and techniques. We have estimated the urinary constant for the human as 0.055, assuming that all of the strontium is accounted for by integration of the excretion to infinity and that about 1/3 of the strontium is excreted in the urine. Although these assumptions have been derived from the data for dogs, rats, and rabbits, the studies of Harrison, et al.[8] with stable strontium in the human have indicated that less than 6 percent of the administered dose is excreted in the feces over a period of 30 days, while about 65 percent is excreted in the urine. This would indicate that the constant for the urine should be closer to 0.15.

The bioassay program, itself, can play an important part in the establishment of these excretion curves. When positive results are obtained for an individual, every effort should be made to obtain a sufficient number of samples to permit the establishment of an excretion curve. Such a sampling program should include both urine and feces so that the comparative rates of excretion and the total quantity involved may be established. In conjunction with data from animal experiments, these rates may then be used to estimate the fraction eliminated per unit time.

EXCRETION PATTERNS FOLLOWING CHRONIC INTAKE

Radioactive materials may be accumulated in the body by the frequent addition of a quantity so small that each addition is not detected as an acute exposure. The cumulative effects of such a condition, however, may result in the deposition of a significant portion of the body burden.

The excretion pattern resulting from this type of chronic exposure will depend upon the frequency of intake as well as the length of time over which it occurs. The 2 limiting cases which are most amenable to solution are the acute or single administration and the continued intake which is completely uniform in time. A short-term chronic intake will appear as an acute administration a long time after the intake has stopped. Thus excretion rates several years after a 1-month chronic exposure may be interpreted as though the intake were acute.

The influence of a continued administration may be estimated by summation of the curves representing each individual intake. As an illustration, if the same quantity of isotope is given at the same time each day, the excretion rate after a given time interval could be obtained by summing the excretion rates for each individual parcel. If it is assumed that the intake is completely uniform over time,

$$(11) \quad E_n = BD_n \int_0^{T_1} (T_2-\tau)^{-m} \, d\tau$$

where D_n is the quantity administered per unit time, T_1 is the time of exposure, T_2 is the time since exposure has stopped, and E_n is the excretion rate. Solution of this equation gives

$$(12) \quad E_n = \frac{BD_n}{1-m} \left[(T_1+T_2)^{(1-m)} - T_2^{(1-m)} \right]$$

The total body burden resulting from the continued administration of D_n must be evaluated from the over-all retention. In the simplest case,

$$(13) \quad q = T_1 D_n$$

where q is the resulting body burden. This equation implies that there is no significant elimination over the period considered. If this value for D_n is substituted in (12),

$$(14) \quad q = \frac{(1-m) E_n T_1}{B \left[(T_1+T_2)^{(1-m)} - T_2^{(1-m)} \right]}$$

If the radioactive decay of the isotope is negligible over the total time period but biological elimination is significant, the total retention[9] from integration of equation (1) is

$$(15) \quad q = \frac{D_n A}{1-n} \left[(T_o+T_1)^{(1-n)} - T_o^{(1-n)} \right]$$

where T_o is the time after administration when the value for the body burden is desired. Substitution in equation (12) gives

$$(16) \quad q = \frac{E_n A(1-m)}{B(1-n)} \left[\frac{(T_o+T_1)^{(1-n)} - T_o^{(1-n)}}{(T_1+T_2)^{(1-m)} - T_2^{(1-m)}} \right]$$

If the radioactive half-life of the isotope is significant, the final body burden may be obtained by integration after accounting for the combined radioactive decay and biological elimination.[9]

Such equations are useful primarily for assessing the required sensitivity of a bioassay procedure and for establishing the shape of curve expected for chronic types of intake. In practice, the chronic case described by these equations is seldom encountered, since exposure levels vary and the aim of most protection groups is to keep contamination levels sufficiently low so that exposure occurs only as a result of an accident.

The effects of chronic exposure on excretion rates are illustrated for radium and plutonium in Figure 1. In these curves, the excretion following 1 year of continuous exposure, at such a level that the permissible body burden for plutonium and 1/10 of the permissible body burden for radium are accumulated, is contrasted with the excretion rates obtained with an acute exposure. The chronic curves have a lower slope in each case.

In Figure 2 the excretion rates 10 days after being exposed to plutonium and radium for periods up to 10 years are plotted. Again the plutonium is permitted to reach the maximum permissible body burden in the time of exposure, while the radium is limited to 1/10 of the maximum permissible body burden. This curve indicates the sensitivity required for detection as the time of exposure increases. Thus in order to detect 1/10 of the maximum permissible body burden for

Figure 1

EXCRETION CURVES - RADIUM AND PLUTONIUM

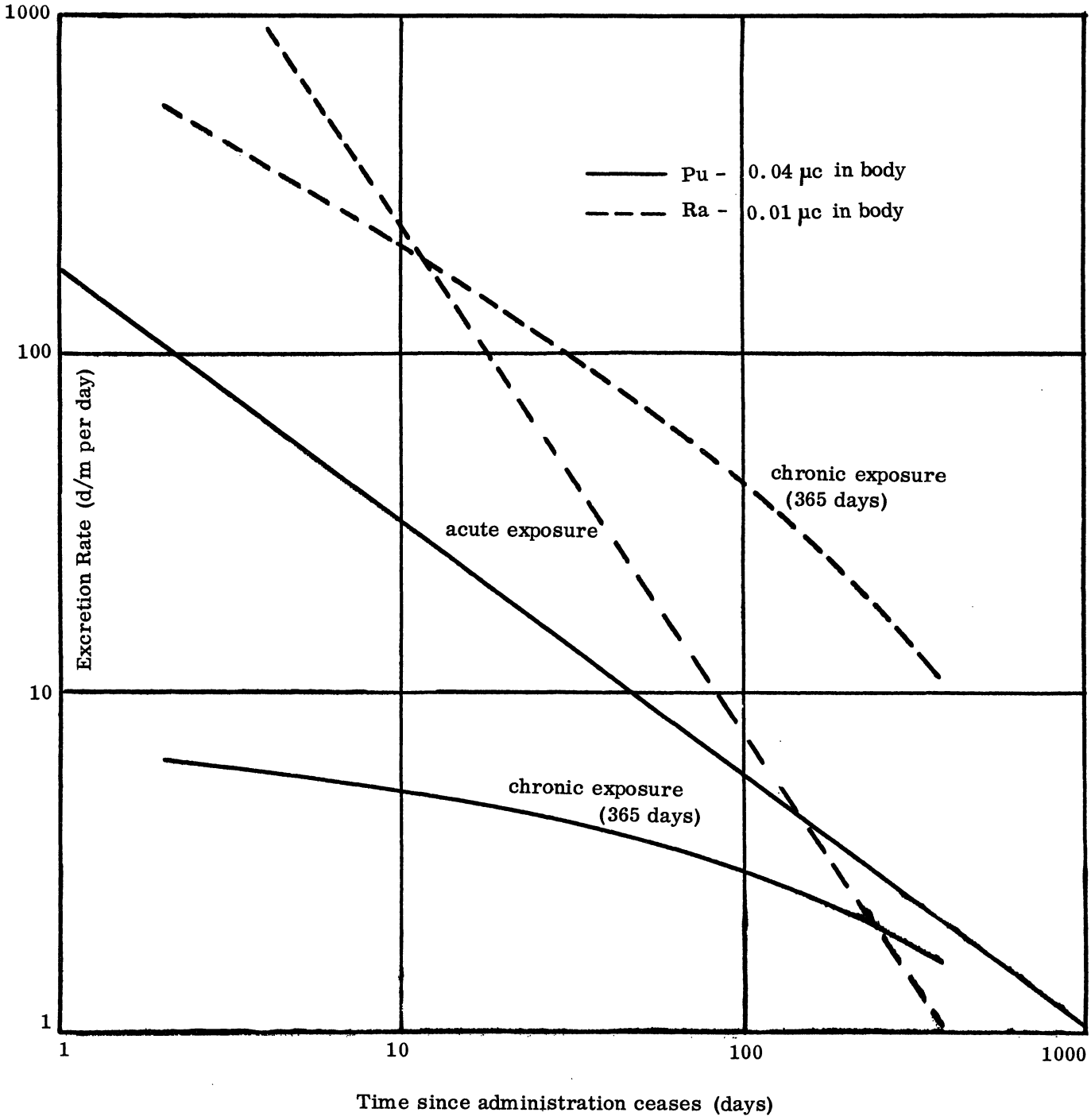

Figure 2

EXCRETION RATES TEN DAYS AFTER EXPOSURE STOPS

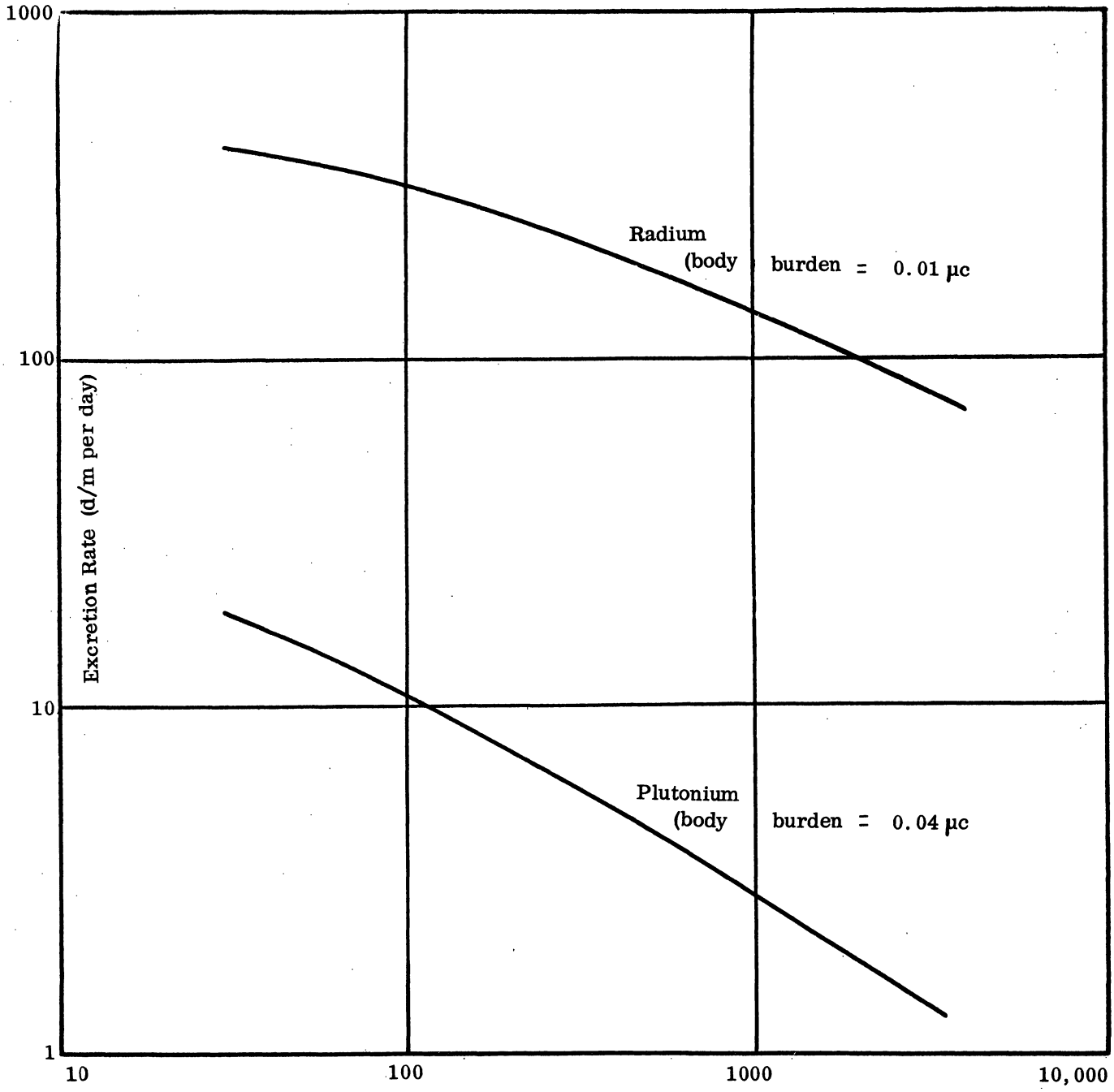

plutonium after 10 years of chronic exposure, the sensitivity limit must be on the order of 0.1 to 0.2 d/m. After 20 years of exposure, this limit is on the order of 0.07 d/m. The attainment of these burdens would require an average absorption to the bloodstream of 3 to 4 d/m per working day for 10 years or 1.5 to 2 d/m per working day for 20 years.

LUNG DEPOSITION

One of the more probable methods of taking radioisotopes into the body is by inhalation. If the isotopes are soluble and easily absorbed from the lung, they will pass into the bloodstream rapidly and will be excreted as predicted by the previous considerations. If the material is relatively insoluble or forms relatively insoluble compounds in the lung, it will be absorbed more slowly. This unabsorbed portion will not be detected by the bioassay methods. Thus a source of material which may gradually be dissolved and transported to the blood will exist. A similar situation will occur in the case of wound contamination, where the isotope is precipitated at the site and absorbs only slowly to the body. These situations result in an excretion rate which is related to chronic exposure, although the intake to the body is an acute incident.

Two mechanisms of clearance of the lung are of importance in this discussion. The first, ciliary action or mechanical movement into the throat where the material is swallowed and subsequently excreted in the feces, occurs during the first few days after exposure. Feces samples during this early period may give high results, with a rapid decrease with time. From feces samples taken at long times ($\sim$30 days) after exposure, it was concluded that this mechanism is negligible for the portion retained for long times, although the I. C. R. P. data would indicate that about 50 percent is eliminated in this fashion. The second mechanism, solubility into the bloodstream, then provides an important clearance mechanism for the relatively insoluble isotopes. Note that in the following discussion the exact location of the insoluble isotope in the body is not important. Thus the same excretion pattern will be followed for the isotope liberated to the bloodstream directly from the lung or for any moved by phagocytosis to the lymph nodes, as long as the relative solubility in body fluids is the same.

Thus, after ciliary action has completed removal of that portion which can be mechanically removed, the remainder is transferred to the bloodstream. The rate of removal is undoubtedly dependent upon the solubility of the particular compound and its access to the body fluids. If it is assumed that the rate of transfer is proportional to the quantity present, then a constant, λ, may be defined as the fraction removed per unit time. The quantity Q remaining in the lung at any time following the exposure is then

$$(17) \quad Q = Q_0 e^{-\lambda t}$$

where Q_0 is the initial quantity present. λ may be divided into 2 portions if desired, λ_s the fraction dissolved and λ_c the fraction removed by ciliary action. Comparison between urine and feces samples will then permit an assessment of the comparative rates of elimination by these 2 processes. In the following derivation, only λ_s is used. The rate of movement to the bloodstream is

$$(18) \quad a = \lambda Q_0 e^{-\lambda t}$$

This results in a chronic exposure condition with the rate of administration decreasing. The total rate of excretion, E_u', may be written as

$$(19) \quad E_u' = B \int_0^{T_1} a(T_1 - \tau)^{-m} \, d\tau$$

$$(19a) \quad E_u' = \lambda B Q_0 \int_0^{T_1} e^{-\lambda\tau} (T_1 - \tau)^{-m} \, d\tau$$

where T_1 is the time since the isotope was deposited. This function must be solved by the use of a table of incomplete gamma functions or by numerical techniques for the particular value of the constants.

In the application of this concept some value for λ, the fractional rate of transfer, is needed. At the present time no correlative study between the physical solubility or other physical characteristics of any material and its biological behavior is available. Marinelli, et al.[10] have measured the rate of turnover of radium sulfate from the lung by external measurements and have obtained a half-life of about 120 days. Application of this figure to the measured excretion rate over a period of time gave a good explanation of the shape of the curve.

For most isotopes, where external body measurements are not available, measurements of the excretion rates over long periods of time (up to 1,000 days) will indicate deviations of the curve from the acute case. For example, Figure 3 illustrates the excretion curves expected for plutonium contained as a slowly soluble deposit. The excretion rates are values of the integral in equation (19a), i.e., $f(\lambda, T_1)$ for several values of λ. The maximum in these curves results from the increase in quantity excreted as a result of chronic administration until the source is significantly depleted so that the rate of administration decreases. It is possible to estimate the value of λ from a fit of these functions to the shape of a measured excretion curve. The accuracy is low but does provide an order of magnitude estimate.

In practice, there is frequently a significant absorption to the body at the time of exposure resulting from a soluble fraction in the contaminant or absorption of a portion of the fraction eliminated by ciliary action. Thus the curve must be divided into 2 parts, using the early points to estimate the acute portion and the difference to estimate the retained lung burden. Figure 4 illustrates one type of excretion curve expected for plutonium, assuming a 1-year half-life in the lung.

The sensitivity of the analysis required to establish such curves for the estimation of the half-life is illustrated by Table 2, in which the excretion rate at the maximum time for a lung burden of 0.016 μc is given for several values of λ.

TABLE 2

MAXIMUM EXCRETIONS FOR 0.016 μc OF Pu IN THE LUNG

Half-life in Lung Days	λ $(\text{Days})^{-1}$	Time of Maximum Excretion Days	Value of $f(\lambda, T)$	E_u' d/m
70	0.01	30-50	7.2	5.1
140	0.005	$\sim$ 50	8.7	3.1
350	0.002	$\sim$ 100	11	1.6
700	0.001	$\sim$ 500	13	0.9

SUMMARY

The interpretation of bioassay data in terms of the quantity of radioisotopes in the body is dependent upon the knowledge of the excretion rate of the substance by the human following acute administration. Other cases including chronic uptake and lung deposition may be evaluated from the acute case if other physical parameters are known. At the present time, one function of the bioassay laboratory should be the accumulation of data from any accidental exposures so that values for the parameters involved may be obtained for the human.

Figure 3

URINARY EXCRETION CURVES FROM PLUTONIUM LUNG DEPOSITION

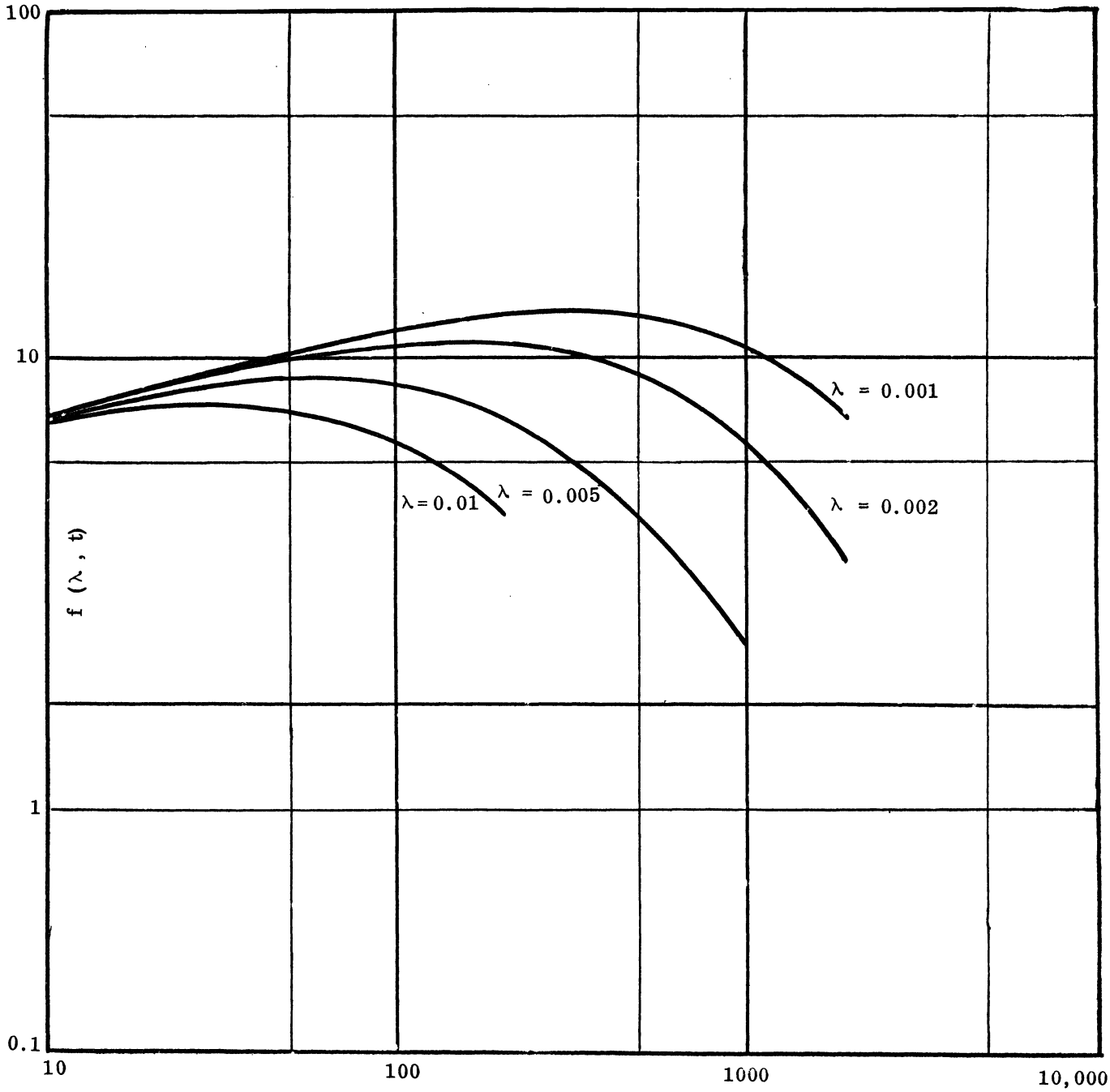

Figure 4

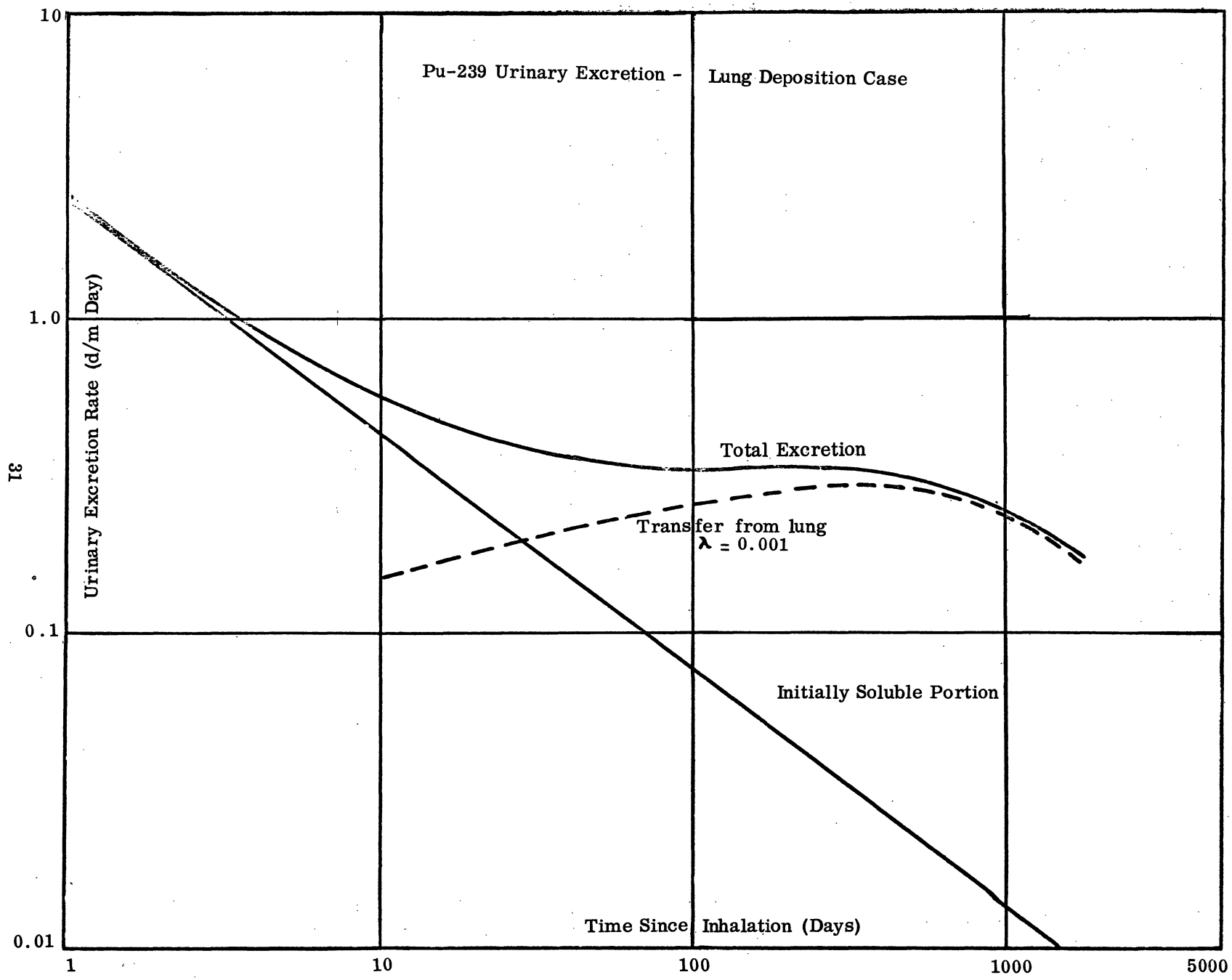
Pu-239 Urinary Excretion - Lung Deposition Case
Urinary Excretion Rate (d/m Day)
10
1.0
0.1
0.01
Total Excretion
Transfer from lung
λ = 0.001
Initially Soluble Portion
Time Since Inhalation (Days)
1
10
100
1000
5000

BIBLIOGRAPHY

1. Thompson, R. C. "Studies of Metabolic Turnover with Tritium as a Tracer. II. Gross Studies on the Rat." J. Biol. Chem., 200:731, 1953.

2. Anthony, D., K. Lathrop, F. Finkle. "Radiotoxicity of Injected Sr^{89} for Rats, Mice, and Rabbits. Part II. Metabolism and Organ Distribution." MDDC-1363, June 1, 1946.

3. Sacher, G. "The Excretion, Retention, Distribution and Clinical Effects of Strontium ^{89} in the Dog. Part II. Statistical Analysis of Excretion and Retention of Strontium ^{89} for Individual Dogs." CH-3866, June, 1946.

4. Langham, W. H. "Determination of Internally Deposited Radioactive Isotopes from Excretion Analyses." Private Communication.

5. Norris, W. P., T. W. Speckman, and P. F. Gustafson. "Studies of the Metabolism of Radium in Man." Am. J. Roen., Rad. Ther. and Nuc. Med., 73:785-802, 1955.

6. Cowan, F. P., L. B. Farabee, and R. A. Love. "Health Physics and Medical Aspects of a Strontium^{90} Inhalation Incident." Am. J. Roen., Rad. Ther. and Nuc. Med., 47:6-, 1952.

7. Swift, W. N., C. L. Prosser, and E. S. Mika. "Effects of Sr^{89} and X-radiation on Goats." CH-3888, June, 1946.

8. Harrison, G. E., W. H. A. Raymond, and H. C. Tretheway. "The Estimation of Barium and Strontium in Biological Materials by Activation Analysis with Special Reference to the Turnover of Strontium in Man." International Conference on the Peaceful Uses of Atomic Energy. Paper A/CONF. 8/P/448, June 20, 1955.

9. Healy, J. W. "The Calculation of Maximum Permissible Concentrations for Long-lived Radioisotopes." Rad. Res. (in press)

10. Marinelli, L. D., W. P. Norris, P. F. Gustafson, and T. W. Speckman. "Transport of Radium Sulfate from the Lung and Its Elimination from the Human Body Following Single Accidental Exposures." Radiology, 61:903-15, December, 1953.

THE DISTRIBUTION AND EXCRETION OF URANIUM IN MAN

S. R. Bernard, J. R. Muir, and G. W. Royster, Jr.

Health Physics Division
Oak Ridge National Laboratory
Oak Ridge, Tennessee

The cooperative study by the Department of Neurosurgery at Massachusetts General Hospital and the Health Physics Division at Oak Ridge National Laboratory has 2 objectives. The first is to obtain data on the excretion of uranium and its distribution in tissues for calculation of Maximum Permissible Concentrations in the body, urine, air, and drinking water of man. The second, which will not be discussed here, is to determine the potentialities which enriched uranium offers in therapy of inoperable brain tumors.

Data on the distribution and excretion of uranium in man are needed for the purpose of determining the internal radiation exposure of production workers who, through handling enriched uranium for long periods of time (10 to 13 years), have inhaled the dusts, mists, and fumes of this material and thus have uranium stored in their bodies. The conclusion that these workers have stored uranium arises from studies of many samples of air they inhale and their excreta. Air samples have shown that the enhanced material is present in measurable quantities, and characterization of the particle sizes places them in the range for penetration into and retention in the lower passages of the lung. Samples of urine reveal variable quantities of uranium. When workers are isolated from the work areas for months, measurements of their urine have shown that the levels drop rapidly after the cessation of exposure. In 1 month the levels fall to one-half, but after reaching this point they decrease more slowly. These findings support the conclusion that the workers' bodies contain stored material.

For the past several years in the Y-12 production area, it has been the practice to remove employees from uranium operations when their cumulative internal exposure exceeds the maximum permissible exposure. The cumulative internal exposure is determined by converting the uranium excreted in the urine into rem delivered to the body. This is accomplished with the following equation

$$(1) \qquad \text{rem} = \frac{0.3}{7 \times 70} \sum_i \Delta t_{i-1}\, d_i$$

Here, d_i is the d/m excreted per day, while Δt_{i-1} is the time interval between measurements. The conversion factor outside of the summation sign merely says that the MPC for urine, 70 d/m/day, corresponds to the elimination from the body when it contains that amount to deliver 0.3 rem per week. This value, 70 d/m/day, is based on the lung as the critical organ and, therefore, corresponds to exposure to insoluble compounds of uranium. When exposure is to soluble types of compounds, the MPC for urine is 80 d/m/day, a negligible difference from the 70 d/m/day.

Figure 1 shows a graph of the cumulative internal exposure for a production worker. Urinary uranium measurements were converted with equation (1). The absorbed dose in rem is plotted on the ordinate while the time is plotted along the abcissa. The Maximum Permissible Exposure line is plotted for comparison. Note that the worker is in excess of the MPE line. His measurements show that he has an absorbed dose of 130 rem and that he should have only 85 rem. His exposure was terminated in 1954 by removing him from the enriched uranium operations and placing him in other work. He cannot return to the area until his exposure is on or below the MPE

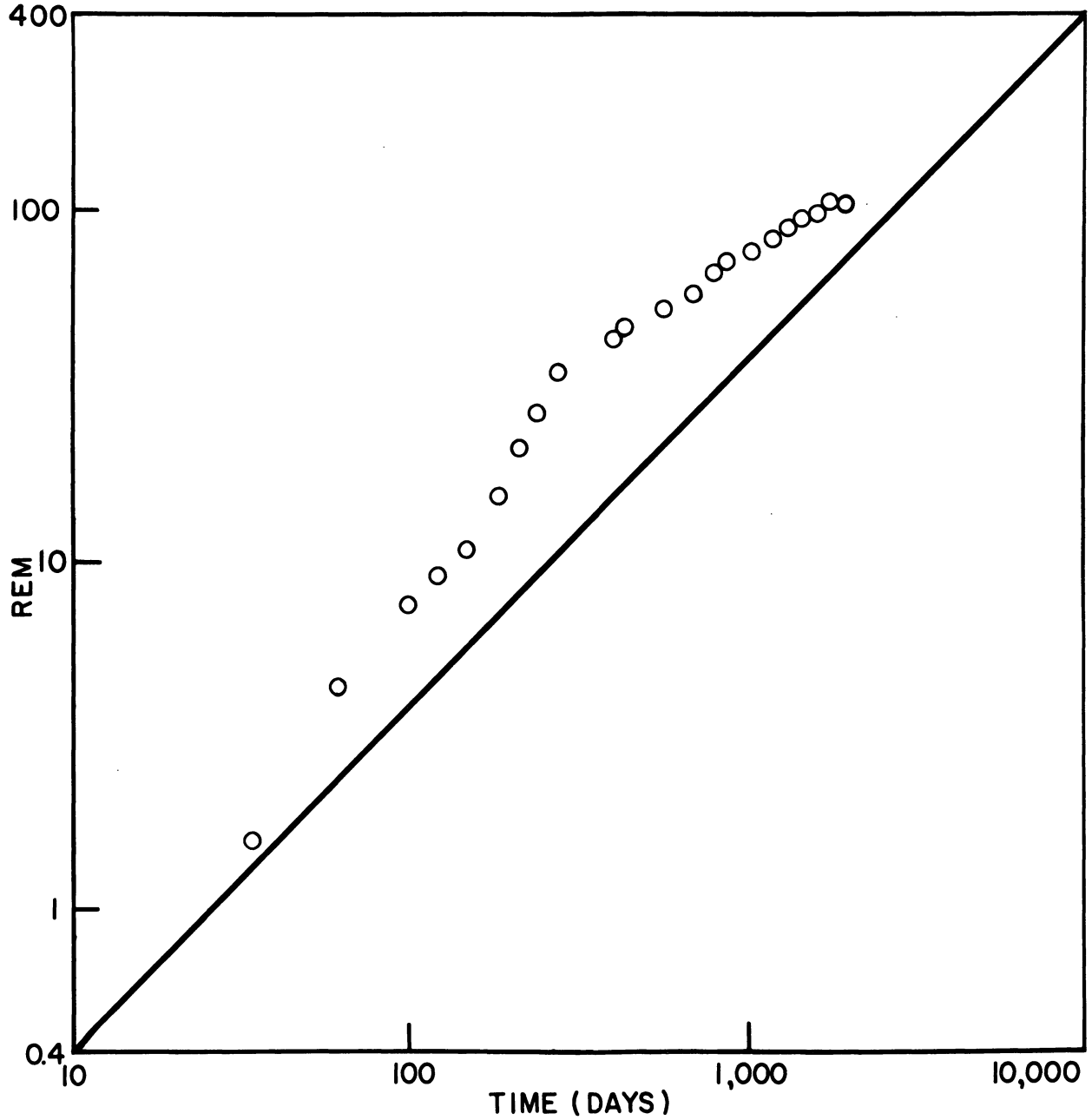

Figure 1. PLOT OF REM TO BODY BASED ON LUNG AS THE CRITICAL ORGAN - ESTIMATED FROM URINARY EXCRETION OF A PRODUCTION WORKER

line. It is estimated that 10 to 15 years will be required to reach this line.

This is not a typical case for production employees, but the highest case on record. There are many others who have been transferred from the uranium operation on this basis; in fact, about 35 have been removed in order to reduce their cumulative internal exposure below the MPE. This method for limiting internal exposure is not different from the practices for limiting external exposure. The philosophy behind its application is noted to be the same. However, the way in which the internal dose is obtained depends upon a factor which is not inherent in problems of external exposure. A reliable measure of internal radiation dose depends upon knowledge of the rate of elimination of uranium from the human body. These exposure cases dictate the need for human measurements. Our value of 70 d/m/day is based upon experimental measurements in dogs and rats.

In an effort to obtain human data for the calculation of MPC's for enriched uranium, the cooperative study of the distribution and excretion in man was initiated several years ago. To date, 11 terminal brain tumor patients have been injected with U-233 and enriched uranium. Many biopsy and autopsy samples have been obtained. All the patients have expired and autopsies were obtained on 9. We shall discuss the results of 6 of these patients here.

At the time of injection all the patients were without evidence of general pathological processes other than their cerebral disease. With the exception of 1 patient, who lived 17 months after injection, all were in a coma or semi-coma. They received the usual hospital care for comatose patients, consisting of indwelling catheters and feeding by gastric tube every 2 hours, which was at times augmented with intravenous fluids. All patients were administered uranium intravenously. Nine received uranyl nitrate hexahydrate compound buffered with a sodium acetate solution, while 2 received the compound UCl_4. The pH of the injection solution ranged from 5.5 to 6.0. Samples of blood, urine, and spinal fluid were obtained every hour during the first 24 hours after injection. Thereafter, blood and urine samples were obtained every 12 hours during the first week, then once per week until expiration.

Figure 2 shows the blood levels plotted versus time. On the ordinate is the percent of injected dose per 10,000 milliliters of blood, while the abcissa is the time of measurement. Patients I through VI were administered the hexavalent state in amounts ranging from 4 to 50 mgms of metal. Note that Patient VII, who was administered 50 mgms of tetravalent uranium, is displaced above the other patients' values. Patient VIII was also injected with 50 mgms but he decreases along the same path as patients who received hexavalent injections. This figure shows that uranium in the blood decreases rapidly. Within minutes after injection only 25 percent remains, while at 20 hours 99 percent has disappeared and only 1 percent remains. Beyond 20 hours the blood levels, shown in Figure 3, are noted to diverge. Patient VI, who received 50 mgms of U(VI), decreases more slowly than those who received amounts ranging from 4 to 15 mgms. Also, note the increased fluctuation as the levels subside. This variation is outside the limits of analytical error.

In Figure 4 the rate of urinary excretion shows clearly a correlation with dose in the first 5 hours. As the injection dose is increased, the levels initiate at lower ordinate values and then rise until they reach a maximum at 3 to 4 hours, when they decrease along a linear path of the power function law. The excretion of tetravalent uranium, Patients VII and VIII, is noted to describe a trend different from hexavalent excretion levels.

The fecal excretion of uranium may be said to be negligible regardless of the valence state injected.

Figure 5 summarizes the measurements made upon autopsy tissues. The bones and kidneys may be said to be the organs which are chiefly concerned with storing uranium. It can be said also that the percent of injected dose in these 2 organs is not significantly different. Since the kidney is the smaller organ, it receives the greater radiation insult. Consequently, it is chosen as the critical organ.

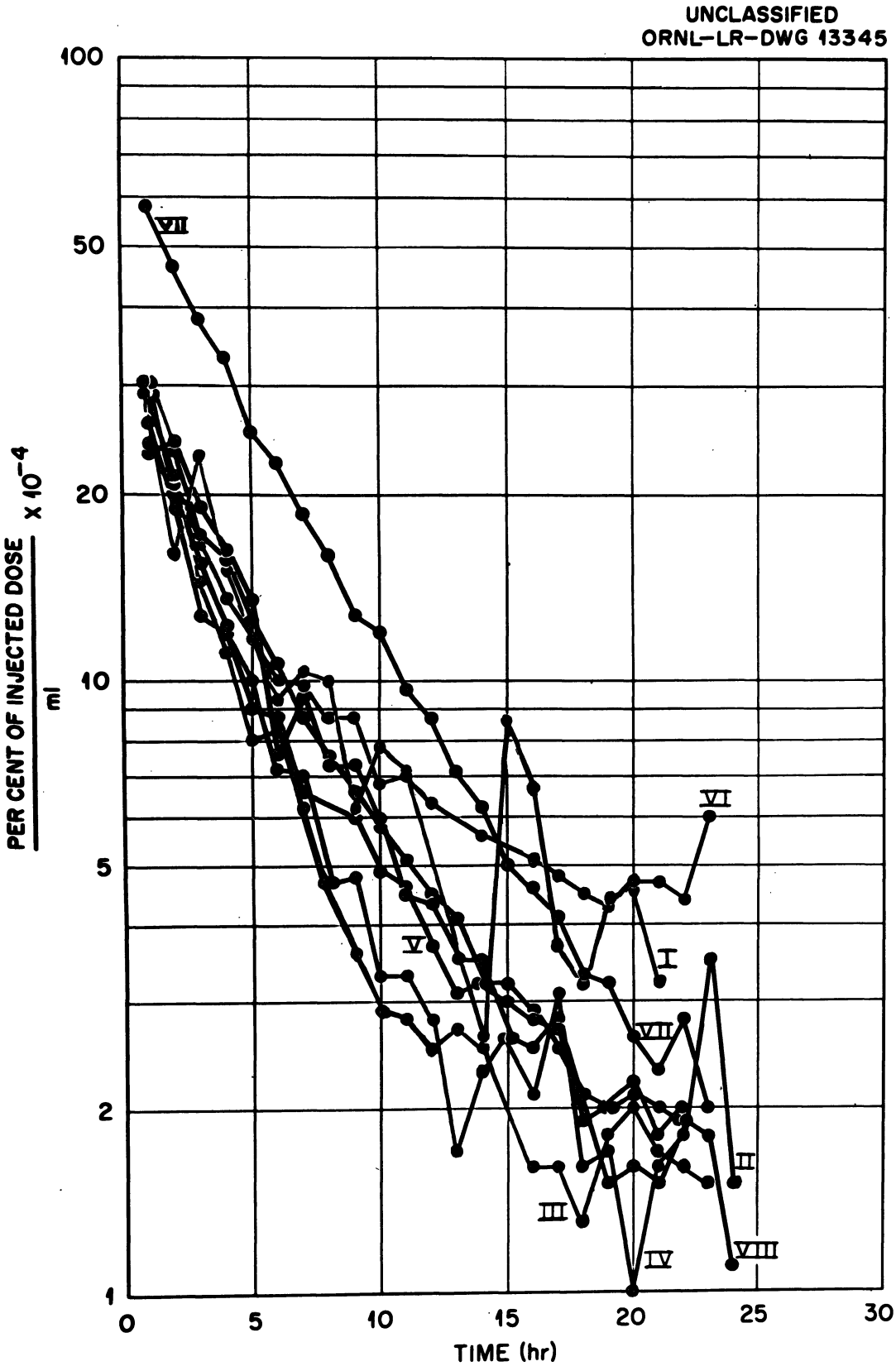

Figure 2. PERCENT OF DOSE PER MILLILITER OF BLOOD DURING FIRST DAY FOLLOWING INTRAVENOUS INJECTION FOR 8 TERMINAL BRAIN TUMOR PATIENTS

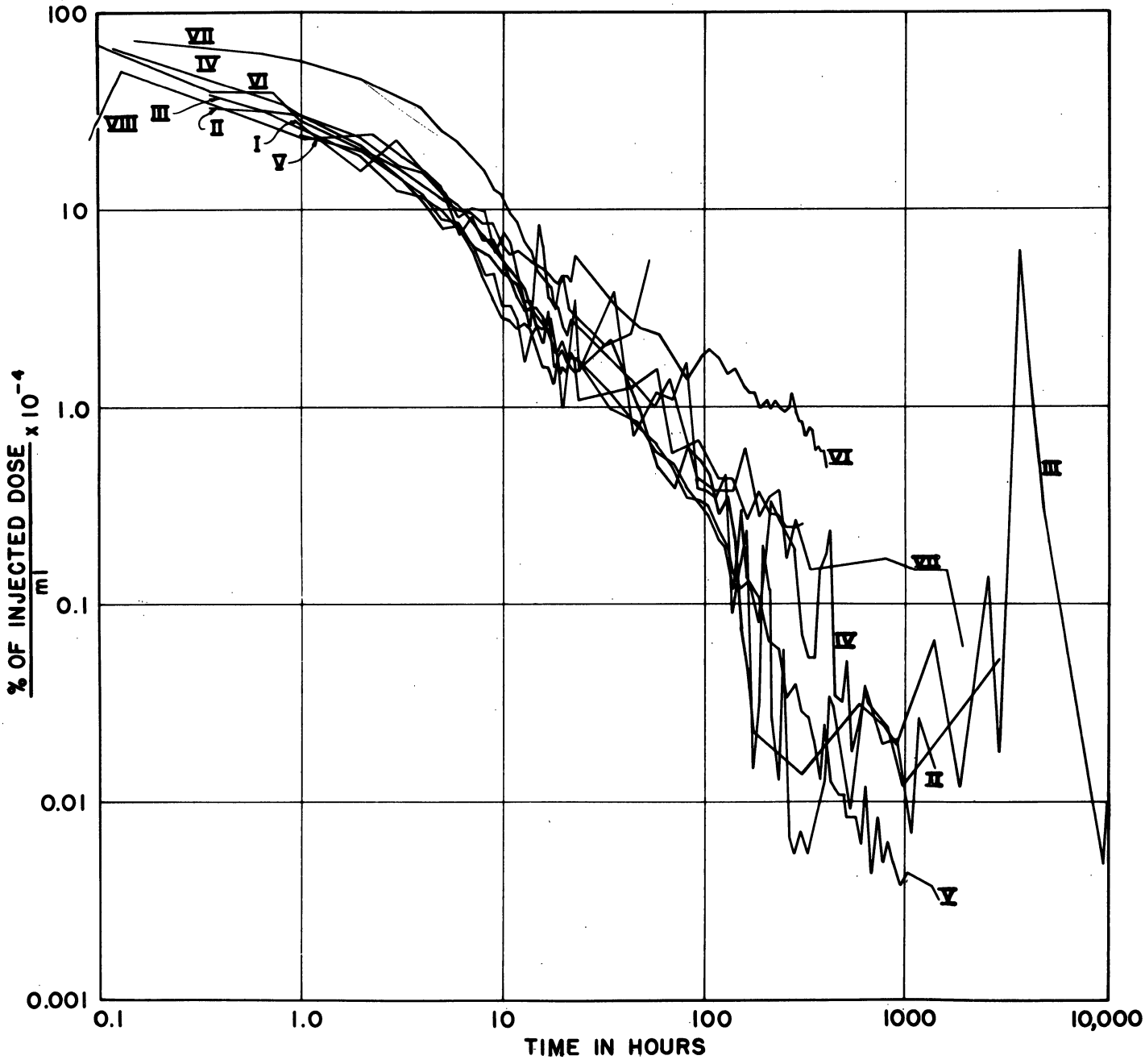

Figure 3. PERCENT OF DOSE PER MILLILITER OF BLOOD FOR 8 TERMINAL BRAIN TUMOR PATIENTS FOLLOWING INTRAVENOUS INJECTION

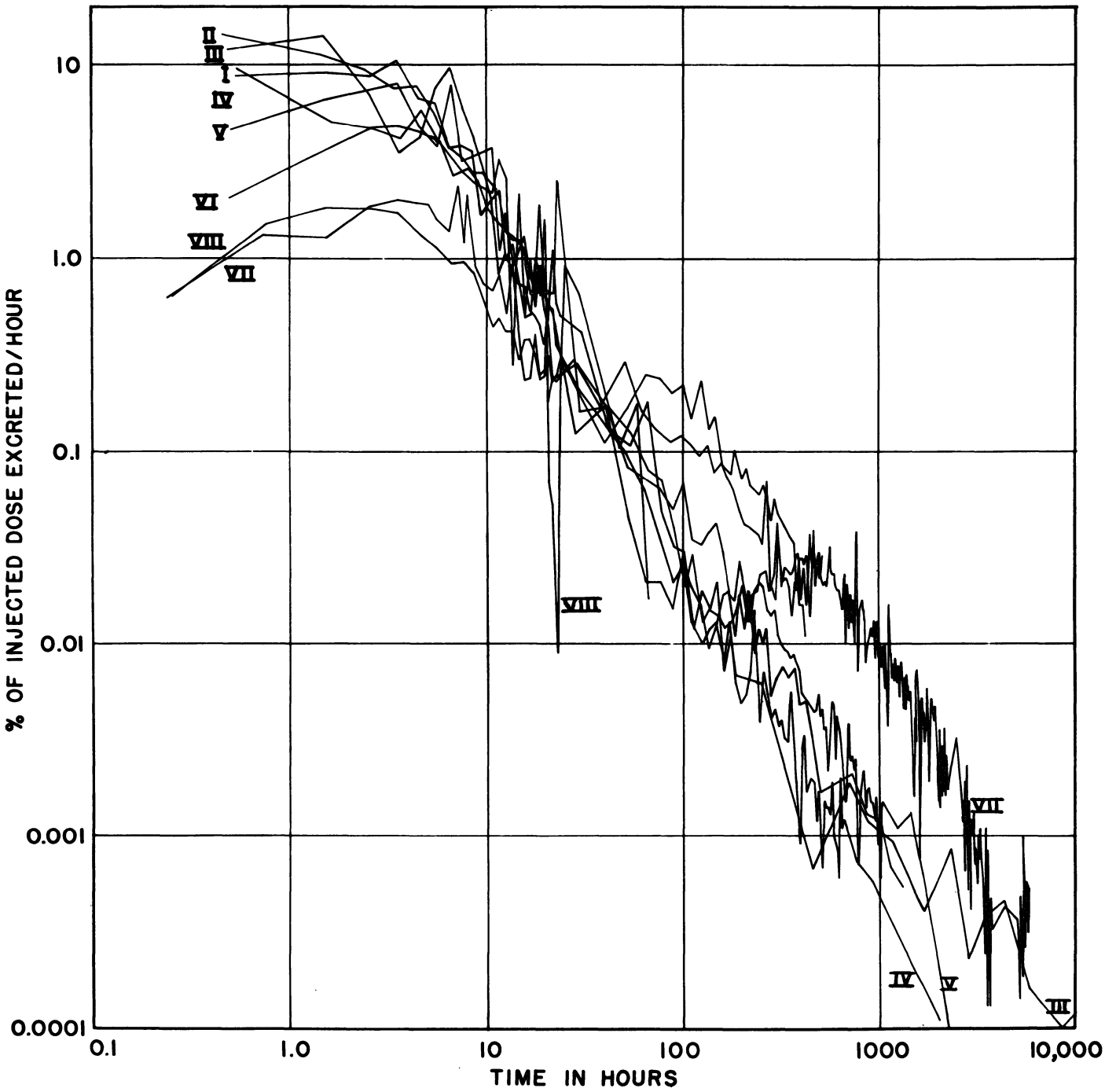

Figure 4. URINARY RATE OF EXCRETION FOR 8 TERMINAL BRAIN TUMOR PATIENTS FOLLOWING INTRAVENOUS INJECTION

INJECTION: $UO_2(NO_3)_2 \cdot 6H_2O$

EXPIRATION TIME IN DAYS		2.5	18	74	139	566
ORGAN OR TISSUE	GRAMS					
BONE	7,000	10.0	4.9	1.4	0.6	1.3
KIDNEY	300	16.6	7.2	0.7	1.2	0.4
MUSCLE	30,000	1.2	2.1	0.9	0.3	0.06
SKIN AND SUBCUTANEOUS TISSUES	6,100	1.8	1.0	0.1	0.06	-----
FAT	10,000	0.6	0.6	-----	-----	0.04
RED MARROW	1,500	-----	-----	0.02	0.03	0.1
YELLOW MARROW	1,500	-----	-----	-----	-----	-----
BLOOD	5,400	1.0	0.2	0.005	0.002	0.004
LOWER LARGE INTESTINE	150	-----	-----	-----	-----	-----
STOMACH	250	0.88	0.02	0.003	0.001	0.001
SMALL INTESTINE	1,100	0.2	0.2	0.03	0.01	0.006
UPPER LARGE INTESTINE	135	-----	-----	-----	-----	-----
LIVER	1,700	1.8	1.1	0.2	0.2	0.05
BRAIN	1,500	-----	-----	-----	-----	-----
LUNGS	1,000	0.5	0.4	0.03	0.02	0.008
LYMPHOID TISSUE	700	-----	-----	-----	-----	-----
HEART	300	0.06	0.02	0.003	0.006	0.002
SPLEEN	300	0.6	0.2	0.1	0.02	0.006
URINARY BLADDER	150	0.03	-----	0.002	0.001	0.0003
PANCREAS	70	0.7	0.008	0.008	0.0006	0.0004
SALIVARY GLANDS	50	-----	-----	-----	-----	-----
TESTES	40	-----	0.01	0.008	0.002	0.002
SPINAL CORD	30	-----	-----	-----	-----	-----
EYES	30	-----	-----	-----	-----	-----
THYROID GLAND	20	-----	0.003	0.0002	0.0001	0.0002
TEETH	20	-----	-----	-----	-----	-----
PROSTATE GLAND	20	-----	0.003	0.0004	0.0004	0.0001
ADRENAL GLAND	20	0.02	0.01	0.003	0.001	0.0004
THYMUS	10	-----	-----	-----	-----	-----
MISC. TISSUES (BLOOD VESSELS, CARTILAGE, NERVES, ETC.)	390	0.3	0.2	0.04	0.002	0.002
URINE (% OF DOSE ACCUMULATED)		61	63	92	84	98.2
BODY CONTENT = 100 - % IN URINE		39	37	8	16	1.8
TOTAL IN TISSUES						

Figure 5. PERCENT OF INJECTED DOSE PER STANDARD MAN ORGAN OR TISSUE FOR 5 TERMINAL BRAIN TUMOR PATIENTS

These human findings can be compared with the results of small animal experiments. The notable differences are:

1. In small animals, U(VI) is stored chiefly in bone. From the human data it can be seen that bone and kidney store identical amounts of uranium.

2. The biological half-life for uranium in rat kidney is ~4 to 6 days. From these data, averaged over a 70-year period, the biological half-life is 300 days.

3. The disappearance of U(VI) and U(IV) from the bloodstream of humans is slower. In rats, 99 percent disappears in as little as 2 hours. Our data reveal that 20 hours are required.

4. In rats, two-thirds of the injected uranium is excreted in 24 hours. On the average, 70 percent is excreted by these patients. However, a correlation with dose appears to exist. Fifty percent of the injected dose is excreted when 50 mgms are injected; 84 percent when 4 mgms are injected.

5. Small animals, when injected with tetravalent salts of uranium, excrete sizeable amounts, 40 percent of the injected dose, in feces. Humans excrete negligible amounts via the G.I. tract.

We have attempted analysis of this dynamic process of distribution and excretion of U(VI) with a linear model shown in Figure 6. This model was based on small animal distribution and excretion data. It permits one to obtain estimates of the amounts of uranium in the chief organs as a function of time. The procedure for its application is to fit the excretion data with 3 exponential terms, thereby determining the parameters of the distribution. This model has been applied to the distribution and excretion data of the second patient in order to illustrate its use. The results of this application appear in Figure 7. Two curves band the excretion measurements to include the error in estimating the parameters. When these 2 sets of parameters are operated upon with the procedure dictated by this linear model, the percent of injected dose may be estimated for the organs. Note in Figure 8 that the model underestimates the percent of injected dose appearing in the kidneys.

This model is presently being modified to give closer agreement with these human experimental results. It appears that better agreement with the experimental data will be obtained by incorporating a mechanism to simulate the diffusible-non-diffusible complex formation in the bloodstream and also to include a pathway from kidney back to blood, thereby simulating reabsorption from the tubules. These modifications are presently being made.

The power function model has been applied to these human data. The excretion measurements were expressed in terms of fraction of injected dose excreted per hour and plotted versus hours. The best fitting equation was found by least squares to be $0.343\ t^{-3/2}$. Figure 9 shows the excretion measurements plotted together with the 95 percent confidence limit of the power function. The outermost confidence limits correspond to the error in a single measurement, while the innermost limits are those for an average measurement. Note that there is a large error associated with a single measurement. The range is wide; a factor of 10 defines the ratio of the upper to the lower limit.

Integrating the excretion equation from time t to infinity yields $0.14\ t^{-1/2}$ (days), the equation for retention in the body. An interesting point for concern arises when we compare this power function estimate with the measured retention. We define measured retention in the body as the difference between the amount excreted and the amount injected. Figure 10 shows the graph of the measured retention for the patients plotted versus the time they expired, together with the power function estimate. Also plotted on this graph is the percent of injected dose in kidneys and bones of the patients. It can be seen that the power function estimate of retention agrees more closely with the organ burdens than with the measured retention values. The greatest discrepancy occurs

UNCLASSIFIED
ORNL-LR-DWG 5816A

Figure 6

THE MODEL:

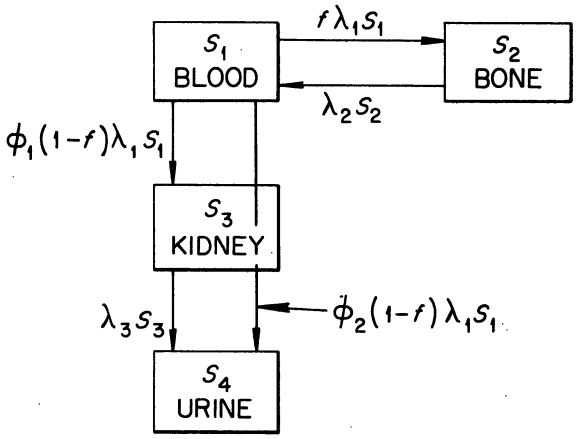

THE DIFFERENTIAL EQUATIONS:

BLOOD

$$\frac{dS_1}{dt} = \lambda_2 S_2 - \lambda_1 S_1$$

BONES

$$\frac{dS_2}{dt} = f\lambda_1 S_1 - \lambda_2 S_2$$

KIDNEY

$$\frac{dS_3}{dt} = \phi_1(1-f)\lambda_1 S_1 - \lambda_3 S_3$$

URINE

$$\frac{dS_4}{dt} = \phi_2(1-f)\lambda_1 S_1 + \lambda_3 S_3$$

THE INTEGRATED EQUATIONS:

BLOOD

$$S_1(t) = \frac{I}{\mu_2-\mu_1}\left[(\mu_2-\lambda_1)\epsilon^{-\mu_1 t} + (\lambda_1-\mu_1)\epsilon^{-\mu_2 t}\right]$$

BONES

$$S_2(t) = \frac{f\lambda_1 I}{\mu_2-\mu_1}\left[\epsilon^{-\mu_1 t} - \epsilon^{-\mu_2 t}\right]$$

KIDNEY

$$S_3(t) = \frac{\phi_1(1-f)\lambda_1 I}{\mu_2-\mu_1}\left[\frac{\mu_2-\lambda_1}{\lambda_3-\mu_1}\epsilon^{-\mu_1 t} + \frac{\lambda_1-\mu_1}{\lambda_3-\mu_2}\epsilon^{-\mu_2 t} + \frac{(\lambda_2-\lambda_3)(\mu_2-\mu_1)}{(\lambda_3-\mu_1)(\lambda_3-\mu_2)}\epsilon^{-\lambda_3 t}\right]$$

URINE

$$S_4(t) = I - \frac{(1-f)\lambda_1 I}{\mu_2-\mu_1}\left[\frac{(\mu_2-\lambda_1)(\lambda_3-\phi_2\mu_1)}{\mu_1(\lambda_3-\mu_1)}\epsilon^{-\mu_1 t} + \frac{(\lambda_1-\mu_1)(\lambda_3-\phi_2\mu_2)}{\mu_2(\lambda_3-\mu_2)}\epsilon^{-\mu_2 t} + \frac{\phi_1(\mu_2-\mu_1)(\lambda_2-\lambda_3)}{(\lambda_3-\mu_1)(\lambda_3-\mu_2)}\epsilon^{-\lambda_3 t}\right]$$

APPLICATION OF MODEL:

GIVEN AN EXCRETION EQUATION

$$\text{URINE} = I - \Sigma_1^3 a_i \epsilon^{-\alpha_i t} \qquad \text{WHERE } \Sigma_1^3 a_i = I$$

THE ROOTS OF

$$x^2 - \Sigma_1^3\left(\frac{1-\frac{a_i}{I}}{\alpha_i}\right)x + \frac{\Sigma_1^3 \alpha_i \frac{a_i}{I}}{\pi\alpha_i} = 0$$

ARE $1/\lambda_2$ AND ϕ_2/λ_3, WITH $\mu_1 < \lambda_3 < \mu_2$

$$\lambda_1 = \mu_1 + \mu_2 - \lambda_2$$

$$(1-f) = \frac{\mu_1\mu_2}{\lambda_1\lambda_2}$$

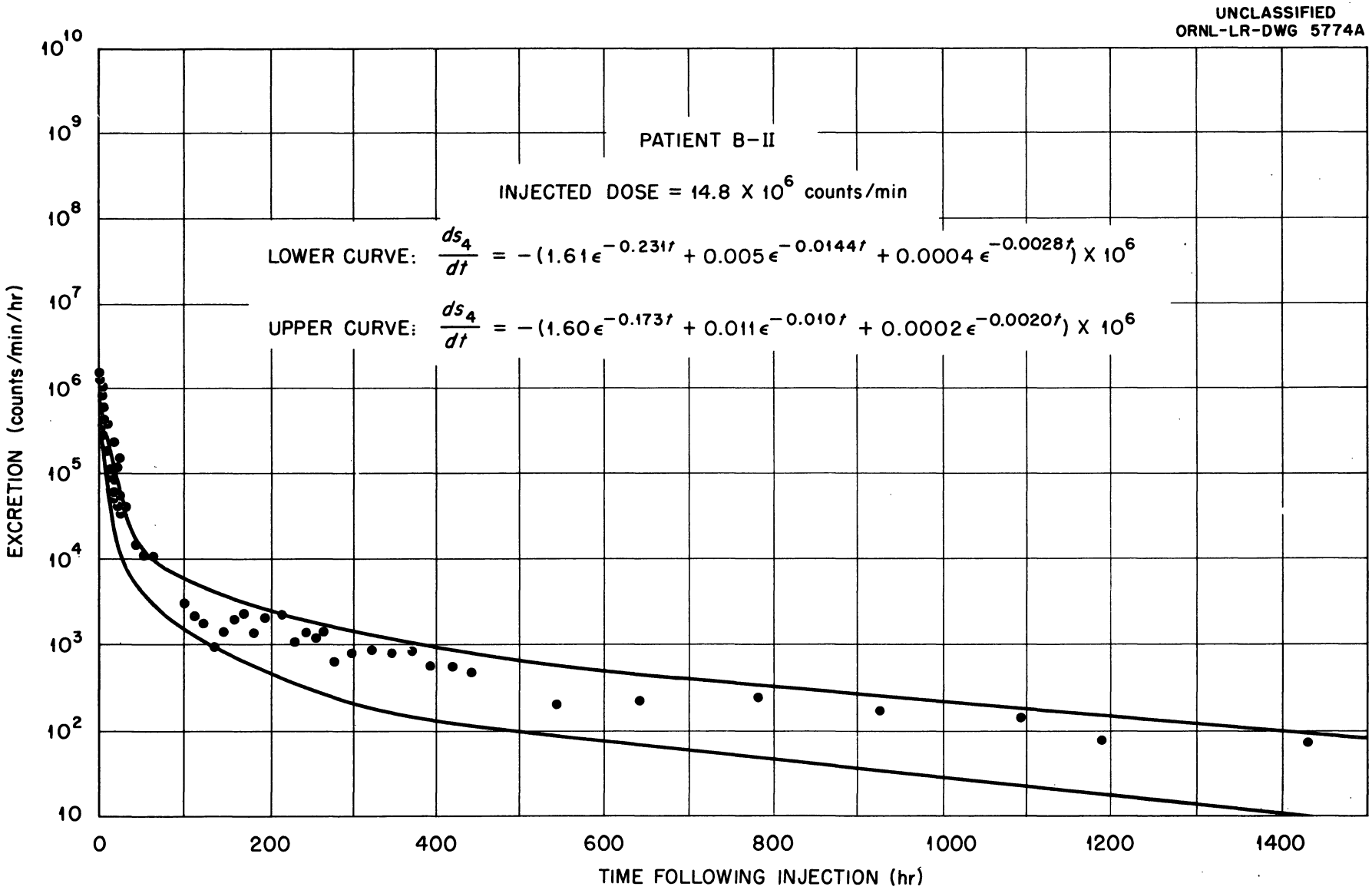
UNCLASSIFIED
ORNL-LR-DWG 5774A
PATIENT B-II
INJECTED DOSE = 14.8 X 10^6 counts/min
LOWER CURVE: ds4/dt = -(1.61e^-0.231t + 0.005e^-0.0144t + 0.0004e^-0.0028t) X 10^6
UPPER CURVE: ds4/dt = -(1.60e^-0.173t + 0.011e^-0.010t + 0.0002e^-0.0020t) X 10^6
EXCRETION (counts/min/hr)
10^10
10^9
10^8
10^7
10^6
10^5
10^4
10^3
10^2
10
0
200
400
600
800
1000
1200
1400
TIME FOLLOWING INJECTION (hr)

Figure 7

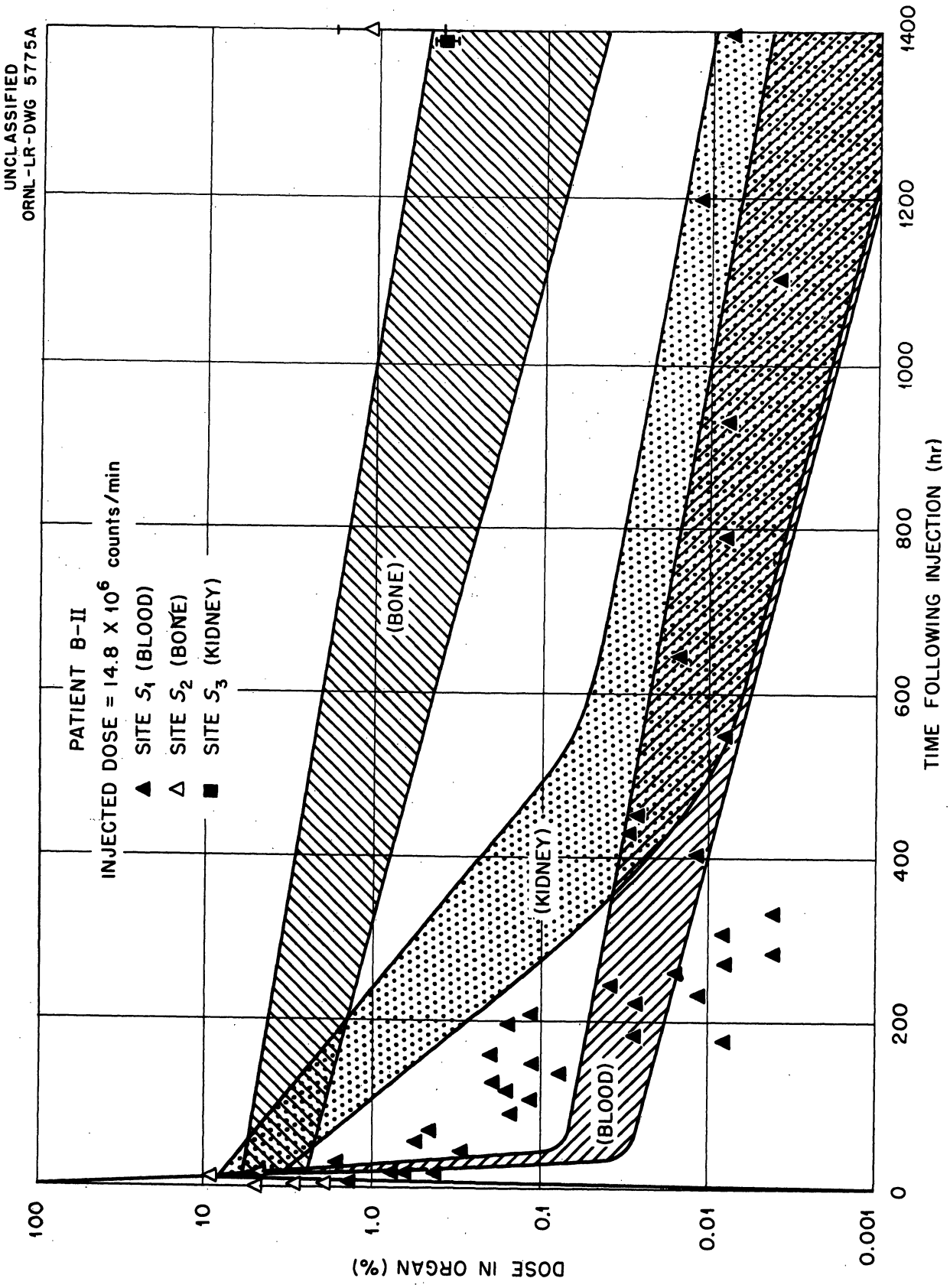
UNCLASSIFIED
ORNL-LR-DWG 5775A
PATIENT B-II
INJECTED DOSE = 14.8 X 10^6 counts/min
SITE S1 (BLOOD)
SITE S2 (BONE)
SITE S3 (KIDNEY)
(BONE)
(KIDNEY)
(BLOOD)
DOSE IN ORGAN (%)
100
10
1.0
0.1
0.01
0.001
0
200
400
600
800
1000
1200
1400
TIME FOLLOWING INJECTION (hr)

Figure 8

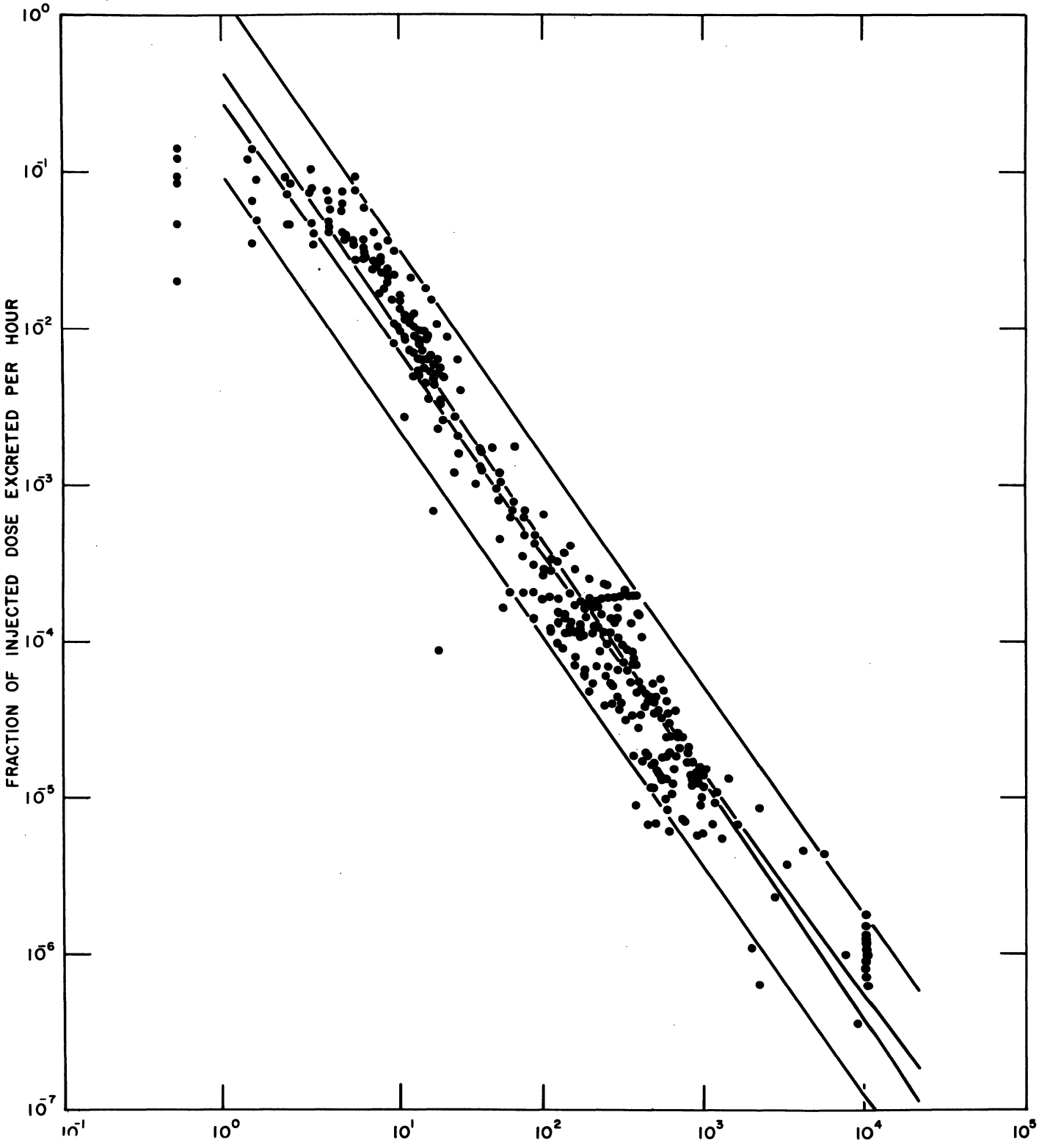

Figure 9. FRACTION OF INJECTED DOSE EXCRETED PER HOUR FOR 6 TERMINAL BRAIN TUMOR PATIENTS

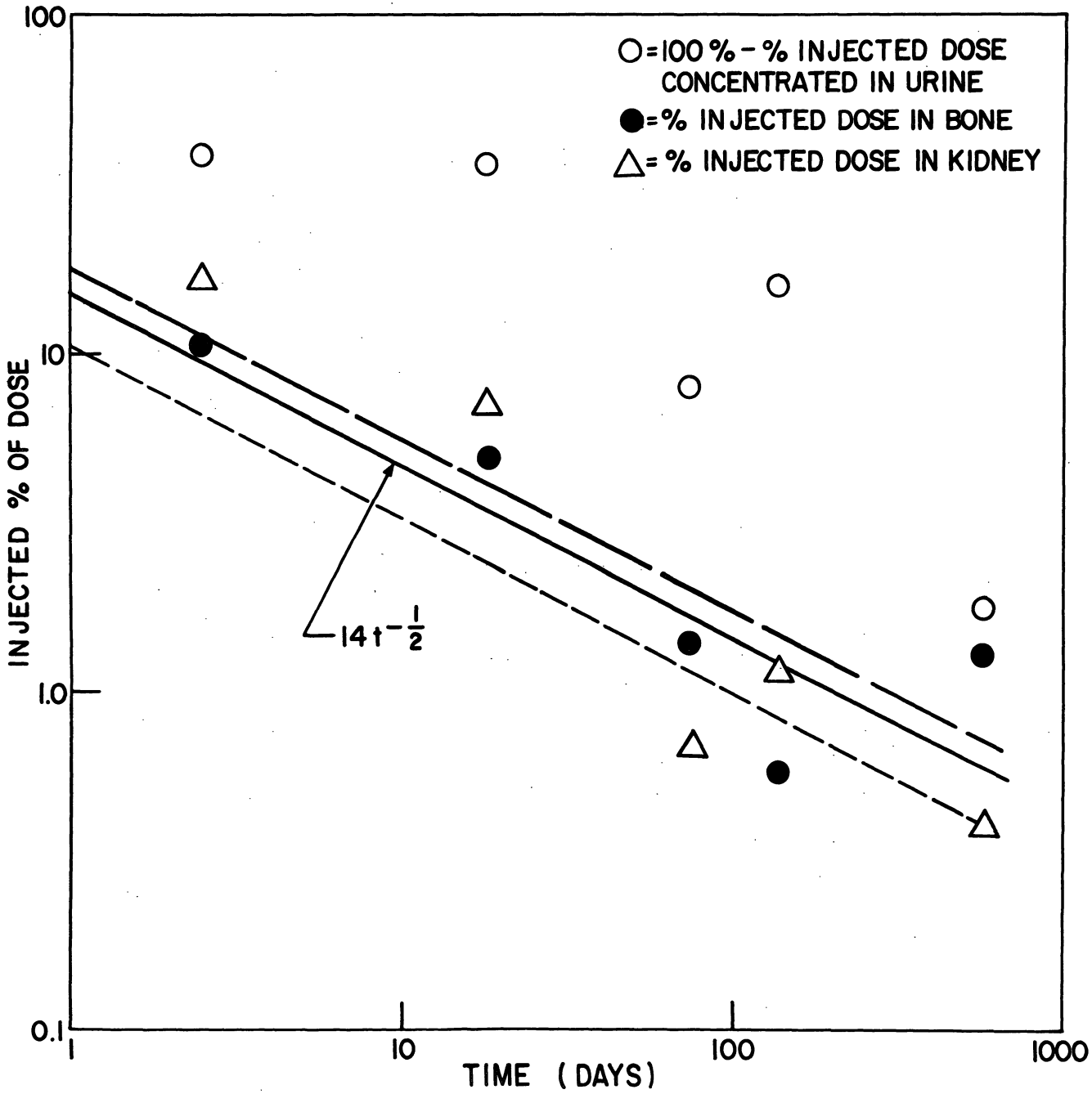

Figure 10. COMPARISON BETWEEN CALCULATED AND MEASURED BODY BURDEN AND ORGAN BURDEN

before 200 days have elapsed. At 2.5 days the measured value for Patient I is 36 percent while the estimated value is 10 percent; at 18 days the measured value is 39 percent, in poor agreement with the estimated value of $\sim$4 percent; and so on. At 566 days, the best agreement is demonstrated. The measured retention here is 1.8 percent (Patient III), while the estimated value is $\sim$0.6 percent. It is believed that the disparity is a result of the different elimination patterns shown by each patient, which in turn can be correlated with the size of the dose injected.

Since the power function estimates the burdens of kidneys and bones with little disparity, it may be used for calculations of MPC's via the method of Norris, et al.[1] Figure 11 shows some tentative MPC values for air and urine. On the left side MPC's for air appear and to the right is the value for urine. The equations for retention in the critical organ, R (t) for a single injection and excretion from the body for a single injection appear at the top of Figure 11. To convert these into continued injection, one multiplies the equations by the differential time, integrates from t = 1 day to t days, adds to this the fraction in the organ at day 0, and multiplies the whole expression by the continuous inhalation level. This obtains qf_2, the number of μc in the critical organ which delivers 0.3 rem/wk to it. Substituting for qf_2 the value 0.006 μc and solving for MPC at 10^4 days, we get 2×10^{-4} μc/day; and converting to inhalation exposure, we get 4×10^{-11} μc/cc, which agrees closely with the current value of 3×10^{-11} μc/cc.[2]

To calculate the permissible excretion level the same procedure is followed, yielding 355 d/m/day, which is higher than the currently employed value of 70 d/m/day. Thus, a factor of 5 is indicated.

In summary, we can say that

1. The critical organ for radiation insult from storage of enriched uranium is the kidney when exposure is to a soluble substance.

2. The disappearance of uranium from the body shows a slight dependence upon the amount injected into the bloodstream.

3. The urinary excretion data can be described using the power function law. Integration of this function yields the retention as a funtion of time. The calculated retention agrees more closely with the retention in the critical organ than with retention in the body.

4. A tentative MPC for exposure to soluble compounds is calculated to be 4×10^{-11} μc/cc on the basis of the power function equation.

5. A tentative MPC for urine is calculated using the power function law. The calculated value is 355 d/m/day, a factor of 5 greater than the present value employed, thereby indicating a margin of safety for exposure to soluble compounds.

ACKNOWLEDGMENTS

We wish to acknowledge the technical assistance of N. L. Gillum and G. J. Dodson who performed numerous chemical analyses.

AIR	URINE
EQUATION FOR SINGLE INJECTION	
$R(t) = 0.14\,t^{-1/2}$	$E(t) = 0.07\,t^{-3/2}$
EQUATION FOR CONTINUOUS INJECTION	
$\int_1^t R(t)\,dt = q = MPC\left[0.14\int_1^t t^{-1/2}\,dt + 0.14\right]$	$\int_1^t E(t)\,dt = MPC\left[0.07\int_1^t t^{-3/2}\,dt + 0.69\right]$
$q = MPC\left[0.28\,(t^{1/2} - 1) + 0.14\right]$	$= MPC\left[0.83 - 0.14\,t^{-1/2}\right]$
$q = 0.006\ \mu c$ FOR KIDNEY	
$\therefore\ MPC = \dfrac{0.006}{\left[0.28\,(t^{1/2} - 1) + 0.14\right]}$	
$= 2 \times 10^{-4}\ \dfrac{\mu c}{DAY}$	$= 2 \times 10^{-4}\ \dfrac{\mu c}{DAY}\left[0.83 - 0.14\,t^{-1/2}\right]$
AT $t = 10^4$ DAYS	AT $t = 1$
	EXCRETION $= 1.4 \times 10^{-4}\ \dfrac{\mu c}{DAY}$, AT $t = 10^4$
$MPC)_a = 4 \times 10^{-11}\ \dfrac{\mu c}{cc}$	
CURRENTLY ACCEPTED $MPC)_a$ IS $3 \times 10^{-11}\ \mu c/cc$	EXCRETION $= 1.6 \times 10^{-4}\ \dfrac{\mu c}{DAY} = 355\ \dfrac{d/m}{DAY}$

Figure 11. TENTATIVE MPC VALUES

BIBLIOGRAPHY

1. Norris, W. P., T. W. Speckman, and P. F. Gustafson. "Studies of the Metabolism of Radium in Man." Am. J. Roentgenology, Radium Therapy and Nuclear Medicine, Vol. 73:785-802, May, 1955.

2. Recommendations of the International Commission on Radiological Protection. Supplement No. 6 (Revised December 1, 1954). British Journal of Radiology. Published by British Institute of Radiology, London, 1955.

CORRELATION BETWEEN URANIUM AIR DUST SURVEYS AND URANIUM URINE DATA

R. L. Hoover*

National Lead Company of Ohio
Cincinnati, Ohio

(*Presently with Combustion Engineering, Inc., Windsor, Connecticut)

In assessing air dust problems associated with the handling of uranium at the National Lead Company of Ohio, it has been found that there is good correlation between air dust levels and uranium urine data.

METHODS

In taking air dust samples, the Industrial Hygiene and Radiation Department uses the Hudson pump or Gast pump modified to accommodate a 1 1/8 inch diameter Whatman No. 41 filter paper. A complete survey is made in each area every 4 months and, in addition, periodic checks are made when the urine program indicates a need for further surveys or when there has been a known release of uranium. There are 2 types of samples taken: general air samples, which give indications of the amount of air-borne material in the particular area monitored; and breathing zone samples of a specified job, which give indications of the levels of uranium to which an individual would be exposed if a respirator were not worn. These samples are all counted in scintillation counters. In the case of air dust samples a tolerance of 70 $d/m/m^3$ is used.

The uranium urine program is divided into 3 types: Type 1, annual samples (actually these are samples taken from new employees and terminations, as well as during annual physicals); Type 2, periodic samples (taken daily, weekly, monthly, or quarterly); Type 3, the incident samples taken after a known release of uranium in a particular plant. These samples are analyzed fluorimetrically and 0.05 mg U/1 is considered as tolerance.

In collecting the periodic samples, an attempt is made to get an indication of body burden by taking the sample the morning after an employee has been away from work for at least 2 days.

In the case of incident urines, the employee involved is asked by his supervisor to void immediately after an exposure and to report to the Medical Department from 1 to 2 hours later to give his first sample. This sample is followed by 4 consecutive morning samples or until the man has dropped below tolerance.

RESULTS

There is good correlation between high air-borne activity present in incident exposures and the amount of uranium found in the urine of the employees involved. In order to point this out, 2 typical cases of incident exposures are presented.

Case No. 1 - The incident occurred when a cylinder of uranium hexafluoride leaked because the valve on the cylinder was not properly closed. Individuals 1, 2, and 3 were in the fumes for the longest period of time. Number 2 finally froze the line with a CO_2 fire extinguisher.

In the first case the results are compromised somewhat because of poor air dust measurements. However, the health physicist investigating the incident was able to calculate the relative exposure of the 6 men involved prior to obtaining the urine results (Table 1).

TABLE 1

EXPOSURE TO URANIUM DUST

Name	Daily Urine Sample	Relative Exposure	Urine Data mg U/1
1	1	Heavy	2.6
	2		0.6
	3		0.67
	4		0.005
2	1	Heavy	1.3
	2		0.064
	3		0.070
	4		0.014
3	1	Heavy	2.1
	2		0.05
	3		0.11
	4		0.005
4	1	Moderate	0.28
	2		0.013
	3		0.02
5	1	Moderate	0.110
	2		0.028
	3		0.048
	4		0.009
6	1	Light	0.013
	2		0.013
	3		0.005

None of the 6 men had been exposed previously to uranium.

Case No. 2 - This incident was caused when the top of a reactor was removed to break a salt cake plugging the reactor. UF_6 and some UF_4 were released when the feed lines were broken and as the reactor was cleaned. A vacuum hose from the central vacuum system was used in an attempt to exhaust the escaping material, but was not effective. Six men were exposed during the cleanout period. Air dust samples indicated that the general air was running 1,910 d/m/m^3 or 27.2 times the MAC (Table 2).

TABLE 2

EXPOSURE TO URANIUM AIR DUST

Name	Approximate Time Exposed - Hours	Relative Exposure	Daily Urine Sample	Urine Data mg U/1
1	2.0	Heavy	1	0.221
			2	0.073
			3	0.016
2	1.5	Heavy	1	0.16
			2	0.021
			3	0.009
3	2.0	Moderate	1	0.062
			2	0.07
			3	0.033
4	0.5	Moderate	1	0.053
			2	0.013
			3	n.d.
5	0.75	Moderate	1	0.044
			2	0.005
			3	0.008
6	0.5	Light	1	0.009
			2	0.005
			3	0.013

Previous to the exposure, all of the men involved were far below the 0.05 mg U/1 tolerance.

DISCUSSION

One can see that when an individual is exposed to an aerosol containing soluble uranium, his urine will readily indicate the exposure.

It has also been found that where the air dust surveys are above tolerance, the men working in the area show above tolerance uranium in their urine.

It should be pointed out, however, that a straight comparison between air dust surveys and uranium urine levels will not always indicate a direct correlation (without a thorough understanding of the situation). This is caused by the fact that certain variables must be taken into consideration. These include the use of respirators during certain high level operations, difficulty in getting breathing zone measurements, changes in the general working habits of an employee when the health physicist is in the area, particle size of the material collected, distribution of the particulate matter, and the difference in the rate of metabolism of soluble and insoluble uranium.

Because the health physicist or monitor responsible for an area cannot devote his entire time to taking air dust surveys, the employee working in the area becomes the most effective sampling device, and a good urine program will become beneficial to the health group assessing the air dust conditions existing in a particular area. Urine data have been useful in finding abnormal conditions, poor ventilation, careless working habits, and defective equipment.

Just recently the ventilation in a plant was found to be inadequate. The air dust surveys indicated that the personnel were working in levels of 70 $d/m/m^3$ or less. At the same time, the men from that plant showed above 0.05 mg U/1 in their urine on annual and periodic sampling. The poor correlation was caused by certain variables encountered in the dust sampling technique. It was found that the men working in the area used greater caution in handling the uranium when the monitor was taking his samples than when there was not a health physicist around, and that the particle size of the material might have been small enough to pass through the Whatman No. 41 filter paper. After a thorough investigation, the industrial hygiene group recommended that the hoods over the equipment be modified and that the ventilation in the hoods be improved. Since that time the urine data has indicated a downward trend.

On another occasion, a group of chemical operators working on a special job showed above tolerance uranium in their urine. Although there were no air dust samples taken, a health physics investigation revealed that these operators were not following the standard operating procedure and that large quantities of uranium dust were generated. The situation was brought to the attention of the foreman and the necessary steps were taken.

In conclusion it may be said that in assessing the air dust levels, the correlation between air dust surveys and uranium urine data is generally good. The uncontrolled variables in the air dust sampling program, however, as stated previously, have led to more reliance being placed on the uranium urine data.

NUCLEAR TRACK TECHNIQUE FOR LOW LEVEL PLUTONIUM IN URINE

L. C. Schwendiman and J. W. Healy

Hanford Atomic Products Operation
General Electric Company
Richland, Washington

Because of the low permissible body burden of plutonium, 0.6 microgram,[1] and the very low excretion rate, it is essential that sensitive methods be available to detect the element in urine. For an acute exposure of plutonium resulting in the maximum permissible body burden, only 4.2×10^{-5} μg (6d/m) per day will be excreted in the urine 100 days after the exposure. For incipient chronic intake which eventually results in a maximum permissible body burden, an even smaller quantity of plutonium is excreted per day because of the nearly complete immobilization of plutonium which occurs with time.

These considerations, and a belief that greater sensitivity, accuracy, and precision could be attained in the bioassay of human urine samples, prompted the undertaking of this work.

The routine procedure used prior to this development required the evaporation of the urine sample to dryness, muffling, and dissolution of remaining salts. Plutonium present was then precipitated with lanthanum as the fluoride. After solution of the lanthanum precipitate, thenoyltrifluoroacetone was used to chelate the plutonium now in the +IV oxidation state. The plutonium chelate was subsequently driven from the organic phase with 8N HNO_3, and the resulting acid evaporated to near dryness. Evaporation was continued to dryness after transfer of the acid to a 1 1/2 inch counting dish. Low background alpha counters were used to record the alpha particles entering the sensitive volume of the counter. The air chambers used were microphonic and much maintenance and operator time were required to keep the sets in control with low backgrounds. A counting time of up to 2 hours was needed to give a detection limit of about 0.4 d/m per sample.

Nuclear track emulsions were considered to replace the electronic counters as the alpha particle detector, since several of the disadvantages of the then currently used electronic detectors could thus be eliminated or minimized. As visualized, the analysis would separate the plutonium from the sample and deposit it uniformly onto a small disc. This disc would be held against the nuclear track emulsion for a period long enough to produce a significant number of alpha tracks upon development. These would then be counted by viewing the exposed area under a microscope. The quantity of plutonium present could then be calculated.

It was first necessary to develop a method for depositing the plutonium contained in the urine sample uniformly on to a small area. An electrodeposition procedure was devised in which plutonium was first oxidized in a basic medium, then electrodeposited on a 7 mm diameter area in the center of a 1/2 inch diameter stainless steel disc. In 1-2N KOH and in the presence of sodium hypochlorite, it was found that nearly quantitative recovery of $\mu\mu$c of plutonium was achieved. The muffling, lanthanum fluoride, and thenoyltrifluoroacetone method for prior separation of plutonium from urine was retained. Hydrochloric acid was substituted for 8N HNO_3 in the extraction, when it was found that nitrate ions caused low electrodeposition yields under the conditions employed.

This paper is based on work performed for the Atomic Energy Commission under Contract #W-31-109-Eng-52.

An electrodeposition cell was developed and multi-position equipment designed to permit simultaneous analysis of as many as 20 samples. Figure 1 shows the Lucite electrodeposition cell and Figure 2 the 20-sample electrodeposition apparatus developed.

The nuclear track emulsion used to record the alpha particle emission from the 7 mm areas is Kodak NTA emulsion 25μ thick on 1 by 3 inch microslides. A study was undertaken to determine optimum conditions for eradication of background latent tracks, exposure, processing, and reading the exposed slides.

As received, the emulsion contains latent track images from alpha-emitting impurities which will appear upon development. For the method to be sensitive, background must be extremely low. Background tracks in the emulsion can be effectively eradicated before development by exposing the emulsion to vapor from 0.3 percent hydrogen peroxide. Desiccation for 3 to 4 hours restores the original sensitivity of the film. A reduction of background by a factor of 10 is thus easily accomplished.

The latent image of a track in an emulsion will be destroyed over a period of time by the same processes which are deliberately accelerated in background eradication. High humidity and warmth are particularly deleterious to retention of the latent track image. It was found that imperceptible fading of latent images occurred in 8 weeks after exposure if the exposed emulsion was held at 5°C during the period following exposure.

Optimum developing time was determined to be 6 minutes in D-19 at 68°F ± 2°. Developing proceeds with no agitation. Fixing requires 45 minutes with agitation, and washing requires 1 hour.

A necessary part of the development was a device to support the 1/2 inch diameter discs against the emulsion. A "radioautographic camera," detailed in Figure 3, was constructed. All cameras used are identical and each permits the simultaneous exposure of 8 discs. The camera indexes the 1 by 3 inch slides in the same position occupied when it is mounted on the microscope stage for track counting. The coordinates of the disc centerlines are reproducible from slide to slide. The emulsion slides are loaded into the camera with as little exposure to safe light (Wratten Series OA) as possible in order to reduce to a minimum the single grain background.

After the discs have been exposed to the emulsion at 5°C for the exposure time, generally 1 week, the slides are removed and processed. A microscopic count of tracks is then made in the exposed areas of the emulsion. Dark field illumination is used. A 43X objective and 10X eyepiece are used, giving a total magnification of 430. Immersion oil is used between the condenser lens and the slide.

A scanning system of counting is employed. A rectangular reticule in the eyepiece delineates a 0.1 mm by 0.2 mm area of the emulsion. From the coordinates of the area to be examined, the lateral limits of the scan (4 mm long) are determined. A stop is positioned on the lateral traverse bar of the mechanical stage. This stop limits the motion of the stage to the length of the scan. A click-stop attachment permits the stage to be moved in 1/2 mm increments perpendicular to the lateral motion. These devices permit several traverses to be made on each exposed area; the total area scanned in the standard procedure is about 4 sq. mm. The number of tracks per sq. mm is thus determined and a conversion to d/m is made using exposure time, exposure area, and film efficiency. Urine spiked with a known quantity of plutonium and blank urine samples are analyzed with each group of samples to maintain control over the process. Film efficiency is also determined routinely by exposing the film to a source of known disintegration rate for a known time.

RESULTS

Figure 4 shows the frequency distribution of the number of tracks found in 3.8 sq. mm of emulsion for 545 blank urine samples analyzed by this procedure. The data fit the Poisson distribution reasonably well and it is assumed that samples with very little plutonium present will also fit

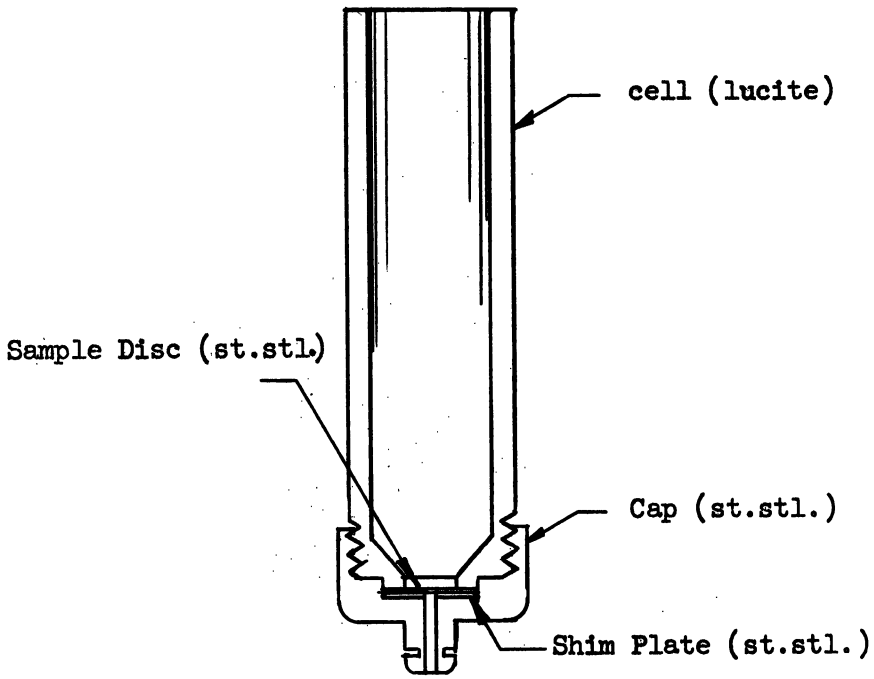

Figure 1. ELECTRODEPOSITION CELL ASSEMBLY-SECTION

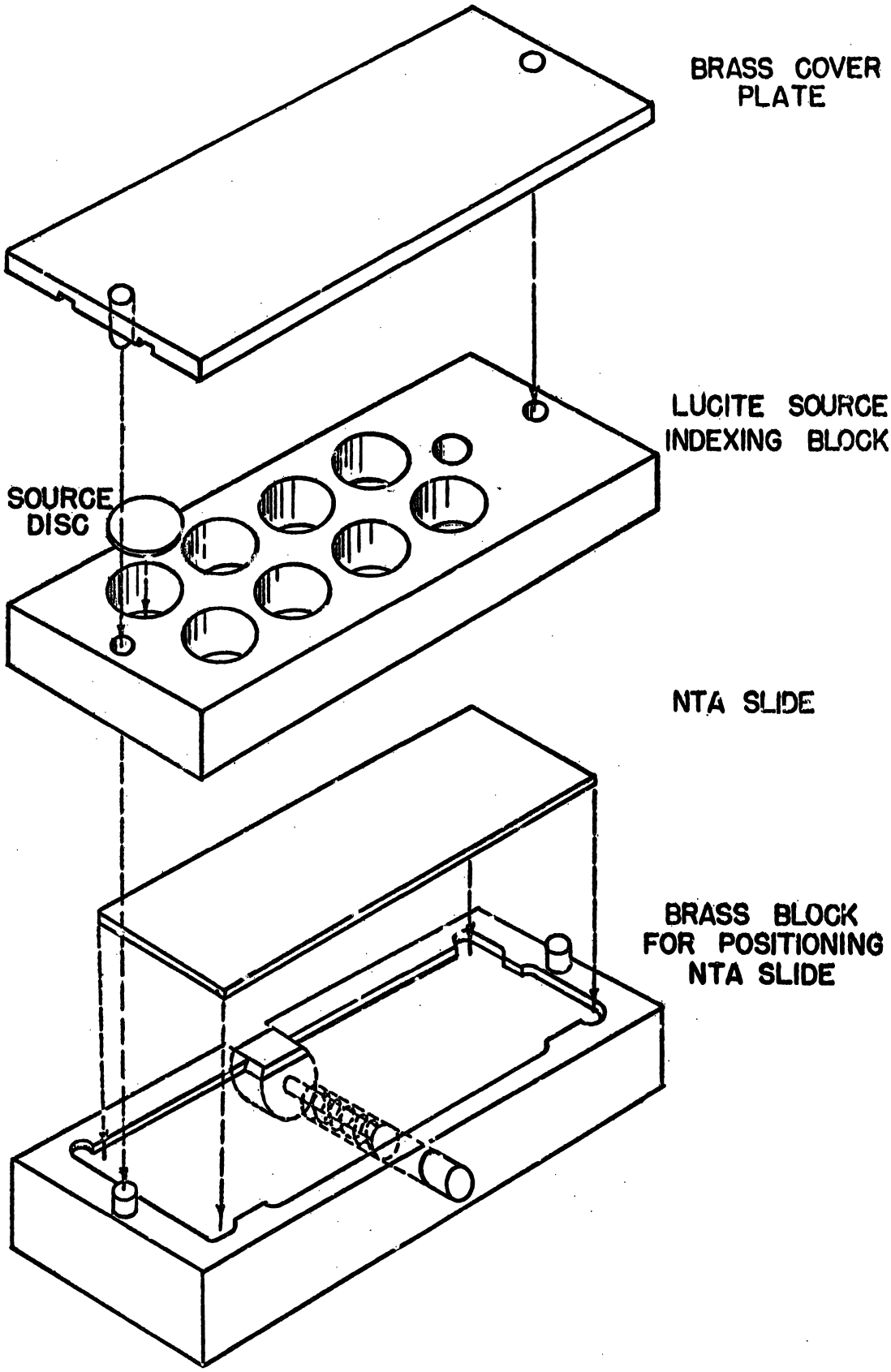

Figure 3. RADIOAUTOGRAPHIC CAMERA

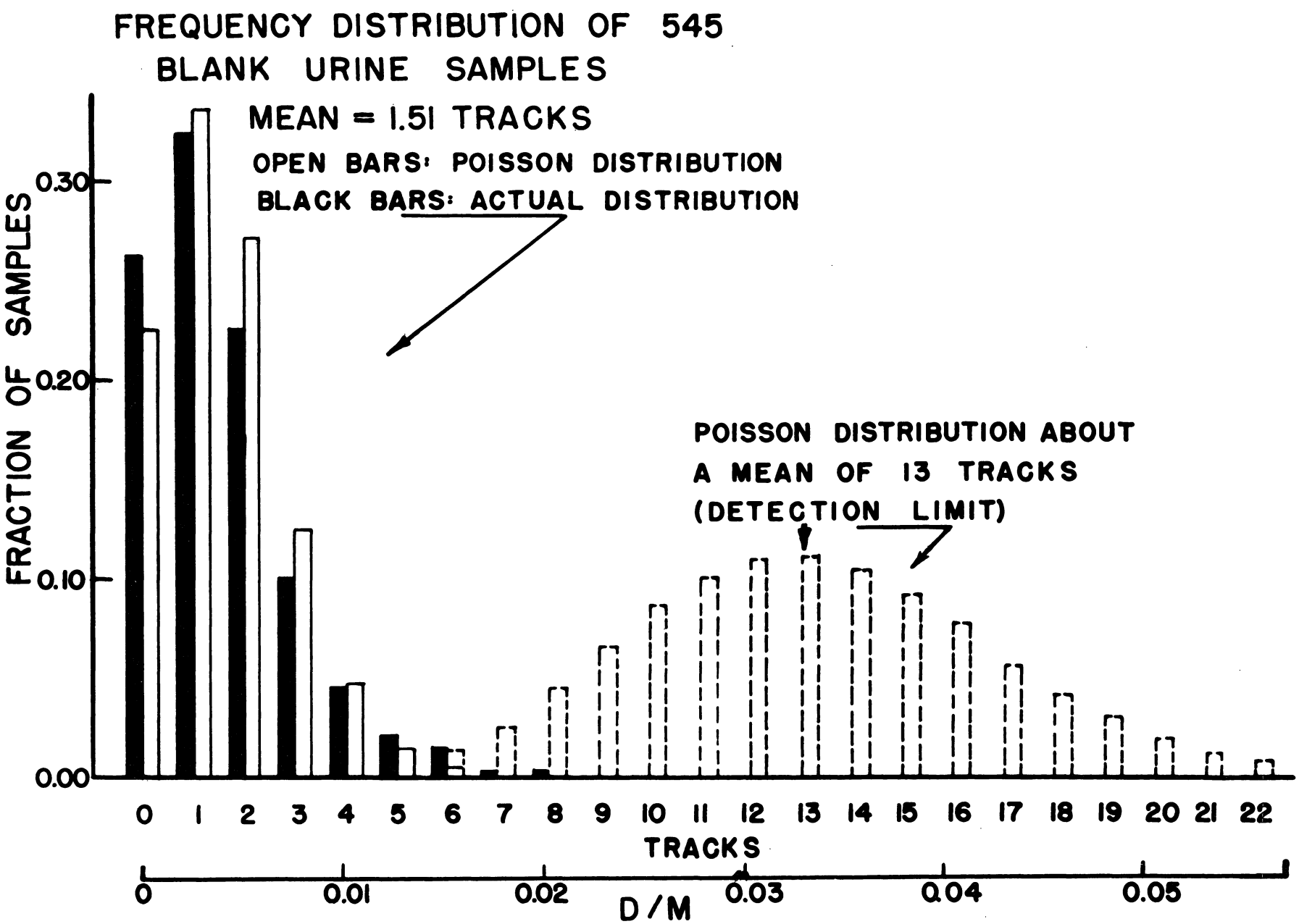

Figure 4. BLANK SAMPLE FREQUENCY DISTRIBUTION AND THE DETECTION LIMIT

the Poisson function. The detection limit is then defined as that average which has a lower 99 percent Poisson confidence limit equal to the upper 99 percent limit of the blank sample distribution. The data, which represents the blank samples analyzed from November, 1955, to April, 1956, indicate a detection limit of 0.035 d/m.

Figure 5 shows the result of the analysis of 553 samples, each spiked with 0.57 d/m of plutonium. These samples were analyzed concurrently with the regular bioassay urine samples. The plutonium solution is calibrated repeatedly using a PC-2A proportional alpha counter. The standard deviation of the 553 results shown is 12 percent. If only random variations from reading the tracks were present, a standard deviation of 7 percent should be demonstrated. The remaining variance results from all other random errors in the process. The long-time average of the over-all process yield is 89 percent, assuming a 50 percent emulsion geometry. Emulsion geometry will, in general, be slightly less than 50 percent, principally because of the inability of the microscopist to record tracks perpendicular to the plane of the emulsion.

The particular advantage of this method is that there is virtually no limit to its ultimate sensitivity, since by a combination of reducing source size and increasing the exposure time, almost any desired sensitivity should be obtained. Experiments have shown that electrodeposition on 1 and 2 mm diameter areas is feasible. Another advantage is the complete freedom from the unpredictable behavior of low background electronic counters, and their attendant high initial and subsequent maintenance costs.

For cases in which plutonium present in urine must be known within a very short time of the incident, the method described obviously is not useful. In these cases, however, the plutonium will appear in the urine in much higher concentrations because of the short delay between exposure and sample collection. For these cases the usual α-counting after a chemical separation is generally adequate. In a routine bioassay program designed to ferret out incipient plutonium exposures and identify such individuals, who may require work with less chronic exposure liability, this method has proved reliable, sensitive, and adequately precise. In this application the lag time required between sampling and recording of result is of little consequence.

SUMMARY

A method for analyzing urine samples for very small quantities of plutonium has been developed. The method requires evaporation of the urine sample, muffling, precipitation, and an extraction with thenoyltrifluoroacetone (TTA). The plutonium is subsequently electrodeposited on a 7 mm diameter area. The disc so prepared is held against a nuclear track emulsion for 168 hours. Techniques were perfected for preparing, processing, and microscopic examination of the emulsion. The detection limit of less than 0.05 d/m per sample currently achieved on a routine basis is low enough to permit early recognition of incipient plutonium deposition.

BIBLIOGRAPHY

1. "Maximum Permissible Amounts of Radioisotopes in the Human Body and Maximum Permissible Concentrations in Air and Water." NBS Handbook 52, March 20, 1953.

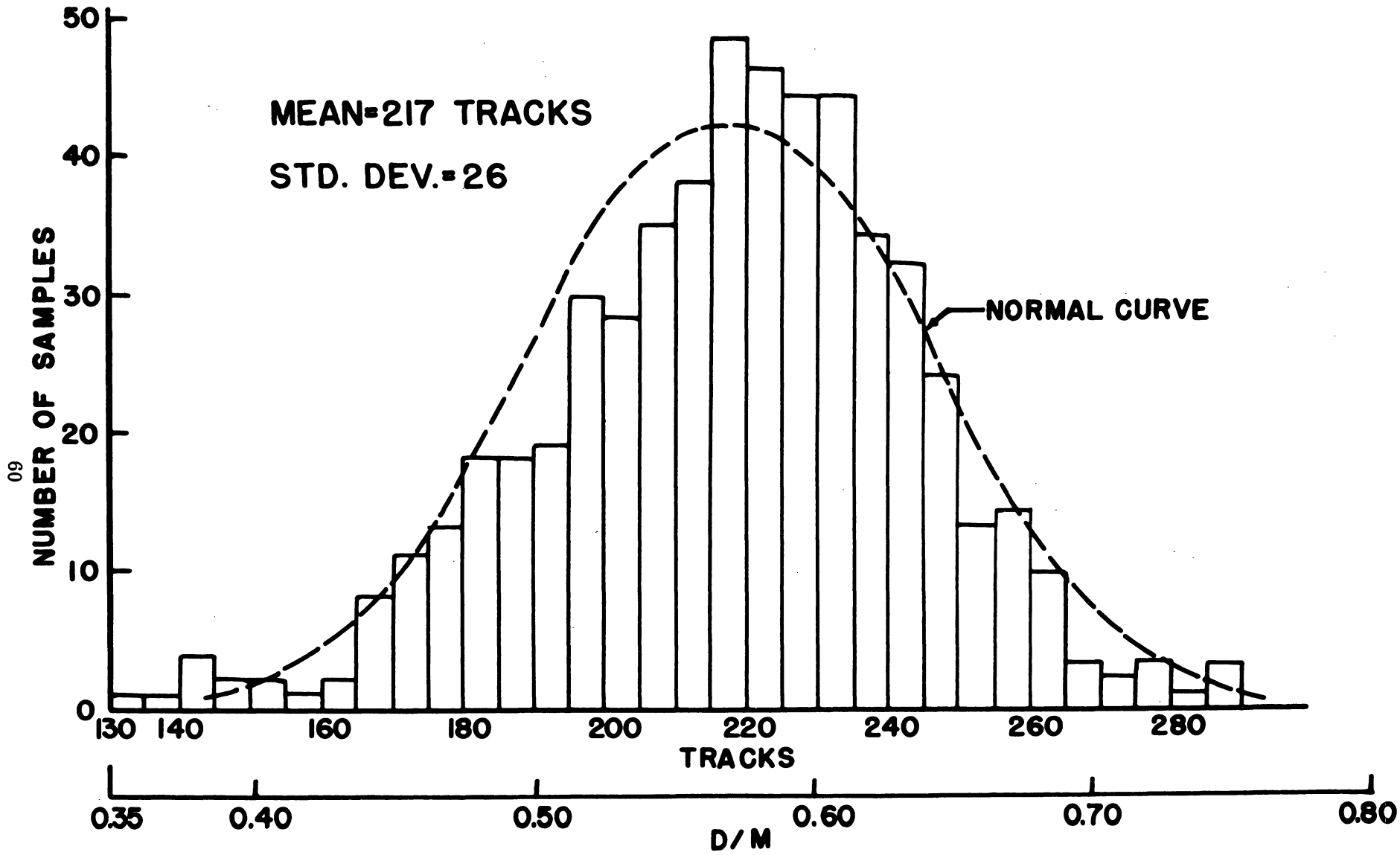

Figure 5. FREQUENCY DISTRIBUTION: 553 URINE SAMPLES SPIKED WITH 0.57 D/M PLUTONIUM

ACUTE UPTAKE OF PLUTONIUM AND URANIUM FOLLOWING WOUND CONTAMINATION

E. L. Geiger and S. M. Sanders, Jr.

Savannah River Plant
E. I. du Pont de Nemours and Company
Aiken, South Carolina

INTRODUCTION

Data accumulated as a result of accidental assimilation of plutonium and uranium can yield valuable information about the metabolism of these elements in the body and the rates of their excretion in the urine. Such data may represent more accurately the rates of elimination by healthy persons of average working age than data obtained from planned research projects with chronically ill or elderly patients. As more data are accumulated from accidental assimilation cases and planned research projects, a more accurate interpretation can be made of bioassay results. For this reason, data obtained in 2 accidental assimilation cases at the Savannah River Plant are presented here.

RESULTS AND DISCUSSION

Plutonium - The first case is that of an employee who received an acute uptake of plutonium as plutonyl nitrate in 4N nitric acid in a hand wound contamination incident.

Ninety-nine urine samples were collected over a 487-day period following the incident. Figure 1 shows an outline of the analytical procedure used to estimate the plutonium content of the urine samples. The plutonium was coprecipitated twice with bismuth phosphate and then twice with lanthanum fluoride. The plutonium was then solvent extracted, using thenoyltrifluoroacetone, leached from the solvent, and electroplated. The disc containing the plutonium was radioautographed and the alpha tracks were counted with the aid of a microprojector.

Some of the samples were collected after drugs had been administered intravenously. These injections caused material to be excreted that interfered with the procedure; therefore, some modifications were necessary for 26 percent of the samples.

Figure 2 shows the data obtained by urinalyses. The individual results are indicated by small circles. The second point is for a urine sample collected over a 3-day period. The third and fourth points are for urine samples collected over 2-day periods. All other points are for daily urine voids. The solid line is the function

$$Y = 141\ t^{-1.07} \text{ for } 11 \leq t \leq 487 \text{ days}$$

where Y = d/m of Pu that is excreted per day

t = time in days since the incident.

The equation was calculated by the least squares method using data from 11 to 487 days. The dashed line, given here for comparison, is the function

$$(1) \quad Y = 43\ t^{-0.77} \qquad 11 \leq t \leq 487 \text{ days}$$

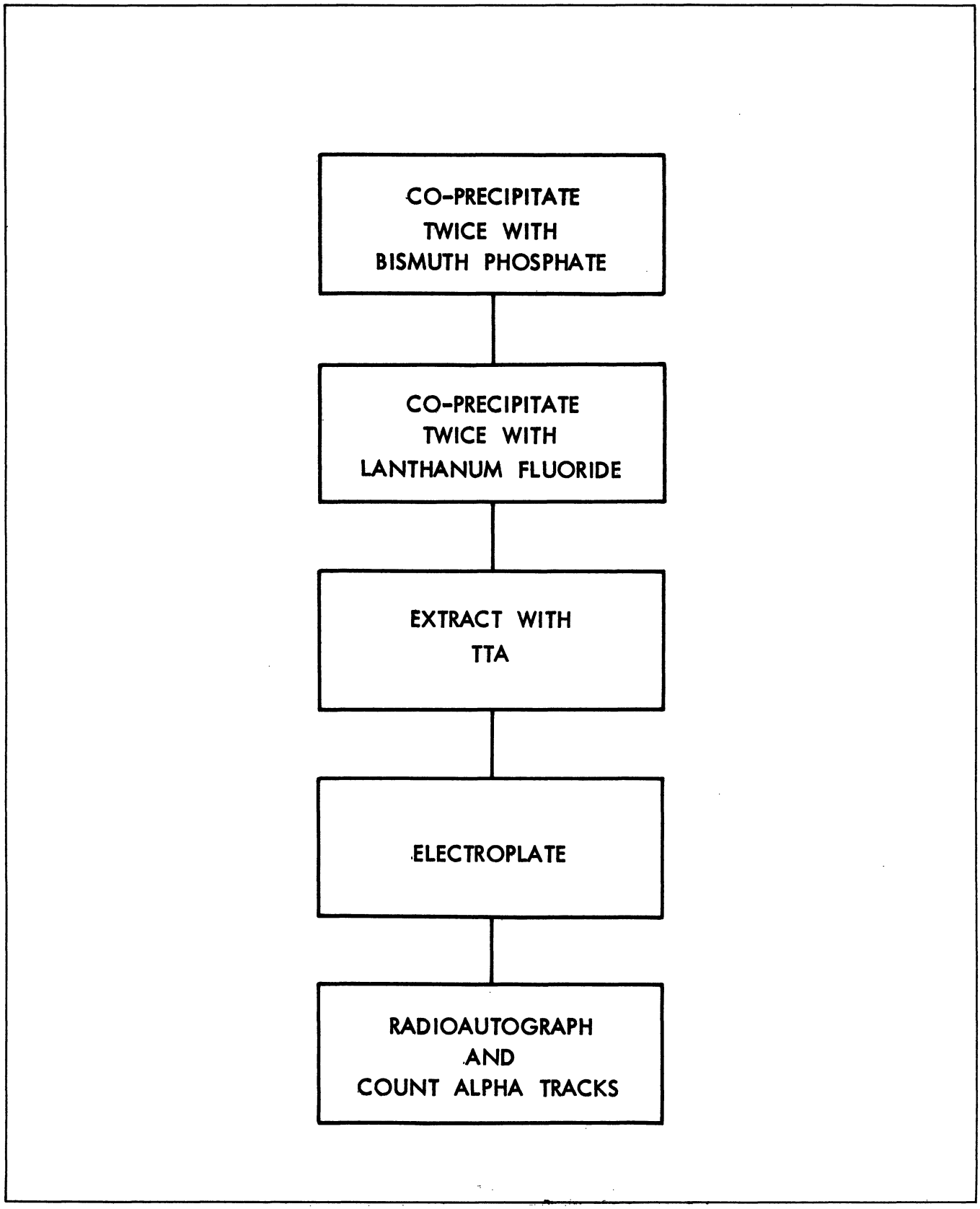

Figure 1. PLUTONIUM PROCEDURE

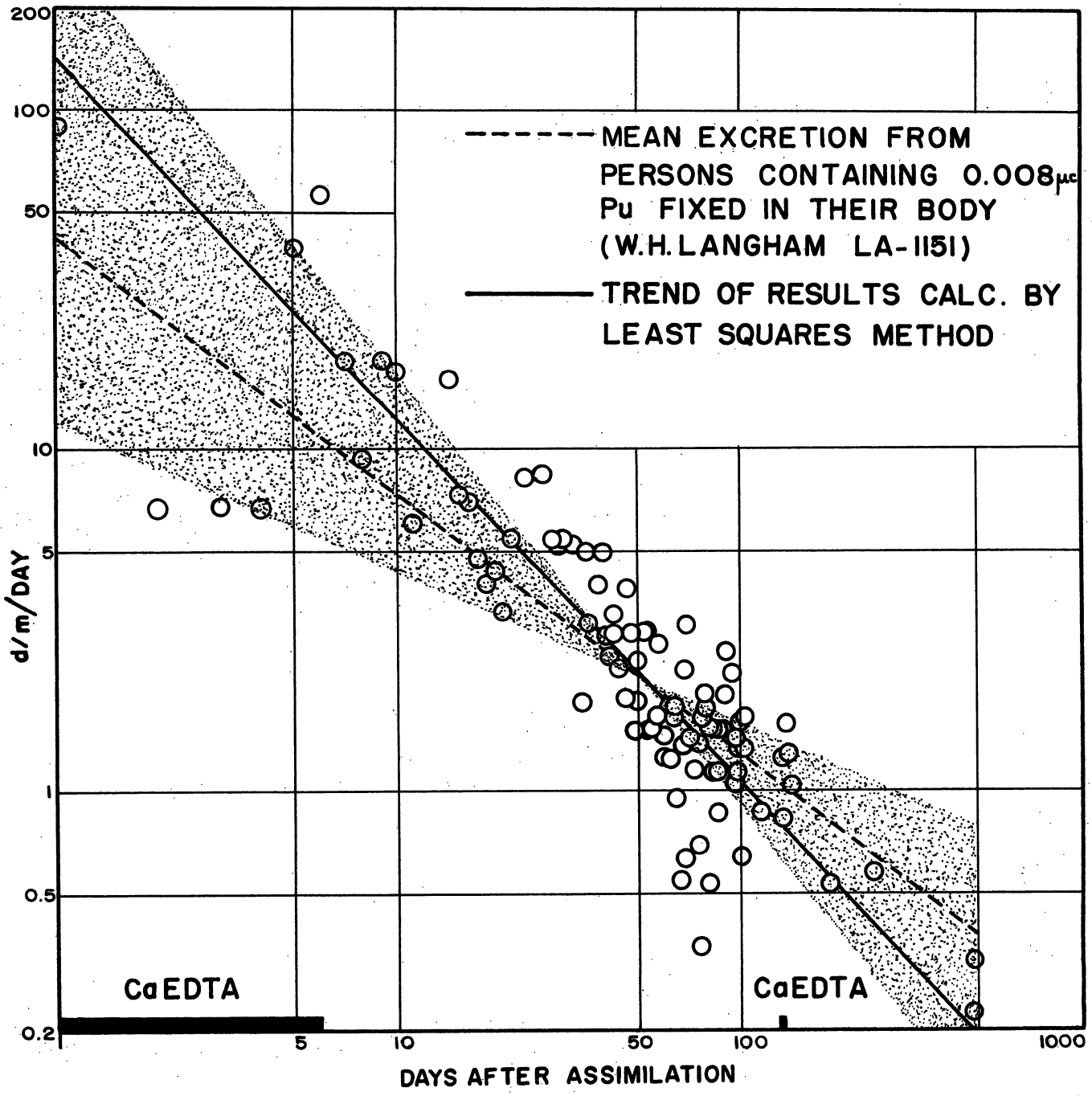

Figure 2. URINARY EXCRETION OF PLUTONIUM

Y and t have the same units as before. The latter expression was obtained by fitting the data to the equation, $Y = at^{-0.77}$, presented by Langham, et al.[1], as the general equation for the excretion of plutonium in urine.

Approximately 3 hours after the accident, 1.2 grams of zirconium in a citrate solution were administered intravenously. One gram of calcium disodium ethylenediaminetetracetate (Ca-EDTA) was administered intravenously the first and second days after assimilation of the plutonium. The Ca-EDTA treatment was repeated morning and evening of the third, fourth, fifth, and sixth days. These injections may have increased the excretion rate slightly, but not as much as the hundredfold increase observed by Foreman, Milligan, and Norwood[2] in a case at the Los Alamos Scientific Laboratory.

Their case involved a 40-year-old female technician who broke a flask containing plutonium nitrate in 1M nitric acid and received a 2 cm laceration across the base of her left thumb. Starting with the fifth day and continuing through the twenty-second day, the subject was given 2.5 grams of Ca-EDTA twice daily except on the ninth and the tenth days. This treatment produced a striking increase in plutonium excretion, particularly on the first day of administration, from a pretreatment level of 12 c/m to over 1,300 d/m. An extreme drop was also noted on the days when the treatment was not administered.

No comparable large increase was noted in the excretion rate of the Savannah River Plant employee after Ca-EDTA treatment. No sharp decrease in the excretion rate was noted when the treatment was stopped. Ca-EDTA was again administered on the 131st to 135th days after the accident. Here a possible twofold increase was observed, which falls very short of the increase observed in the case at Los Alamos.

The question arises as to whether the 2 curves shown in Figure 2 are significantly different. The -0.77 exponent of t given in the general equation (1) is the mean determined for several cases. The hatched area represents the distribution of these cases if plotted individually. The exponent of t for these cases ranged from -0.46 to -1.31. The dashed line is the mean. The solid line, which is the best fit for the Savannah River Plant data, varies no more from the mean than do some of the cases used to calculate the mean. The equation determined for the latter data was

$$Y = 141\, t^{-1.07} \pm 0.09.$$

The probability that $t^{-0.77}$ fits these data as well as $t^{-1.07}$ is only 1 in 1,000. This suggests that individual excretion rates may be different; however, it does not invalidate the use of a general equation to make early estimates of the internal exposure to plutonium.

Uranium - The second case is that of an employee who assimilated approximately 30 mg of uranium transdermal. This exposure resulted from the employee's being splashed about the legs with a hot acid solution of uranyl nitrate. He was given medical treatment for his burns, and all of his urine was collected for the first 30 hours. A 40-hour period followed during which no urine was collected. After the analysis of the first samples, the employee was placed on an around-the-clock sampling program. Within hours of the start of this program, his burns were diagnosed as third degree and he was hospitalized. With the exception of 2 days, complete daily urine voidings were collected through the fortieth day when the employee returned home.

Aliquots of the urine samples were analyzed by a fluorophotometric method. The results of these analyses are given in Figure 3.

The excretion rate decreased slowly for the first 9 days. Between the ninth and fifteenth days, however, the daily excretion rate dropped a hundredfold. From the fifteenth to the fortieth day the biological half-life for elimination was approximately 6 days.

The solid line, shown here for comparison, was taken from data reported earlier by S. R. Bernard and E. G. Struxness.[3,4] The curve represents the excretion observed for 2 brain tumor

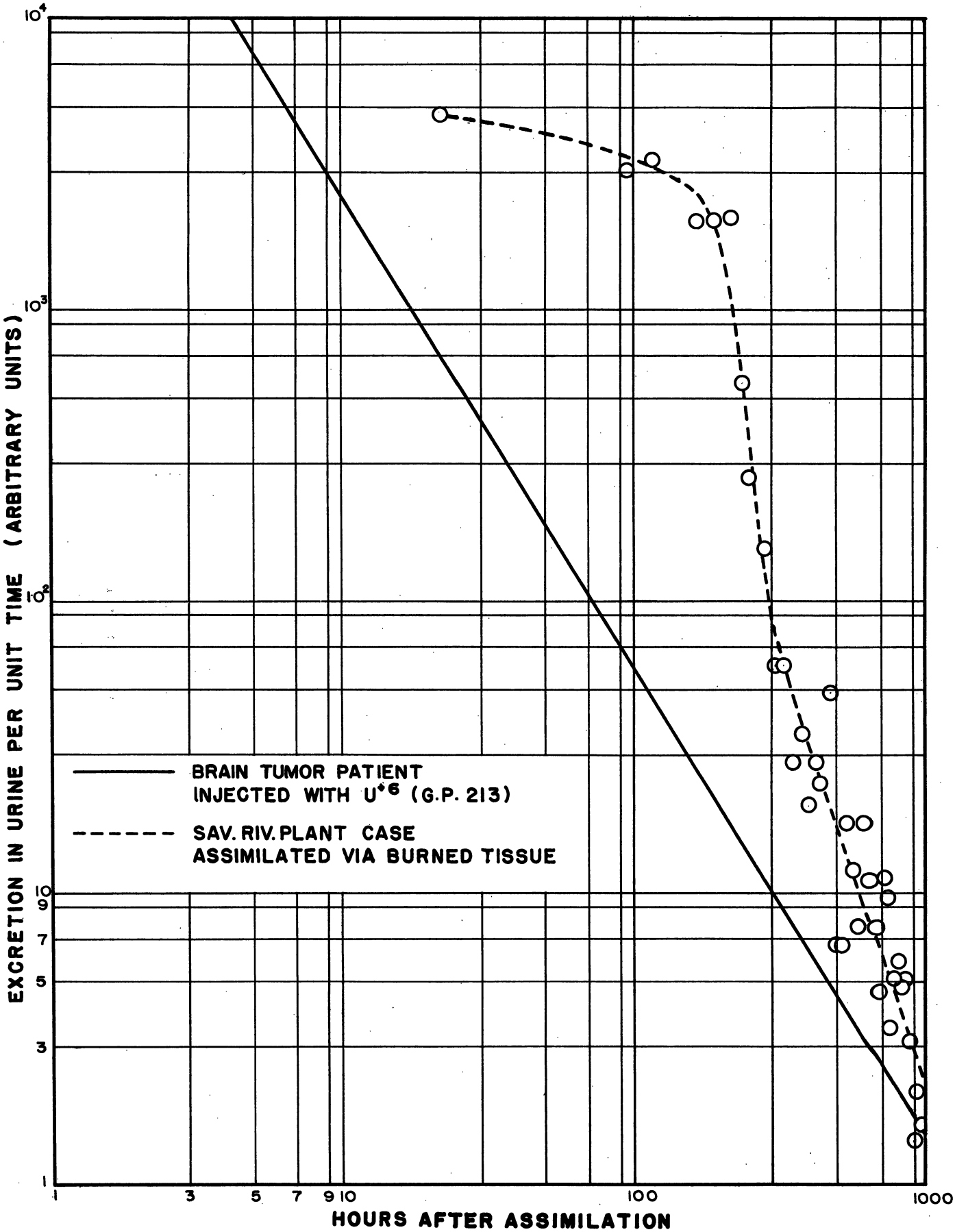

Figure 3. EXCRETION OF URANIUM IN URINE

patients injected with hexavalent uranium. The rapid decrease in the excretion rate in the case of injected uranium may be contrasted with the relatively slow decrease for the first 9 days in the case of the burned employee. This comparison may indicate that the uranium was leached slowly from the burned tissue into the blood. Expression of these data requires a more complex mathematical treatment than that presented by Bernard.[3]

SUMMARY

Plutonium - Urinary excretion of plutonium during a 487-day period after an acute uptake by wound contamination was followed by the analyses of 99 urine samples. The data may be approximated by the function

$$Y = 141\ t^{-1.07}$$

where Y is the plutonium disintegrations per minute in a daily voiding after t days. The probability that the Langham equation[1] for the excretion of plutonium fits the Savannah River Plant data as well as the above equation is only 1 in 1,000. The data, however, differed no more from the Langham equation, which is a mean equation, than data from some of the cases used to calculate the mean.

Zirconium citrate solution, administered intravenously approximately 3 hours after the accident, and Ca-EDTA, administered intravenously during the first 6 days after the accident, produced only a slight increase in the rate of plutonium excretion. Ca-EDTA was again administered on the 131st to 135th days after the accident and only a slight increase in the rate of plutonium excretion was observed.

Uranium - A second case followed was that of an employee hospitalized for burns caused by hot uranyl nitrate solution. Contrary to excretion data obtained from persons injected with soluble uranium, the excretion rate in this case decreased only slowly for the first 9 days following the accident. Between the ninth and fifteenth days, however, the daily excretion rate dropped a hundredfold. From the fifteenth to the fortieth day, the biological half-life for elimination was approximately 6 days. The data may indicate that the uranium was leached slowly from the burned tissue into the blood.

BIBLIOGRAPHY

1. Langham, W. H., S. H. Bassett, P. S. Harris, and R. E. Carter. "Distribution and Excretion of Plutonium Administered Intravenously to Man." LA 1151, 1950.

2. Foreman, H., P. A. Fuqua, and W. D. Norwood. "Experimental Administration of Ethylenediaminetetracetic Acid in Plutonium Poisoning." AECU-2923, 1954.

3. "Distribution and Excretion of Uranium in Man," Health Physics Division Semiannual Progress Report for Period Ending January 31, 1955, ORNL 1860, pp. 1-12.

4. "Distribution and Excretion of Uranium in Man," Health Physics Division Semiannual Progress Report for Period Ending July 31, 1955, ORNL 1942, pp. 1-6.

VETERINARIAN HEALTH PHYSICS

F. J. Bradley and L. Johnson, D.V.M.

Office of Radiation Safety
The Ohio State University
Columbus, Ohio

Much has been written concerning the radiation problems connected with radiology departments in hospitals, but few persons are familiar with similar problems that confront a veterinarian. There is usually a lag of several years between the use of ionizing radiation on man and its practical application in Veterinary Medicine. Today at the Veterinary Clinic, approximately 1 out of every 3 animals admitted receives either a therapeutic or a diagnostic dose of ionizing radiation.

Most radiographs on small animals are taken with a G. E. stationary diagnostic unit. Someone must hold the animal while the radiograph is taken unless the animal is put to sleep, which is seldom done. As opposed to the situation in human diagnostic X-ray procedure, where a technician is seldom in the room, there are always 2 or 3 persons in the room under these circumstances.

Film badges were placed in 2 positions to monitor the soft radiation: (1) near the tube, in approximately the same position the person holding the animal stands, the exposure averaged 54 mr/wk; (2) on the control panel, which is also in the room with the X-ray equipment, the monitor film badge indicated that the operator received only a very small dose. Usually the persons holding the animal are veterinary students and are on X ray only 1 week out of 13. All students are instructed in the proper procedure before they are assigned to this work and the standard lead aprons and gloves are worn by personnel holding the animal.

For the radiographs of the extremities of larger animals, mainly horses and cows, a portable G. E. unit is used. The procedure that is followed is shown in Figure 1. The plate is held remotely by a person wearing lead gloves and apron. Pocket meters are worn and the highest body dose is 2 mr per exposure. One might contrast the number of persons required to take animal and human radiographs. In the human case 1 person is normally required, while with animals usually 3 to 4 persons are involved, with no permanent lead barrier for protection.

The recommendations of NBS Handbooks 41 and 60 for checking such X-ray units were followed. While both units are rather old, they have the proper shielding on the tube head. Filters and cones, however, are not used very often. Each unit surveyed is posted as to proper operating conditions and includes a list of personnel authorized to use the unit. Authorized personnel have taken the prescribed radiology course in the Veterinary College. All permanent personnel in the Diagnostic X-ray Department wear film badges and have blood counts taken approximately every 6 months, mainly for the record.

The diagnostic use of radioisotopes in animals has been reported in the literature. These tests are usually duplications of well-known tests that have been used in man. In fact, most human diagnostic tests, such as thyroid function, blood space, sodium space, etc., are applicable to animals, but as Dr. Rudy has stated, people are reluctant to spend the money for such tests on pets or farm animals.

For therapeutic use a G. E. 250 KV unit is used. During irradiation the operators are in a shielded cabin with the control panel, and the animal is watched by means of side-view mirrors on the cabinet. Scattered radiation was not detected in the cabin. Outside the cabin, however, it was 5 to 15 mr/hr, and it was greater than 20 mr/hr outside the door of the room 18 feet from the tube head. This door was later covered by 1/8 inch of lead.

This unit is used to treat neoplasms or tumors of small animals under general anesthesia, and gives a dose of 36 r/min at 50 cm.

Under Dr. Johnson's direction, it also has been used for the relief of pain in the legs of horses suffering from bursitis and certain types of arthritis. For several days prior to the actual treatment, time had to be spent in training the horse to stand still during irradiation. This procedure was not always effective, especially among nervous thoroughbreds in whom these disabilities are prevalent.

Dr. Johnson contacted Dr. U. K. Henschke, then in the Radiology Department at the University Hospital, regarding the possibility of using radioisotopes. Together they worked out a system using, at first, approximately 100 mc of radium in 6 brass tubes.

A canvas strap containing metal tube holders is tied to the horse's leg over felt. By means of special surgical tongs, the tubes containing the radioisotope are removed from their lead storage container and put in the metal tube holders on the horse's leg (Figure 2). Everything is prepared before removing the radioisotope from the container. The total exposure time, therefore, is only 2 to 4 minutes, and removal of the tubes requires 1 to 2 minutes.

Table 1 gives the exposure data as recorded in surveys over the last 2 years.

TABLE 1

EXPOSURE DATA

		Body Dose		Dose-Rate $(\frac{mr}{hr})$	
		Pocket Meters	Film Badge	Hands	Outside Stall
1954 - 1955					
(used Ra mainly)	100 mc	3-5 $\frac{mr}{exposure}$	247 $\frac{mr}{wk}$ *	all tubes in place 300	20 - 30
(1 person doing work)			(worn mainly on wrist)		
1955 - 1956					
(used Co-60 mainly)	60 mc set	37 $\frac{mr}{wk}$	40 $\frac{mr}{wk}$	340	30 - 40
(2 persons doing work)	120 mc set	(worn mainly on body)	(worn mainly on body)	400	40 - 50

* The wearer of this badge had a habit of leaving the badge near the isotope container, so that the reading is probably higher by a factor 1.5 to 2 above the actual dose received.

Blood counts have been taken on exposed persons every 6 months and they have never deviated from normal. Because of the hardness of the radiation we have relied mainly on speed, a long

pair of tongs, and rotation of personnel to reduce the exposure. It has been found that the direct-reading pocket meters which have been in use for the last 8 months have been very useful both in controlling exposure and also for psychological reasons, because they give a quantitative value to radiation that one cannot feel or touch.

Although radium was used at first, the ability of the horses to work the tubes loose by chewing and rubbing indicated that Co-60 would be far safer. Over-all experience with Ra and Co-60 here has been very favorable, both safety-wise and in the results obtained. In fact, one member of the thoroughbred industry stated that their use represented the most forward step yet accomplished in the industry. In this clinic over 300 horses already have been treated in the last 3 years; each horse received 6 applications, for a total of 1,800 isotope treatments.

Drs. Catcott, Tharp, and Johnson[1] are using the beta rays from Sr-90 provided by a commercial β-ray applicator to treat inflammatory lesions and neoplasms in the eyes of animals. This unit gives a surface dose of 38 rep/sec. A survey indicated that the dose was 20 mrep per hr at 1/2 inch on the end of box where the Sr-90 was located.

The procedure for handling the applicator is shown in Figure 3. Since the greatest hazard is to the fingers, small tongs are used to push the eyelids apart following administration of a topical anesthesia to the eye. This applicator is returned to the manufacturer every 6 months for a smear test. These applicators in the hands of a skilled veterinarian produce excellent results, but because of the extremely high surface dose and the possibility of breaking the seal on the Sr-90, they can represent a very dangerous hazard in unskilled hands.

Veterinarians' contact with ionizing radiation may not stop here. Because veterinarians are called upon to inspect meat to determine its wholesomeness for human consumption, an added function in the future may be the testing of meat that has been sterilized by ionizing radiation. Furthermore, in the coming nuclear age it will also become imperative for them to know how to detect meat contaminated with radioactivity.

ACKNOWLEDGEMENT

We wish to acknowledge the assistance of Dr. R. Rudy, Veterinary Radiology Department, in carrying out this study.

BIBLIOGRAPHY

1. Catcott, E. J., V. L. Tharp, and L. E. Johnson. "Beta Ray Therapy in Ocular Diseases of Animals." Am. J. Vet. Med. Assn., 122:172-175, March, 1953.

A THEORETICAL APPROACH TO BIOLOGICAL EFFECTS OF RADIATION

L. H. Krohn, M.D.

Central Hospital
Detroit, Michigan

The experiments of Hofman and Muller[1] suggest that primary mechanisms of radiation injury involve 1 or more systems of chemical reactions. Lethal doses of ultrafractionated radiation given to a number of test groups of insects were found to vary widely with frequency of fractionation. Using a spinning sectored disc to pulse radiation with periods varying from 0.1 millisecond to 1 second, as many as 5 maxima and minima for lethal effectiveness may be observed, while mitotic periods are much longer than the pulse times. Plausibility for the assumption that chemical reactions are responsible for the large variations of effectiveness observed arises from the existence of radio-mimetic drugs such as the nitrogen mustards, and production of mutations in plants by chemicals.

Analysis has led to a quantitative theory based on the law of mass action. This gives rise to an ordinary differential equation involving the substance of interest as the dependent variable. The equations are generally non-linear, first order. At this point we are unable to pin down particular substances. We are only looking into types of possible reactions and determining reaction constants from experimental results. For instance, the quantitative theory allows for a completely arbitrary number of chemical reactions to take place.

We consider that ionizing radiation produces substances foreign to the biological system as well as substances not uncommon to the system. We are interested only in the lethal substances in this case. As a first approximation, it is assumed that the principal effect is caused by a single substance much more toxic than other toxins which may be produced. This substance is removed from the system by detoxification reactions and by its toxic reactions.

Analysis indicates that dependance upon pulse time depends upon the degrees of chemical reactions involved in the toxic and detoxifying actions. The usage of degrees here refers to the number of fundamental particles of the toxic substance taking part in a reaction. For example, if three alkaloidal molecules must be attached to an enzyme to block it, this is a third degree reaction from the standpoint of the alkaloid.

We have shown that a consideration of mixed degrees of reactions, restricted to first and second degrees, will produce agreement in form with experimental results. Quantitative comparison is being carried out by means of a digital computer working out a 5-parameter system of equations.

BIBLIOGRAPHY

1. Hofman, D. and K. Muller. Strahlentherapie, 96 Band, heft 3, 403-407, May, 1955.

DETERMINATION OF GROSS BETA ACTIVITY IN URINE WITH K-40 CORRECTION

E. R. Ebersole and J. K. Flygare, Jr.

Health and Safety Division
U. S. Atomic Energy Commission
Idaho Falls, Idaho

Under policies established by the Health and Safety Division, a urinalysis service is provided contractors at the National Reactor Testing Station for the detection and estimation of absorbed, ingested, or inhaled radioactive materials. Urine specimens collected at regular intervals from personnel working in areas containing radioactive materials, as well as specimens taken immediately following an accidental "spill" or release of radioactive materials, are sent to the Analysis Branch of the Health and Safety Division for analysis.

Because of the varied nature of the experimental work being done at the NRTS, the Analysis Branch seldom knows what radioactive isotopes may be expected in a given individual's urine specimen. In some areas general fission products are a potential source of exposure, while in other locations isotopes produced by irradiation of various materials may represent a greater potential source of exposure than fission products. Since the analyst does not know what chemical species may be expected in a given sample, a simple and rapid method of determining low levels of gross beta activity regardless of chemical species is desirable for monitoring of personnel handling radioactive materials. Such a method would be extremely useful in screening routine urine samples, as well as samples from individuals known to have been exposed, before time-consuming chemical separations are undertaken.

Direct gross beta counting of evaporated urine samples[1] for low levels of beta activity suffers from two disadvantages: (1) self-absorption by the solids found in urine, and (2) the natural activity of K-40 found in urine. Removal of organic material by wet-oxidation and proper choice of sample size minimize the first disadvantage. Determination of the potassium content and subsequent correction for K-40 activity eliminate the second disadvantage. A gross beta counting method for urine samples which incorporates removal of organic material and correction for K-40 activity based on actual potassium content of the sample has been in use in this laboratory for over 3 years.

Briefly, the procedure consists of wet-ashing a 50 ml aliquot of the urine specimen to remove organic material. The residual salts are dissolved in a small portion of dilute nitric acid, transferred to a 10 ml volumetric flask, and brought to volume with distilled water. A 1 ml aliquot is evaporated to dryness on a 1-inch watch glass under an infrared lamp and counted for 512 counts. Potassium concentration is determined on the remainder of the 10 ml sample by means of the Beckman D. U. flame photometer. The activity contributed by the K-40 is read from an experimentally established curve and subtracted from the net activity of the sample to obtain that caused by foreign materials.

PREPARATION OF SAMPLE

The urine specimen, as received, is mixed thoroughly and a 50 ml aliquot transferred to a 250 ml beaker. Ten milliliters of concentrated nitric acid are added, the beaker is covered with a watch glass, and the sample placed on the hot plate. The sample is evaporated to dryness and allowed to char. Some samples may break into flame at this point, but the flame is confined by the watch glass and does not become violent. After the sample has charred, the beaker is removed from the hot plate and cooled for 2 to 3 minutes. A second 10 ml portion of concentrated nitric

acid is added and the sample is again evaporated to dryness. If appreciable organic material still remains, this treatment should be repeated until the carbonaceous material is gone. However, the majority of urine samples require only 2 evaporations with nitric acid, while 3 evaporations with nitric acid will remove the organic material from all but an occasional sample.

Four to 5 milliliters of 30 percent hydrogen peroxide and 4 to 5 ml of concentrated nitric acid are then added to the residue and evaporated to dryness. Warning! Addition of 30 percent hydrogen peroxide to organic material may lead to rapid reaction. Care should be exercised at this point to ensure that essentially all organic material has been destroyed by nitric acid prior to addition of the 30 percent hydrogen peroxide and that the concurrent addition of 4 to 5 ml of nitric acid is not omitted. Several thousand urine samples have been run in this laboratory using the above procedure. After this treatment, a white residue of inorganic salts remains. Prolonged heating at this stage should be avoided, if possible, to prevent baking of the salts on the beaker.

The residual salts are dissolved in 4 to 5 ml of water and 4 to 6 drops of concentrated nitric acid. This solution, plus any undissolved solids, is transferred quantitatively to a 10 ml volumetric flask and brought to volume with distilled water.

Since any undissolved solids may carry radioactive materials insoluble in dilute nitric acid, the solution is thoroughly mixed to disperse the solids and a 1 ml aliquot is transferred to a 1-inch watch glass and evaporated to dryness under an infrared lamp for counting purposes.

CHOICE OF SAMPLE SIZE

A 1 ml aliquot of the prepared sample - the equivalent of 5 ml of original urine - was chosen for counting purposes to minimize self-absorption and to facilitate mechanical handling. Figure 1 illustrates the self-absorption of urine salts for a 0.7 Mev maximum beta emitter and for a 1.4 Mev maximum beta emitter. The percent correction for absorption is plotted against mg per cm^2 salt thickness. For most urine samples the plated salts will lie between the vertical dashed lines shown on the curve or between 20 and 40 mg per cm^2 thickness. Thus we see from this curve that for a beta emitter with a maximum energy of 0.7 Mev or greater, the correction factor will be above 75 percent and no correction for self-absorption need be made. Also, mechanically, a 1 ml aliquot is readily handled on a 1-inch watch glass for counting purposes.

POTASSIUM CORRECTION

Potassium concentration is determined on the remaining portion of the 10 ml of prepared sample, using a Beckman D. U. flame photometer equipped with a red-sensitive phototube. The determination is made at a nominal wave length of 768 millimicrons and a slit width of 0.04 mm. Figure 2 is a potassium calibration curve with percent transmission plotted against milligrams of potassium chloride per milliliter of solution. This curve was obtained by using reagent grade potassium chloride in water solution. No correction for sodium or nitric acid concentration is necessary since counting variations overshadow any small errors in the potassium determination caused by these materials. In fact, no error has been observed in the potassium determination in the presence of 3 times the normal urine sodium concentration.

In order to establish an experimental curve of K-40 activity in urine, 61 samples were obtained from unexposed personnel and the K-40 activity determined by counting the prepared samples under the same conditions used in the regular determination procedure. The potassium concentration was determined by means of the flame photometer. Figure 3 is a plot of K-40 activity in counts per minute versus potassium concentration as potassium chloride per milliliter of solution. The straight line A drawn through the points represents the best fit obtained by the least squares method. The dashed lines represent 2 standard deviations of the determination from this line. The solid line B represents the curve obtained by using reagent potassium salts. The excellent agreement between the curve from reagent potassium salts and the curve from the actual urine specimen suggests that reagent potassium salts may be used to obtain a standard curve for K-40 activity in the future. Figure 4 is a working curve showing potassium transmission plotted

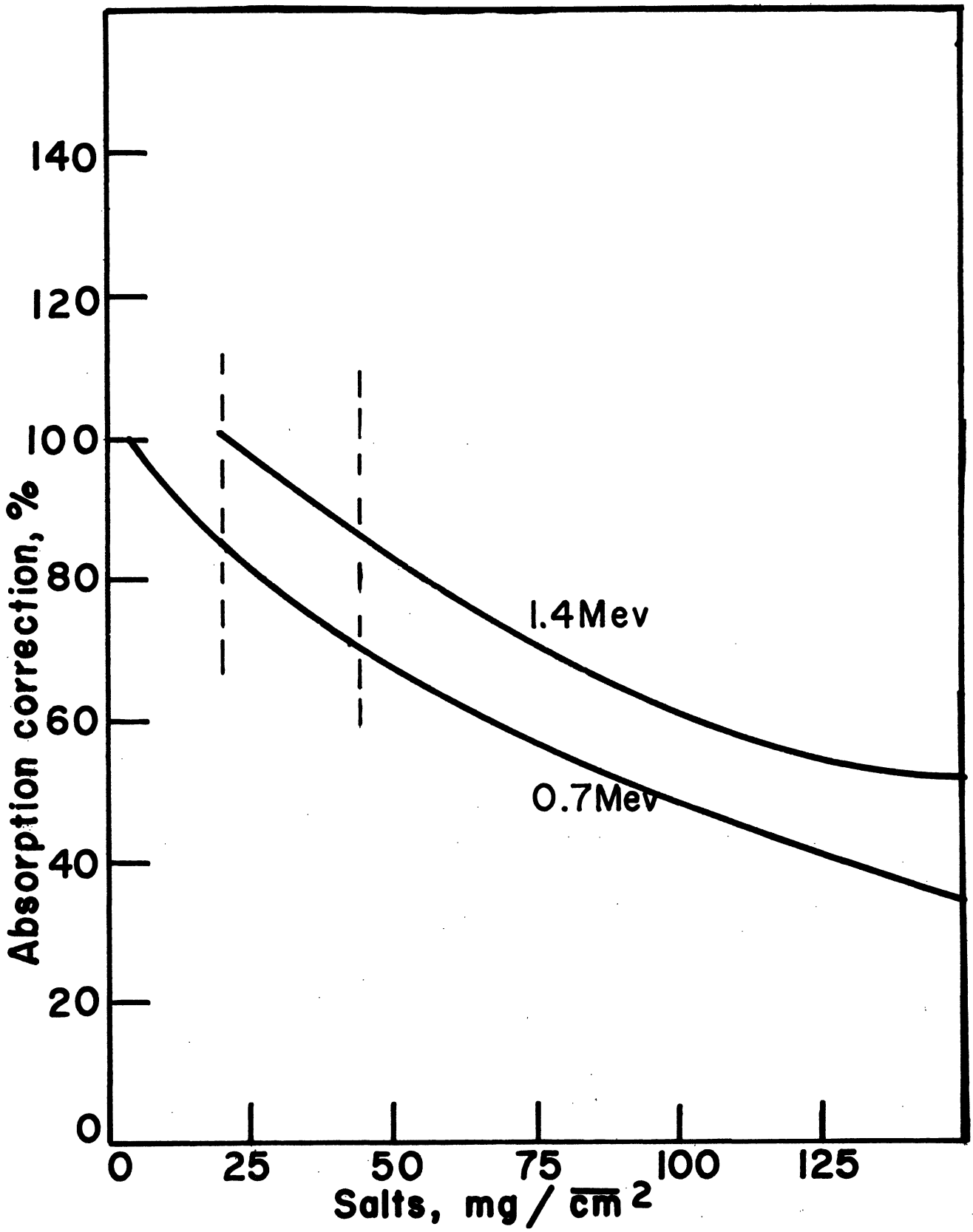

Figure 1. BETA ABSORPTION BY URINE SALTS

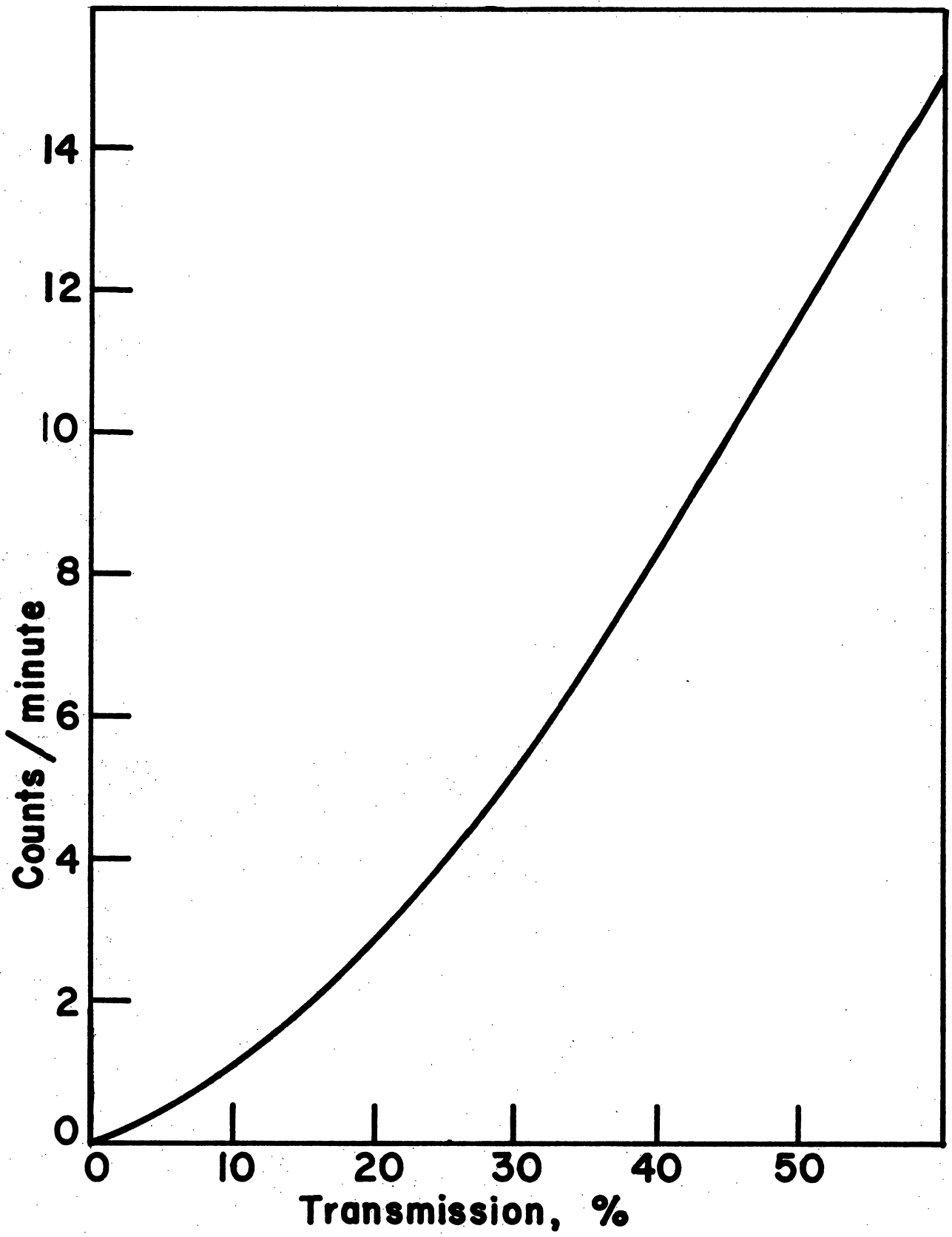

Figure 2. WORKING CURVE

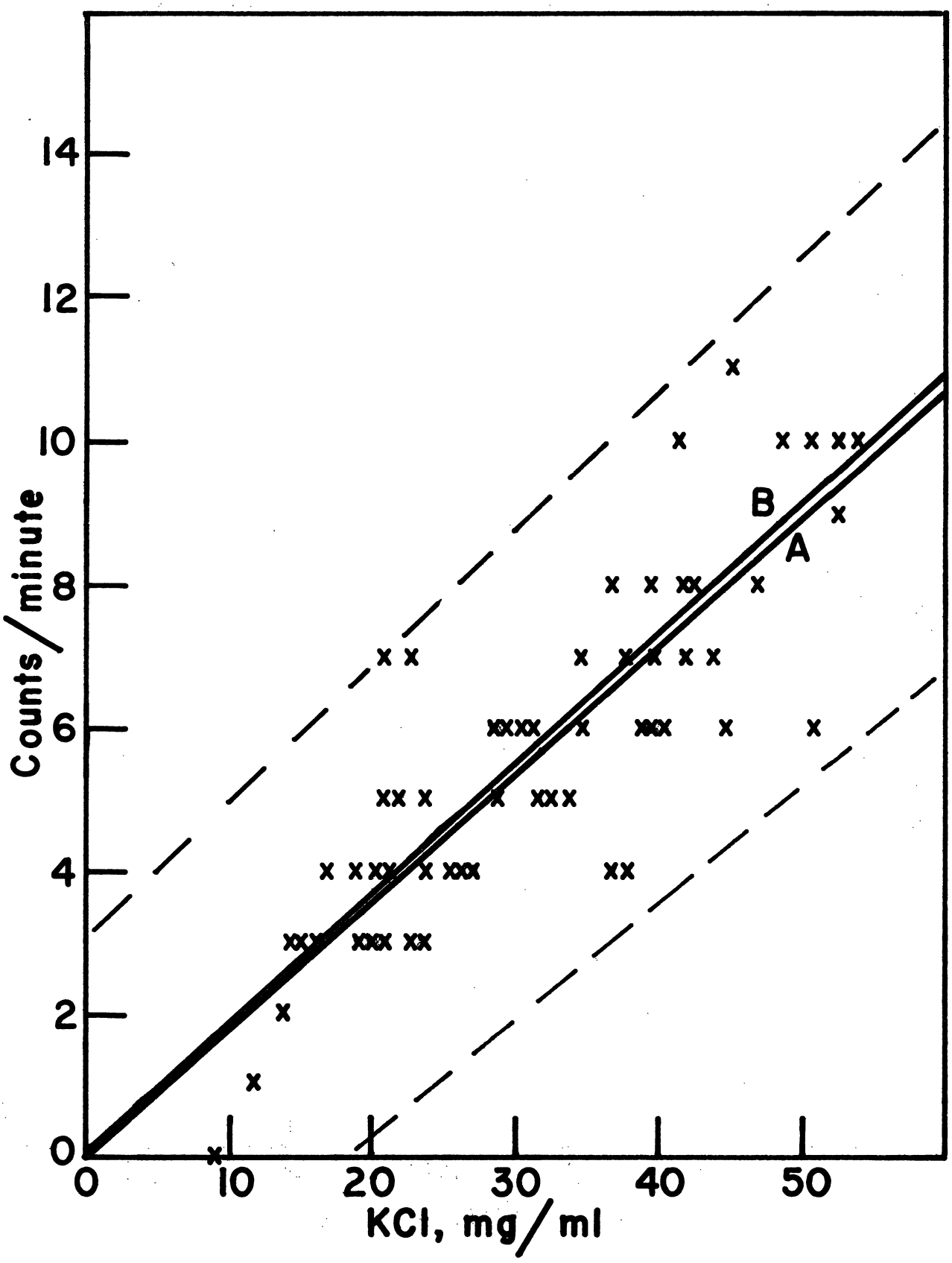

Figure 3. K-40 ACTIVITY VERSUS KCl CONCENTRATION

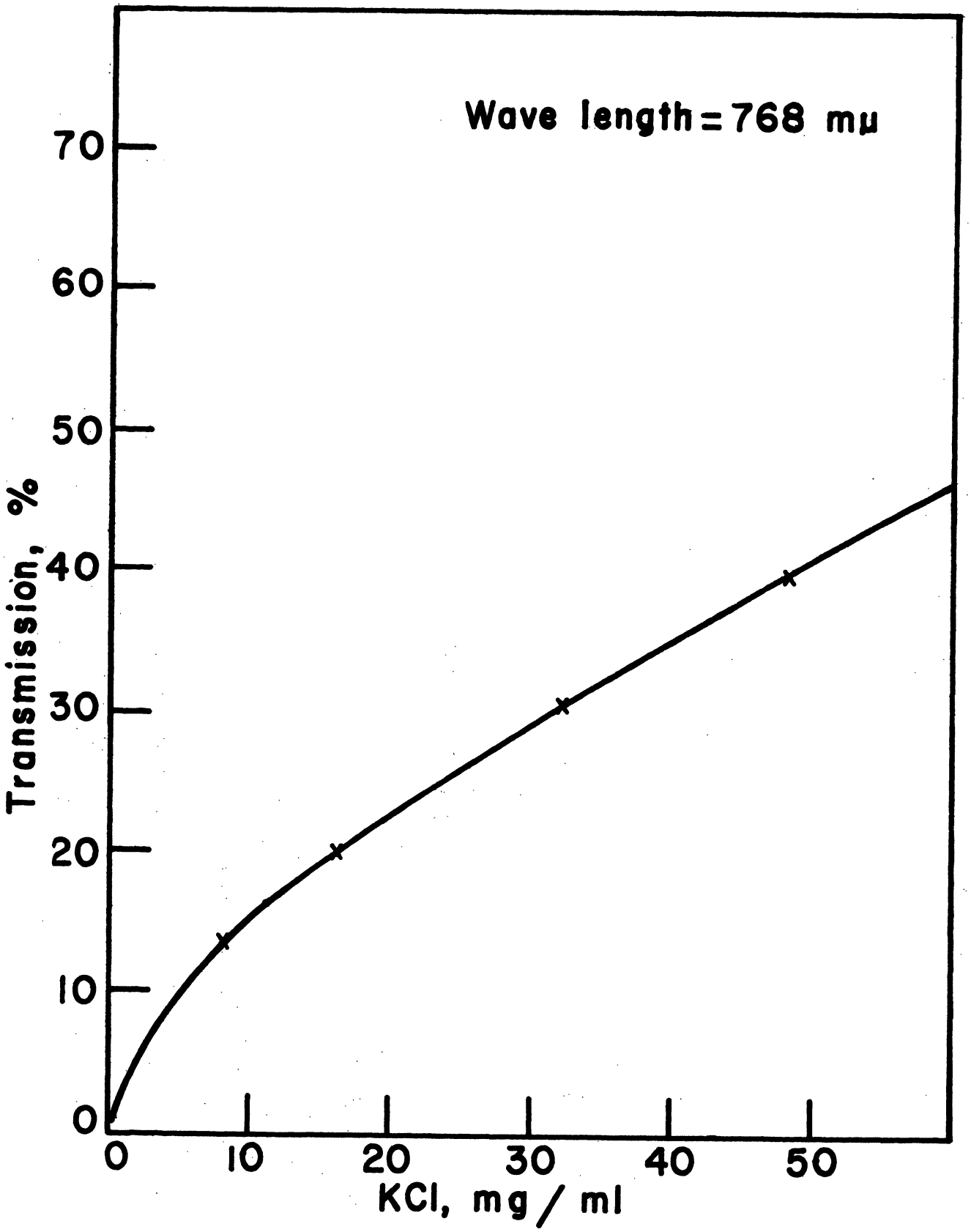

Figure 4. CALIBRATION CURVE

against K-40 activity, and is a crossplot of Figures 1 and 2. The percent transmission on an individual urine specimen is obtained by means of the flame photometer and the activity caused by K-40 is read directly from this curve. This activity in counts per minute is subtracted from the total activity of the sample in counts per minute to give the foreign or unnatural activity in counts per minutes.

Consideration must be given to counting statistics in obtaining this difference so that differences caused only by counting variations are not taken as significant. The detection limit is defined as the foreign activity that is equal to twice the standard deviation of its determination. For example, under our conditions the standard deviation of the determination at the background level is approximately 2 counts per minute. Thus the detection limit is twice the standard deviation or approximately 4 counts a minute. We assume that most foreign activity will be mixed fission products, for which our counting efficiency is 10 percent. Thus our detection limit is 40 disintegrations per minute of foreign activity per 5 ml of original urine, which corresponds to 4×10^{-6} microcuries per ml of original urine, or approximately $6 \times 10^{-3} \mu c/day$. Thus, the detection limit is approximately 1.5 times the total excretion per day of Sr^{90}-Y^{90} as calculated by Morgan and Ford[2] for chronic exposure that has resulted in an equilibrium condition in which the person has accumulated a maximum permissible body burden.

The counting is done under an end-window G. M. tube on automatic sample changers and does not require personnel in attendance during the counting period. One man can prepare for counting and determine the potassium content of 50 to 60 urine samples per 8-hour day. Thus a maximum number of urine specimens may be screened for activity by a minimum number of people.

BIBLIOGRAPHY

1. Cowan, Frederick P. and Jerome Weiss. Nucleonics, 10. No. 2:33, 1952.

2. Morgan, K. Z. and M. R. Ford. Nucleonics, 12. No. 6:32, 1954.

MEASUREMENT OF RETENTION AND EXCRETION OF RADIOISOTOPES OF THE ALKALI METALS BY MICE AND RATS, USING AN ANNULAR LIQUID SCINTILLATION COUNTER*

K. T. Woodward,** C. R. Richmond, and W. Langham

The Los Alamos Scientific Laboratory
University of California
Los Alamos, New Mexico

INTRODUCTION

The importance of excretion, retention, and distribution data to the determination of the potential health hazards of internally deposited radioactive materials was recognized by Hamilton and co-workers.[1-3] They began systematic studies of the metabolism of radioisotopes in rats as early as 1942 and devoted special attention to the heaviest elements and to the products of nuclear fission. Because of the number of nuclides being considered, they attempted to correlate metabolic properties with position of the various elements in the periodic table. This early work still provides the majority of data available on many nuclides.

The development of in vivo whole body liquid scintillation counters for mice, rats, dogs, monkey, and humans[4, 5] has provided a rapid approach to the study of the excretion and retention of the gamma-emitting isotopes by all these species. Because of the characteristics of the large volume liquid scintillation detectors, it is possible to administer very small amounts of radionuclides to experimental animals and still obtain high in vivo counting rates through several biological half-times. Such studies can be made on humans without administering more than 0.1 to 0.01 of a maximum permissible body burden.

The purpose of this study was to determine (by in vivo counting methods) the retention of the alkali metals in mice, rats, dogs, monkeys, and man, as part of a general program to reinvestigate the metabolism of the more common gamma-emitting radionuclides. From such data inter-specific correlations might be possible, and some common metabolic parameter established for all species. If no such parameter were found, the results might still be of value in calculating maximum permissible levels of radioisotopes in the body and in air, water, and food.

This report gives primarily the data collected on mice and rats. Because of the current interest in cesium, in relation to world-wide fallout from atomic tests, measurements of Cs-134 retention in 1 man following oral administration are given also.

METHODS AND MATERIALS

Male Sprague-Dawley rats and female CF_1 mice were given single doses of Na-22, K-42, Rb-86, or Cs-134 via oral and intraperitoneal administration. Six rats and 12 mice were used in each experiment. Each rat was given $\sim$0.4 μc and each mouse $\sim$0.2 μc, and all animals that received the radioisotopes orally were fasted 18 hours prior to administration. The animals were placed in standard metabolism cages and urine and feces collected until the excreted radioactivity dropped essentially to the limits of detection. During the experiment the dietary regimen consisted of Purina chow and water ad libitum, and the animals were weighed periodically to assure normal growth and maintenance.

* Based on work done under the auspices of the U. S. Atomic Energy Commission.
** Major (MC) USA. Now stationed at Walter Reed Army Hospital, Washington, D. C.

The whole body gamma radioactivity in individual animals was determined immediately after administration of the radionuclides and periodically thereafter by in vivo counting in the Los Alamos small annular liquid scintillation detector (shown in Figure 1). Standards of each radionuclide were prepared by pipetting an amount of the isotope equivalent to that administered to the animal into polyethylene bottles containing a quantity of water approximating the average weight of the rats or mice in each experimental group.

Urine and feces samples were collected every 24 hours and counted in the same counter. To ensure reasonable geometric counting duplication, water was added to the rat and mouse urine samples to make the total volumes approximately that of the animals. Feces were collected and counted in small waxed paper drinking cups.

One healthy mature man was given orally 1.2 μc of Cs-134 and his whole body activity determined at subsequent intervals in the Los Alamos human counter.[4] Periodic urine and fecal samples also were collected and counted.

Because of the high counting rates, statistical accuracy was obtained in very short times. Even when the counting rate of the sample was a factor of 4 below background (background 100 c/sec), the statistical precision of the measurements was determined to < 5 percent in 2 to 4 minutes counting time. The counts were corrected for physical decay and the results expressed as percent of administered dose.

RESULTS

Retention and excretion data for the individual animals were averaged and plotted against time on semilog paper. Figures 2 and 3, showing body retention and fecal and urinary excretion of Na-22 by mice and rats, respectively, are representative of the data obtained by the in vivo counting method.

Whole body retention or excretion at any time may be expressed by a multiple-component rate function of the form

$$R = a_1 e^{-k_1 t} + a_2 e^{-k_2 t} + \ldots + a_n e^{-k_n t}$$

in which a_1, a_2, a_n and k_1, k_2, k_n are the intercept and slope constants, respectively, of the individual or first-order components of the composite retention or elimination process. The values for a_1, $a_2 \ldots a_n$, and k_1, $k_2 \ldots k_n$ were determined from the data by the standard kinetic approach.[6] The half-times for each first-order component of the retention or elimination process were calculated by the expression

$$t_{1/2} = \frac{0.693}{k}$$

Values of the various parameters for retention of Na-22, K-42, Rb-86, and Cs-134 by mice and rats following oral and intraperitoneal administration are given in Table 1.

One group of mice was maintained on a low sodium intake (3 meq/100 gm food) following intraperitoneal injection of Na-22 and their sodium retention measured. After 21 days on the low sodium regimen, they were placed on the standard diet (90 meq Na/100 gm food) and the Na-22 retention measurements continued. These results are shown in Figure 4 and the values for the various parameters of the retention process are given in Table 1.

The whole body retention curve for cesium in 1 human volunteer is shown in Figure 5. Since the experiment is not completed, an equation expressing the entire retention process is not given. To date, however, 1 exponential rate of loss from the body is apparent; this component having a half-time of about 150 days.

Figure 1. SMALL ANIMAL COUNTER

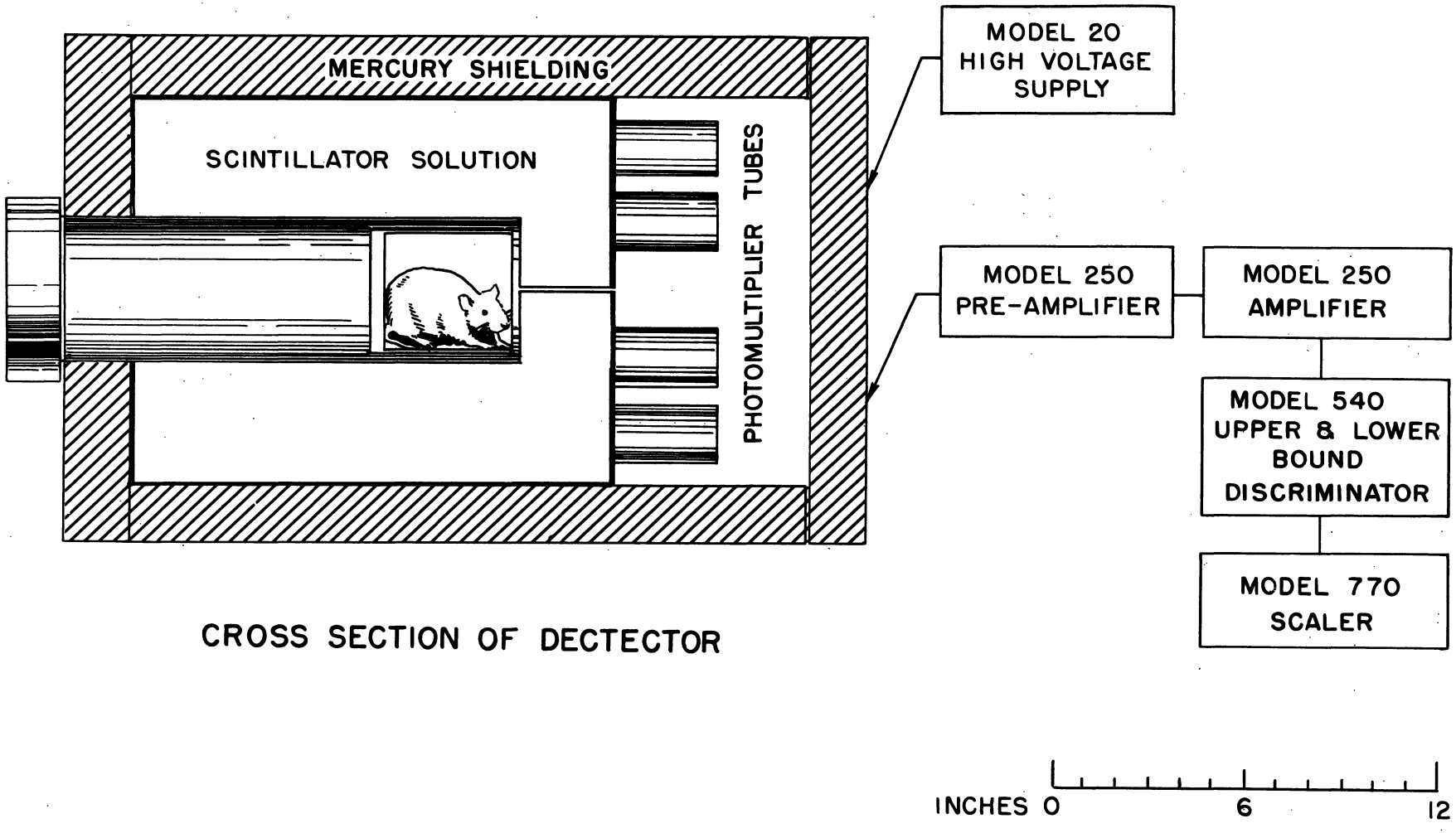

Figure 2. BODY RETENTION AND FECAL AND URINARY EXCRETION OF Na-22 BY MICE

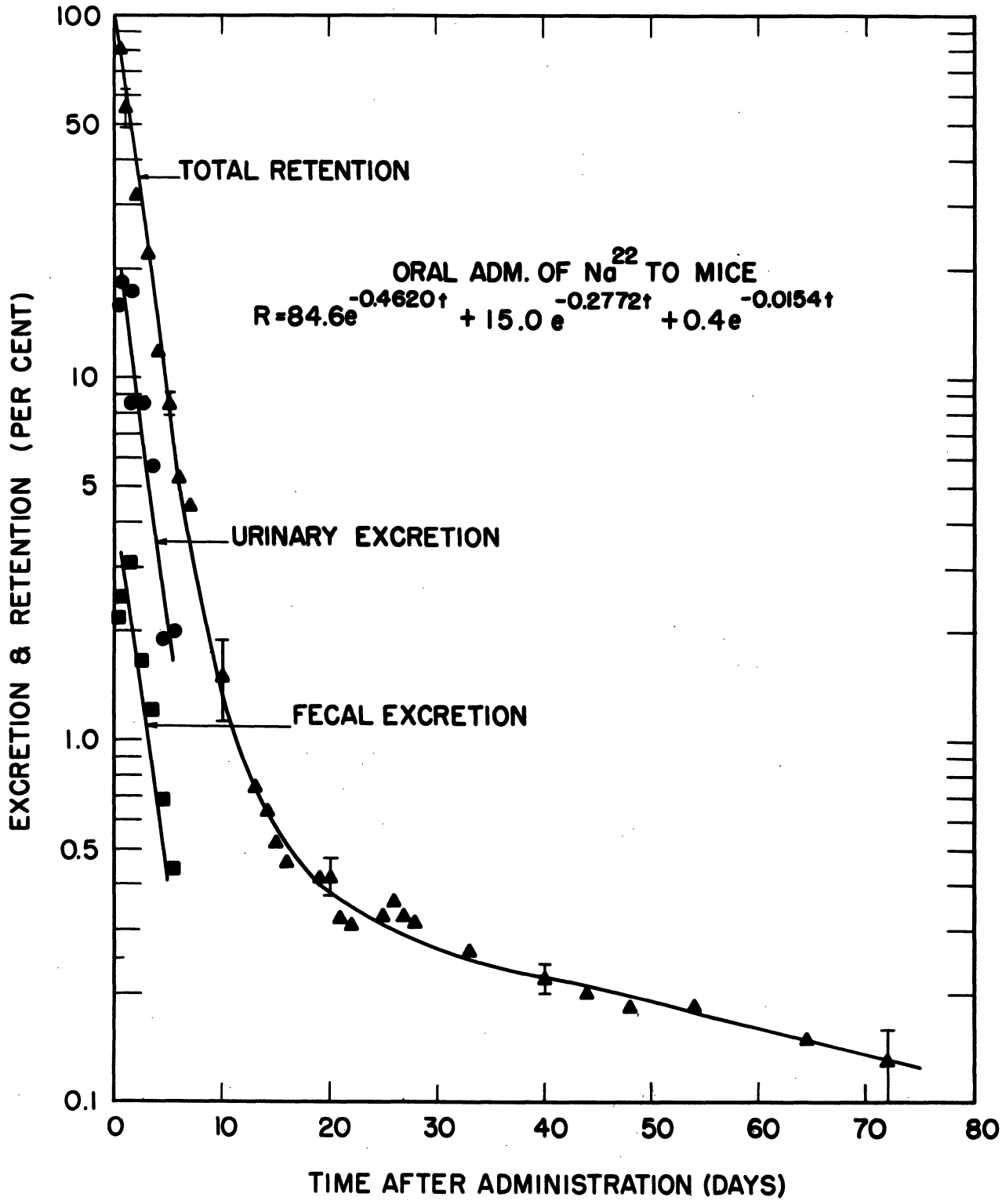

Figure 3. BODY RETENTION AND FECAL AND URINARY EXCRETION OF Na-22 BY RATS

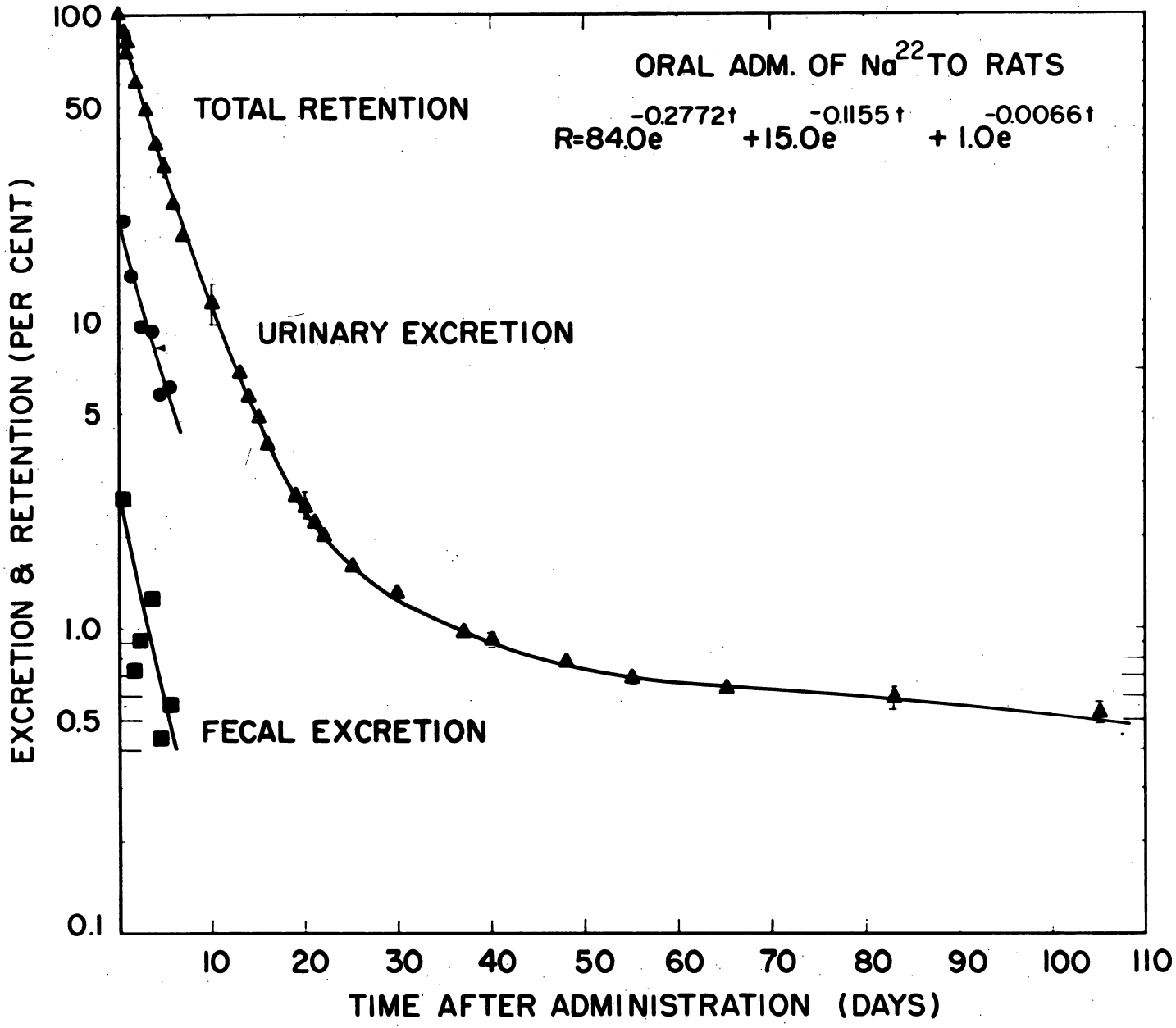

Figure 4. BODY RETENTION OF INTRAPERITONEALLY ADMINISTERED Na-22 BY MICE AFTER 21 DAYS ON LOW SODIUM DIET

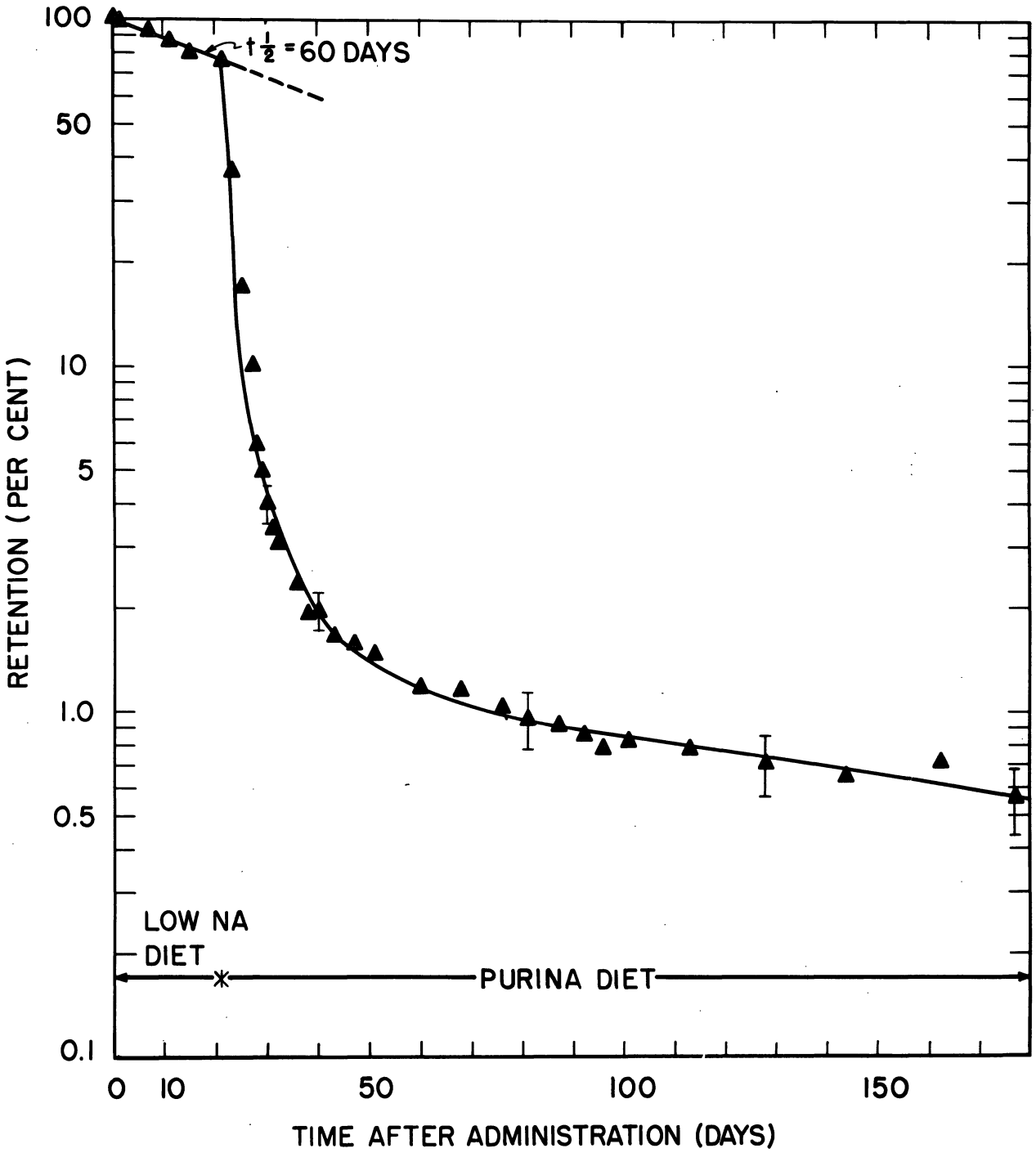

Figure 5. BIOLOGICAL HALF-TIME OF ORALLY ADMINISTERED Cs-134 IN A NORMAL MAN

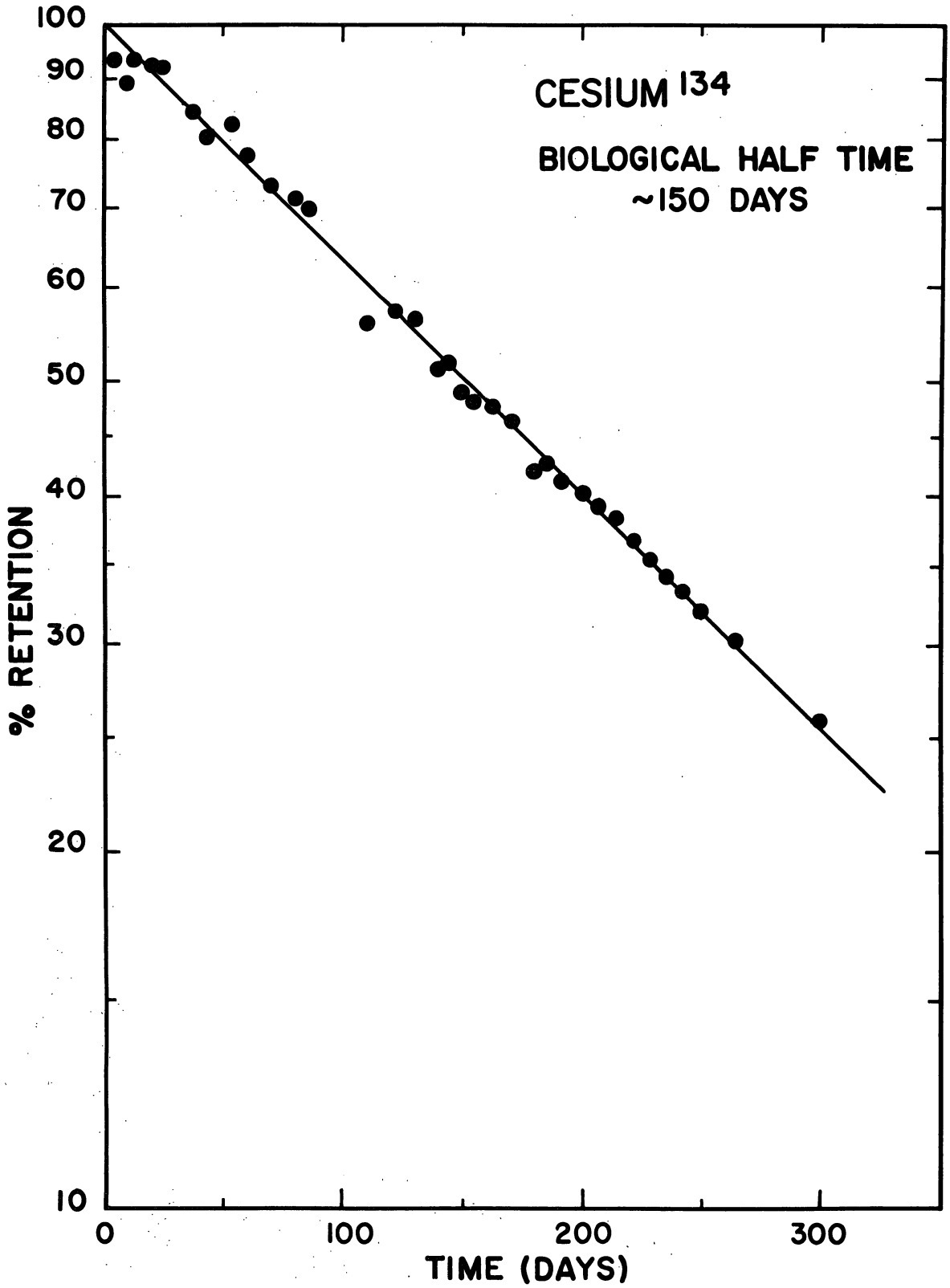

TABLE 1

VALUES FOR THE PARAMETERS* OF RETENTION OF ALKALI METAL IONS BY MICE AND RATS FOLLOWING ORAL AND INTRAPERITONEAL ADMINISTRATION

Isotope	Species	Route	a_1	k_1 (Days)	$(t\,1/2)_1$	a_2	k_2 (Days)	$(t\,1/2)_1$	a_3	k_3 (Days)	$(t\,1/2)_3$
Na-22	Mice	Oral	84.6	-0.462	1.5	15.0	-0.277	2.5	0.4	-0.015	45.0
Na-22	Mice	I. P.	87.3	-0.576	1.2	12.0	-0.247	2.8	0.7	-0.031	22.0
Na-22	Rats	Oral	84.0	-0.277	2.5	15.0	-0.115	6.0	1.0	-0.007	105.0
Na-22	Rats	I. P.	61.0	-0.385	1.8	38.0	-0.147	4.7	1.0	-0.007	105.0
K-42	Mice	Oral	90.0	-0.462	1.5	10.0	-2.310	0.3	-	-	-
K-42	Rats	Oral	80.0	-0.119	0.5	20.0	-1.386	0.5	-	-	-
Rb-86	Mice	Oral	100.0	-0.182	3.8	-	-	-	-	-	-
Rb-86	Mice	I. P.	69.0	-0.187	3.7	31.0	-0.577	1.2	-	-	-
Rb-86	Rats	Oral	80.0	-0.060	11.5	20.0	-0.198	3.5	-	-	-
Rb-86	Rats	I. P.	79.5	-0.067	10.4	20.5	-0.346	2.0	-	-	-
Cs-134	Mice	I. P.	32.4	-1.386	0.5	46.0	-0.289	2.4	21.6	-0.105	6.6
Cs-134	Rats	I. P.	23.0	-0.462	1.5	32.0	-0.099	7.0	45.0	-0.049	14.0
Na-22 (Low Na diet for 3 weeks)	Mice	I. P.	92.9	-0.533	1.3	5.5	-0.086	8.0	1.6	-0.005	136.0

* From the general equations $R = a_1e^{-k_1t} + a_2e^{-k_2t} + \ldots + a_ne^{-k_nt}$ and $t\,1/2 = \frac{0.693}{k}$

DISCUSSION

The application of first-order kinetics to describe the physiological processes of retention, especially in conjunction with tracer experiments, has been elucidated by several workers.[7-9] It should be emphasized, however, that the ability to express a process in mathematical form does not preclude the possibility of an erroneous physiological interpretation. Retention of Na-22 as a function of time after intraperitoneal and oral administration to mice and rats (Figures 2 and 3) is best expressed by a multiple-component rate function. Of the 3 components which describe the loss of Na-22, the slowest can probably be attributed to loss from bone. The 2 faster components may represent initial loss from the vascular system and loss from the connective and soft tissue.

Mice on a low sodium intake (3 meq/100 gm of food for 21 days) showed an exponential rate of elimination of intraperitoneally injected Na-22 (Figure 4). The half-time of elimination was 60 days. After resumption of the standard dietary regimen (thirtyfold sodium increase), the loss of Na-22 increased immediately and ultimately was best described as a multiple-component rate function composed of 3 exponentials. The slowest moving component represented 1.6 percent of the dose and had a half-time of about 136 days. These data suggest that a low sodium diet favors greater fixation of Na-22 in bone.

Because of the relatively short physical half-life of K-42 (12.4 hours), the whole body gamma ray activity of the mice could be determined for only 3 1/2 days. It was possible to determine the activity of the rats for 6 days by using graded doses in 2 groups of animals and normalizing the combined data. In both species the retention process was best described as a 2-component rate function. These components apparently represent initial loss from the vascular system and loss from the intracellular reservoir, since potassium is the major intracellular cation in muscle. Potassium enriched with K-40 would provide a means of following the physiological processes of retention and excretion for longer times.

Loss of Rb-86 from mice after oral administration followed a single exponential rate. This may be interpreted as representing average loss from several tissues of a basic type, i.e., loss of the ion from all soft tissues. Zilversmit, et al.[7] showed that a single exponential function may represent the sum total of multiple transfer rates and not a simple transfer into a single tissue or phase.

The 2 exponential rates which describe the loss of Rb-86 from mice after intraperitoneal administration may reflect differences in the relative loss from the vascular system and other soft tissues as a result of different rates of absorption from the gastrointestinal system and the peritoneal cavity. However, this difference between routes of administration and the number of components representing body retention of the rubidium was not seen in the rat. Sheldon and Ramage[10] reported that bone is the only adult tissue lacking rubidium in man, and that the muscle mass is the chief storehouse for the temporary retention of this ion. Freedberg, et al.[11] found that Rb-86 was concentrated mainly in the muscle and other soft tissues of several species of animals.

The retention of Cs-134 administered intraperitoneally to mice and rats showed 3 exponential components. The slowest component observed in rats given Cs-134 intraperitoneally represented 45 percent of the dose and had a half-time of 14 days. Since cesium primarily concentrates in soft tissue,[12,13] the 3 components may represent initial loss from the vascular system, loss from the muscle mass, and loss from other soft tissues. The results on urine and fecal excretion from mice given Cs-134 intraperitoneally are in good agreement with those of other investigators.[13] As expected, the urinary and fecal excretion curves were parallel to each other and to the curve for total body retention.

The rate of loss of Cs-134 from 1 healthy human male was about 0.0046 percent per day and the biological half-time was 150 days. It appears that cesium is concentrated in the muscle mass of the body, much as potassium is. The retention of Cs-137 by 3 humans presently is being followed in this laboratory to determine if there is also an early fast-moving component associated with the loss of cesium from man.

BIBLIOGRAPHY

1. Hamilton, J. G., et al. "Metabolism of Carrier-Free Fission Products in the Rat." U. S. Atomic Energy Commission Report, MDDC-1275, 1947.

2. Hamilton, J. G., et al. "Metabolism of Fission Products and the Heaviest Elements." Radiology, 49. No. 3:325, 1947.

3. Hamilton, J. G., et al. "The Metabolism of the Radioactive Elements Created by Nuclear Fission." New England J. Med. 240:863, 1949.

4. Anderson, E. C., et al. "The Los Alamos Human Counter." Nucleonics, 14. 1:26, 1956.

5. Van Dilla, M. A., R. L. Schuch, and E. C. Anderson. "K-9: A Large 4π Gamma Ray Detector." Nucleonics, 12. 9:22, 1954.

6. Comar, C. L. Radioisotopes in Biology and Agriculture. pp. 18-40. McGraw-Hill, New York, 1955.

7. Zilversmit, D. B., et al. "On the Calculation of 'Turnover Time' and 'Turnover Rate' from Experiments Involving the Use of Labeling Agents." J. Gen. Physiol. 26:325, 1943.

8. Solomon, A. K. "Equations for Tracer Experiments." Jour. Clin. Invest. 28:1297, 1949.

9. Burch, G. E., S. A. Threefoot, and J. A. Cronvich. "Theoretic Considerations of Biological Decay Rates of Isotopes." Jour. Lab. Clin. Med. 34:14, 1949.

10. Sheldon, J. H. and H. Ramage. "A Spectrographic Analysis of Human Tissues." Biochem. Jour., 25. 2:1608, 1931.

11. Freedberg, A. S., H. B. Pinto, and A. Zipser. "Distribution of $Rb_2^{86}Co_3$ in Mouse, Guinea Pig, Dog, and Man." Fed. Proc., 11. 1:49, 1952.

12. Hood, S. L. and C. L. Comar. "Metabolism of Cs^{137} in Laboratory and Domestic Animals." Univ. of Tenn. Report ORO-91, May, 1953.

13. Weeks, M. H. and W. D. Oakley. "Biology Research Annual Report. Gastrointestinal Absorption, Distribution and Retention of Cesium Fed Chronically in Various Forms to Rats." AEC Research and Development Report HW-35917, pp. 50-55, 1954.

A NEUTRON FILM DOSIMETER

J. S. Cheka

Health Physics Division
Oak Ridge National Laboratory
Oak Ridge, Tennessee

The film badge used at Oak Ridge National Laboratory from 1943 until a few years ago is shown in Figure 1. It contained 2 dental-sized gamma films of overlapping sensitivities, and 1 film coated with nuclear emulsion. A 1 mm cadmium sheet shielded half the area of the films. This shield served both to evaluate the quality of the electromagnetic radiations on the gamma films and also to filter out thermal neutrons from part of the neutron film. Consequently, in the neutron film, only recoil protons from fast neutrons were recorded behind the shield, while in the unshielded portion, in addition, there were recorded the 0.6 Mev protons from the N-14(n, p)C-14 reaction due to thermal neutrons. In this manner, the quality of the incident neutron radiation was indicated.

However, the problem was not solved. The track count was a measure of neither dose nor flux, the latent images were not stable, and the film was much less sensitive than one desires for a monitoring medium.

The measurement of neutron flux is not a measure of dose since dose per neutron is a function of energy. Snyder and Neufeld calculated total or multiple collision dose per neutron incident on a body normally, based on tissue composition and the probable histories of neutrons of several specific energies. These values are used to determine MPE. However, since a film badge is worn next to the body, so that reflected neutrons again impinge on the film, a first collision dose curve will give a better measure of the body dose. Such a curve was calculated on the basis of the cross sections published by Hughes' group in 1952. In general, its magnitude is about 2/3 of the total dose. This curve is shown in Figure 2.

Film response to neutrons is also a function of neutron energy, as the number of recoil protons depends on the collision cross sections of neutrons with hydrogen. The emulsion will record the passage of a proton irrespective of whether the proton is formed in the emulsion or outside it, and it takes a proton with an energy of approximately 0.25 Mev to generate a 3-grain track, while tracks of less than 3 grains cannot be identified positively. The track count per neutron due to recoil protons formed in a 30μ emulsion by neutrons of various energies appears as Curve 1. It is found by multiplying the H atom density by the collision cross section and by the probability of the transfer of at least 0.25 Mev of energy.

The contribution of the film base is Curve 2. In this case, in addition to the previous type of calculation, account must be taken of the ranges and directions of the recoil protons, and only those counted which will enter the emulsion with a residual energy of at least 0.25 Mev. The film base thickness is just the range of a proton of 4.5 Mev energy and, as can be seen, for energies above this value the track contribution falls off with the H collision cross section.

This paper also appeared in Nucleonics, Vol. 12, No. 6, p. 40, 1954.

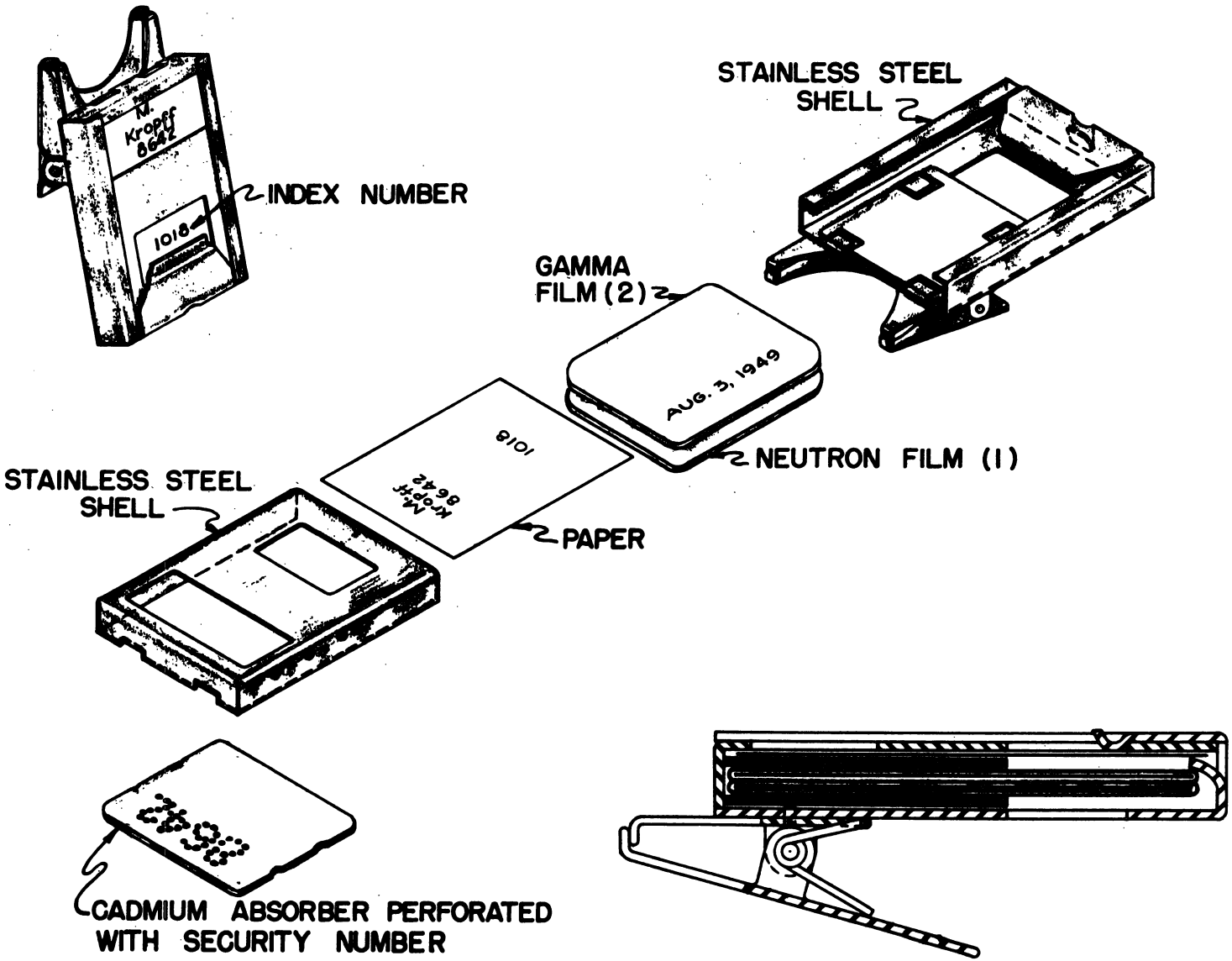

Figure 1. FILM BADGE

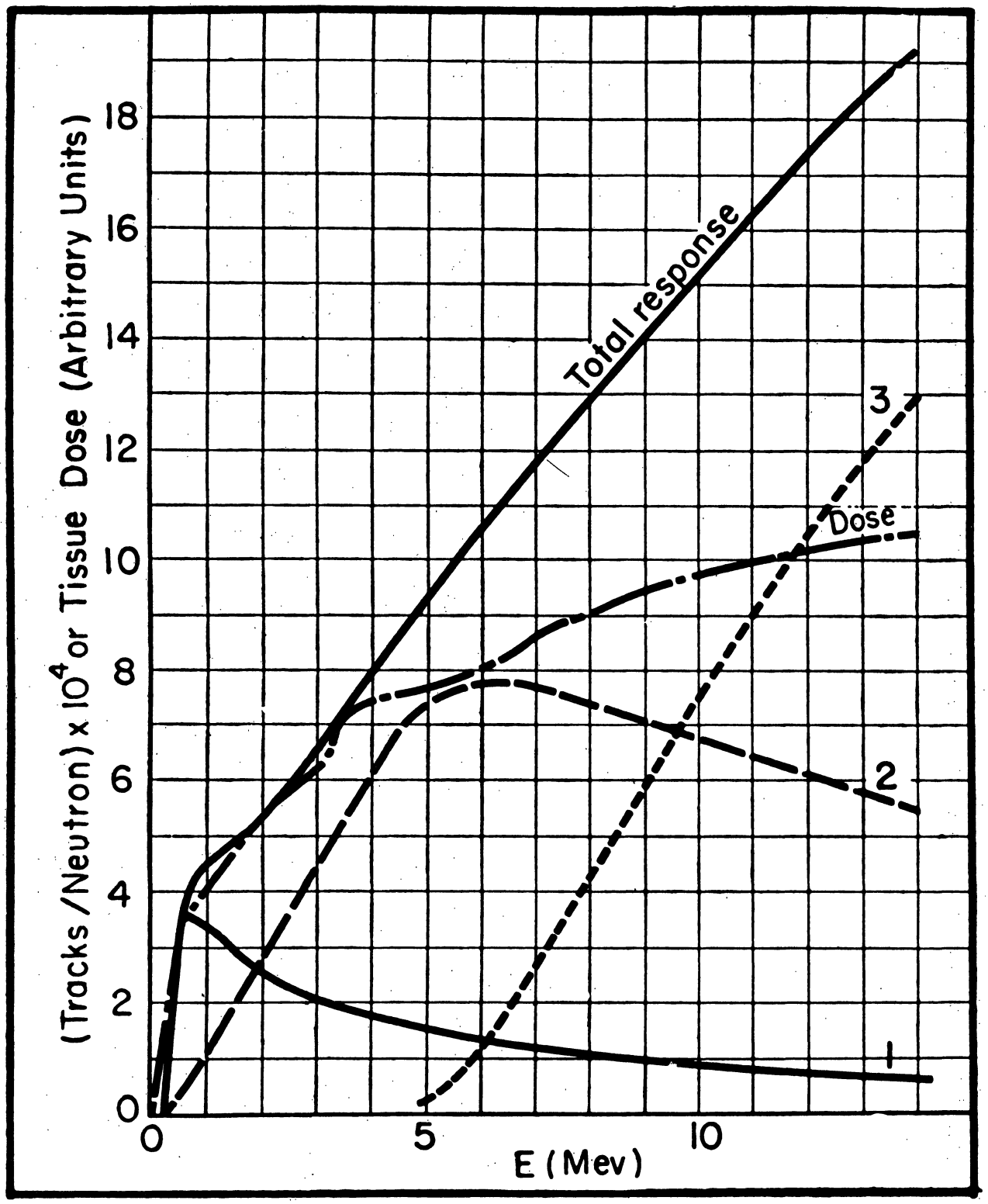

Figure 2. NEUTRON RESPONSE OF UNMODIFIED FILM BADGE

The proton contribution of the film wrapper and other external hydrogenous substances is represented by Curve 3. In this case the contribution to track count has to be calculated as that of a shielded radiator, the film base supplying the shield.

The sum of these 3 is the curve marked "total response." The response we are seeking, however, is the first collision dose curve as indicated. As can be seen, the total response curve corresponds to the dose curve up to about 4 Mev; beyond there it becomes increasingly too high until, at 14 Mev, it is about twice that required. If the film were shielded by a thick, non-hydrogenous material, the response would show fair agreement with the dose curve up to about 7 Mev, beyond which it would become increasingly too low.

By replacing the usual black paper between the film and wrapper with a 27 mg/cm^2 aluminum foil, one makes the total shielding of the Al + film base $\sim$6 Mev. This brings the response curve into agreement with the dose curve up to $\sim$10 Mev, which is sufficient for use around reactors or Po-Be sources. For energies up to 14 Mev, one builds up the radiator formed by the wrapper to 45 mg/cm^2 of cellulose equivalent, and adds 85 mg/cm^2 of aluminum shield, followed again by cellulose.

To make the film meter less directional, it was specified that an additional film base face the emulsion. The latter is coated with No. 5302 emulsion and thus serves as a very high range, or catastrophe gamma detector. Table 1 shows the structure of this dosimeter packet. Eastman has been supplying such a packet for over a year.

Its response is shown in Figure 3. The solid line is the first collision dose curve, which we try to approximate. The dashed line shows how well the dose curve can be fitted if several laminations are used. The dotted line shows the response of the packet we are using. This consists of the original 0.008-inch film base packaged as before, except that a 27 mg/cm^2 Al foil replaces the black paper used originally. The response of this combination is seen to be within $\pm$ 8 percent of the dose curve throughout, and, since one seldom encounters monoenergetic neutrons, the errors should probably tend to cancel each other.

There is, however, an inherent source of error in this method. The response shown here is calculated on the basis of 2.7 percent H_2O in the emulsion. This is the equilibrium value that the gelatin of the emulsion will absorb at 50 percent R.H. and accounts for $\sim$20 percent of the H in the emulsion. Thus, in a dry climate the response is low, and in a wet climate the response is high at low energies, where most of the protons recorded are formed in the emulsion itself.

While photographic latent images are fairly stable, those in nuclear emulsions are much less so. The rate of deterioration is a function of temperature and humidity, especially the latter. The effects on track populations of 3 different sets of storage conditions between exposure and development are shown in Figure 4. The steepest curve shows the result of storing the exposed film in Tennessee in the summer. This was to simulate field conditions. Temperatures run in the 80's and 90's and R.H. is high. As 12 percent of the tracks are lost in about 1 week, we make such a correction when reading films which have been worn a week. The next curve shows the results of storage at 50 percent R.H. at $\sim$70°, i.e., in an air-conditioned laboratory. Here a 12 percent track loss occurs in about 3 times as long a period. The flat curve shows the result of storing in a desiccator at 70°. Here the 12 percent track loss does not occur for 2 months.

There would be several advantages to packaging a dry film in a moisture-proof wrapper. First, with a known, constant moisture content the response of the film would be uniform and known. Then, with the low moisture, the latent images would be more stable, enabling a longer monitoring period. This would cut the time spent in processing and reading the film. It would also increase the track density for a given rate of exposure, thereby improving the statistical accuracy of the readings.

The maximum permissible exposure rate to fast neutrons over a period of 1 week produces $\sim$3,000 recognizable tracks/cm^2. The figure for thermal neutrons is almost the same. Considering

the small size of the developed silver grains, i.e., a few tenths of a micron, and that tracks down to 3 grains are counted, it is necessary to use high magnification and dark field illumination. At 950X the area of one field is 2×10^{-4} cm^2 and consequently a maximum permissible exposure rate for 1 week produces $\sim$0.5 track/field. If discrete fields are read - even if 20 or 30 are read - the track total representing 1 week MPE is a small number, and statistical significance is poor. A much larger area may be scanned by using a traverse instead of discrete fields. Figure 5 shows a film holder used for this purpose. The film is placed in the recess between a glass slide and the body of the holder. The bosses hold the slide in place. The viewing slits are so placed that through one, one sees the shielded portion of the film and through the other, the open window. However, the slits can be milled in any other position to accommodate any other shield pattern the badge may contain. The lead weights are added to ensure flatness of the film.

TABLE 1

LAMINATIONS OF HYDROGENEOUS MATERIAL AND ALUMINUM FOIL AROUND NTA FILM TO ADJUST TRACK RESPONSE TO FAST NEUTRON TISSUE DOSE

Material	Thickness (mg/cm^2)	Energy of Proton Whose Range Equals Cumulative Thickness of Material to Emulsion (Mev)
Cellulose (or front film)	≥ 76	≥ 14
Aluminum	85	11.05
Cellulose	24.2	8.0
*Cellulose (film wrapper)	10.3	6.6
*Aluminum	27	5.9
*Film Base	28.5	4.37
*Emulsion		
*5302 Coated Film	28.5	4.37
*Aluminum	27	5.9
*Cellulose (film wrapper)	10.3	6.6
Cellulose	24.2	8.0
Aluminum	85	11.05
Cellulose	≥ 76	≥ 14

* These constituents are present in the packet as supplied by the manufacturer.

A stop is set at each end of the mechanical stage to ensure a predetermined distance of travel. Then the area scanned is the product of this distance by the diameter of the field of view. Thus, one can scan the equivalent of a large number of fields without counting the fields, and statistical uncertainty can be reduced to a desired level.

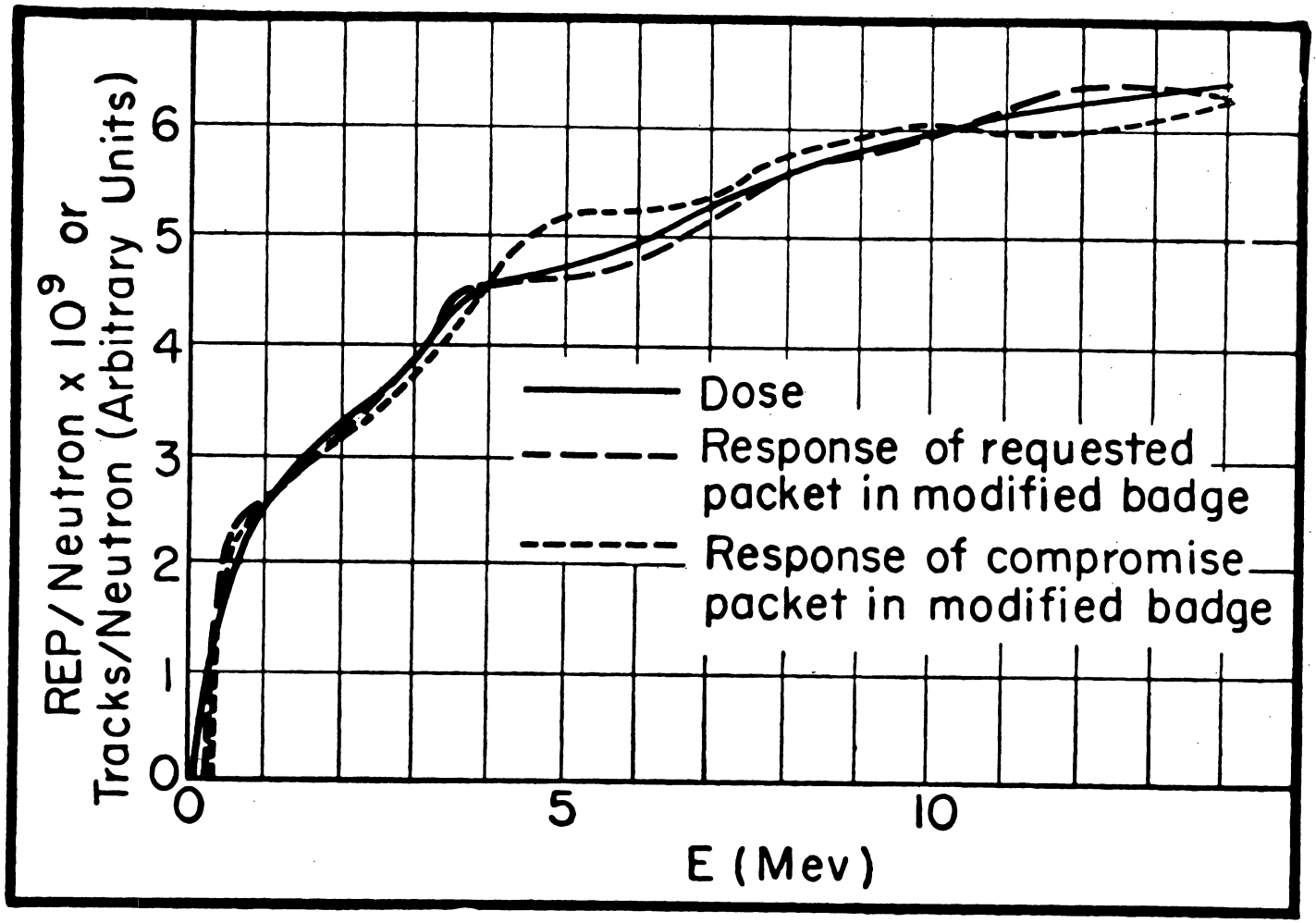

Figure 3. FILM RESPONSE FITTED TO CALCULATED FIRST-COLLISION DOSE

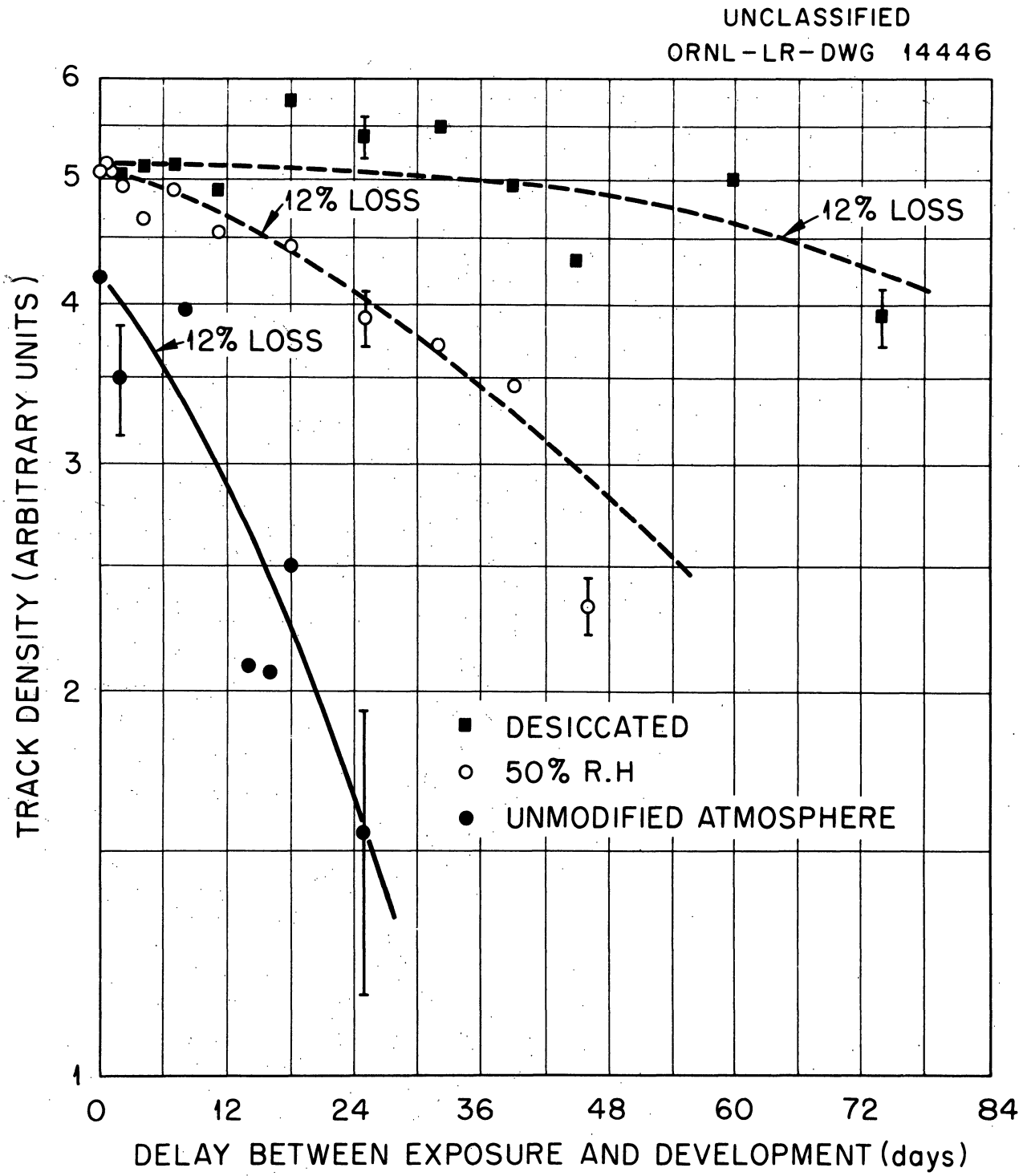

Figure 4. EFFECT OF RELATIVE HUMIDITY ON LATENT IMAGE STABILITY

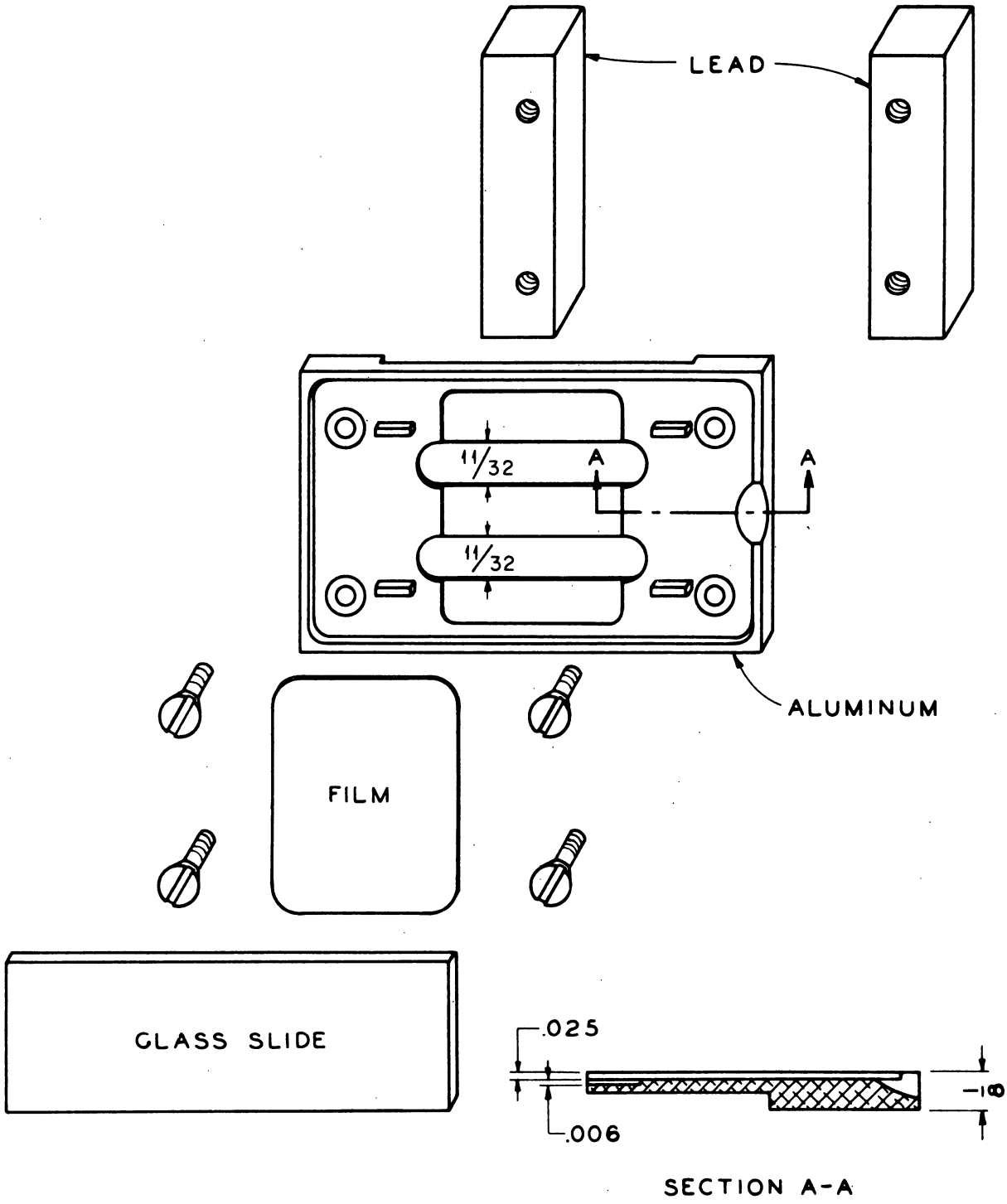

Figure 5. EXPLODED VIEW OF FILM HOLDER

The traverse method of film scanning has not been field-tested here, but is being used at the Naval Research Laboratory. It was reported by Garcia[1] that ± 20 percent accuracy can be obtained in traverse reading in as little or less time than ± 50 percent accuracy can be obtained by use of the discrete field method.

If all these features are incorporated, such a film badge meter supplies the best available means of personnel neutron monitoring which is accurate in the range of the present MPE. It does require processing and scanning by microscope. As yet there is no satisfactory, direct-reading, integrating, fast neutron meter which can be worn by personnel.

After processing, such a film also serves as a permanent record of exposure and requires little storage space. In addition, the presence of the high range gamma films enables the use of the packet for coverage in case of accident of personnel not exposed to neutron radiation. For this purpose, the film packet remains in the badge for an extended period. In this connection, by changing to a more sensitive emulsion, the packet may be used as a long-range, integrating, gamma dosimeter.

BIBLIOGRAPHY

1. Garcia, Luis. Personal Communication.

A SIMPLIFIED FAST NEUTRON FILM DOSIMETER

S. W. Ross* and E. Tochilin

U. S. Naval Radiological Defense Laboratory
San Francisco, California

(*Presently with Radiation Detection Company, Palo Alto, California)

At the present time only nuclear track plates are used for fast neutron personnel monitoring. To read many track plates under a high power microscope is a lengthy and extremely tiresome procedure. Also, it is far more difficult to train qualified operators for this type of work than to read a comparatively simple densitometer and interpret density in terms of dose. It was therefore attempted to develop a film badge with which fast neutron dose could be obtained directly from density measurements.

The Navy Department is particularly interested in such a badge for use around installations such as shipboard reactors. Under such circumstances a considerable number of people work in a close space around a reactor and simple monitoring methods are needed. For these reasons we are particularly interested in a badge that is usable with a fission or moderated fission spectrum. In this comparatively low energy region, proton recoil tracks are extremely short and difficult to distinguish from background grains. At the University of California Radiation Laboratory, 1.5 tracks per field under a magnification of 430X are counted for a weekly tolerance dose of 10^7 n/cm^2 for a fission spectrum.

The sensitivity of film to fast neutrons is not great enough to register a weekly tolerance dose. We have observed that 100 rep of fission neutrons are required to produce blackening equivalent to one r of Co-60 gamma rays. Similar measurements with thermal neutrons showed that a flux of 10^{10} n/cm^2 would produce the same results. Investigations by Rausa[1] have shown that film sensitivity to thermal neutrons could be greatly increased by activation of foils placed in contact with the film. We have modified this technique for the detection of fast neutrons by first thermalizing them in a suitable moderator and then measuring the thermalized component of the neutron flux.

Preliminary exposures were made with thermal neutrons, using silver foils as the capture material. Silver, when activated by thermal neutron capture, emits 1.7, 2.2, and 2.8 Mev betas with a maximum half-life of 2.3 minutes. This short half-life allows the film to be developed within 15 minutes after an exposure without any loss in sensitivity. The high energy betas can penetrate the entire film packet, consisting of wrapper and 2 films, without appreciable attenuation. Films wrapped with silver were exposed in the thermal column of a water boiler reactor. With an optimum thickness of 0.015-inch silver, 10^7 thermal n/cm^2 produced a density equivalent to 40 mr of Co-60 gamma rays. This represents an upper limit of sensitivity for our system.

Thermalization of fast neutrons was accomplished by the use of a polyethylene moderator placed in front of the silver. Additional thermalization results from the human body at the back of the badge. Experimental studies with bare gold foils in a 6-inch polyethylene cube showed that with a Po-Be source, maximum activation of the gold occurred at about 2 1/4 inches, and that with fission neutrons and with neutrons from 12 Mev protons on a thick beryllium target, the peak was at about 1 1/2 inches. Comparisons of fast and thermal flux measurements with fission neutrons and with the proton beam indicated that beyond the thermal peak, the 2 slopes were essentially the same. In this region thermal neutrons can be considered proportional to the fast neutron flux.

For the badge, a moderator thickness of 3/4 inch was chosen. This resulted in a sensitivity loss of about 20 percent but produced a reasonably small badge that was comfortable to wear.

The complete badge, as shown in Figure 1, consists of a 3/4-inch polyethylene moderator with a slot for the film packet, plus a 1/8-inch plastic back with a metal clip to hold the badge on the belt. It is important that the badge be worn close to the body, which acts as an additional thermalizer and backscatter medium. Inside the unit, the metal foils are held in 2 oval depressions in each plate. The upper hole contains 0.015-inch silver backed by 0.025-inch tin. The lower one contains 0.050-inch tin. The combination is matched in such a way that no difference in film density is observed under the 2 windows for Co-60 gamma rays. The filters also tend to minimize energy dependence with low energy X rays. In this manner the badge serves as a monitor for both neutrons and gamma radiation.

For calibration purposes, the badge was exposed to the cyclotron neutron spectrum resulting from the bombardment of a thick beryllium target by 12 Mev protons. As can be seen from Figure 2, this spectrum is slightly harder than that of the Godiva critical assembly at Los Alamos. Under these conditions, a weekly tolerance dose of 10^7 n/cm^2 produced film blackening equivalent to 30 mr of Co-60. Calibrations with the Godiva assembly are under way and preliminary results show the same sensitivity as with the cyclotron neutrons.

The neutron film badge in its present form is restricted in use to a fission type neutron. High energy spectra such as are found around accelerators will produce insufficient film blackening, as the degree of thermalization and the scattering cross sections are too small. Another limitation of the system involves the presence of any significant gamma radiation. Enough blackening can be produced so that differences in reading between the 2 shielded regions become insufficient to be measured accurately. For such a case the badge contains a nuclear track emulsion which can then be used to determine neutron exposure.

The badge is also affected by the presence of thermal neutrons. It is not possible to shield these out as they will scatter back into the badge through the body. Under such circumstances the dose would be overestimated. This condition was observed when fast neutron exposures were made with a fission plate located in a large opening of a thermal column with from 3 to 10 times more thermal than fast neutrons. This, however, is a situation that will seldom be encountered in a nuclear power plant.

In conclusion, we would like to say that this badge acts as both a fast neutron and gamma ray dosimeter. The badge contains a sensitive gamma-ray film (Eastman Type K or DuPont Type 555) together with a nuclear track emulsion. Under normal conditions the dosimeter film is used to determine neutron exposure. The nuclear emulsion is read whenever a high gamma exposure or a serious overexposure is indicated or under any condition where a more accurate evaluation of the fast neutron dose is warranted.

BIBLIOGRAPHY

1. Rausa, G. D. University of Rochester Report UR-253, 1953.

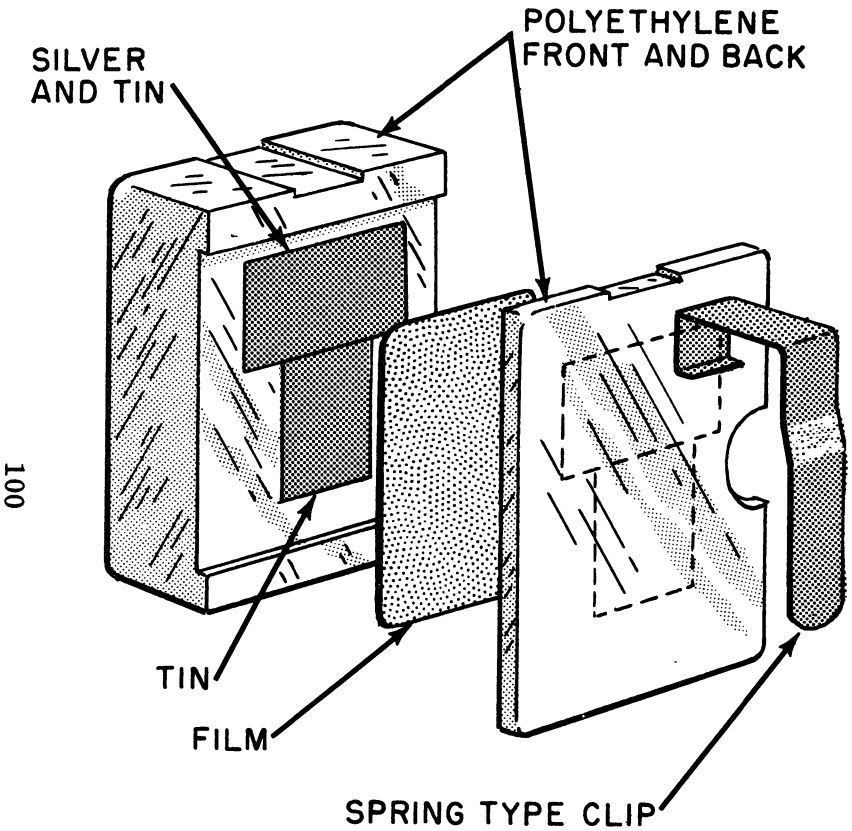

FAST NEUTRON FILM BADGE

Figure 1. A SIMPLIFIED FAST NEUTRON FILM DOSIMETER

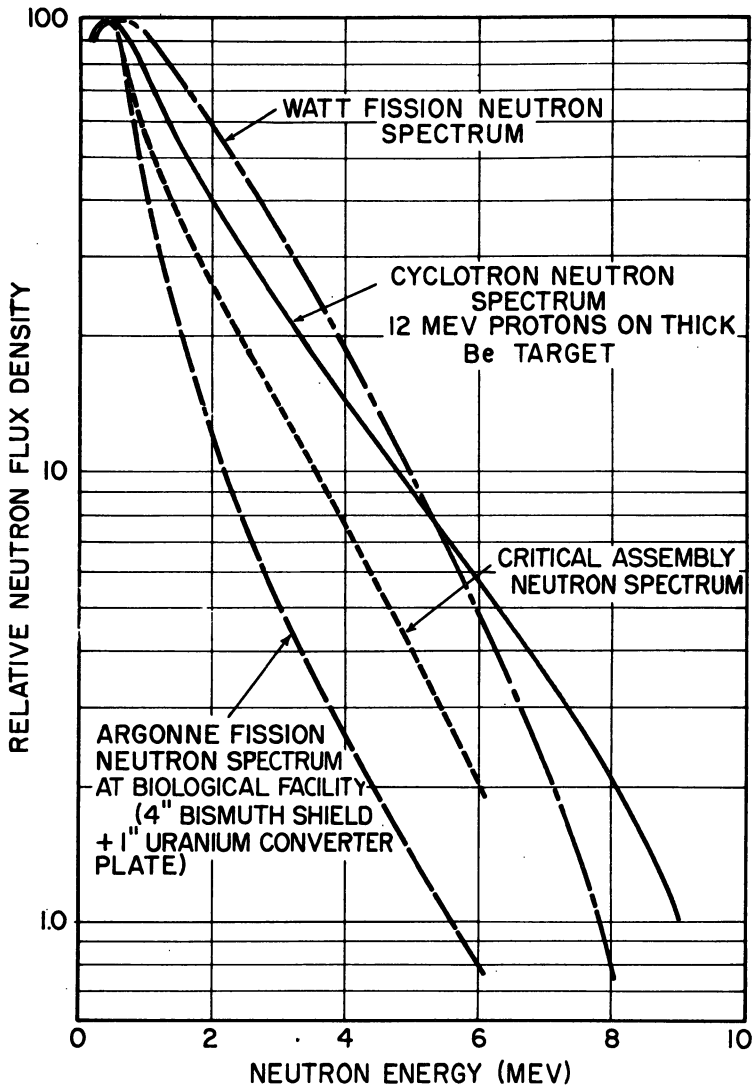

Figure 2. COMPARISON OF VARIOUS FISSION NEUTRON SPECTRA

A SCINTILLATION TYPE DOORWAY MONITOR

D. A. Campbell and L. D. Test

Hanford Atomic Products Operation
General Electric Company
Richland, Washington

INTRODUCTION

The clothing of personnel exposed to possible radioactive contamination is monitored manually as a routine procedure at Hanford. As an additional safeguard, a doorway-mounted instrument for automatically monitoring the clothing of all personnel in certain specific locations was considered to be desirable.

The objective was to produce a reliable, inexpensive instrument for the detection of hard beta contamination on the clothing of personnel. It was required that the monitoring be accomplished without interrupting the normal activities of the employees; therefore, the detectors were installed in the plant exit doorways. Detectors having a low gamma background were required because of the short period of time a radioactive source would be in the vicinity of the detectors.

SELECTION OF A DETECTOR

Various detectors were tested under standardized conditions to determine which was most satisfactory for this application. The detectors tested were a GM tube, a liquid scintillator, and several crystal scintillators. The principal criterion used in making the choice was the count-to-background ratio. The detector chosen was a thin anthracene scintillator attached to the photocathode of a Du Mont Type 6292 multiplier phototube.

PRODUCTION OF A THIN ANTHRACENE SCINTILLATOR

Various methods for producing a thin anthracene scintillator were tried. Attempts to saw or shave off thin layers from a large crystal were not successful because the thin layers were fragile and pieces of uniform thickness could not be produced. A fairly simple method which was quite satisfactory consisted of mixing anthracene powder with a transparent adhesive and applying the mixture to the cathode of the multiplier phototube. Two adhesives tried were Lucite powder dissolved in acetic acid, and rubber cement thinned with xylene. The use of dissolved Lucite powder results in a more rugged and permanent scintillator.

The detector is completed by forming aluminum foil over the scintillator to exclude external light and to reflect the light produced in the scintillator. Three layers of 1/3 mil aluminum foil were used to prevent the alignment of pinholes which were present in the thin aluminum foil. Black scotch electrical tape is used to hold the aluminum foil in place and as a light shield to cover the remainder of the multiplier phototube.

THE WIDE-ANGLE BETA DETECTOR

An experimental doorway monitor was assembled, using the scintillators previously described; but it was found that the directional characteristics of the detectors were not satisfactory.

As a first approximation, the sensitivity of a thin scintillator at a fixed distance from a point source of radiation varies directly with the solid angle subtended by the scintillator. It can be seen that with the movement of a point source along a line parallel to the plane of a disc-shaped detector, there will be a great change in this angle. This is shown in Figure 1. Both the inverse square law and the decreasing projected area of the detectors contribute to a rapid decrease in sensitivity of such a monitor as the distance between the source and the plane of the doorway is increased. The sensitivity is also low between adjacent detectors in the plane of the doorway.

To improve the sensitivity to radiation from the sides, Lucite hemispheres covered with anthracene scintillator were attached to the multiplier phototubes. It is obvious that the projected area along a line parallel to its flat surface will be more nearly constant for a hemisphere than for a disc. As shown in Figure 2, with equal sensitivities for a source in front of the detectors, the hemispherical scintillator has a 4 to 1 improvement in sensitivity to radiation from the sides.

The Lucite hemispheres were attached to the multiplier phototubes using polyvinylacetate, a transparent thermoplastic material produced by the Bakelite Company. The hemispheres were then dipped in Lucite dissolved in acetic acid, and powdered anthracene was liberally sprinkled over the surface. After drying, the excess anthracene was shaken off and a second layer applied in the same manner. Finally, a protective film of Lucite was applied to prevent the anthracene from being rubbed off. These scintillators have proved very satisfactory in this application.

ARRANGEMENT OF DETECTORS

After the selection of a suitable detector for the doorway monitor, the principal problem was to determine how many detectors would be required. On first consideration of this problem, it might seem that the more detectors used the better the sensitivity would be. This, however, is not true. The sensitivity is determined by the ratio of the source count to the background count. Since all the multiplier phototubes contribute equally to the background count and only a few are effective in counting a source carried through a doorway, the optimum number is the fewest which can be used while maintaining adequate sensitivity at all points in the doorway. A reasonable criterion for the minimum allowable sensitivity at any point in the plane of the doorway is that it should not be significantly less than the sensitivity midway between the sides.

It was found that with detectors at 1, 3, and 5 feet from the floor along the sides of the doorway and 1 detector overhead at 7 feet, the sensitivity between adjacent detectors was approximately the same as the sensitivity midway between the sides of the doorway. Calculations showed that the addition of detectors at 2, 4, and 6 feet from the floor along the sides of the doorway would have a negligible effect on the sensitivity along the centerline. Near the sides of the doorway, the sensitivity would be improved for a source near an added detector, but would be poorer for a source near an existing detector. Therefore, the additional detectors were not used.

THE COMPLETE INSTRUMENT

Figure 3 is a block diagram of the complete instrument. Pulses from the 7 detectors are combined in an additive mixer which also provides for gain equalization adjustments. Following the mixer, the pulses are amplified by a linear amplifier which also includes an amplitude discriminator for rejecting low energy background pulses. The output of the amplifier discriminator is connected to the input of a Technical Measurements Corporation counting-rate meter. This counting-rate meter is equipped with an alarm circuit which can be adjusted to operate a light and buzzer at any desired counting rate. An Esterline-Angus recorder is connected to the recorder output of the counting-rate meter.

A photograph of a typical doorway monitor installation is shown in Figure 4. Metal guards are used to protect the detectors from accidental damage, since the aluminum foil covering can be torn easily.

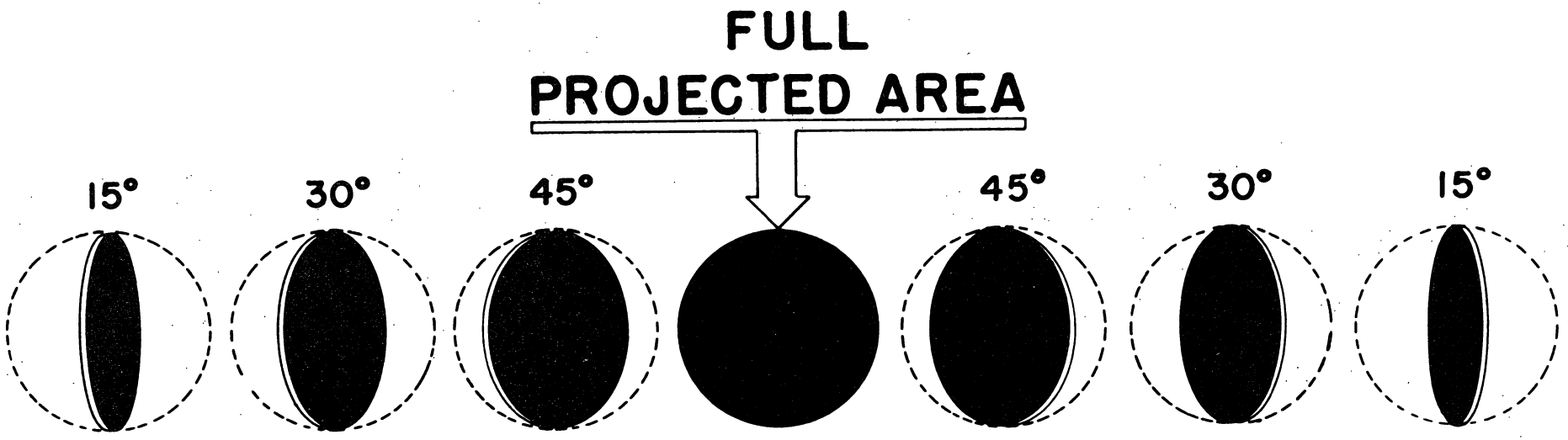

Figure 1. THE PROJECTED AREA OF A DISC DETECTOR AS A FUNCTION OF POSITION ALONG A LINE PARALLEL TO THE PLANE OF THE DISC

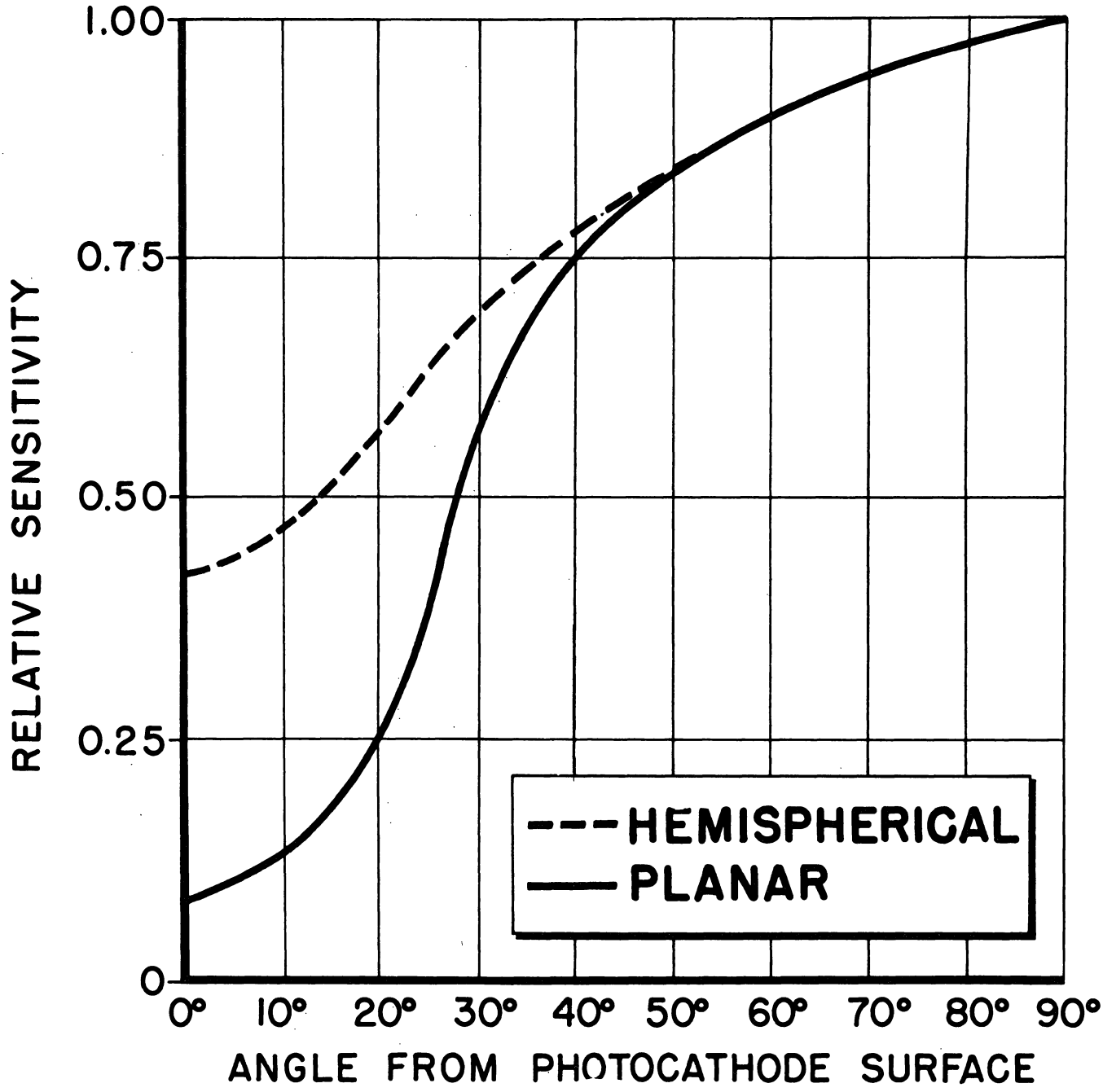

Figure 2. SENSITIVITY VERSUS ANGLE FOR PLANAR AND HEMISPHERICAL SCINTILLATOR SURFACES

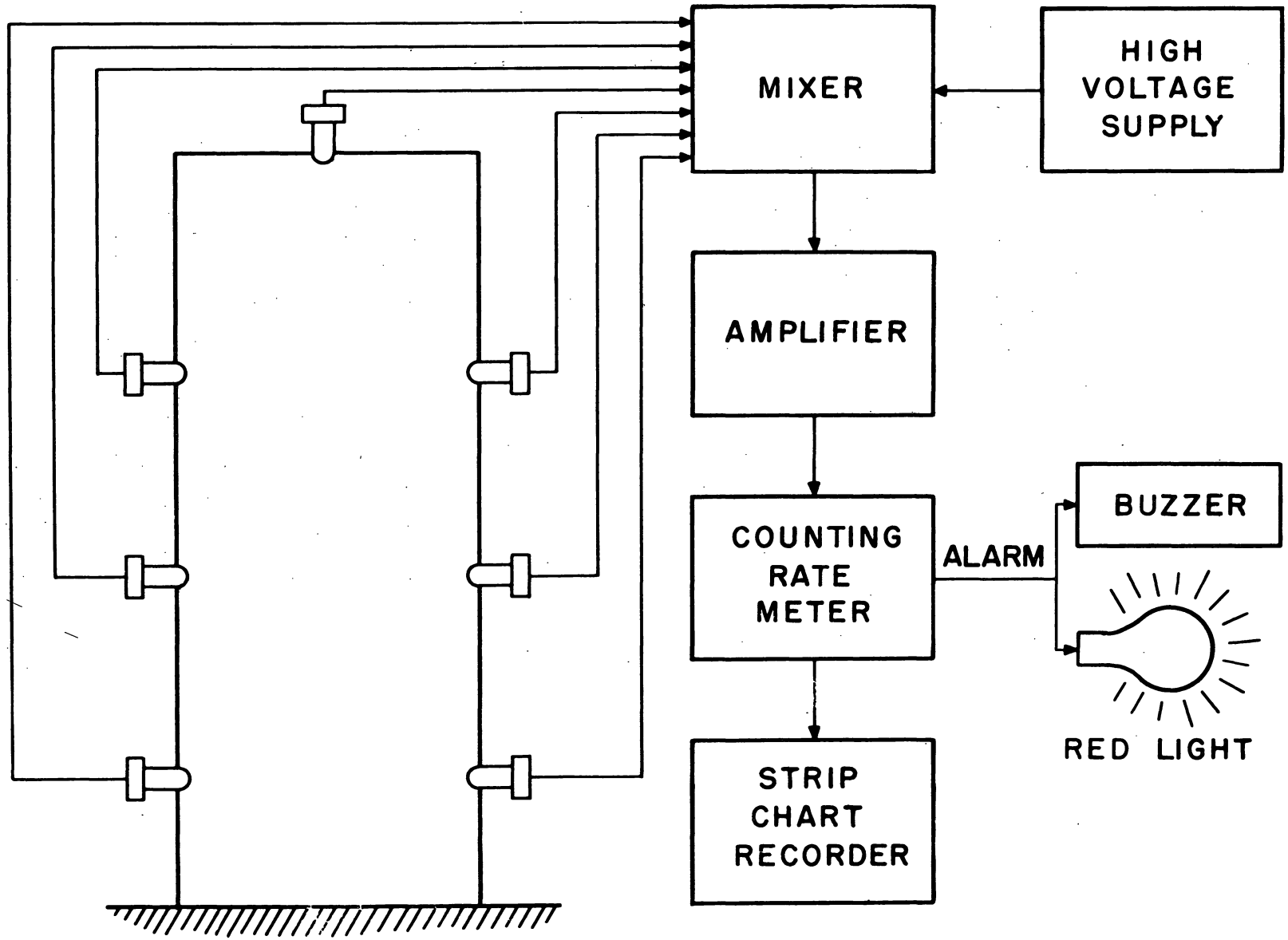

Figure 3. BLOCK DIAGRAM OF THE DOORWAY MONITOR

PERFORMANCE

The normal background for a doorway monitor is adjusted to 200 counts per minute. Since the counting-rate meter must respond rapidly, however, considerable meter fluctuation results. This requires the alarm to be set at 400 to 500 counts per minute to avoid operating on random fluctuations. A 0.5 microcurie source of 3.5 Mev beta radiation will readily trip the alarm when carried through the doorway at a normal walk.

CONCLUSIONS

The doorway monitor satisfactorily performs the function for which it was intended. A similar instrument for detecting other types of radiation could be assembled easily, using a different number and type of detector.

THE VARIATION OF NEUTRON DOSE WITH NEUTRON ENERGY AND GEOMETRY

W. S. Snyder

Health Physics Division
Oak Ridge National Laboratory
Oak Ridge, Tennessee

It is difficult to give precise information concerning the dependence of neutron dose on neutron energy or the geometry of the source and irradiated phantom. The discussion here will be far from a complete and detailed analysis of the problem, but it does attempt to give rough limits on the degree of variability to be expected.

For the most part, the discussion will be concerned with the site of maximum dose and will attempt to give methods of estimating it which, while far from precise, may still be of value in many practical cases.

The dose at any site in the irradiated phantom will be separated into a "first collision dose" and a "build-up dose." The "first collision dose" consists of the absorbed energy that is released by a neutron making its first collision or interaction with an atom of the phantom. All the rest of the dose is termed the "build-up dose," and consists of energy released by subsequent interactions of the neutrons with the atoms of the phantom. The only reason for making this separation is that, for neutron energy less than 10 Mev, the first collision dose is easily calculated. It is given in rads for a beam source by

$$(1) \qquad D = 1.6 \times 10^{-8} \, I \, e^{-\sigma T} \left\{ \sum_i \sigma_i \frac{2M_i E}{(M_i+1)^2} + \sum_i \sigma_i(\text{capture}) \, E_i \, A_i \right\}$$

The first group of terms represents the dose caused by elastic collisions and the second group of terms the dose caused by capture collisions.

In (1), I is the intensity in $n/cm^2/sec$; σ_i and σ_i(capture) are, respectively, the macroscopic cross sections for an elastic collision and a capture collision with the i^{th} type of atom of the phantom; $\sigma = \sum_i \sigma_i$, that is, the total macroscopic cross section; T is the thickness of phantom material the neutron must traverse to reach the site in question; E is the neutron energy and E_i the energy released by a capture collision with an atom of type i, both in Mev; M_i is the mass number of an atom of type i; and A_i is a "fudge factor" to represent the fraction of energy produced by capture which is absorbed at the site.

Actually, the formula assumes that all the energy of the recoil atoms is absorbed at the site where the collision occurs, and the same assumption should therefore be made for the protons and alphas produced by the capture collisions. Thus, all the A_i may be taken as 1 except in the case of gamma rays. The precise knowledge of A_i for gamma rays requires an integration over the phantom and thus is not entirely simple. For a small body we may take T = 0 and the A_i corresponding to gamma rays as 0, since in a very small volume of tissue only a negligible fraction of the gamma energy will be absorbed. This simplified formula, i.e., with T = 0 and also the A_i corresponding to gamma rays set equal to 0, will be referred to as the first collision dose. It corresponds roughly to the dose in a small phantom irradiated by neutrons. Strictly, the phantom should be small compared to the mean free path of the neutrons so that the attenuation is negligible,

but should be large compared to the range of the recoils and protons produced since it assumes all their energy is absorbed. Since the formula neglects inelastic collisions, it is not strictly accurate above a few Mev, but the discrepancy due to neglect of inelastic collisions should not be gross below 10 Mev. Figure 1 shows the various terms of (1) as functions of the neutron energy as well as the biological dose obtained by weighting each term by the appropriate RBE and summing. The RBE used are those recommended by the National Committee for Radiation Protection.

For an isotropic point source, the intensity I is given in n/sec and a factor of $1/4\pi R^2$ is inserted to take account of the inverse square attenuation for a site at distance R from the source.

Consider a phantom irradiated by a broad beam of monoenergetic neutrons and let M be the site of maximum dose. Clearly, the first collision dose as defined above cannot exceed the dose at M. Thus we have an easily calculated lower bound on the maximum dose. If the phantom is enlarged by the addition of material which does not shield it from the beam, then the dose at M is increased (see Figure 2). If the phantom is a convex body, this can be rigorously proven mathematically and is physically obvious. Indeed, for a convex body the path of a neutron scattered from one site to another in the body does not leave the body; hence, the energy absorbed at M from the "build-up dose" as multiple scattered neutrons is unaffected by the added material. In addition, some neutrons will be scattered from the added material into M and thus the dose at M is increased. We may, therefore, enlarge the phantom to a slab of material and get an upper bound on the maximum dose. Thus we have the rule: The maximum dose in a convex body cannot exceed the maximum dose in a slab which will contain the body. Actually, minor departures from convexity can hardly cause gross deviations from this rule, and we may conclude that the maximum dose in any approximately convex body will lie between the first collision dose and the maximum dose in a slab which will contain the body.

These 2 bounds do not differ too greatly for fast neutrons. Figure 3 shows the variation of the maximum dose with slab thickness for several thicknesses and energies. These values were computed[1] using Monte Carlo methods, and these studies are far from complete. It can be seen from the figure that for a slab of tissue 30 cm thick, the ratio of maximum dose to first collision dose does not exceed a factor of 1.6 for neutrons with energy between 0.1 Mev and 10 Mev. The ratio then rises as the neutron energy decreases, being about 3 at 0.02 Mev and becoming of the order of 500 at 0.1 kev. This rapid and extreme variation makes the ratio of doubtful practical importance for computation in such cases. It simply reflects the fact that at these energies, the dose in a thick slab is largely caused by the scattered radiation which is not taken into account in the first collision dose. The graph shows approximately how thin the slab must be to bring this ratio reasonably close to 1, say within 10 percent. Further studies are in progress, however, and the results presented here are to be regarded as preliminary.

We may derive some further information from the ratio considered above. The dose caused by fast neutrons at any point on the irradiated surface of the phantom cannot fall below the first collision dose, nor can it exceed the maximum dose. Thus the variation of fast neutron dose over a plane surface irradiated by fast neutrons cannot exceed 60 percent and is generally much less. For example, the maximum dose to the head cannot differ from the maximum dose in the trunk by more than this amount.

Preliminary computations indicate that similar bounds are valid for isotropic sources and for beams not oriented normally to the surface.

It should be strongly emphasized that the bounds given here apply only to the maximum dose, which for the thick slab is near or at the irradiated surface. Deep within the slab the build-up dose becomes far more important and the first collision dose may be a small part of the total dose. For neutrons of intermediate or thermal energy the build-up dose is also of major importance for large phantoms, and the size at which the first collision dose again becomes the preponderant part of the dose is not well defined as yet. Studies now in progress along the lines indicated in Figure 3 may provide useful formulae for these cases as well.

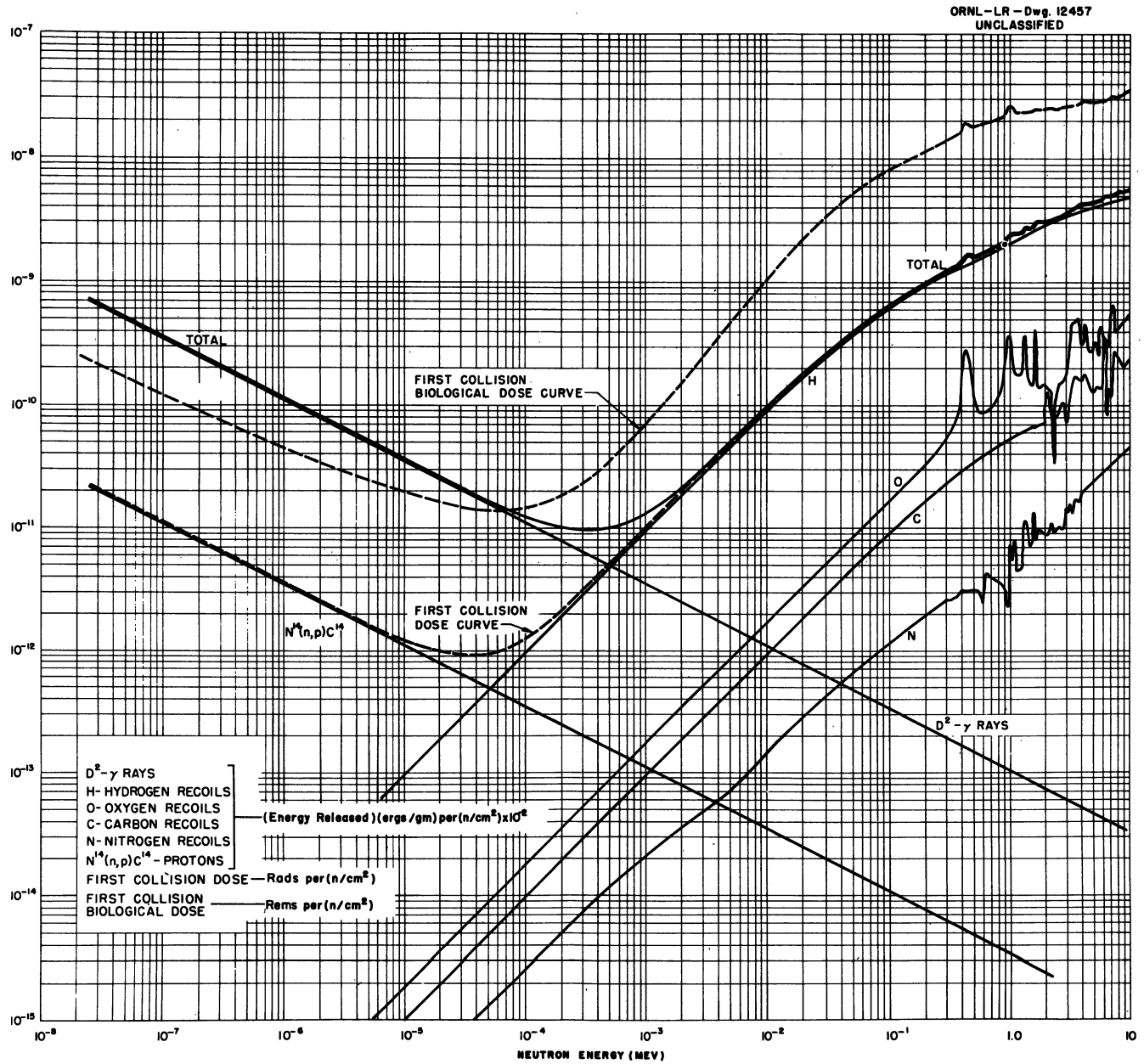

Figure 1. FIRST COLLISION DOSE CURVE

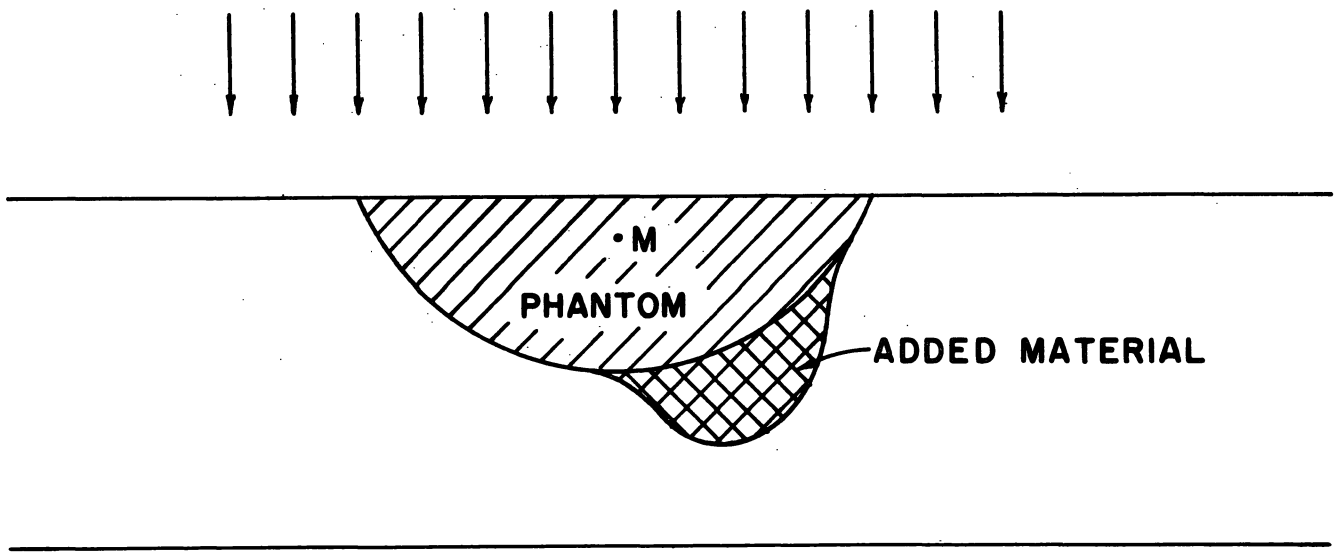

FIRST COLLISION DOSE AT SURFACE $\leqq$ DOSE AT M $\leqq$ MAX DOSE IN SLAB

Figure 2. VARIATION OF MAXIMUM DOSE WITH THE SHAPE OF THE PHANTOM

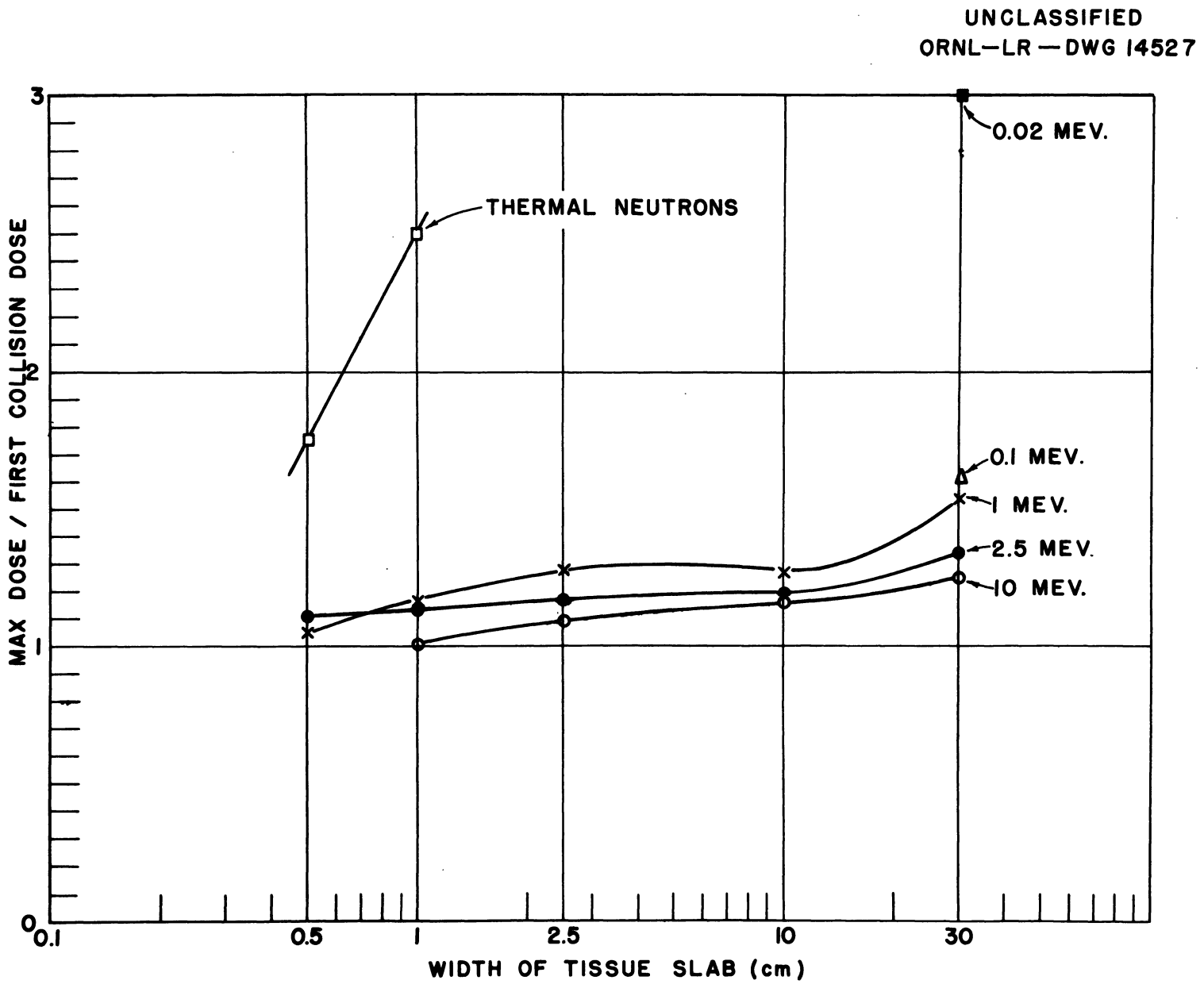

Figure 3. RATIO OF MAXIMUM DOSE AND FIRST COLLISION DOSE

BIBLIOGRAPHY

1. Snyder, W. S. and J. Neufeld. "Calculated Depth Dose Curves in Tissue for Broad Beams of Fast Neutrons." Brit. J. Radiol. XXVIII, No. 331:342, 1955.

ESTIMATION OF EFFECT OF RADIATION UPON HUMAN HEALTH AND LIFE SPAN

H. B. Jones

Donner Laboratory
University of California
Berkeley, California

Recent evidence that long-range effects of radiation simulate aging effects comes from a variety of sources and is consistent with information relating radiation effects with genetic change and changes in cell-population numbers and quality. Evidence and logic support an argument that small increments of radiation-induced morbidity persist as small permanent changes in body functional structures which become detectable as aging, neoplastic disease, and genetic change. It remains to be prooved experimentally, however, that these effects do occur as the result of small irradiation exposures. The testing of this question is not likely because it would involve great technical difficulties. Attempts to procure some evaluation of the problem relating small-dose (5 r to 10 r) effect to life span would involve study under uniform conditions of perhaps several million mice. It is pointed out that in order to establish the effect of the smallest doses as yet measured for genetic effect, namely 25 and 50 r, the geneticist, Curt Stern, and his associates worked for 6 years and examined approximately 50,000,000 individual flies. They came to the acceptable conclusion that these small exposures have the same effect per roentgen upon gene mutation as would be predicted from observations made at higher exposures to radiation. Ionizing radiation effect, in the depression of blood-forming function and blood-forming cells, is proportional to radiation dose even down to 5 r(Hennessy and Huff[12]). Other effects upon blood cells, leading to abnormal doubling of the cell nucleus, are now reasonably established by Dobson in the range of 0.1 to 0.3 r of single exposure, but are not yet tested for proportionality.

There is no reason to doubt the general evidence of a proportional effect of radiation, but it is also possible that linear extrapolations of higher doses to the small-dose range may not give a true representation of the problem. It is known for some kinds of cellular response to radiation that there can be no effective change in function until 2 or more similar critical entities within the cell are affected. Some kinds of observed injury, however, appear to depend upon the effect on one critical entity per cell, and other observed injuries may be the result of damage to any one of a number of critical functional parts. The response that depends upon a chain of 2 or more detrimental changes shows a lesser apparent effect in proportion to radiation exposure at the low-dose ranges. Although this kind of irradiation response does not argue against extrapolation of radiation effect, it may explain a factor of 2 or 4 buffering against detectable radiation effect in the lowest exposure ranges; or it may even have the opposite effect, because radiation effect can add onto partially initiated dysfunctional changes in structures that otherwise would have remained functional.

Radiation effect is most frequently estimated in animals that are rather uniformly irradiated over the whole body. Thus, we are usually generalizing from the observed result of whole body exposure. In some studies (Kaplan[16]), shielding a relatively small portion of the bone marrow from radiation may protect the animal from generation of thymic tumors. In other experimental situations, local irradiation is associated with induction of cancer in that region, quite independently of exposure or shielding of the remainder of the body.

The unfolding of understanding of radiation effects began with association of radioactivity with a kind of burn, the prime observation being the burn on Becquerel's belly brought about by his carrying a souvenir radium sample. Thus, in the first observation of radiation effect is the

element of response to great exposure. In most of the subsequent study of radiation effect, the concern has been the effects of radiation in far smaller amounts. Erythema, the mild, sunburn-like, delayed response of the skin to ionizing radiations, established several of the major concepts of radiation injury, which are: delayed tissue response, effects from which there is recovery, and threshold levels of radiation exposure below which, in the test system, no effect is observed. Most studies on radiation effect have measured physiologic responses which develop within a few hours, or weeks, following radiation exposure; and, in this regard, events such as burns, necrosis, tissue involution, weight loss, metabolic change, radiation-sickness, and survival measures exhibit uniform evidence for a recovery or repair process which follows the initial evidence of radiation damage. Further the latent period between time of exposure and time of development of biological effect decreased with increasing exposure to ionizing radiation; and thus, it became apparent that the threshold effect of radiation represents some balance between quantity of ionization damage and the effectiveness of the repair processes. It is important to keep in mind that the threshold response and the recovery processes associated with radiation effect appear as the response of complex, multicellular systems; on the other hand, as radiation effect has been subjected to analysis at the cellular level, there is less evidence of recovery and more of a quantum change irreversible in kind. Finally, at the molecular level of observation, effects of radiation form a system of generally permanent changes in the basic structure of matter. Grossly simplified, the problem of recovery is the generation of replacement units from relatively less damaged biological functional units. In intermediate ranges of radiation exposure, cells ranging from relatively undamaged to completely destroyed should be present. This is because of the random, quantum action of radiation effect; and, indeed, most cell populations follow a "hit" type of survival as a function of radiation exposure.

The quantitative reaction of mammalian cells to radiation exposure of the whole animal is such that functional reserves are depressed about 0.3 percent of cell function per rep for several days following irradiation. Table I gives values for some of the functions which measure cell destruction.

It appears, then, that each roentgen unit destroys about 3 cells in every 1,000 mammalian cells of the marrow or lymphatic tissue. It is this kind of cell damage which appears to accompany immediate effects of radiation such as burn, radiation-sickness, weight loss, etc. Each roentgen of exposure to X rays also produces in each cell about 100 ionization events, on the average; and, with respect to the mammalian gonadal tissue, each roentgen of exposure produces approximately 2 new mutations per 1,000 cells (based on the estimate that 50 r produces a new mutation in 1 of 10 germ cells [21]). Thus, it appears that, at the cellular level, destruction of radiosensitive cells and gene mutation of the germinal tissue are events of nearly the same probability of occurrence per roentgen in spite of the gross differences in ease of detection of each of the effects, while the average ionization event in the cell is about 40,000 times more likely to occur than either mutation or cell destruction:

$$\text{per r:}\quad \frac{\text{100 ion pairs per single cell}}{\text{2 to 3 cell destructions or mutations per 1,000 cells}}$$

$$\text{ratio} = 1/40{,}000$$

The aftermath of tissue injury, whether by radiation effect or other morbidity-inducing agent, is that damage expressed as cell destruction is largely repaired by the great capacity of the tissues to form new cells. Thus even at 0.3 percent destruction of cells per roentgen, or 26 percent ($1\text{-}e^{-0.003 \times 100}$) destruction at 100 r, cell replacement may be very prompt. Tissue such as marrow can replace 1 cell in every 10 cells during each 24-hour period (Kelly[17]). Thus, radiation damage of the most sensitively responding tissues by a dose of 100 r corresponds to cell destruction which may require 3 days for replacement (100 percent / 74 percent = $e^{0.1 \times \text{days}}$). Whether, in recovery, a tissue system is able to regenerate fully the number of cells contained in it before radiation exposure is difficult to answer. The long-term effects of radiation on life span and functional qualities are probably related to this question.

TABLE I

Source	Time after irradiation	Percent depression per roentgen
Patt[19]		
Lymphopenia	3 days	0.37
Lymph Node Pycnosis	5 hours	0.28
Lymph Node Pycnosis	3 days	0.34
Thymus Involution	3 days	0.31
Spleen Involution	3 days	0.28
Duodenal Lymphocyte Pycnosis	5 hours	0.03
Thymus Cells	6 hours	0.18
Blood Lymphocytes	5 hours	0.14
Thymus Lymphocytes	22 hours	0.40
Thymus	6 hours	0.18
	Radiation Source and Exposure Time	
Jacobson and Marks[14]		
Leukocytes in blood (rabbit, guinea pig, mouse)	X rays 20-40 days chronic irradiation	0.23
Lawrence[18]		
Leukocytes in:		
Leukemia	P-32 therapy	0.23 to 2.5
Polycythemia	1 month	0.3 to 0.7
Hennessy and Huff[12]		
Depression of marrow red cell formation	X ray	0.3

The Long-term Effects of Radiation on Health and Life Span

The estimation of effects of radiation beyond the period of acute manifestation and recovery requires observation over the life span and statistical treatment of events associated with disease and risk of death over the life span. The biological history of the individual animal is marked by certain events which occur with increasing frequency as age increases. As a basic model of the relation between aging and deterioration of body function, we may visualize a system in which certain functional parts are no longer reproducible or fully repairable, so that the loss of a component, such as a finger, a hand, or any appendage, is not replaced. Since there is, at any time in life, a certain average probability that extremities (as a single example of a functional part) may be lost, the number of extremities remaining will decrease on the average as age of the individual increases. Thus, the average loss of extremities is the integrated probability of loss of extremity per unit time over the duration of life lived. Additionally to be considered is the problem that, as the total functional capability of the body decreases with age through loss of general functions, the probability of loss of function per unit time may in itself increase. It is not surprising, then, to find (as has been well known for at least a hundred years) that incidence of morbidity and mortality increases logarithmically with age in adult life. In all human populations, morbidity and mortality are doubling every 8.5 years, and in each animal species at a characteristic rate such as 3.5 months for the mouse and 8 days in the case of the fly.

The remarkable thing is that, regardless of the choice among several mathematical models available for analyzing aging changes in disease and death rate, each species shows a similar and consistent time change function, even though any 1 population sample of that species may vary considerably in level of morbidity or mortality at a given age. Physiologic age, in terms of extent of degeneration of function and appearance of internal disease, may be relatively either advanced or retarded in that population at some reference age. Whether health at an adult age is good or poor, however, the relative increase of risk of death as age increases is at a characteristic rate for that species. Thus, it appears that, in each animal species, including man, health is being degraded by a system which always has the same time characteristic by species. Among all species there exists a similar function for the increase in relative probability of degenerative disease as age increases. This is important because it provides a convenient bridge between species for estimating radiation effect upon the life span; but before we attempt to use such a system for that purpose, it is important to consider general interpretations of the system of aging and appearance of disease.

The average increase of disease with increasing age is a process of great regularity when either morbidity or mortality is used as a measure. Over the adult life span, an increase of 200-to 1,000-fold occurs in mortality rates. The regularity of this increase makes it unlikely that more than half of the individuals in a population are a factor of 2 away from the average trend; indeed, in populations containing admixtures of people having different basic death rates, the combined mortality function clearly reveals that inhomogeneity.

The remarkable feature about the average trend in development of disease is that health in any portion of the life span seems, on the average, to predict health in all subsequent time lives; in other words, health in a reference age as judged from average mortality figures is adequately predicted by health in earlier periods of time. This inspection of the pattern of disease leads to a generalized concept of health as being the sum of unrepaired effects of morbidity experience which grow as systems of disorder or dysfunction into frank manifestations of disease. In general, it may be shown that all of the major diseases of internal origin are interrelated, that the diseases of infancy and childhood are prognostic of the internal disease of adult life, and that there is a very general quantitative relationship of morbidities leading to mortality.

Whatever the projected effect of childhood health upon adult health, it appears that, the younger the individual experiencing morbidity, the greater the effect of that morbidity upon the health later in life. This enhancement of deleterious events of the early periods of life seems to involve several mechanisms: (1) Any injury to function appears to accumulate a greater total

effect upon the individual as time increases; the earlier in life the injury occurs, the greater the total compounding of the effect to a given age. (2) Embryological development and growth have specific requirements for exact continuity of cell life, especially of certain key cells. Small developmental errors due to induction of cell death may become magnified by the process of growth and the interplay of homeostatic functions. (3) Morbidity events occur relatively close together in early life; if radiation-induced morbidities are superimposed at this time, there is then a greater chance that chain-reacting effects will be initiated. In a sense, every stage of embryological development and growth is critical, and frequently one is dependent upon the other, as in a chain of events. Each state of development is subject to modifications which, even though within normal limits, will have a lasting effect upon that individual's functional capacity. Thus viewed, life in utero has a series of developmental stages in which permanent plus or minus changes to health may occur in a way that is entirely similar to the estimated effect of any morbidity upon health.

In quantifying events which can influence the course of human health, the factors of childhood morbidity appear to have an irreversible effect upon tendency toward disease in later life; in this respect they are similar to the long-term radiation effect. The significance of childhood morbidity can be seen in the relationship between adult mortality and childhood mortality for the past century in Europe; it is apparent that the death rate at age 5 predicts the death rate at age 50 despite the random effects of all other factors modifying health in the intervening 45 years of life span.

Adverse physiological phenomena such as overweight, smoking, high blood pressure, lipoprotein disturbance, diabetic state, and other metabolic disorders appear to act as constant factors of increase in the induction of mortality at any age. In the presence of one of these conditions, the death rate at any age is effectively multiplied by a factor characteristic of that condition in that species of organism. When the condition terminates, the death rate tends to return to its former value. Thus, these factors appear to be distinctly modifiable by physiologic change and in this respect are different from irradiation effects and changes induced during the developmental period, which have a large component of permanency.

These increases in mortality risk, which are associated with environmental and physiologic status and which appear to be constant throughout life, act as though they are weighting factors to be multiplied by some more basic system of change that involves the aging system representing physiologic decay. Table II reviews a number of factors which can modify health.

Radiation effect differs from the factors which modify health at the physiologic level of action in that it seems to act directly upon primary systems responsible for aging. Thus, through periods of chronic radiation exposure, the rate of apparent aging increases proportionally to the amount of exposure. Stated mathematically, the death rate shows an exponential increase, the exponent being proportional to the rate of exposure. This is in contrast to toxic systems or systems of improved hygiene which, operating at a physiologic level of modification of body function, alter the risk of morbidity and mortality but do not change the basic rate of increasing susceptibility to aging during the action of the toxic event. An example of this kind of action is smoking; individuals smoking one package of cigarettes per day have twice as great a death rate from any cause as nonsmokers at any age. In this case, however, there is a specific enhancement of 100 times in the tendency for lung cancer to occur, even though the main effect of increased morbidity and mortality is the twofold increase in common diseases.

Table II gives a rough comparison of a large number of factors which can weight the relative risk of morbidity and mortality at any age. It may serve as a useful background of information from which to view radiation effects and to estimate factors which may enhance or diminish radiation effect on life span and mortality.

Life-Shortening Effects

The life-shortening effects of radiation have been observed to occur under a variety of experimental conditions. An experiment of particular significance because of the large numbers of animals and the range of exposure was the exposure of mice to nuclear detonation at "Operation

Greenhouse" (Furth, et al.[4]). The fraction of life span lost per unit of radiation exposure appears to be essentially the same for a number of species, including the mouse, the rat, the guinea pig, the rabbit, and man. The largest number of experimental observations concern the mouse. In the mouse, the fraction of the life span lost per unit of whole-body radiation exposure is acceptably constant over a wide range of variation in radiation exposure. The tentative conclusion is that radiation effect simulates aging itself, and that a unit of radiation exposure, regardless of the intensity and duration time of exposure, produces approximately the same relative disturbance to body structure, in adults of mammalian species. On the human life-span scale, these effects of radiation summarized from small-animal data suggest that 1 roentgen of radiation exposure is equivalent to 5 to 15 days of physiologic aging. This prediction is confirmed directly in man (with reasonable technical reservations) by Doctor Shields Warren's recent investigation of life span of radiologists compared with physicians not using radiation in their practice of medicine. The average age at death is approximately 6 years less for radiologists than for physicians in general practice or pathologists, both selected as being relatively unexposed to radiation. The estimation of accumulated radiation exposure in radiologists is uncertain, but has been approximated as 300 r to 500 r. Thus, the life span loss, if attributed to radiation, is:

$$1\ r = \frac{-6 \text{ years} \times 365 \text{ days per year}}{300 \text{ r to } 500 \text{ r}} = -7 \text{ days to } -4 \text{ days per roentgen of whole-body exposure.}$$

Such a number is still subject to considerable possible revision; but many different estimates give values of 1 to 30 days lost per roentgen of radiation exposure, and the probable value is in the range of 5 to 10 days lost per roentgen.

A question exists whether it is justified to extrapolate effects such as life-span lost per roentgen from measures that are mostly determined in the range of 100 to 1,000 r. The evidence is that, over the range that can be tested, the effect is linearly proportional to the radiation exposure; and the information fits an extrapolation to zero shortening of life-span at zero artifical radiation exposure. There is additional evidence in the effects of radiation upon cells (as distinguished from entire organisms), in which lethal damage to cells per roentgen also appears to be proportional to total radiation exposure. Such estimates agree for cells in the mouse, the rat, the rabbit, the guinea pig, and man. This experimental evidence that effect of radiation on cells is in linear proportion to radiation exposure of from 15 to several thousand roentgens provides a reasonable basis for understanding the life-shortening effects of radiation.

Furthermore, the life-shortening effects are consistent in order of magnitude with the genetic effects of radiation upon cells (2 to 3 cells affected per 1,000 cells per roentgen). The genetic effect of radiation has been shown to be acceptably proportional to radiation exposure from 25 r to 8,000 r.

The sum of systematic evaluations of such effects of radiation as mutation induction, cell destruction, and life-span shortening indicates that these effects are permanent and represent the quantum interactions of radiation randomly affecting body cellular structure. The concept of quantum interactions with matter justifies extrapolation to the probability that a single quantum of radiation reacts with an individual molecule.

Although all recent evidence suggests that radiation effect is proportional to radiation exposure, such effects must be viewed together with other common environmental factors that modify health. A scheme is used here in which the effect upon health is expressed as an induction of aging (this is expressed as loss in lifetime, or minus time, written "-n years") or as postponement of aging (expressed conversely as lifetime gained, or plus time, "+n years")*. These

*This estimation of life span lost or gained is in terms of relative physiologic age change. Change in life expectancy may be estimated by determining life expectancy at a given age in comparison to a given age + n years' change in apparent age. Thus, a person, age 40, has a life expectancy of 31.1 years. If his physiologic age is 50 (because of a sum of factors predicting -10 years age over the average), his life expectancy is 22.8 years, or an average loss of life span of 8.3 years. Thus life expectancy lost is somewhat less than physiologic time lost.

factors all appear to have a general action upon disease tendency, and the effect is about the same at any adult age. The following list of relative displacements of physiologic age is given for factors which accentuate aging or loss of life span (expressed as minus time) or retard aging (expressed as plus time). These measures are derived directly from human records. They are grouped according to whether they appear to be reversible or to be permanent. Most of the effects which are not partial measures of the same state are apparently additive, in the few instances that can be tested for this property.

TABLE II

Relative displacements of physiologic age by factors that accentuate aging or loss of life span (minus time) or retard aging (plus time).

Reversible	Years
Country versus city dwelling[35]	+5
Married status versus single, widowed, divorced	+5
Overweight[32]	
25 percent overweight group	-3.6
35 percent overweight group	-4.3
45 percent overweight group	-6.6
55 percent overweight group	-11.4
67 percent overweight group	-15.1
or, an average effect of 1 percent overweight	-0.17
Occupational exercise versus sedentary occupation[36]	+5
Smoking[37]	
1 package cigarettes per day	-9
2 packages cigarettes per day	-18
Atherosclerosis[24]	
Fat metabolism	
In 25 percentile of population having "ideal" lipoprotein concentrations	+10
Having average lipoprotein concentrations	0
In 25 percentile of population having elevated lipoproteins	-7

Permanent	Years
Female versus male sex[35]	+3
Familial constitutions:[33]*	
2 grandparents lived to 80 yr	+2
4 grandparents lived to 80 yr	+4
Mother lived to age 90 yr	+3
Father lived to age 90 yr	+4.4
Both mother and father lived to age 90 yr	+7.4
Mother lived to age 80 yr	+1.5
Father lived to age 80 yr	+2.2
Both mother and father lived to age 80 yr	+3.7
Mother died at 60 yr	-0.7
Father died at 60 yr	-1.1
Both mother and father died at age 60 yr	-1.8
Recession of childhood and infectious disease over past century in Western countries	+15
Life Insurance Impairment Study:[33]	
Rheumatic heart disease, evidenced by	
Heart murmur	-11
Heart murmur - tonsillitis	-18
Heart murmur - strep infection	-13
Rapid pulse	-3.5
Phlebitis	-3.5
Varicose veins	-0.2
Epilepsy	-20.0

Reversible	Years
In 5 percentile of population having highest elevation of lipoproteins	-15**
Diabetes[31]	
Uncontrolled before insulin 1900	-35
Controlled with insulin	
1920 Joslin Clinic record	-20
1940 Joslin Clinic record	-15
1950 Joslin Clinic record	-10
Antibiotics	+

Permanent	Years
Skull fracture	-2.9
Tuberculosis	-1.8
Nephrectomy	-2.0
Trace of albumin in urine	-5.0
Moderate albumin in urine	-13.5

*As measured in 1900 (Beeton and Pearson[33]). These effects may be measurably less now, as environment is changing to produce greater differences between parents and progeny. Also, in 1900, it was a greater feat to live to be 80 or 90 than now.

**This 70 percent difference in distribution of lipoproteins, between 25 percent versus 5 percent highest is equivalent to a total of 25 years in relative displacement of physiologic age.

Certain of these circumstances that modify health are partially interrelated; others may be independent of each other. Estimates of effect upon physiologic age may be added, depending upon the extent to which they are independent. Thus, country versus city dwelling may be suspected to include the factor estimated as exercise benefit. The lipoprotein test already contains information that can be estimated partially by relative overweightness, and the lipoprotein test already accounts for a portion of the smoking effect. Familial inheritance is independently extimated from each ancestor; male versus female differences are equally added to city versus country effects, and presumably each separate disease-sign in the impairment study is additive.

In further support of the additive nature of partial effects upon health, each morbidity circumstance that can be quantitatively estimated produces an effect proportional to its intensity. Examples of proportional change in mortality risk with morbidity severity are:

1) Overweight -0.17 year for each percent overweight

2) Smoking -0.45 year per cigarette used per day

3) Radiation -5 to -10 days per r of whole-body radiation

   3 cells killed per 1,000 cells per r (marrow and and lymphatic tissue)

   4 cells with chromosome breaks per 10,000 cells per r

   1.4 percent increase in leukemia per r

4) Atherosclerosis)
   Diabetes) End effects are proportional
   Nephritis) to severity of metabolic error

5) Accidents are porportional to exposure risks

A somewhat similar tabulation can be made of an estimation of the cost of industrial and transportation progress in this century in terms of years of life span lost by accidental death, distributed to the average individual in the population of the United States. These values are approximately comparable to the preceding values based upon changes in physiologic age.

Statistical distribution of lifetime shortening by travel and industrial accidents. (Calculation based on Vital Statistics of 1949, values for adult white males 20 years and older.)

All accidental deaths	-2.3 yr per individual in U.S.A.
Travel accidents	
Accidents involving railways	-0.06 yr per individual in U.S.A.
Accidents involving ships	-0.04 yr per individual in U.S.A.
Motor-vehicle accidents involving driver and passengers	-0.67 yr per individual in U.S.A.
Assuming only half of population spends appreciable time in automobiles	-1.3 yr per individual at risk
Pedestrian motor-vehicle accidents	-0.2 yr per individual in the U.S.A.
Assuming this effect largely involves the urban portion of the population	-0.4 yr per individual at risk
Aircraft accidents	-0.05 yr per individual in U.S.A.
Assuming that 1/4 of the population (actually, probably much less) uses airplanes	-0.2 yr per individual at risk
Accidents involving industrial machinery	-0.04 yr per individual in U.S.A.
Assuming only 30 percent of males are employed using industrial machines	-0.27 yr per individual at risk

These values are based upon numbers of deaths attributed to accidents; the estimates of life span lost are actually perhaps slightly low because survivors who are maimed, and hence have reduced life expectancy, are not included in these estimates.

In about the same way, we can tabulate the effects on life span of radiation received.

Estimation of radiation effect upon health and life span.

Radiation received	If 1 r = -5 days*	If 1 r = -10 days*
50 r	-0.7 year	-1.4 years
100 r	-1.4 years	-2.7 years
200 r	-2.7 years	-5.5 years
400 r	-5.5 years	-11.0 years

*Two columns are given because of uncertainty whether 1 r = -5 days or -10 days.

Thus, it is observed that, although the estimated effect of radiation upon life span is a number worth attention, its magnitude of effect at low accumulated dosage is slight compared with many public health problems. It must be remembered that major problems such as smoking and overweight and fat metabolism are so subtle that they are estimated and established not by clinical methods but rather by statistical researches involving large population samples. The effect of smoking 1 package of cigarettes per day, for example, appears equivalent in reduction of health and life span to the effect of between 200 and 400 r of accumulated whole-body radiation. This is several times as great as the 50 r limit currently recommended for occupational exposure; and 50 r, in turn, is of the order of 10 times as much as the individual would accumulate through fallout. If the life-span loss is estimated as 5 to 10 days per roentgen of whole body exposure, the loss resulting from 50 r falls within the range of -0.7 year to -1.4 years of life span. This effect is greatly exceeded by the magnitude of the smoking problem, the obesity problem, the problems of atherosclerosis, diabetes, and all the chronic diseases; the benefits of marital status; etc. The effect of 50 r of whole body exposure to the general populace can also be viewed as being in the same category of life-span loss as that which results in the population of the United States from use of the automobile. This estimation, however, does not include the problem of the mutation burden in the next generations following such radiation exposure.

The problem of estimating radiation effect and making recommendations concerning it is not the simple problem of avoiding exposure at levels at which there is a detectable or predictable response. This is especially true when considering radiation effect through systems that allow proportional extrapolation to very small radiation exposures. It is always important to keep radiation exposure to a minimum, but it is also important in the understanding and evaluation of the relative importance of radiation effect to establish its place in the entire climate of factors that can modify health. Similar - and, at times, greater - effects upon health can be shown to result from a large number of common environmental factors. Also, the problem is not simply that of effect of body irradiation upon health. It is necessary to evaluate the effect upon human beings of all known phenomena resulting from the onset of the atomic age, including general socio-economic factors related to our well-being, which are dependent upon progress and the development of useful energy.

The sum of evidence would lead to the conclusion that radiation probably does affect man's health subtly, and - like spending money and time - it should be exchanged for equivalent advantages.

Since the usefulness of atomic energy, including material and energy gain and defense measures of prime importance, is a positive result of the atomic age, atomic energy usefulness minus harmful radiation effect must be equated to the net gain. It is critically important, therefore,

to estimate hazard quantitatively, and to be comparatively mindful of other factors while doing so. There is, however, no unanimity of opinion at this time as to the precise balance that should be achieved between advantages and disadvantages of use of atomic energy, because certain qualifying factors are still too poorly known. Uncertainties exist which can mean either underestimation or overestimation of the effect of radiation.

BIBLIOGRAPHY

Life Span Effects

1. Boche, R. D. "Symposium on Low Level Irradiation." Argonne National Laboratory, 1948.
2. Blair, H. A. "Peaceful Uses of Atomic Energy." Vol. II. University of Rochester A. E. C. Reports 206 and 207, United Nations, New York, 1956.
3. Brues, A. M. and G. A. Sacher. "Analysis of Mammalian Radiation Injury and Lethality." Symposium on Radiobiology, James J. Nickson, Editor, J. Wiley and Sons, New York, 1952.
4. Furth, J., A. C. Upton, K. W. Christenberry, W. H. Benedict, and J. Moshman. "Some Late Effects in Mice of Ionizing Radiation from Experimental Nuclear Detonation." Radiology, 63:562-570, 1954.
5. Jones, H. B. "Aging and Life Span (estimation made that 1 r = -5 days for man)." Am. Assoc. Adv. Sci., Berkeley, December, 1954.
6. Jones, H. B. "A Special Consideration of the Aging Process, Disease, and Life Expectancy." Adv. in Biology and Med. Physics, Vol. 4, Academic Press, New York, 1955.
7. Jones, H. B. and G. A. Sacher. Highland Park Conference, Nat. Res. Council, 1956.
8. Muller, H. J. "Radiation Damage to the Genetic Material." Science in Progress, Yale Univ. Press, New Haven, Connecticut, 1951.
9. Sacher, G. A. "On the Statistical Nature of Mortality with Empirical Reference to Chronic Radiation Mortality." Radiology, 67:250, 1956.
10. Warren, S. "Longevity and Cause of Death from Irradiation in Physicians." J. Am. Med. Assoc., 16:464-468, 1956.
11. Yockey, H. "An Application of Information Theory to the Physics of Tissue Damage." Radiation Research, 5:146, 1956.

Effect on Blood Cells And Developing Embryos

12. Hennessy, T. G. and R. L. Huff. "Depression of Tracer Ion Uptake Curve in the Rat Erythrocytes Following Total Body X-irradiation." Proc. Soc. Exp. Biol. Med., 73:436, 1950.
13. Hicks, S. P. "Developmental Malformations Produced by Radiation." Am. J. Roent., Rad. Therapy and Nuc. Med., 69:272, 1953.
14. Jacobson, L. O. and E. K. Marks. "Plutonium Project: Hematological Effects of Ionizing Radiations In Tolerance Range." Radiology, 49:286, 1947.

15. Jones, H.B. "Some Physiological Factors Related to the Effects of Radiation in Mammals." Symposium on Radiobiology, James J. Nickson, Editor, John Wiley and Sons, New York, 1952.

16. Kaplan, H.S. "On the Etiology and Pathogenesis of the Leukemias: A Review." Cancer Res., 14:535-548, 1954.

17. Kelly, Lola S. "Effects of Radiation on DNA Synthesis in Mammalian Cells." Prog. in Biophysics, J.A.V. Butler and J. T. Randall, Editors, Pergamon Press, London, 1957.

18. Lawrence, J.H. Polycythemia, Grune and Stratton, New York, 1955.

19. Patt, H.M. "Factors in the Radiosensitivity of Mammalian Cells." Annals N.Y, Acad. Sci., 59:649, 1954.

20. Russell, L.B. "X-ray Induced Developmental Abnormalities in the Mouse and Their Use in Analysis of Embryological Patterns." J. Exp. Zoo., 114:545, 1950.

21. "Radiation Hazards to Man." British Report Cmd 9780, Her Majesty's Stationery Office, 1956.

22. "The Biological Effects of Atomic Radiation." Report to the Public, National Academy of Science, Washington, D.C., 1956.

23. "The Biological Effects of Atomic Radiation." Summary Report, National Academy of Science, Washington, D.C., 1956.

Fat Metabolism

24. Gofman, J.W. "Serum Lipoproteins in the Evaluation of Atherosclerosis, Experimental Methods for the Evaluation of Drugs in Various Disease States." Annals N.Y. Acad. Sci., 64:590, 1956.

25. Gofman, J.W. and H.B. Jones. "Obesity, Fat Metabolism and Cardiovascular Disease." Circulation, 5:514, 1952.

26. Gofman, J.W., O. deLalla, F. Glazier, N. K. Freeman, F.T. Lindgren, A.V. Nichols, B. Strisower, and A.R. Tamplin. "The Serum Lipoprotein Transport System in Health and Metabolic Disorders, Atherosclerosis and Coronary Heart Disease." Plasma (Milano), 4:413, 1954.

27. Gofman, J.W., H. B. Jones, B. Strisower, and A. R. Tamplin. "Evaluation of Serum Lipoprotein and Cholesterol Measurements as Predictors Clinical Complications of Atherosclerosis." Appendix A. Circulation, 14:725, 1956.

28. Gofman, J.W., B. Strisower, O. deLalla, A.R. Tamplin, H.B. Jones, and F. T. Lindgren. "An Index of Coronary Artery Atherogenesis." Mod. Med., 21:119, 1953.

29. Jones, H.B., J.W. Gofman, F.T. Lindgren, T.P. Lyons, D.M. Graham, B. Strisower, and A. V. Nichols. "Lipoproteins in Atherosclerosis." Am. J. Med., 11:358, 1951

30. Lyon, T.P., A. Yankley, J.W. Gofman, and B. Strisower. "Lipoproteins and Diet in Coronary Heart Disease, A Five-Year Study." Calif. Med., 84:325, 1956

Diabetes

31. Joslin, E.P., H. F. Root, P. White, and A. Marble. The Treatment of Diabetes Mellitus, 9th Edition, Lea and Febiger, Philadelphia, 1952.

Effects of Overweight

32. Dublin, L.I. and H. H. Marks. "Mortality Among Insured Overweights in Recent Years." Presented 6th Annual Meeting Association Life Insurance Medical Directors, Metropolitan Life Ins. Co., 1951.

Physical Impairment

33. Society of Actuaries, Impairment Study. Peter F. Mallone Inc., New York, 1951.

Accidents

34. U. S. Vital Statistics, Fed. Sec. Agency., Pub. Health Service, Natl. Office of Vital Statistics, U.S. Government Printing Office, Washington, D. C., 1951.

Sex Differences, Urban Rural Differences

35. Vital Records of Denmark, Great Britain, Holland, and Sweden

Occupational Exercise

36. The Registrar General's Decennial Supplement, England and Wales Occupational Mortality Part I, 1951, Her Majesty's Stationery Office, London, 1954.

Effects of Smoking

37. Hammond, E. C. and D. Horn. "The Relationship Between Human Smoking Habits and Death Rates." J. Am. Med. Assoc., 155:4, 1954.

DUAL ION CHAMBER NEUTRON DETECTOR

J. C. Hunter

Radiation Laboratory
University of California
Livermore, California

The purpose of this instrument is to measure the fast neutron flux as encountered with pulsed neutron sources, and in particular those pulsed at rates beyond the dead time and frequency response of conventional type portable neutron detectors. Other methods such as film, the response of which is not well defined for 14 Mev neutrons, and the saturation of a silver foil are not suitable for immediate evaluations. This instrument is not intended to give an absolute value of a neutron flux, but to have an accuracy comparable with most field type neutron detecting instruments.

A further requirement of this instrument is that it should be capable of measuring a neutron flux in the presence of up to 1/2 r/hr of X or gamma radiation.

The ionization current caused by gamma radiation was eliminated by using 2 ion chambers, one of which is sensitive to both neutron and gamma radiation while the other is sensitive only to gamma radiation. The ionization current from both chambers flows through a common grid resistor. If the chambers are balanced for equal sensitivity to gamma radiation and if both chambers see the same flux intensity, there will not be voltage drop across the grid resistor. However, since one chamber is sensitive to neutrons, a neutron flux will produce an unbalance which can be measured. This principle is not new but is quite effective and the construction of the dual ion chambers is unique.

The construction of the dual ion chambers, and the associated electronics, can be seen by referring to Figure 1. Two brass cylinders, closed at 1 end, are mounted on a common Lucite insulator. Also mounted on the Lucite insulator is a T-shaped brass common center electrode which extends into both chambers, and is connected to the input grid of an electrometer tube. One ion chamber is of the proton recoil type, and has a 1/8-inch polyethylene liner extending the complete length of the chamber wall. This polyethylene liner is coated with a 2,000-angstrom thick layer of aluminum which is thin enough to pass the proton recoils formed in the polyethylene liner, yet has enough conductivity to ensure that a voltage gradient will exist between the center electrode and the outside shell. This chamber has the function of collecting the ionization caused by fast neutrons and gamma radiation.

The second chamber consists of simply a brass shell, the common center electrode, and a desensitizing liner. The function of this chamber is to collect ionization caused by gamma radiation only, and it must have a sensitivity equal to that of the proton recoil chamber.

Both chambers are filled with a mixture of argon-CO_2 to atmospheric pressure.

Because of the difference in wall material in the 2 chambers, even though the volumes are the same, there is quite a difference in sensitivity for gamma radiation. It should be noted also that for the same reason this difference in sensitivity varies with the energy of the gamma radiation.

There are several methods for reducing the sensitivity of an ion chamber and each has certain disadvantages in this application. The method to be described was chosen because it doesn't add capacitance to the grid circuit, doesn't provide a source of insulator leakage, and is quite simple to construct and adjust.

An insulating liner, preferably of some non-hydrogenous material, having sufficient length to cover enough wall to reduce the gamma sensitivity to that of the proton recoil chamber, is placed in the gamma sensitive chamber. This liner effectively reduces the chamber volume by absorbing electrons emitted from the chamber wall, and to some extent reducing the area about which the voltage gradient exists. The disadvantage in this method is that this liner may tend to build up a charge from the space charge, and become an active section of the chamber again; however, any such effects have not been noticed in the tests of the instrument.

The dual chambers were tested for saturation effects and no deviation from a linear response was noted with a chamber voltage of 60 volts.

The electrometer is a conventional d.c. amplifier having an input resistance of 10^{13} ohms, and utilizes the Victoreen 5803 electrometer triode. The drift rate after a 5 minute warm-up period is less than $\pm$ 0.5 microampere per hour.

Figure 2 shows the response to Po-Be neutrons. It requires 10 neutrons per cm^2/sec to give a meter deflection of 1 microampere. The response is quite linear and reproducible even when the dual chambers are placed in a gamma flux of 1/2 r/hr.

In its present stage of development, it is believed that this instrument would be useful in measuring fast neutrons in permanent installations where the energies of the gamma radiation is known, and the dual ion chambers are balanced for these energies.

Also, an external means of balancing the gamma sensitive chamber for a given range of gamma radiation, such as adjusting the length of the desensitizing liner, would enhance the use of this instrument for field measurements.

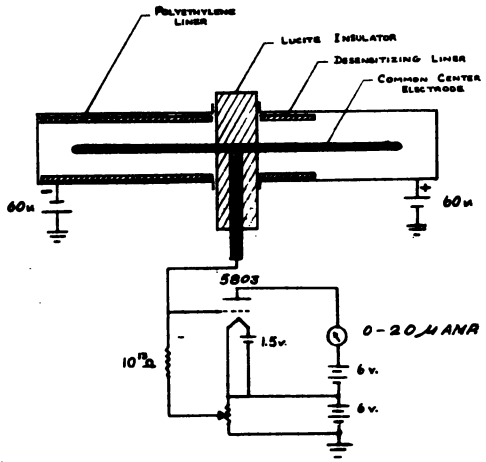

DUAL ION CHAMBER FAST NEUTRON DETECTOR

Figure 1

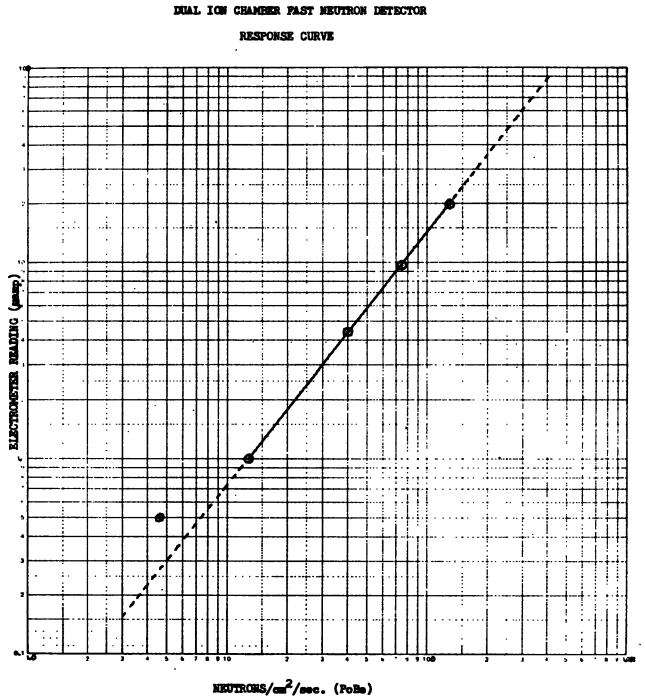

Figure 2

VERSATILE FAST NEUTRON DETECTOR

J. B. McCaslin

Radiation Laboratory
University of California
Livermore, California

The following is a short description of an adaptation of, and uses for, a proton recoil fast neutron detector described by B. J. Moyer[1] and B. Thompson.[2]

It is necessary, for a number of applications, to have at our disposal a fast neutron detection instrument which can serve for:

1. general survey,
2. semi-permanent area monitoring,
3. determination of average energies of fast neutron fields,
4. beam alignment and tune-up indication for various accelerators.

The instrument (Figure 1) consists of an argon-CO_2 filled cylindrical chamber, a preamplifier, and an amplifier-scaler. The chamber is lined with 1/8-inch polyethylene which has a thin, evaporated aluminum inner surface.

In order to meet the requirements of portability for general survey work, the detector probe, which also houses the preamplifier in its handle, was made entirely of aluminum. The cabling between the probe and the scaler is of particular interest because of its size and weight. A Microdot[3] shielded high voltage cable and a Tensolite[4] shielded preamplifier cable are used. Each of these cables is about 1/16 inch in diameter and has been covered with a 1/4-inch diameter plastic sleeve. The assembled cable weighs only 7 1/2 grams/foot or 3 1/2 pounds for a 200-foot cable.

The preamplifier has a gain of 17 and is cathode-coupled to the scaler through the subminiature cable. It uses 3 type 5840 subminiature pentodes. These tubes, in addition to being extremely small, are also very rugged and dependable. Tubes may be changed in seconds by unscrewing the cap on the probe handle (Figure 2). In fact, the entire preamplifier can be replaced, as can the chamber, in a few seconds.

This instrument was checked against 3 calibrated neutron sources of different average energies in order to determine if, within these energy ranges, it maintained its energy-flux-density characteristics. Po-Be, mock fission, and Po-Li sources, with average energies of about 4.6 Mev, 2.5 Mev, and 250 kev respectively, indicated that the instrument was operating satisfactorily as an energy-flux-density meter at these energies.

One rather interesting use for this type of instrument lies in its ability to determine the average energy of an unknown fast neutron spectrum when used in conjuction with a cadmium-shielded Hansen-McKibben long counter. Since the polyethylene-lined chamber provides a response which is proportional to the product of the average energy and flux density, and the Hansen-McKibben counter provides the number of neutrons/cm^2/sec, the former divided by the latter reveals the average neutron energy.

Since, however, the low energy cutoff of the energy-flux-density chamber probably lies around 100-200 kev, because of both the discriminator setting and the range of the recoil proton in the hydrogeneous liner and in the inner conductive coating, and since the Hansen-McKibben counter experiences no such cutoff, a possible source of error arises if this part of the neutron spectrum is not considered.

In an attempt to test the response of the instrument at higher energies, it was exposed to 14 Mev neutrons from a Cockcroft-Walton Accelerator. The target pit is completely surrounded by concrete except for the roof, and therefore was a source of neutron energy degradation. The beam also was contaminated with 2 Mev (d, d) neutrons. The average energy as shown by the combination of the 2 instruments was 6.5 Mev.

On another occasion, this instrument was used to determine the extent of deuterium absorbed on the walls of an accelerator by noting the d, d reaction. The average energy of these neutrons was also checked and found to be 1.9 Mev. In view of degradation of energy by surrounding equipment, floor, and walls, this is surprisingly close to the theoretical value of 2.2 Mev.

The sensitivity of this instrument, when the discriminator of the amplifier-scaler is adjusted above 200 mr per hour of gamma radiation, is 0.9 Mev for 1 count per minute. A typical background for an 8-hour period is 0.83 count per minute.

BIBLIOGRAPHY

1. Moyer, B. J. "Survey Methods for Fast & High Energy Neutrons." Nucleonics, May, 1952.
2. Thompson, B. W. "Fast Neutron Scintillation Survey Meter." Nucleonics, May, 1954.
3. Microdot #50-3903, Microdot Division, Felts Corporation, South Pasadena, California.
4. Tensolite #1920F-3, Tensolite Insulated Wire Company, Tarrytown, New York.

A LARGE BISMUTH FISSION PULSE IONIZATION CHAMBER

W. N. Hess, H. W. Patterson, and R. Wallace

Radiation Laboratory
University of California
Berkeley, California

The ion chamber to be described here was intended for health physics surveys of neutron and proton fields, as well as for applications in cosmic ray and high energy nuclear physics research. The methods of chamber design developed in the course of this work are applicable to the construction of any pulse ion chamber in which it is desired to have a plate area of the order of 50 square feet. The large electrical capacity of such a chamber has been a barrier to its use in the past. The approximate sensitivity which has been achieved is 1 count per 300 very high energy neutrons/cm^2.

In order to eliminate response to gamma rays and nuclear star events, it was decided to use a material with a high fission threshold to coat the ion chamber plates, and then operate the device so that only fission events could be detected. At energies above 1 Mev, bismuth is the only element suitable for this purpose.[1] Its fission threshold is near 50 Mev for both neutrons and protons, and at 270 Mev the cross section has risen to 180 millibarns. No measurements at higher energies have been reported, but there is reason to believe that the cross section does not rise much above this value.

The range of the fission fragments from bismuth is of the order of 1 mg/cm^2, and there is some evidence that only the top 0.5 mg/cm^2 of a bismuth coating can be considered as "effective" in producing detectable fission events. As a result, it was decided to space the plates 1/4 inch apart. This provides approximately 1 mg of gas path length when the pressure is 1 atmosphere and the fragment travels perpendicular to the plates. Because of the very limited effective depth of the bismuth, it is necessary to provide a very large area in order to have a significant counting rate. Bismuth fission chambers which have been made before[2] have had much less area than the present one. The total area of the plates in the present chamber is 63,000 cm^2, so there are 31.5 grams of effective bismuth even though the coating is actually 1 mg/cm^2 deep.

The vacuum-tight case of the ion chamber shown in Figure 1 is made of 1/2-inch aluminum with a flange, gasket groove, and lid at each end to facilitate assembly. Inside the chamber, as shown in Figure 2, 43 plates 12 inches in diameter and 0.040 inch thick are spaced 1/4 inch apart on 8 rods and insulated from each other and the rods by ceramic spacers. The rods are fastened at each end to heavy rings, which are in turn held in place in the case by 8 radial set screws. This rugged construction was chosen to reduce microphonic response. The plates are coated on each side, by vacuum evaporation, with 1 mg/cm^2 of bismuth.

It was intended at first to connect the plates in series, using a voltage of about 5 Kv across the whole stack to provide a field strength of about 200 volts/cm. Series connection did not provide uniform or adequate sensitivity across the stack, that is, a fission occurring on any plate could not be detected with equal sensitivity. In addition, the high voltage necessary for the series connection caused high voltage breakdowns. A simple connection of alternate plates in parallel permitted a low voltage to be used, but introduced an electrical capacity of about 8,000 $\mu\mu$f, which made the signals much too small to detect. In order to isolate each plate and yet take advantage of the large total area, half of the plates were each connected to an individual triode and the plates of

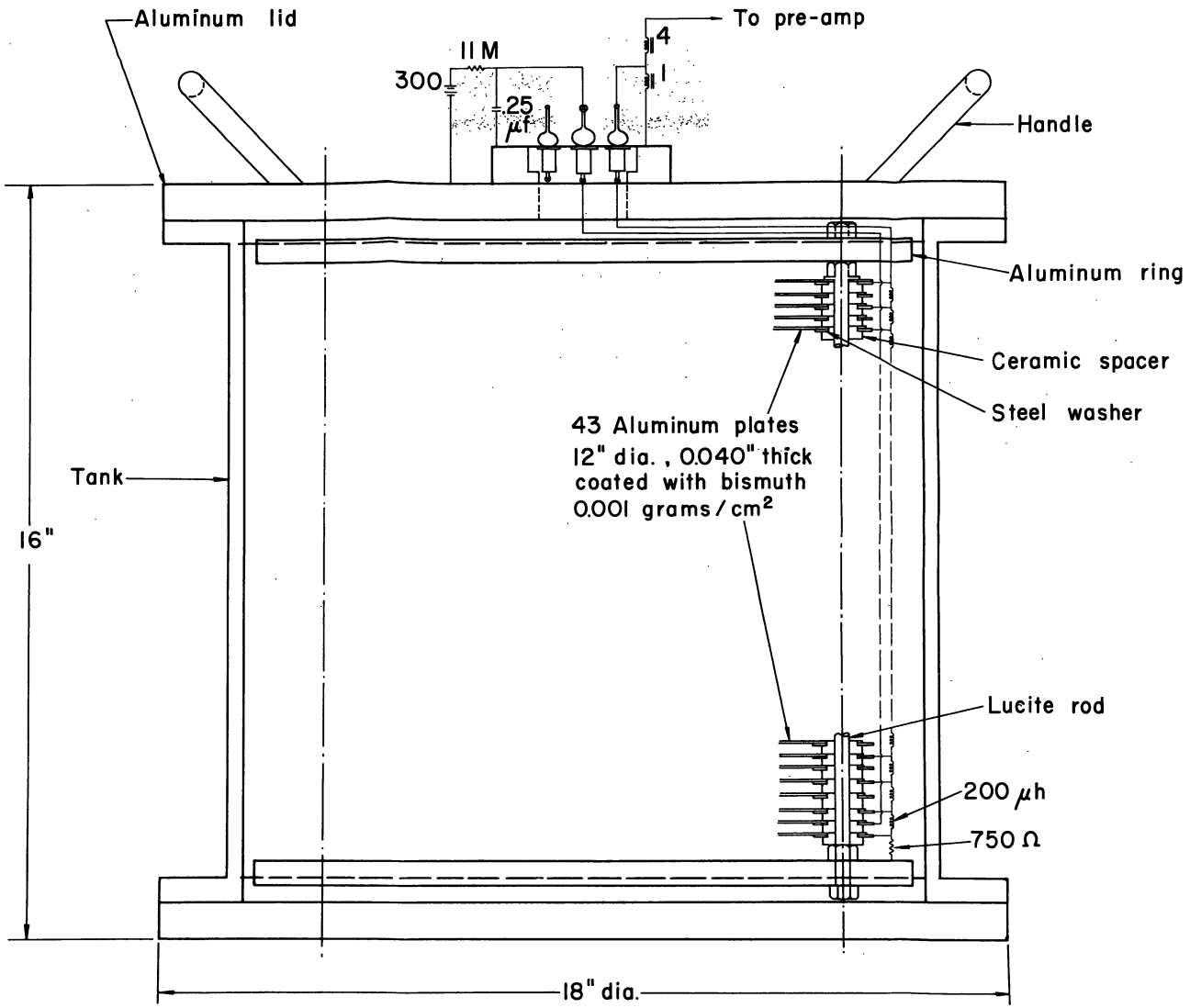

physical arrangement of the bismuth fission chamber.

Figure 2

the triodes tied together. This system did not work, since the noise of all the triodes was competing with a desired signal from only one.

What was needed was a method allowing 1 of each pair of plates to be connected to the input of the preamplifier when a signal was available between that particular pair of plates; but, when such a signal was not present, allowing the capacity of that pair of plates to be disconnected. This desirable arrangement (as suggested by William Goldsworthy and James Robison of this laboratory) is achieved by the connections shown in Figure 2. One set of alternate plates is connected directly to the negative side of a 300-volt battery through a simple filter. The other set of plates is inter-connected by 200-microhenry inductances forming, in conjunction with the inter-plate capacitances, a delay line. To eliminate reflections, one end of this line is terminated in its characteristic impedance by a 750Ω resistor. The other end of this delay line is connected to an auto pulse transformer giving a 5 to 1 voltage gain. This provides better impedance matching to the input of the preamplifier.

There is a 5-microsecond delay down this entire line. A particular signal, therefore, may be delayed from 0 to 5μs. If it is desired to do coincidence work to better than 5μs, both ends of the delay line could be brought out, and if the resulting double pulses were photographed, the location of the pulse in the chamber along with its resulting delay could be determined to perhaps 1/4μs.

The signal from the pulse transformer is amplified 100 db by a low noise preamplifier and a low noise linear amplifier of UCRL design. The average signal coming from the pulse transformer is about 100 microvolts. Since counting rates with this chamber are often quite low in spite of the large amount of effective bismuth, the pulses coming from the linear amplifier are both photographed and recorded in duplicate on registers in order to have a check on the long-time stability of the electronic circuits. A conventionally driven sweep oscilloscope and moving film camera are used. Calibration pulses of a known size are automatically fed into the circuit between the pulse transformer and preamplifier at regular intervals and recorded on the film as a check of reliability. The discriminators controlling the registers are gated off when the calibration pulses are being fed in.

The chamber is filled to 20 lb/in^2 absolute with 95 percent A and 5 percent CO_2. This is an optimum pressure, since more pressure increases recombination and less pressure allows the average fission fragment to hit the opposite plate before the end of its range. It has been found, by reversing the polarity, that the bismuth is effective on both the delay line collector set of plates and on the high voltage set. That on the high voltage set of plates is about 2 to 3 times as effective as that on the delay line set.

Since the 184-inch Synchrocyclotron is not in operation at present, the chamber has been partially calibrated during a run at the UCRL Bevatron. Protons of 6.2 Bev struck a target, producing a variety of particles. The magnetic field of the Bevatron deflected all the charged particles away from the chamber, leaving principally neutrons and gamma rays of several Bev.. A transition curve was run, using 0, 1/2 inch, 2 inches, 6 inches, and 12 inches of lead (Figure 3). A twin chamber having no bismuth was used to subtract any effect caused by the aluminum plates. Above a few volts bias this correction proved to be small. The small slope of these curves is consistent with the attenuation of neutrons by lead, which is equivalent to a mean free path of about 200 grams/cm^2. This is as close to the geometric cross section mean free path for lead of 180 grams/cm^2 as can be expected from these rough preliminary measurements. Apparently the response to gamma rays, known from other experiments to constitute about 1/3 the neutral particle beam, is quite small, since the steep attenuation characteristic of gamma rays is not observed.

The relative integral bias curves for the chamber with bismuth and the twin control chamber without bismuth are shown in Figure 4. It is seen that under the worst conditions, at 10 volts, the ratio is 4 to 1, but that this rises to 25 to 1 at 20 volts and above 20 volts is as much as 500 to 1. The difference in slopes of the bismuth and non-bismuth curves is interpreted as an indication that the processes responsible for the pulses are fundamentally different, namely heavy element fission on the one hand and light element star formation on the other.

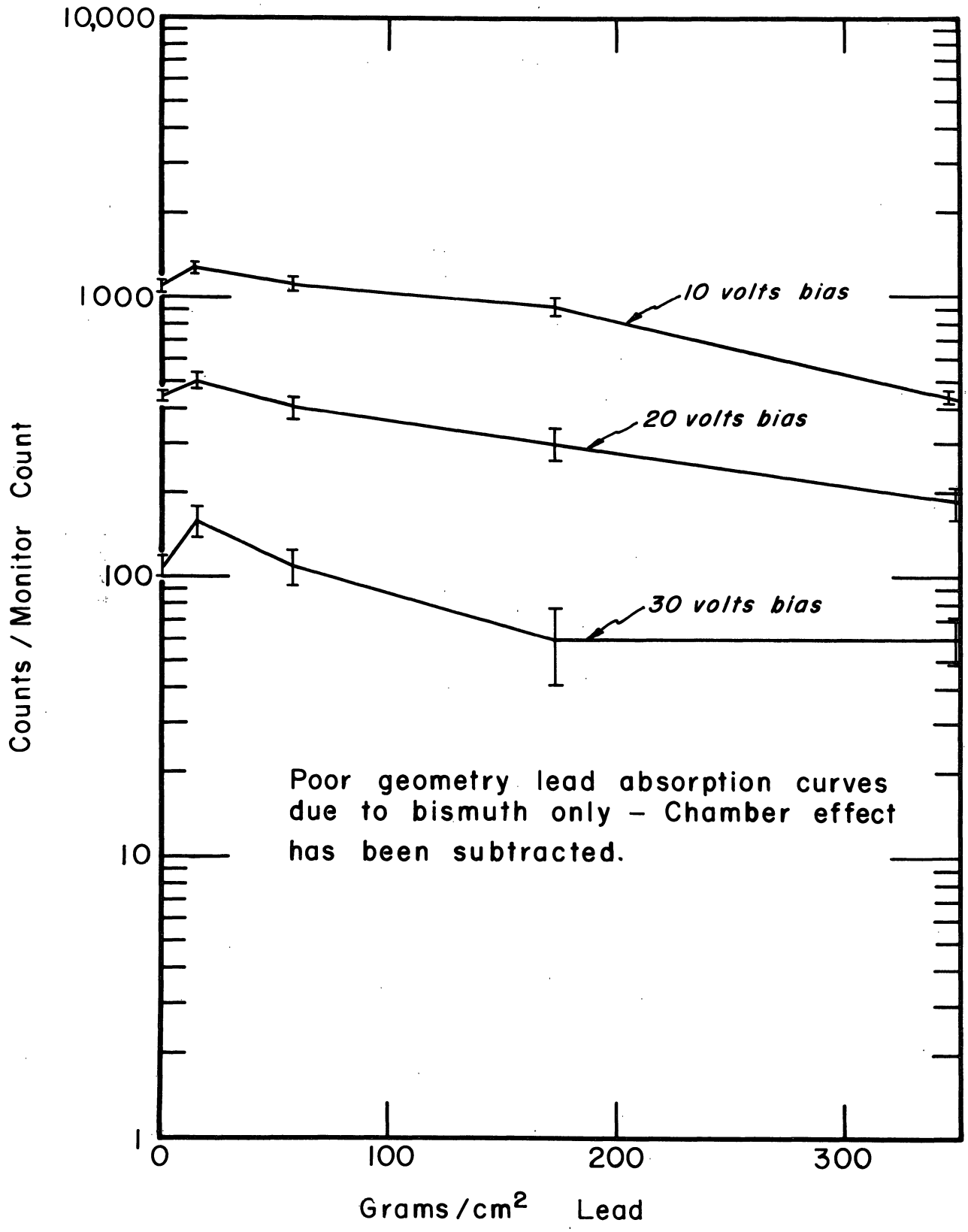
10,000
1000
100
10
1
Counts / Monitor Count
10 volts bias
20 volts bias
30 volts bias
Poor geometry lead absorption curves due to bismuth only – Chamber effect has been subtracted.
0
100
200
300
Grams / cm2 Lead

Figure 3

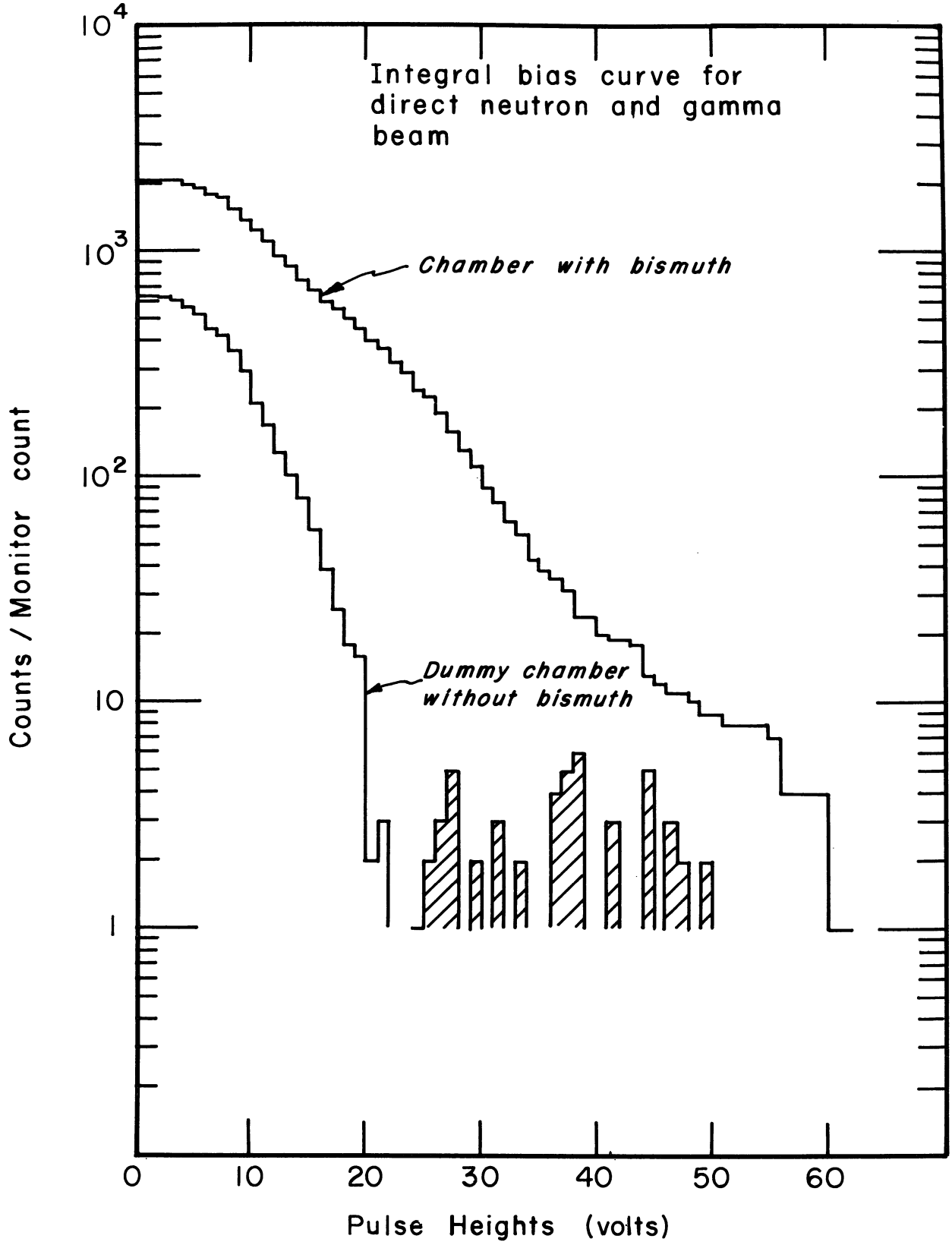
Integral bias curve for direct neutron and gamma beam
Chamber with bismuth
Dummy chamber without bismuth
Counts / Monitor count
Pulse Heights (volts)
10^4
10^3
10^2
10
1
0
10
20
30
40
50
60

Figure 4

During the Bevatron run a comparison was made with a previously calibrated chamber containing 1 gram of effective bismuth and having a sensitivity of 1 count per 10^4 neutrons/cm^2 at 290 Mev. It was found that the large chamber had a counting rate, extrapolated to zero bias, 37 times that of the little chamber. This is to be compared with a ratio of about 21 in effective bismuth contained. This measured ratio gives a sensitivity of about 1 count per 300 very high energy neutrons per cm^2, assuming that the fission cross section does not vary rapidly with energy above 300 Mev.

A Cf-252 spontaneous fission source has been incorporated into each chamber, but for simplicity has not been shown in Figure 2. The high voltage to this source can be switched off or on from the outside, allowing a fairly high counting rate of bona fide fission pulses to be available at any time for circuit test and calibration purposes. The integral bias curve arising from 500 Cf-252 pulses is shown in Figure 5. That the slope of this curve is much steeper than that arising from the bismuth fissions is interpreted to be a result of the difference in the mechanics of the 2 fission processes themselves, and the fact that the Cf-252 is extremely thin.

This chamber will sometimes be used in the presence of charged particles such as very high energy protons and pions which can initiate fissions as easily as neutrons can, since their energy is so far above the coulomb barrier potential. In order to separate the effect of the charged particles, a complete blanket of Geiger tubes is being constructed for the bismuth containing chamber, and each fission event will be recorded as being either in coincidence with a Geiger pulse or not.

The authors wish to thank the operating crews of the UCRL 184-inch Cyclotron and Bevatron for their cooperation in the experimental calibrations of this fission chamber.

BIBLIOGRAPHY

1. Kelly, E. L. and Clyde Wiegand. Phys. Rev., 73:1135, 1948.

2. De Juren, James. R. S. I., 19:790.

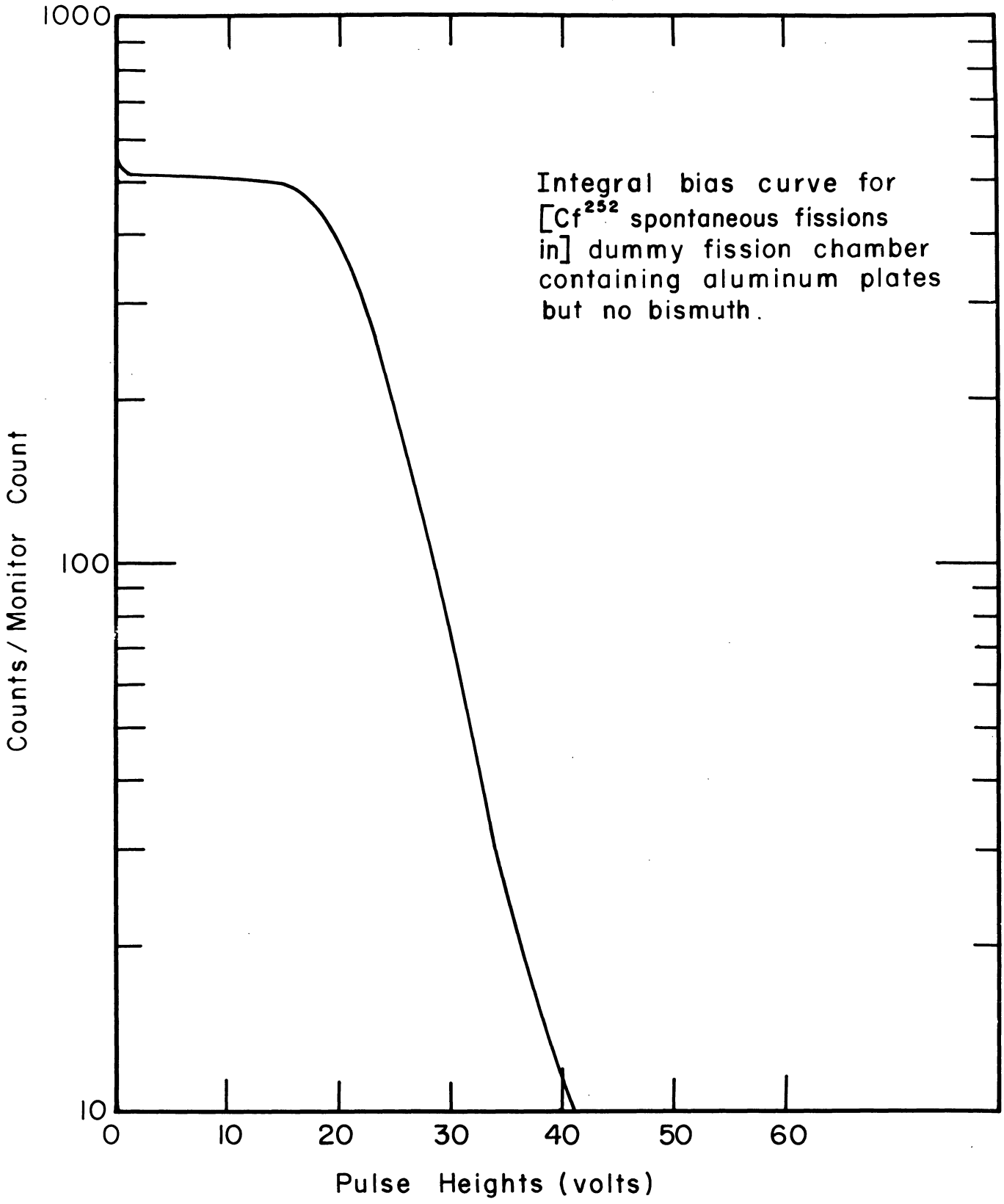
1000
100
10
Counts / Monitor Count
Integral bias curve for [Cf252 spontaneous fissions in] dummy fission chamber containing aluminum plates but no bismuth.
0
10
20
30
40
50
60
Pulse Heights (volts)

Figure 5

AN AUTOMATIC ISODOSE PLOTTING DEVICE

C. S. Simons.

Alice Crocker Lloyd Radiation Therapy Center
University Hospital
Ann Arbor, Michigan

INTRODUCTION

The development of a device for rapidly locating and recording the dose rate distribution of radiation in a water phantom was undertaken in connection with the development of certain treatment plans utilizing Co-60 gamma radiation. The 1,900-curie source is housed in a AECL model "B" beam therapy unit, the Theratron which is shown in Figure 1. The attachment of an adjustable diaphragm to the Theratron permits a wide variety of field sizes to be selected, but this flexibility requires that the isodose curves for many field sizes become rapidly available to the radiation physicists.

The design criteria for the instrument include the following points:

1. The finished curves should present a 1:1 correspondence between the location of the iso-intensity lines in a water phantom and the location of the isodose lines on a piece of paper.
2. The motion of the detecting element (the probe) should be along rectangular coordinates in 1 plane with the recording pen showing at all times its location.
3. The speed of motion of the probe should not be greater than the ability of the servo system to respond to a change in radiation intensity.
4. The time required to present a complete set of isodose curves for a single field should be in the order of 2 hours or less.
5. The unit must be controlled at a point remote from the radiation field.

Regarding the first 2 points, the Brown "ElectroniK" strip chart recorder which has reversible chart motion and a 2-second full scale speed was selected. The vertical motion of the probe is transmitted by means of selsyns to produce vertical motion of the chart. The horizontal motion of the pen is governed by the voltage taken off of a 40-turn Helipot, which is driven by the same motor that drives the probe in a horizontal plane.

The voltage that arises from the interaction of radiation on the probe is compared to some pre-set reference voltage. The servo motor drives the probe until there is no difference between these 2 voltages. The pre-set voltage values are selected to be 90, 80, 70, etc., percent of the voltage which is produced at the maximum radiation rate.

MECHANICAL ASPECT OF ISODOSE PLOTTER

1. Horizontal Drive

The motion of the probe in a horizontal direction is powered by a 2-phase reversible motor, which drives a 20-pitch screw at a maximum speed of 108 rpm. The maximum speed of the

probe's motion is 5.4 inches per minute; this permits the full scale motion of the probe to take place in about 2 minutes. The motion of the screw is transmitted by gears to the Helipot so that its wiper makes 40 turns while the carriage (Figure 2) which holds the probe moves 11 inches.

2. Vertical Drive

A similar motor drives a second 20-pitch screw to produce the vertical motion of the probe up to a maximum speed of 5.4 inches/minute. In the recorder, the receiving selsyn requires 20 turns to produce an inch of chart motion. Since the transmitter selsyn, attached directly to the vertical screw, also will experience 20 turns for each inch of vertical motion of the probe, the paper and the probe will move at identical speeds. Limit switches are employed to terminate the motion in case the probe should be driven to either extremity of the travel.

3. Electrical Drive System

The power for the vertical and horizontal drives comes from 2 independent sources, either of which can be applied to either drive motor. One source is an autotransformer which enables the operator to select any speed of drive (patrol speed) up to the maximum. The second source of voltage is a Brown Servo amplifier. Its output voltage depends on the amplitude of d.c. signal from the detecting circuit, and its phasing depends on the polarity of the d.c. signal. The output of the probe is initially opposed by an equal but opposite polarity signal from the reference voltage. Whenever the probe experiences a change in output, caused by a change in radiation incident on the probe, the difference in the 2 voltages produces an input signal to the servo amplifier, as shown in Figure 3. The motor then drives in such a direction as to reduce to 0 the difference (error voltage) between the probe output voltage and the reference voltage. The hunting signal is applied to the horizontal drive motor whenever the gradient in the radiation rate is greatest in the horizontal direction; the patrol signal is applied at the same time to the vertical screw. At such locations where the gradient is steep toward the vertical direction, the input signals are manually switched to be applied in the opposite manner; that is, the hunting voltage is applied to produce the vertical screw motion, and the patrol voltage is fed into the horizontal drive motor.

RADIATION PROBE AND DETECTION CIRCUITS

The sensitive element in the detection system is an ionization chamber having internal dimensions of 3 mm diameter, 12 mm length, and a wall thickness of 0.5 mm. This probe, shown in Figure 4, is made of polystyrene; it is coated internally with a thin film of colloidal graphite. The central electrode is a No. 30 aluminum wire. The ionization chamber and its guard ring assembly are connected to a modified version of Johns' d.c. amplifier. When a relatively constant radiation source such as a long half-life radioisotope is involved, only 1 d.c. amplifier is needed to provide the hunting signal. However, if an X-ray source which has a varying output is involved, a second probe (monitor) and amplifier are used to replace the reference voltage. Consequently, when there is a change in source output, the output voltage of both probe amplifiers will be changed by equal amounts, thus retaining the same relationship to each other as if the source had remained constant.

During the actual recording of isodose curves, the microammeters that are used in adjusting the circuits must be switched out of the circuit and replaced by resistors of value equal to the resistance of the microammeters. If this is not done, the emf generated by their fluctuation will appear as a spurious voltage that will cause excessive hunting in the servo system.

It was found that for large error signals the Brown amplifier would be overloaded, and would produce a distorted wave form which would prevent the maximum speed of the drive from being attained. An automatic gain control circuit has been developed which reduces the sensitivity of the amplifier when large error signals are present, but permits the desired sensitivity when the error signal is small. This circuit will be described elsewhere.

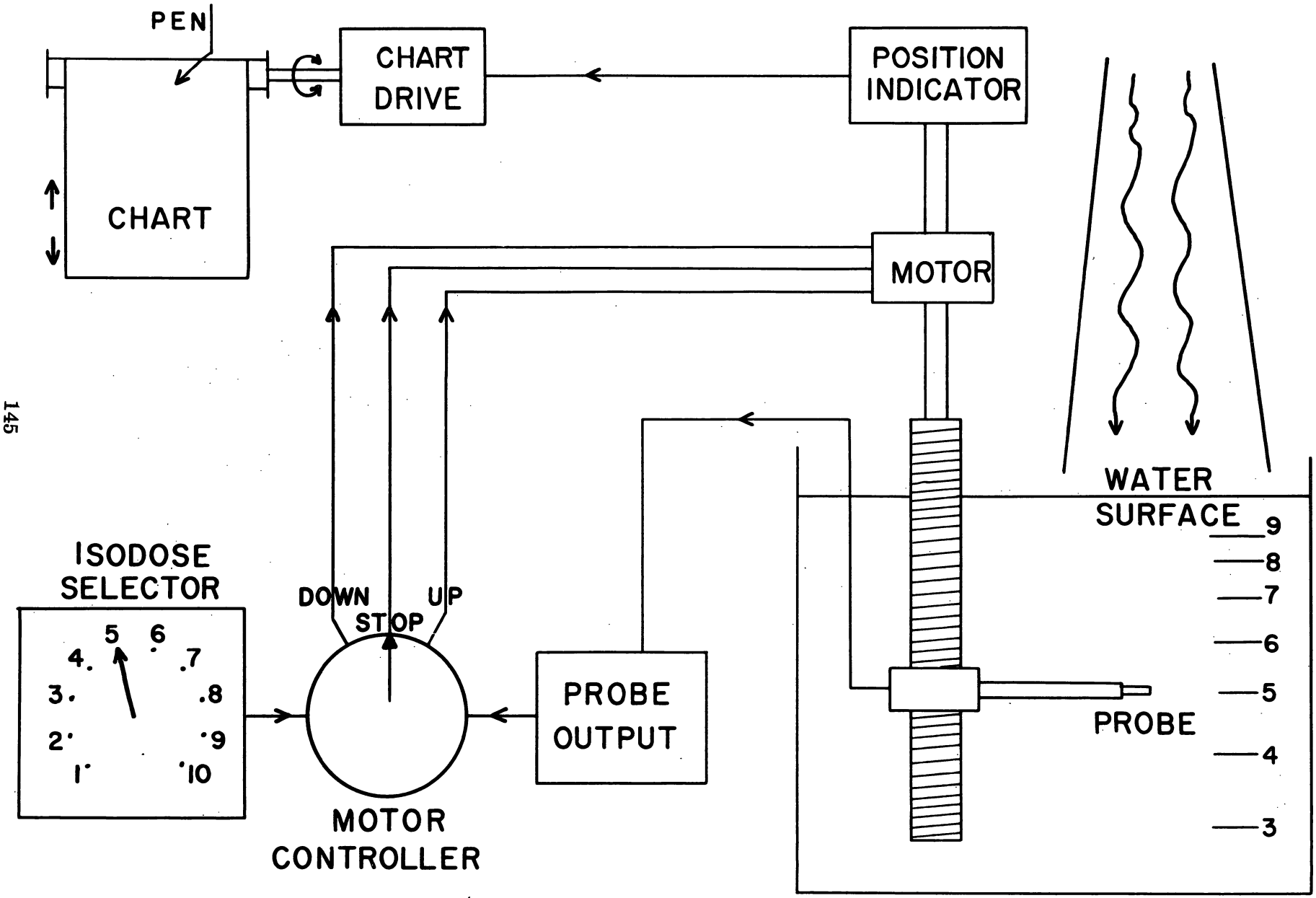
PEN
CHART
CHART DRIVE
POSITION INDICATOR
MOTOR
WATER SURFACE
9
8
7
6
5
4
3
PROBE
PROBE OUTPUT
ISODOSE SELECTOR
5
6
4
7
3
8
2
9
1
10
DOWN
STOP
UP
MOTOR CONTROLLER

Figure 3

OPERATIONAL SEQUENCE

The carriage, containing the horizontal and vertical drives, and the probe, are mounted on top of a sheet metal tank (Figure 5) which is filled with water to dimensions of 80 cm by 50 cm by 25 dm deep. This water "phantom" is placed so that when the radiation beam is turned on, it will strike the open surface of the water. The initial position of the probe in the beam is located visually by means of the light localizer in the Theratron or X-ray unit. The probe is driven, by manual control, to the depth where the maximum dose rate is encountered. The reference voltage is adjusted so that it is equal to the output of the probe's d.c. amplifier. This reference voltage is arbitrarily called 100 percent, and the percentage Helipot is set to read 100 units. When this Helipot is adjusted to 90, the probe will be driven by the servo system toward one edge of the beam until a point is reached (at the same water level) where the radiation dose rate is 90 percent of the maximum. The patrol voltage is then applied to the vertical drive and the probe moves deeper into the water at a constant speed; at the same time, the servo system moves the probe in a horizontal direction in order to maintain the pre-set radiation rate. At such time as the operator observes a rapid sustained drive in the horizontal direction, the patrol voltage is switched over to the horizontal drive motor and, simultaneously, the probe output is applied to the vertical drive motor. This maneuver prevents excessive hunting conditions and permits a more accurate plotting of the isodose lines.

When the probe has returned to the initial horizontal plane below the water surface but on the other side of the central axis of the beam, the percentage Helipot is changed to 80 and the probe proceeds to plot the 80 percent line. This process is continued out to the 5 or 10 percent line. The entire operation takes less than an hour.

Since the control panel, shown in Figure 6, must be located in the radiation control area, 40-foot long cables are required. This location permits the operator to observe the action of the plotter indirectly by watching the pen and chart motion, or directly by looking through the view window into the treatment room.

ISODOSE CURVES

The principal use of the isodose plotting device has been to obtain the isodose curves for the Cobalt-60 gamma rays in a water phantom. Figure 7 shows 1 set of typical curves as obtained from the plotter. Figure 8 illustrates the same curves after they have been traced onto cleared X-ray film base, using India ink. The plotter has also been used to map isodose curves pertaining to radium tubes and to X-ray therapy units.

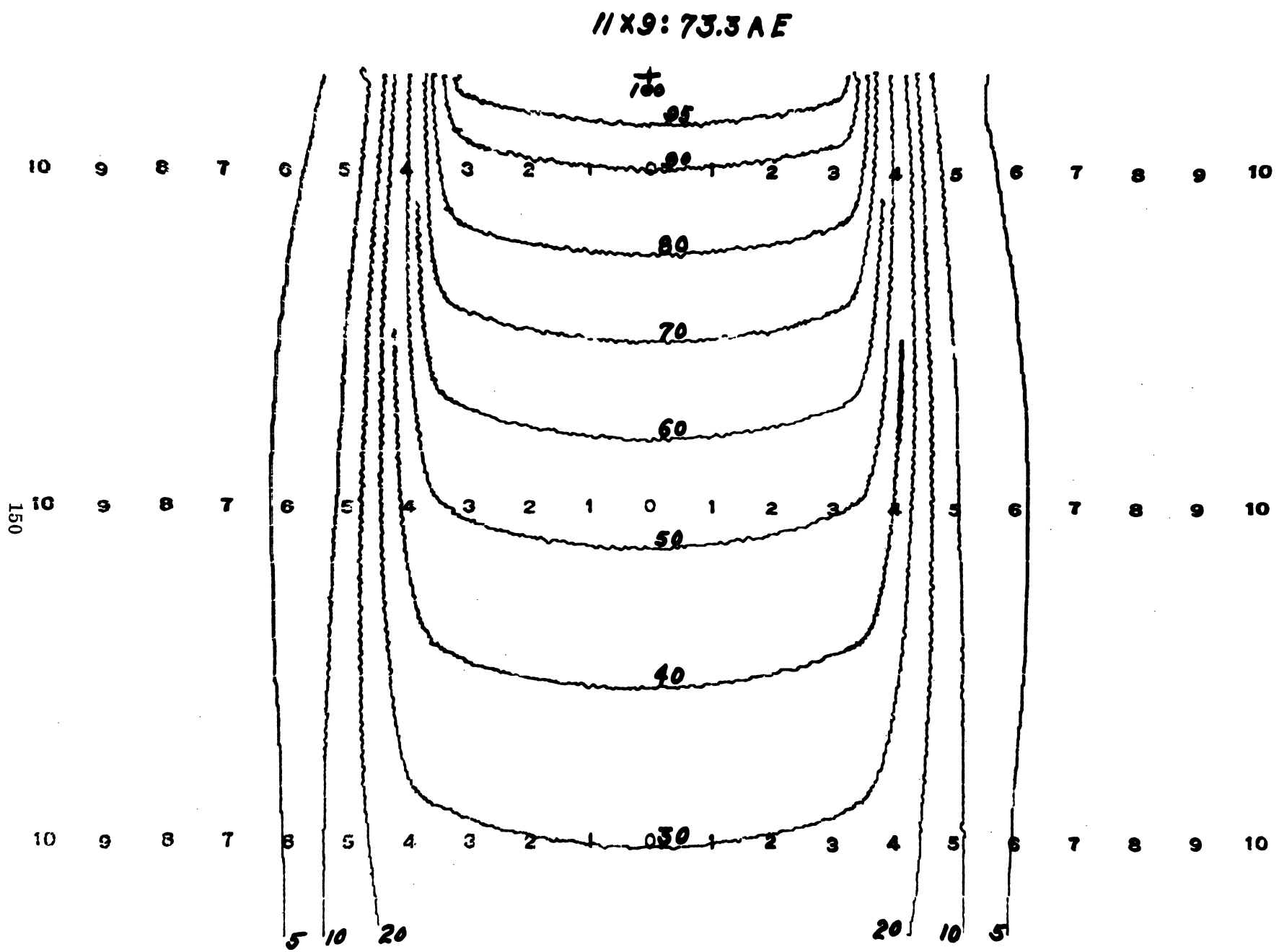

Figure 7

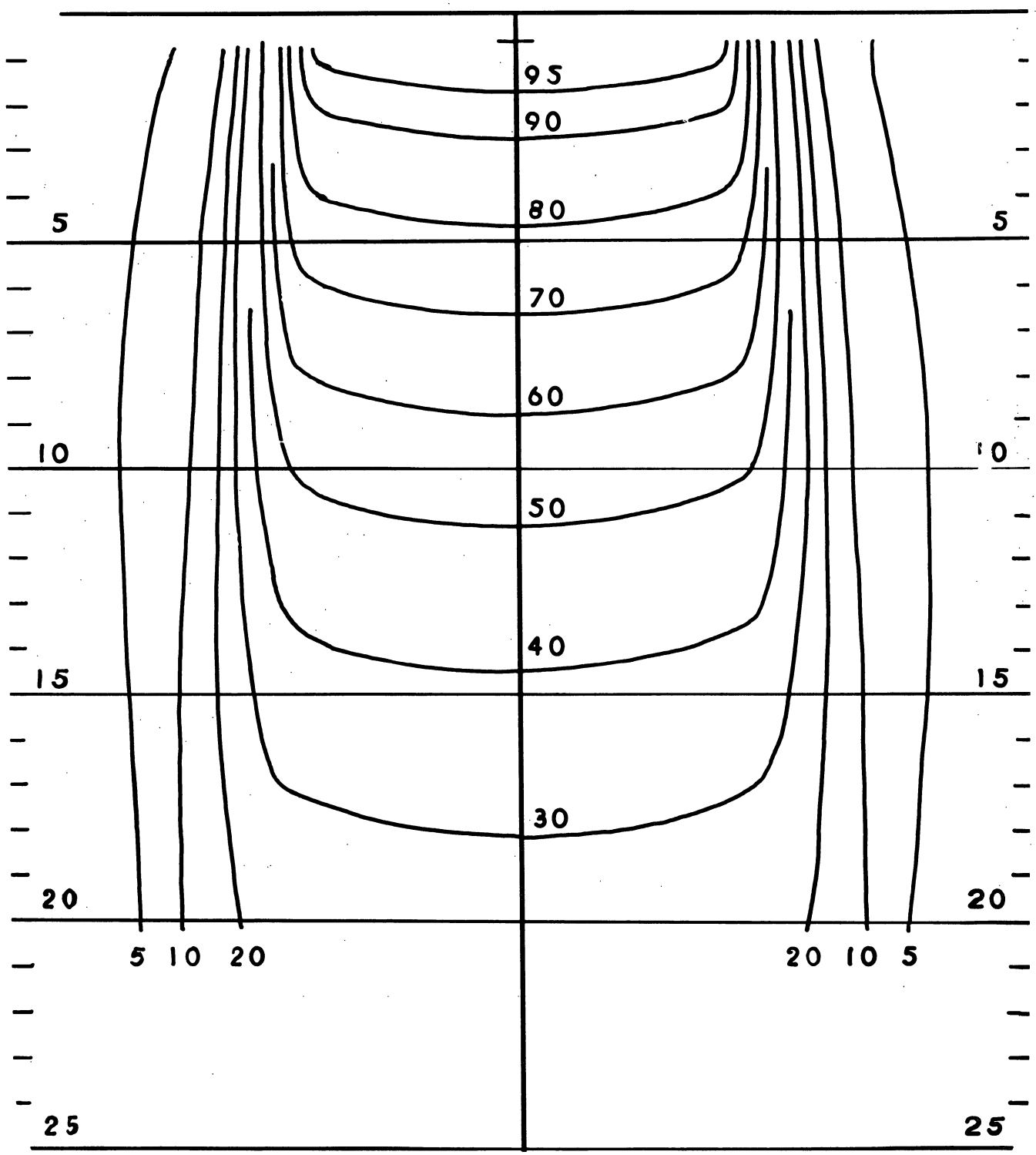

Figure 8

PROBLEMS IN THE INCINERATION OF RADIOACTIVE WASTE

H. S. Jordan

Health Division
Los Alamos Scientific Laboratory
Los Alamos, New Mexico

INTRODUCTION

The magnitude of the waste disposal problem at institutions and installations handling radioisotopes continues to increase with time. The incineration of contaminated combustible waste inevitably comes to mind as a possible means of reducing the volume of such material. A number of installations have issued operational reports on this method.[5, 3, 11, 4, 10] Those by A. D. Little, Inc.[9] and Larson and Simon[8] of the Knolls Atomic Power Laboratory indicate some of the factors to be evaluated in considering the feasibility of incinerating radioactive waste. In view of the fact that all radioactive incinerators erected at various AEC sites have ceased operation, however, there would appear to be a need for a more critical appraisal of the process.

This paper, therefore, attempts to develop criteria for evaluating incineration as a process to assist in the disposal of contaminated waste, to indicate features that should be considered in the design of an incinerator for a large installation, and to evaluate the usefulness of the process for a small installation. It should be stressed, however, that although incineration is a method for processing combustible waste, it is not a means for final waste disposal.

FEASIBILITY OF INCINERATION

Before any method of waste disposal is adopted, the basic factors that must be determined are the possible effectiveness of the method and its cost. An accurate determination must be made both of the total volume of waste to be handled for final disposal and of that percentage of the total which could be considered combustible. Care should be taken to include large noncombustible items that constitute an irregular but real part of the total waste. The method of collecting combustible trash within the laboratories may give misleading data on relative volume if containers are too large. For example, laboratory workers often will seal and mark for removal a half-filled container in order to be rid of a potential hazard.

Once the total waste volume has been determined, a cost analysis can be completed, assuming some final disposal of both combustible and noncombustible waste. The maximum saving to be accomplished by incineration is that proportion of the total cost represented by the percentage of combustible trash. The actual saving, however, will be this maximum minus the following items:

1. Initial cost of the incinerator building depreciated over a 10-year period.
2. Cost of incinerator equipment depreciated probably over a 5-year period.
3. Cost of secondary fuel.
4. Cost of labor for operation of incinerator.

5. Cost of maintenance services (this has been computed by A. D. Little, Inc.,[9] as 5 percent of total initial cost per year, but it probably could be computed at a higher rate in the majority of cases).

6. Cost of health services. This will include direct monitoring at the incinerator, air-pollution control, biological assays on incinerator personnel, and provisions for their protective clothing.

7. Increase in unit cost for final disposal. This probably will be a factor, because of the presence of certain fixed costs in the final disposal process and the decrease in volume for final disposal.

8. Increase in unit cost of collection. Waste will have to be segregated within the laboratories, with combustible waste delivered to the incinerator and noncombustibles to the final disposal point. In addition, ashes from the incinerator will have to be packaged and handled for final disposal.

9. Cost of treating waste water used in air-cleaning train.

Most of these items are self-evident, but their contribution to the total cost seldom is evaluated before adopting incineration as a method of waste treatment.

INCINERATOR DESIGN

Operating experience at Los Alamos and reports in the literature indicate that the following factors should be given consideration in the design of an incinerator for radioactively contaminated waste at large installations.

1. A separate fireproof storage facility, equipped with automatic sprinklers, should be provided for storage of radioactive combustible material between collection and incineration, and for holding materials for radioactive decay. In any event, at a minimum, an overnight facility equipped with automatic sprinklers should be provided. Careful consideration should be given to transporting the waste from storage to charging unit with minimum handling.

2. Charging should be by a minimum of 2 air locks, with provisions for ensuring air movement from the workroom into the first charging chamber. This is necessary because conventional charging doors as used in ordinary municipal or institutional incinerators are completely unsatisfactory. The design of the air-lock doors should be as simple and foolproof as possible, and the doors should be interlocked to prevent accidental disruption of the air lock. A manual override of the interlocking feature should also be provided.

3. Construction of the grates should be such that any irregular noncombustible item capable of being charged into the incinerator can also be discharged by the grates without requiring manual removal from the combusion chamber. All mechanical features (bearings, operating grates, etc.) should be designed for operation at high temperatures.

4. Ash-removal facilities also should be designed so that any item charged into the incinerator will be discharged in the normal manner. Local exhaust control will be required at the ash-discharge point, whether the ash is wet or dry. Ash-removal equipment should be designed to minimize the spread of contamination and to facilitate cleanup.

5. Careful attention must be given to the actual composition of the contaminated trash at each installation, and the design modified accordingly. Experiments to determine the efficiency of combusion and air cleaning should be accomplished with comparable

waste. Difficulties were encountered at Los Alamos as a result of failure to anticipate the adverse effect that a relatively small number of rubber surgeon's gloves would have on combustion and air cleaning.

6. Pumps and other equipment handling contaminated water from ash-control equipment, air-cleaning equipment, or condensation of stack vapors should be mounted in trays provided with drains to the contaminated waste system.

7. The ash from the incinerator should be kept wet at all times. This requires careful handling of the contaminated water from any de-watering process so that water lines do not become plugged.

8. The design of the incinerator and the materials used in its construction should be such that it can be easily decontaminated. To date, this has been taken to mean that stainless steel is the most desirable construction material.

9. The incinerator and all openings to the incinerator should be capable of maintaining a seal when subjected to a positive internal pressure of 15 to 20 inches of water. Such pressures are not uncommon in incinerators burning unknown materials from experimental laboratories. There is not general agreement as to the necessity or desirability of providing a rupture disk with a separate stack to handle "puff outs" of greater magnitudes.

10. Adequate view ports should be incorporated into the entire material-handling train.

11. A suitable system to quench the fire in the incinerator quickly and effectively in the event of an emergency and for routine control purposes should be provided.

12. The design of the incinerator should be such that complete combustion of all combustible material is assured. This has not been the case in previous incinerator designs. Complete combustion will reduce the load on the air-cleaning train and aid in the final disposal of the ashes.

13. Combustion air should be supplied by a forced air blower with the intake outside the workroom in order to prevent "puff outs" blowing contamination into the room.

14. Instrumentation should be provided, with recording devices located at a central control board, in order that the operator may be aware of all operating conditions.

15. The primary design criterion for the air-cleaning train is that it be virtually trouble-free and capable of being serviced without creating a radiological health hazard to maintenance personnel.

16. Condensation of vapors in the stack gases makes it necessary to provide suitable contaminated drains throughout the air-cleaning train and to ensure that the equipment in the train is leakproof.

17. Because of their flexibility and self-cleaning aspects, wet collectors are generally included in the air-cleaning train for the incinerator. If they are used, however, provision must be made for the safe handling and ultimate disposal of the contaminated sludge and liquid resulting. As noted before, design features should be included to prevent plugging of lines and equipment. Corrosion of ducts and equipment also becomes a major problem after stack gases pass a wet collector, unless the gas is reheated. Facilities should be provided for adjusting the pH of the scrub water.

18. The final cleaning unit is generally a high-efficiency dry filter. Special mountings or holders must be designed to permit removal of contaminated filters in a safe manner. Conventional holders are generally not acceptable.

NONCONTROLLED INCINERATORS

Every installation will not require the same design or operating features, and varying degrees of control for the various levels of radioactivity in the material incinerated will be specified by the health group concerned. The limiting case, designated herein as a noncontrolled incinerator, would be characterized by:

1. Standard commercial incinerator without special provision for charging, ash removal, and stack-gas cleaning.

2. Operators with little or no skill and training.

3. Health personnel not available for daily supervision.

4. Ordinary channels utilized for final disposal of ashes.

This situation would be satisfactory in the case of a hospital or institutional laboratory working with isotopes at low activity levels. For this type of facility, the combustible waste could be such a high percentage of the total waste as to make incineration economically feasible. Even in this case, however, several factors must be borne in mind before such a program is initiated. In the first place, facilities handling radioisotopes almost invariably increase the scope of their work and levels of activity with time. Waste treatment and waste disposal, in general, are not assigned a proportionate percentage of the funds available for this expansion. In the second place, work habits and procedures do not change as rapidly or as effectively as programs. Thus, it is entirely conceivable that a dangerous situation could arise without notice. It is safe to predict that, in the future, a large percentage of radiation injuries will occur in such installations rather than in well-controlled installations handling high levels of activity. In the third place, stringent control procedures will be required in laboratories served by a noncontrolled incinerator to prevent accidental loss to waste of any relatively high level source.

Presuming, however, that incineration in a noncontrolled incinerator is economically feasible and operationally desirable, there remains the problem of determining permissible levels of activity that may be incinerated without creating a health hazard.

C. W. Kruse, et al., in their report entitled, "Behaviour of Institutional Incinerators When Used to Burn Radioactive Wastes,"[7] indicate that the principal factor to be considered in a noncontrolled installation would be the level of activity in the ash. To prevent the creation of a health hazard by the ashes, it was determined that the maximum charges for I-131 and P-32 were 2 and 4 microcuries, respectively, per pound of refuse per hour. Based on a burning rate of 200 pounds per hour, 6 hours per day, and 5 days per week, a total of 12 millicuries of I-131, or 24 millicuries of P-32, could thus be handled per week. There is a distinct possibility, however, that continuous handling of this quantity of activity could create health hazards in the workroom and result in the spread of contamination. Initial plans, therefore, should not anticipate steady loading at this rate.

C. W. Kruse also reported that, with 170 times the maximum allowable concentration of I-131 in the stack gas, below-tolerance air samples were obtained on the ground in a down-wind direction from the stack. It is our feeling that the concentration of activity in stack gases may be much higher than this figure without creating a health hazard. This feeling is based on the following assumptions and calculations:

Sutton's equation for diffusion of stack gases upon differentiating and maximizing reduces to

$$X\,(\text{max.}) = \frac{2Q}{\pi e \bar{u} h^2}$$

X = maximum ground concentrations in units/M^3
Q = emission rate in units/sec
$\bar{u}$ = mean wind speed in m/sec
h = effective stack height in meters

If a minimum value for $\bar{u}$ (of approximately 0.5 mile/hr or 0.23 m/sec) is assumed, a factor of safety is introduced and the equation reduces to

$$X = Q/h^2$$

Also, since the contemplated AEC regulation is that the yearly average shall not exceed the maximum permissible concentration,[1] for a plant operating 5 days a week, 8 hours a day, the maximum permissible concentration could be increased by a factor of 168/40 or 4.2 Further, it is assumed that any point on the ground will not be within the zone of maximum ground concentration more than 50 percent of the time. Combining the above with the reduced equation results in the following approximation:

$$Q = 10\,X\,h^2$$

since

$$Q = CR$$

when

C = concentration of activity in stack gases in units/M^3
R = flow rate of stack gases in M^3/sec

and if X is set equal to the MPC for nonoccupational exposures,

$$C = MPC\ (10h^2/R)$$

It is apparent from this approximation that with normal relationship between stack height, stack diameter, and stack-gas velocities, the stack concentration could exceed the maximum permissible concentration by a considerable factor. Thus, it would appear from this assumption and from the work of Kruse, et al. and that of Silverman and Dickey,[12] that the limitation placed on the loading rate by the health hazard associated with the ash-removal operation is much lower than the limitation based on permissible levels of activity in the effluent gases, and that air cleaning is not necessary or desirable for a noncontrolled incinerator.

It is evident, therefore, that for a noncontrolled incinerator the lack of a health group makes it mandatory that an extremely low level of activity be fixed as a maximum charge. If a health group is available for routine checks and evaluation of health hazards, it is possible for the levels to be increased within flexible limits.

In connection with disposal of radioactive waste, brief mention should be made of 2 other methods. The first is the so-called dilution method, in which radioactive material is disposed of through ordinary municipal waste channels. This method, in general, is not attractive to people experienced in handling radioactive waste. Basically, however, it is probable that the same standards established for a noncontrolled incinerator would apply to this method of disposal.

The other method recently investigated is that of open-field burning.[6] The authors concluded that the health hazards associated with this method were essentially nonexistent and that widespread use of the procedure would "significantly reduce the volume and weight of materials to be disposed of" by AEC installations. The objections to it not dealt with in the report are:

1. The open-dump burning of municipal trash is and has been an unsatisfactory method of municipal waste disposal. The objections are lack of control, lack of proper incineration, and the possible spread of fires under uncontrolled weather conditions. In the case of an open fire burning contaminated waste with unknown levels of activity, the possibility of spreading contamination is not negligible.

2. The authors do not clearly indicate if this is a method of waste processing or waste disposal, but presumably the field in which burning is accomplished would eventually have to be considered a contaminated dump.

3. In tending an open-dump fire, personnel are exposed to numerous hazards, particularly if maximum volume reductions are accomplished. To achieve volume reductions on the order of 90 percent, as reported, requires extraordinary amounts of labor.

It is felt that these objections are such as to remove this method of waste treatment from consideration as a routine method. It would appear to have considerable merit in disposing of a large accumulation of combustible material in a controlled dump, if the process is carefully supervised by a health and safety group.

BIBLIOGRAPHY

1. Atomic Energy Commission. "Standards for Protection Against Radiation." Notice of proposed rule making, 2nd draft, 1956.

2. Corey, R. C., H. Perry, and C. H. Schwartz. "Off-Site Disposal of Radioactive Incinerator Residue." Report 4223, U. S. Bureau of Mines, Pittsburgh, Pennsylvania.

3. Crego, F. T., W. B. Moen, C. S. Sullivan, and A. Muller. "The Development of a Destructor for Processing Solid Combustible Radioactively Contaminated Waste." Air Reduction Sales Company, Inc. Report ARSC-31, April, 1950.

4. Hampson, Donald C., E. H. Hykon, and R. Walton. "Basic Operational Report of the Argonne Active Waste Incinerator." Argonne National Laboratory Report ANL-5067, February, 1953.

5. Haring, M. M. and P. S. Schauer. "Pilot Plant Work on Solid Burnable Waste Disposal for Mound Laboratory." Mound Laboratory Report MLM-232, Monsanto Chemical Co., Dayton, Ohio, November 1, 1948.

6. Harris, W. B. and M. S. Weinstein. "Open Field Burning of Low Level Radioactive Contaminated Combustible Wastes." Paper presented at the American Industrial Hygiene Association's annual meeting in Philadelphia, Pennsylvania, April, 1956.

7. Kruse, C. W., P. V. Freese, A. Machis, and V. C. Behn. "Behaviour of Institutional Incinerators When Used to Burn Radioactive Waste." Johns Hopkins University Report NYO-4517, November 1, 1952.

8. Larson, R. E. and R. H. Simon. "Solid Waste Disposal at the Knolls Atomic Power Laboratory." Knolls Atomic Power Laboratory Report KAPL-936, June 15, 1953.

9. Little, Arthur D., Inc. "Report on Design for Volume Reduction of Combustible Radioactive Wastes by Incineration to Argonne National Laboratory." C-57867, June 3, 1950.

10. Rodger, W. A. and D. C. Hampson. "Operating Characteristics and Economics of a 100 cubic foot per day Incinerator for Radioactive Wastes." Paper presented at the meeting of the Air Pollution Control Association, Detroit, Michigan, May, 1955.

11. Schell, F. N. "A Report on the Development and Operation of a Pilot Incinerator for Contaminated Combustible Solid Wastes." Knolls Atomic Power Laboratory Report KAPL-610, October 1, 1951.

12. Silverman, Louis B. and R. K. Dickey. "Reduction of Combustible, Low Level Contaminated Wastes by Incineration." Paper presented at a conference on Radioisotopes in Agriculture, Michigan State University, Lansing, Michigan, January, 1956.

13. Worsham, M. L., W. G. Neall, and A. F. Owings. "Possible Health Hazards from the Burning of Combustibles Contaminated with Radioactivity." Naval Radiological Defense Laboratory Report AD-134 (14), June 17, 1949.

AUTOMATIC WATER SAMPLING DEVICE

C. T. Nelson and R. L. Koontz

North American Aviation Company
Downey, California

INTRODUCTION

In sampling the effluent from radiochemical laboratories, it is necessary to sample gas as it enters the atmosphere and liquid waste as it enters the sewage system. Many reports have been written on the sampling of air and many excellent methods have been used for constant air sampling and monitoring. Activity records should be kept on liquid effluent, permitting better hazard evaluations to be made just as hazard evaluations are made for air. By the following collection method, liquid sampling similar to the film badge program, in that the average activity - say over 1 week - can be evaluated, is feasible.

In sampling liquid waste from the radiochemical laboratories, the problems at Atomics International are very similar to those at any other laboratory. It is necessary to determine the radioactivity of liquid waste that flows into the public sewer lines.

The liquid which passes through the drains in the radiochemical laboratories is first collected in a dilution tank or sump before passing on with the plant waste into the public sewer lines. Two or 3 years ago at Atomics International the sampling was done by hand. The sump cover was removed, a container lowered into the liquid, and a sample of liquid, floating debris, etc. removed for analysis. From a 500 cc sample the solid residue amounted to several planchets of material for radioactive assay. This cumbersome method of sampling was used at infrequent intervals. If the liquid is sampled only once a week, radioactivity entering the drain between samplings may very well pass undetected. It follows that representative sampling must be taken at close intervals or continuously.

MATERIALS AND METHODS

The sampler designed to fill this need consists of a pump, timing devices, sequence collecting tube, and miscellaneous equipment. The pump is of a constant displacement type, manufactured by Atomics International, and shown in Figure 1. The pump is ideal for this application because of its simplicity - it has no vanes, gears, or diaphragms. The liquid is propelled by squeezing the flexible rubber tubing between the rollers and roller housing. The pump will lift the liquid at least 15 feet at approximately 1 cc per second. The pump is powered by a 6 rpm Bodine motor. By changing the speed of the motor, the flow rate can be changed accordingly. The pump will run for several months, depending on its usage, with no maintenance except replacement of the rubber tubing. Two clamps hold the tubing in place, facilitating rapid replacement.

The sampling probe is shown in Figure 2. It is comprised of a copper tube surrounded by a screen and a float. The float keeps the probe head between floating debris and the mud in the bottom of the tank. The screen aids in keeping large particles from entering the tube. With the use of this sampling probe, a sample of water can be evaporated with hardly more residue than tap water.

Figure 1

PUMP AND MOTOR

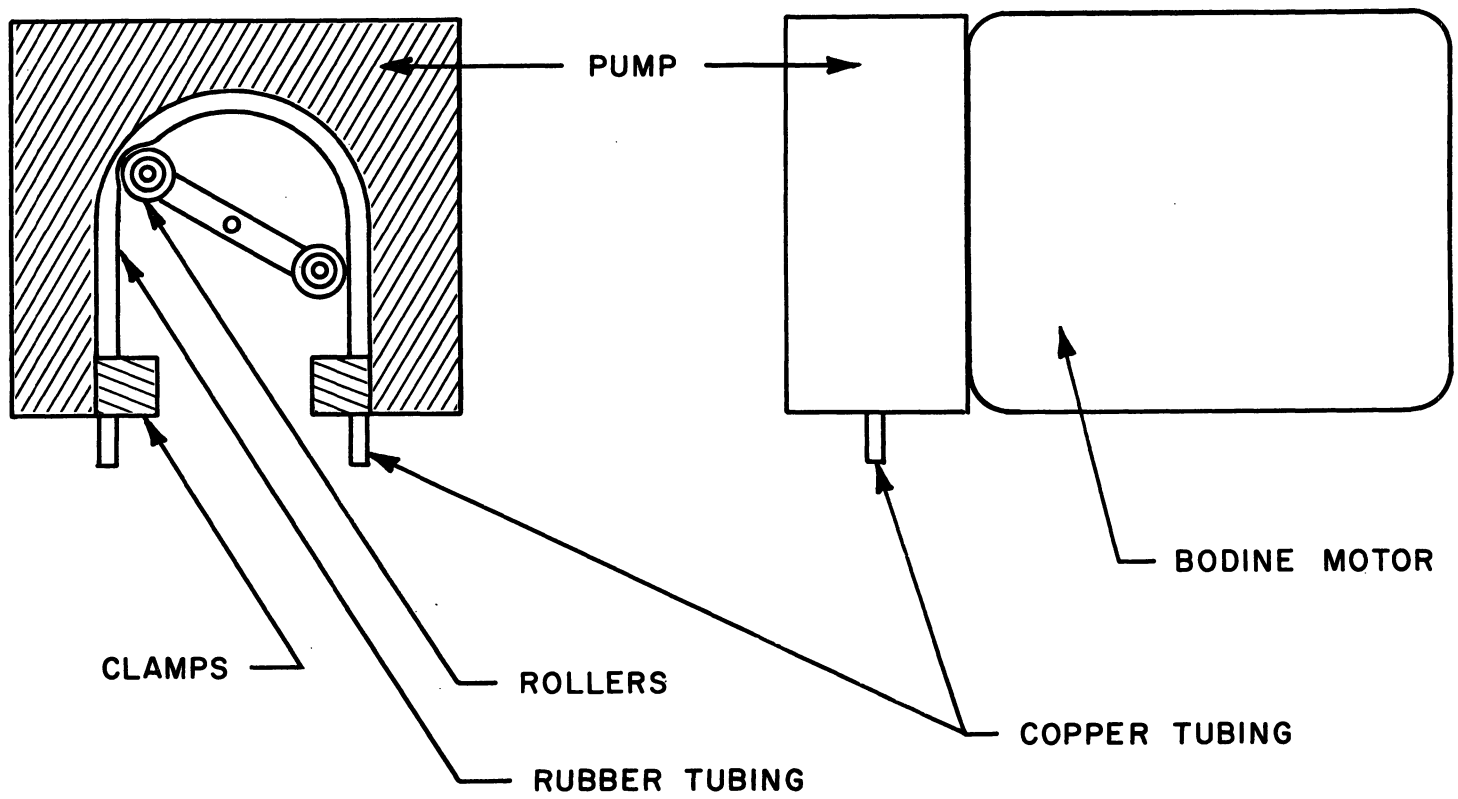

The main timing mechanism is shown in Figure 3. The timer is a type A Tandem Recycling Timer made by the Industrial Timer Corporation. The timing elements, models ET-3M and ET-3H, permit one side of the cycle to vary from 2 seconds to 3 minutes and the other part of the cycle to vary from 2 minutes to 3 hours. The cycle can be reversed by switching the load switch to either T_1 or T_2. After the initial adjustment, each cycle of the operation will follow the other continuously in regular sequence. This particular control unit is adjusted to 20 and 20, so that a sample is collected for 20 seconds every 20 minutes. If the unit operates for 9 hours a day, a sample of approximately 500 cc is collected. The Tandem Timer is connected to a 7-day calendar switch such as the type used to turn on and off lights in store windows. The calendar device determines the sampling period, such as from 7:30 a.m. to 5:30 p.m. daily Monday through Friday. The sampling period can be continuous, 24 hours a day, 7 days a week.

The sequence collecting tube is shown in Figure 4. It consists of a slanting tube with 1 inlet and 4 outlets. As many outlets as needed can be added. The liquid goes down the tube into the empty bottle at the lower end. Since the liquid seeks its own level, the bottles are filled in sequence. The advantage of this tube is that it is easily cleaned and has no moving parts. There is surprisingly little mixing of the activity from one bottle to another. In operation, the samples of liquid are being taken from 1 tank of varying activity, so a small mixture between one bottle and another does not matter. One bottle a day or 1 bottle a week can be collected by this method.

RESULTS AND CONCLUSION

The sample rate can be varied from 100 cc or less per week to 3,000 cc per hour. The pump is self-priming and requires little maintenance. The labor involved is reduced to a minimum. As a result of the automatic sampler, a more representative sample of water can be taken from a large source which is ever-changing in its radioactivity.

Figure 4

FLOW DIAGRAM

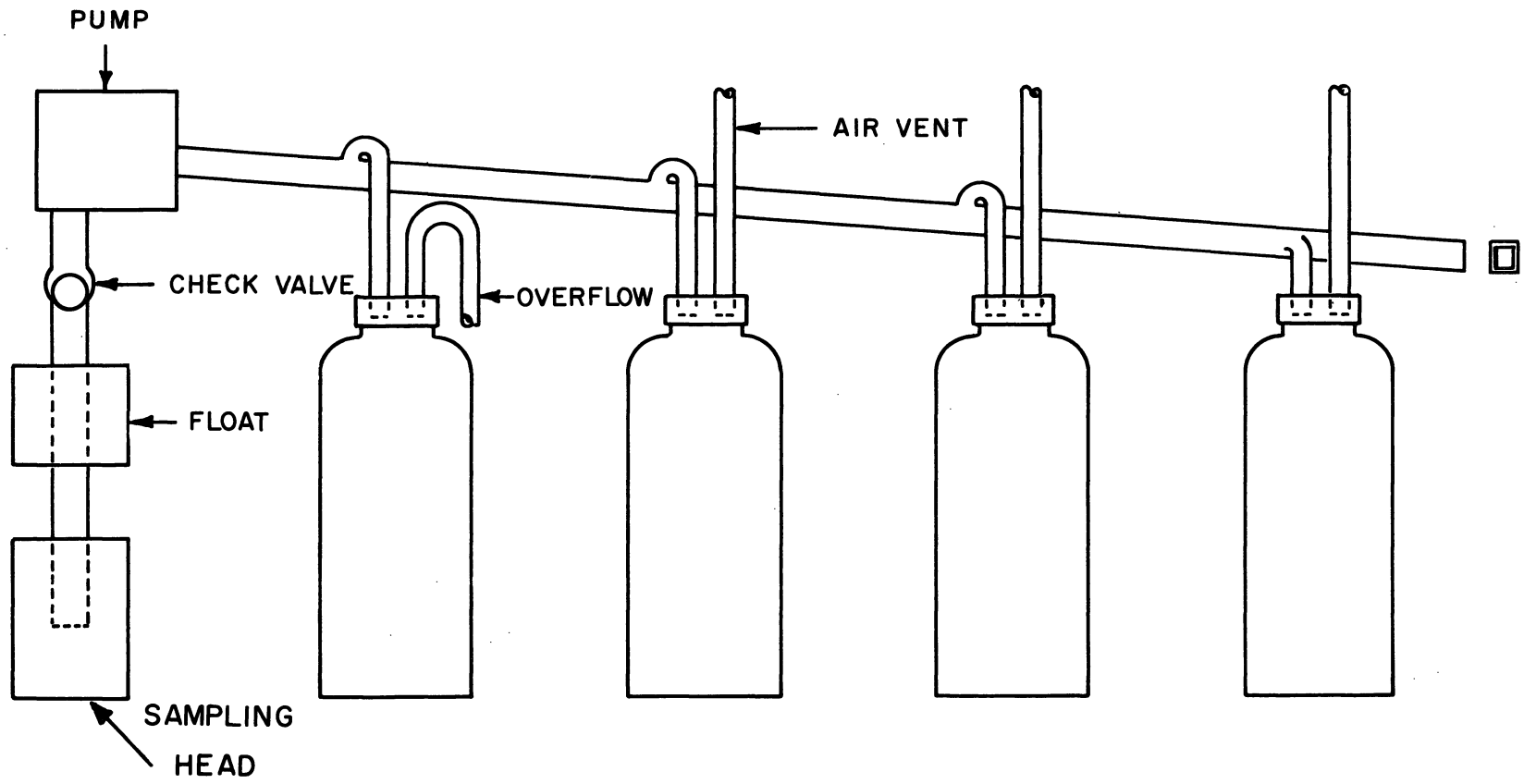

AEROSOL PENETRATION THROUGH SAND

R. E. Yoder

Health Physics Division
Oak Ridge National Laboratory
Oak Ridge, Tennessee

All methods involving the storage of high level power reactor wastes require a medium for the de-entrainment of aerosols produced by the boiling of these wastes.

It is unnecessary to state to an audience of health physicists the urgency of this problem. It is important from the health hazard standpoint of individuals in the waste area and also from the area contamination standpoint.

As this is a problem in aerosol filtration, one immediately thinks of a high efficiency filter medium such as fiberglass, AEC No. 1, or Chemical Corps No. 6 filter media. Since these materials are relatively expensive, we have turned our efforts to a cheap, more abundant material, namely, sand. In addition to being cheap and abundant, it is very resistant to corrosive atmospheres.

A present concept of liquid waste disposal involves the mixing of the liquid wastes with a clay material and various fluxes. By self-heating, this material fuses into a non-leachable mass. When reactor wastes are introduced into a pit, the temperature will rise to about 900°C. As the temperature rises, the water will be driven off as a vapor unless bubbling occurs. Also, volatile materials will be driven off or carried off with the water. It is difficult to state at what size a particle becomes an aerosol, so all particulates in the air will be referred to hereafter as aerosols.

From preliminary data it has been shown that there exists an aerosol size for maximum penetration for heterogeneous river sand at a gas velocity through the sand of 0.8 cm/sec. The aerosol size for maximum penetration was about 0.3 μ radius. The first portion of our work, therefore, was to develop a rapid method of particle size determination for homogeneous aerosols throughout the 0.1 μ to 1.0 μ radius range. All methods heretofore developed were time-consuming and limited to small sections of this range.

We packed a 3-foot length of glass pipe 1 1/2 inches in diameter with No. 11 lead drop shot. These shot are reasonably homogeneous and nearly spherical.

The column was calibrated by using several fundamental methods of particle size estimation: gravity settling for particles greater than 0.3 μ radius, the diffusion battery for particles less than 0.35 μ radius, and polarization for particles between 0.15 μ and 0.18 μ radius.[1,2] When 2 or more methods were used simultaneously on the same aerosol, the results agreed to $\pm$ 10 percent. The positions of the Tyndall bands were noted and used as a check on all the larger sized aerosols.

Figure 1 is a photograph of the lead shot column. It is fitted with adapters at each end to allow the aerosol to pass up or down the column. A screen placed in each end prevents the shot from falling into the tubes leading to the column.

The 2 top curves of Figure 2 correspond to a superficial velocity through the column of 1.49 cm/sec and the lower 2 curves correspond to a superficial velocity through the column of

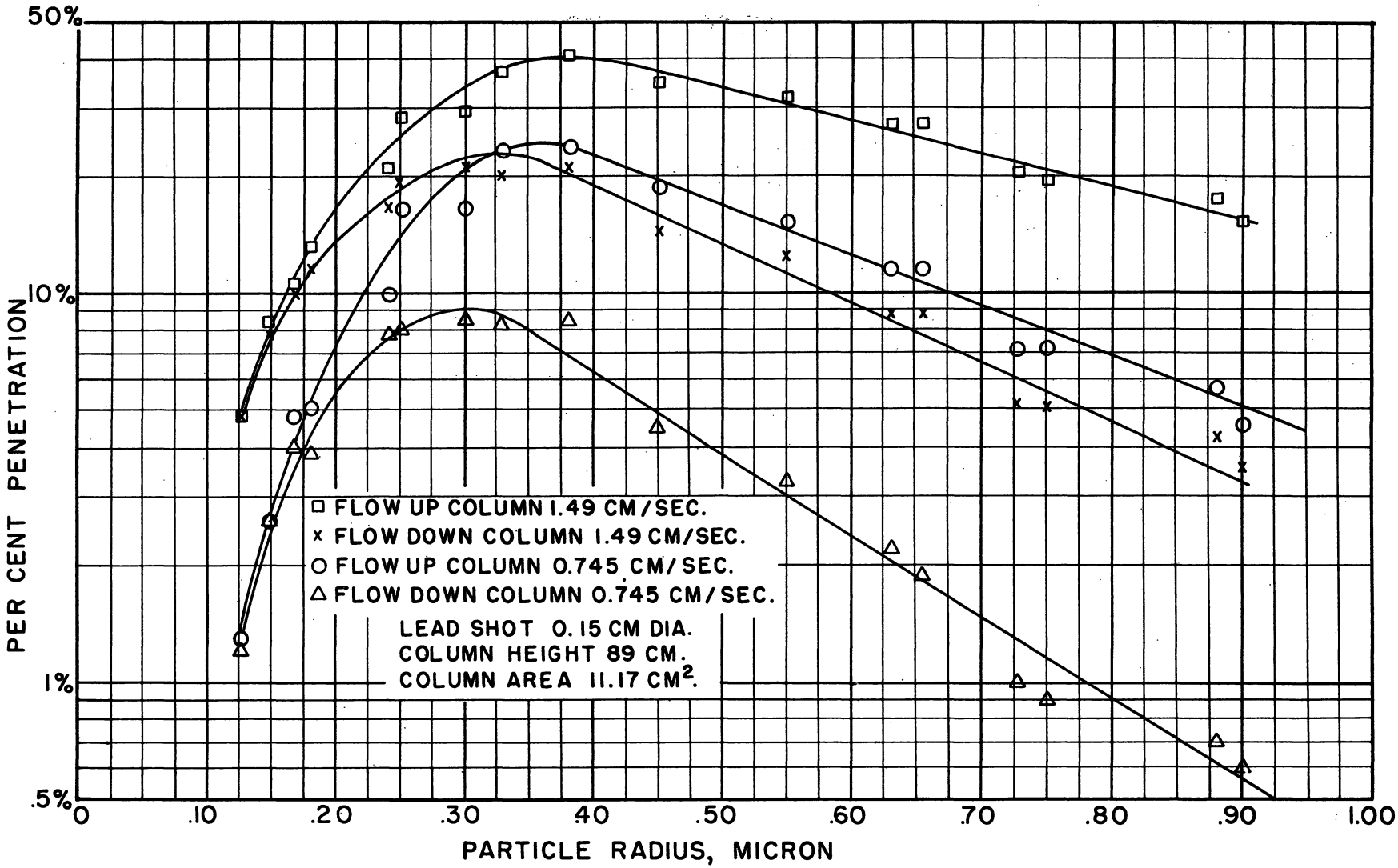
50%
10%
1%
.5%
PER CENT PENETRATION
0
.10
.20
.30
.40
.50
.60
.70
.80
.90
1.00
PARTICLE RADIUS, MICRON
□ FLOW UP COLUMN 1.49 CM/SEC.
x FLOW DOWN COLUMN 1.49 CM/SEC.
○ FLOW UP COLUMN 0.745 CM/SEC.
△ FLOW DOWN COLUMN 0.745 CM/SEC.
LEAD SHOT 0.15 CM DIA.
COLUMN HEIGHT 89 CM.
COLUMN AREA 11.17 CM²

Figure 2

0.745 cm/sec. The superficial velocity is defined as the volumetric flow rate in cc/sec divided by the cross-sectional area of the empty column in cm^2. An NRL E-3 Smoke Penetration Meter was used throughout to measure the aerosol concentration.[3]

One can see from the curves that a particle size for maximum penetration exists. The aerosol size for maximum penetration varies between 0.3μ radius and 0.38μ radius, depending upon the conditions present in the column, i.e., direction of flow and superficial velocity.

The main mechanisms of aerosol removal at these low velocities are gravity settling for large aerosol particles and diffusion for small aerosol particles. When the aerosol goes down the column the force of gravity acts in the direction of aerosol travel, while in up flow the force of gravity acts opposite to the direction of aerosol travel. From this one can see that there might be a difference in penetration depending upon flow direction. The experimental results show a much larger difference than one might anticipate, a factor of 2 at the size for maximum penetration, increasing to a factor of 10 for a 0.9μ radius particle.

As the particle size gets smaller, gravity settling becomes less important, as is evidenced by the coming together of the curves for up and down flow. Diffusion begins to play an important part in the filtration process for aerosols between 0.3μ radius and 0.4μ radius, and becomes the predominant mechanism at particle sizes less than about 0.2μ radius. The converging of the curves is to be expected at the very small particle sizes because gravity settling is not important here and diffusion is independent of flow direction and gravity.[4]

Particle sizes can be determined by passing the aerosol up and then down the column at 1.49 cm/sec, calculating the fraction penetrating the column, and reading the radius from the graph. The whole operation takes only 3 to 5 minutes, with a resulting error of only 10 percent. An inhomogeneous aerosol will not yield the column penetrations predicted by the calibration curves. For example: for an aerosol of 0.5μ particle radius, at a velocity of 1.49 cm/sec through the column, one would expect the penetration values of 34 percent for up flow and 14 percent for down flow. If the same aerosol contained a large number of particles different from 0.5 μradius, one would get penetration values of, say, 34 percent for up flow and 9 percent for down flow. Penetration values of 34 percent and 9 percent give the aerosol particle size 0.5μ radius and 0.61μ radius. The greater the difference in particle size obtained for up flow and down flow, the more inhomogeneous the aerosol.

The column has been checked from time to time and no evidence of clogging or changing of penetration values with particle size has been found. That the columns are reproducible was evidenced by the construction of 3 additional ones.

This completed work on the lead shot column as a rapid method of particle size estimation. In all sand filter work, the lead shot column is used as the only method of particle size estimation.

The main objective of the sand filter work was to study the removal of aerosols arising from pits containing radioactive wastes. The gas velocity in these pits is expected to be 0.0007 foot/sec or 0.02 cm/sec. This is a much lower velocity than any other experiments have reported. Laboratory experiments have used velocities as low as 0.054 cm/sec and as high as 2.2 cm/sec.

Velocities were not extended below 0.054 cm/sec because of the difficulties involved. At these very low velocities, sand has essentially no pressure drop to aid in distributing the flow evenly. Also, the size of a container necessary at these low velocities becomes unwieldy for laboratory use. These will not be problems in a full scale experiment because the sand filter will be placed directly above, if not in contact with, the aerosol source; therefore the aerosol will be uniformly distributed upon entering the filter.

So far in the laboratory 3 types of sand have been used. The first was a Pennsylvania sand used for sand blasting, the second was some Clinch River sand, and the third was the Ottawa

Standard Testing Sand. As will be noted later, the grains of these sands are quite different in shape; they therefore will show variation in filtration.

The Pennsylvania and Clinch River sands were screened into as many fractions as was feasible. To obtain large quantities in each size range, about 100 pounds of each were used.

Figure 3 is a photograph of the Pennsylvania sand in the sand holders. The height of the sand columns increases by a factor of 2 beginning on the right; the first is 1 1/2 inches high, the next is 3 inches high, and so on. The tallest column is 12 inches high. The columns have a diameter of 5 1/2 inches.

The columns were found to be exponential in their filtering action, that is, the expression for aerosol removal is similar to that expressing the attenuation of gamma rays in matter. This allows some freedom in extrapolating the results to thick beds. Beds may be several feet thick, since one of the objectives is to obtain a decontamination factor of 10^{12}.

Figure 4 shows some data taken on the different sands under identical conditions. The D_g is the diameter of the sand grains and is determined by taking the mean value of the openings of the collecting screen and preceding screen. For example: A number 20 screen has an opening of 0.084 cm and a number 30 screen has an opening of 0.059 cm. The D_g of sand collected on a number 30 screen is 0.071 cm, the mean of these 2 figures.

One may well ask why the Pennsylvania sand gives higher penetrations or lower efficiencies than the Ottawa or Clinch River sands. The Pennsylvania sand gives penetrations 5 times greater than the Clinch sand at the size for maximum penetration.

The void fractions, or the ratio of the interstitial volumes to total volumes, are approximately the same, being 0.41 for the Pennsylvania sand, 0.385 for the Clinch River sand, and 0.354 for the Ottawa sand. Upon microscopic examination of the sand grains, one finds the Pennsylvania sand to have a smooth surface even though it is a very angular sand with a prismatic shape. The Ottawa sand has a smooth surface and a spherical shape. The Clinch River sand, on the other hand, neither angular nor spherical, had a rough porous surface. The data indicate that the rougher the sand grains, the greater the sand's efficiency as a filter material.

Figure 5 is a comparison of different size sands at different flow rates. The sand used here is the Clinch River sand. The 3 upper curves were obtained using the largest sand grain size fraction, D_g = 0.161 cm; the lower 3 curves were obtained using the smallest sand grain fraction, D_g = 0.036 cm.

The column heights are the same, 1 1/2 inches. Here one definitely can see the advantage of using a small grained sand in a filter. At 0.109 cm/sec, the largest sand size gives penetrations 100 times greater than the smallest grain size at the same velocity. The difference in pressure drop across the filters at these low velocities is almost independent of the sand grain size.

Figure 6 shows data which were taken in some preliminary work on unsieved Clinch River sand. The important thing to note here is that the penetrations are of the same order of magnitude as those obtained from graded sand.

The expression for the removal of aerosols by sand initially takes the form of a simple exponential equation:

$$C = C_0 e^{-Kz}$$

where

C = effluent concentration of aerosol from filter
C_0 = influent aerosol concentration of aerosol to filter
K = an attenuation function
z = column height.

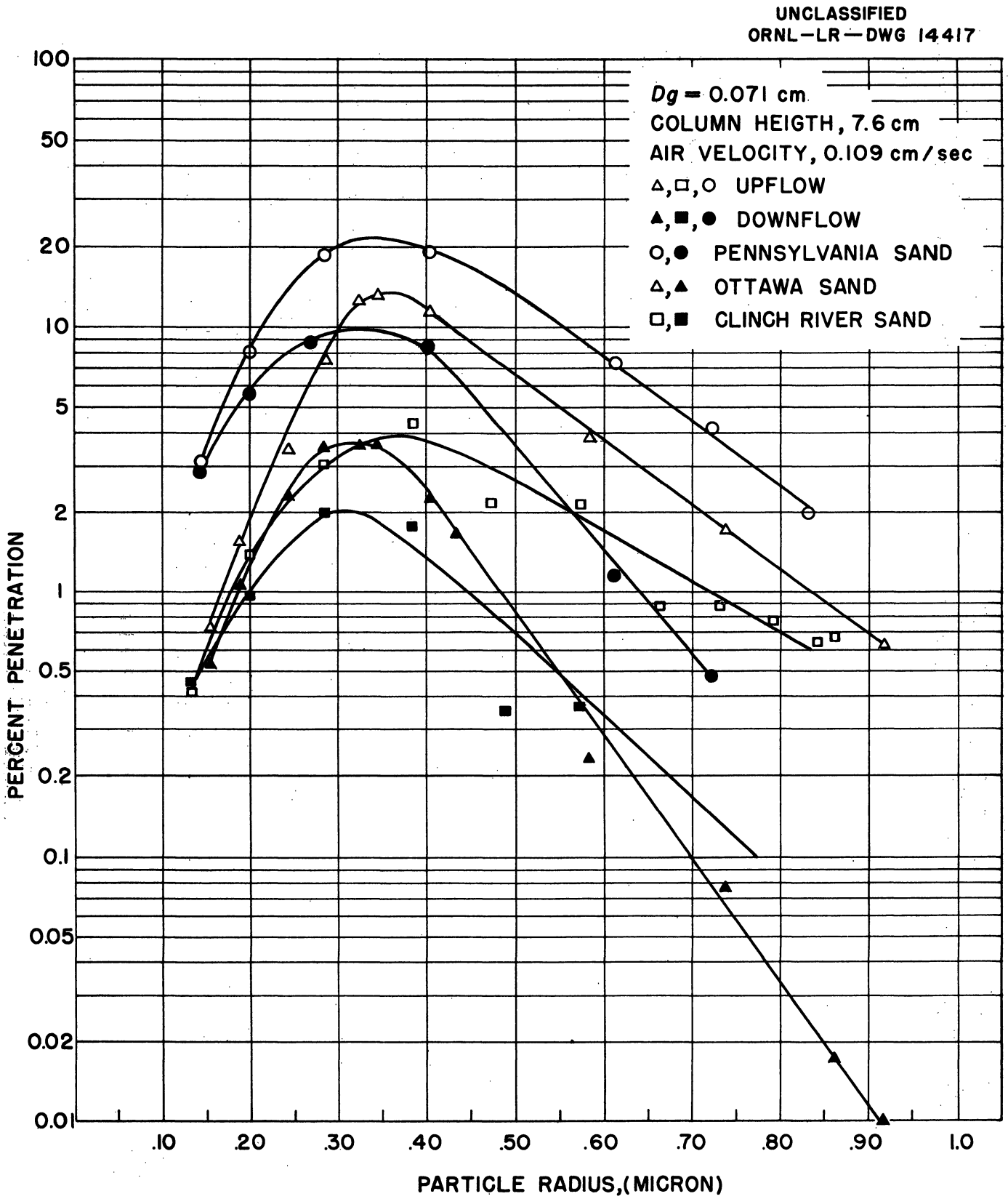
UNCLASSIFIED
ORNL-LR-DWG 14417
Dg = 0.071 cm
COLUMN HEIGTH, 7.6 cm
AIR VELOCITY, 0.109 cm/sec
△,□,○ UPFLOW
▲,■,● DOWNFLOW
○,● PENNSYLVANIA SAND
△,▲ OTTAWA SAND
□,■ CLINCH RIVER SAND
PERCENT PENETRATION
100
50
20
10
5
2
1
0.5
0.2
0.1
0.05
0.02
0.01
.10
.20
.30
.40
.50
.60
.70
.80
.90
1.0
PARTICLE RADIUS,(MICRON)

Figure 4

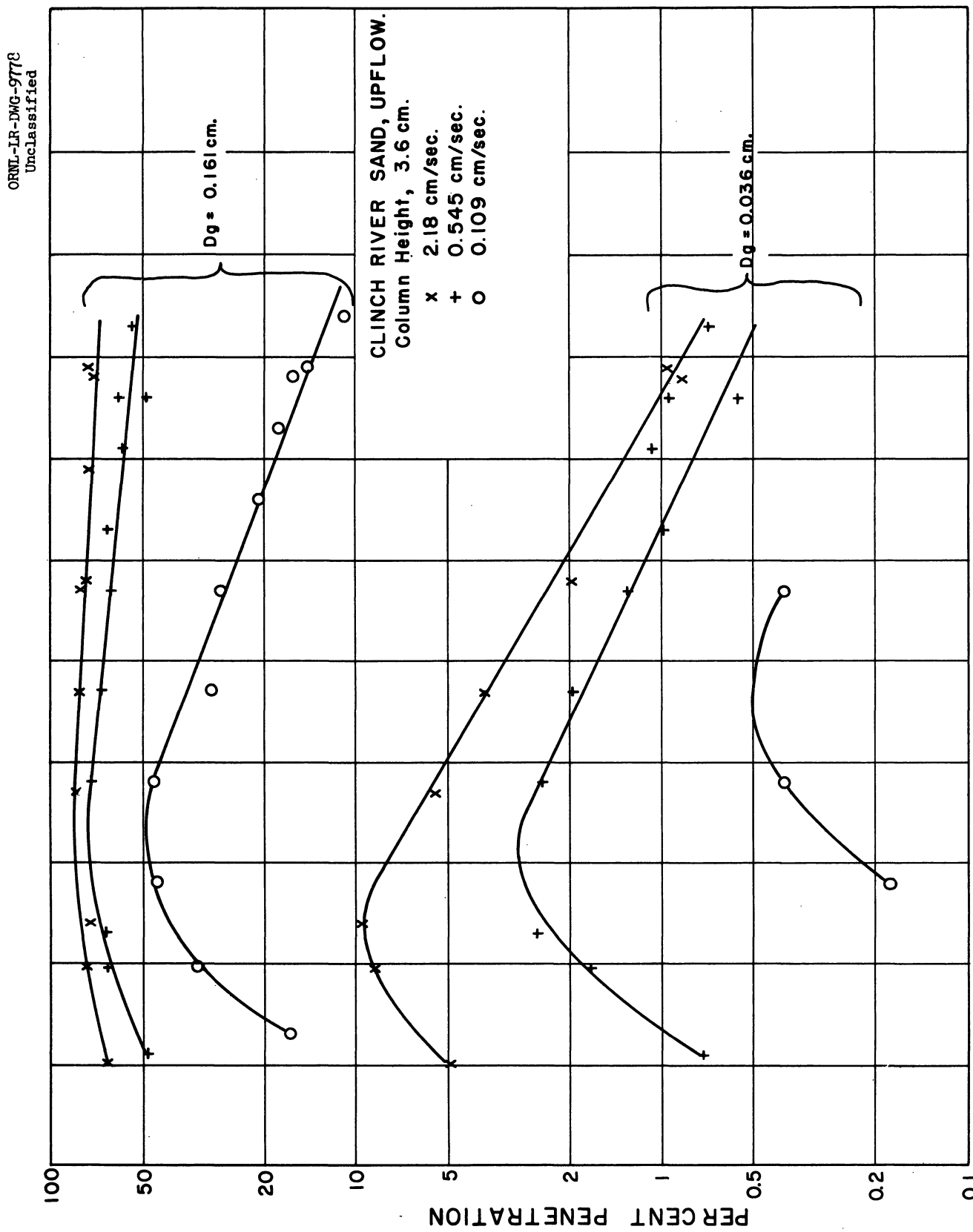
ORNL-LR-DWG-9778
Unclassified
CLINCH RIVER SAND, UPFLOW.
Column Height, 3.6 cm.
x 2.18 cm/sec.
+ 0.545 cm/sec.
o 0.109 cm/sec.
Dg = 0.161 cm.
Dg = 0.036 cm.
PER CENT PENETRATION
PARTICLE RADIUS, (MICRON)
100
50
20
10
5
2
1
0.5
0.2
0.1
0
.1
.2
.3
.4
.5
.6
.7
.8
.9
1.0

Figure 5

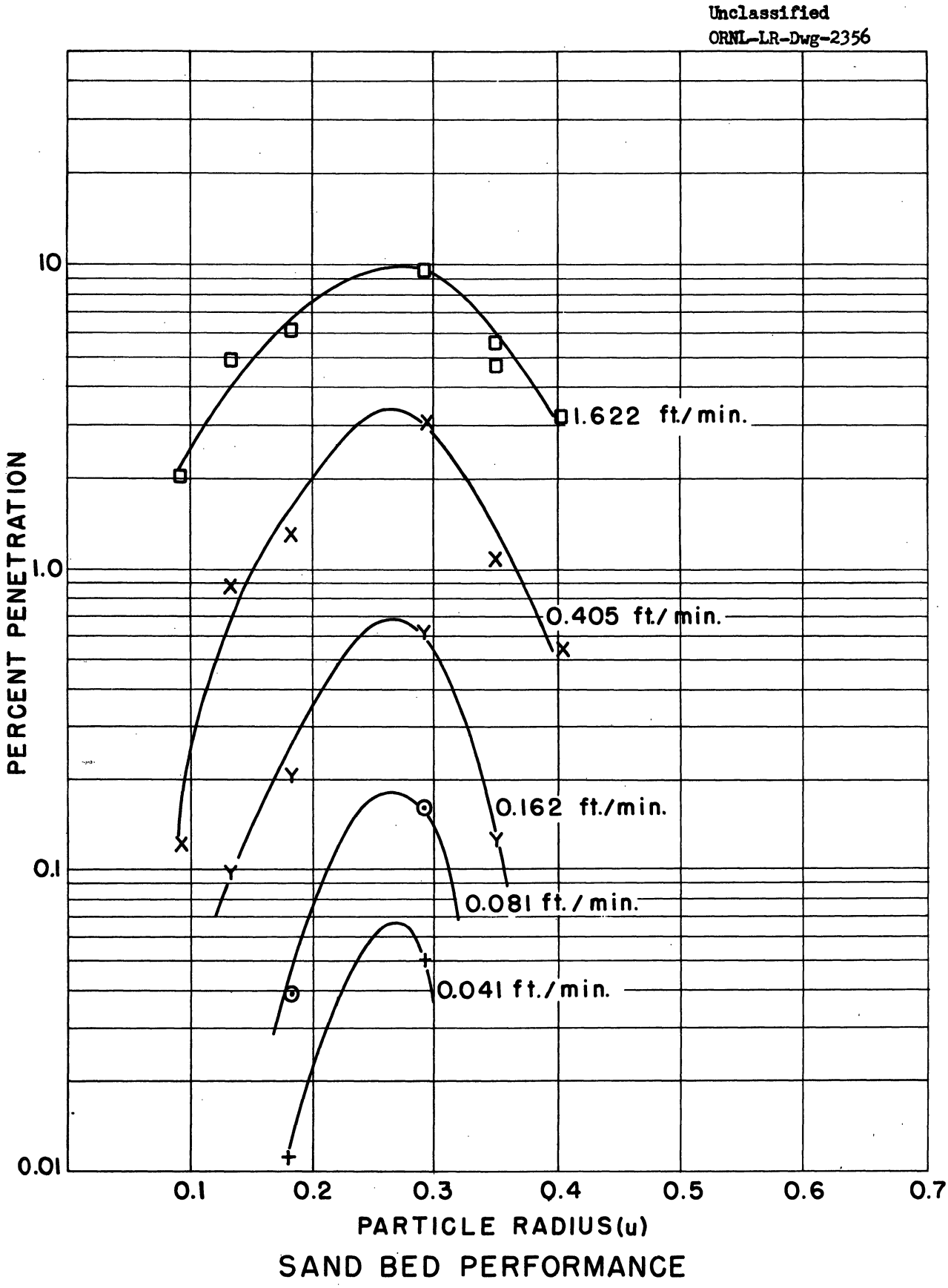

SAND BED PERFORMANCE

Figure 6

With the aid of Dr. Jury, an expression for K was obtained from the most reliable published theories and his own thoughts on the matter. He indicated the expression for K would be of the form

$$K = E\,(A + Br^3)$$

where E is a function of the particle radius r and the grain size D_g, A and B are functions of velocity.

Empirical evaluation of the constants of this expression yields the function

$$K = \frac{10^{-3}}{D_g}\,(1 - \alpha)\,\frac{1}{r}\,(1 + \frac{0.087}{r})\,(2.09\,V^{-0.57} + 22\,V^{-0.78}\,r^3)$$

where

D_g = sand grain size (cm)
r = aerosol particle radius ( )
α = void fraction of the filter
V = superficial aerosol velocity (cm/sec)

The data so far have been obtained using dry sand. Radioactive tracers were used in the aerosol well to study the filtration of aerosols in the presence of condensing water vapor. The aerosol well, Figure 7, is a stainless steel (347) tank, 3 feet in diameter, 20 feet deep, equipped with heaters and thermocouples. It is equipped with a sand filter holder and condensing system which allows collection of all the moisture which passes the filter.

Defining the decontamination factor as the ratio of the activity per cc of well water to the activity per cc of condensate, one finds that by boiling water containing Au-198 as a tracer, one obtains a decontamination factor of 2×10^5. When the water vapor is filtered with 1 foot of sand before condensing it, one obtains a decontamination factor of 2×10^6. This indicates that wet sand gives a decontamination factor of 10 per foot.

From laboratory and field experiments using sand as an aerosol filter one may conclude that

1. A decontamination factor of 10^{12} seems, at the present time, a rather high number for wet sand but a realistic one for dry sand.

2. Having established the aerosol size for maximum penetration, one can now design a dry sand filter to give any degree of protection desired.

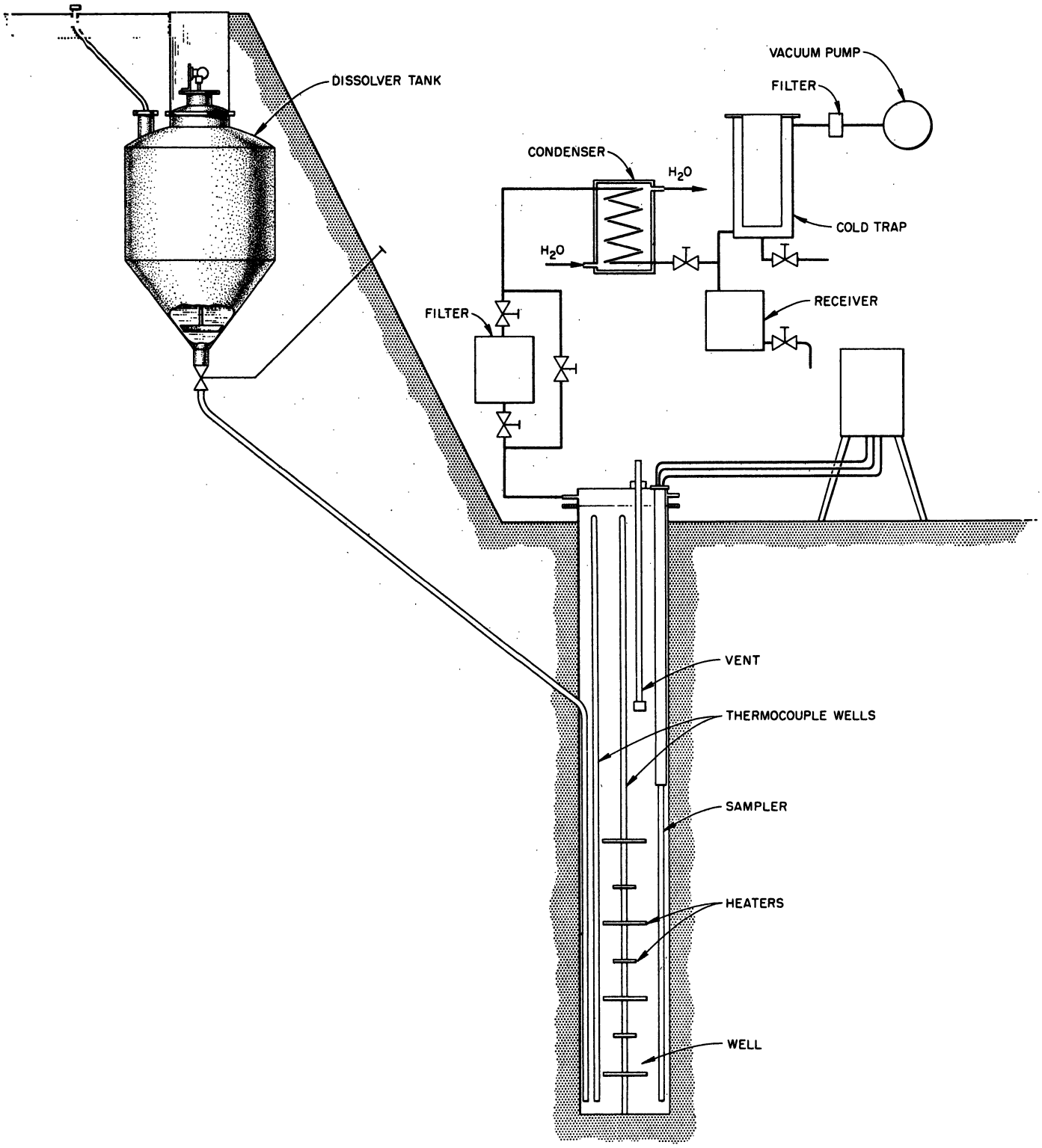

AEROSOL WELL

Figure 7

BIBLIOGRAPHY

1. LaMer, V. K., P. R. Gendron, and R. S. Gruen. Progress Report, AEC Contract AT(30-1)-651, NYO 511, Columbia University, January 30, 1950.

2. LaMer, V. K., et al. "Studies of Filtration of Monodisperse Aerosols." Final Report, AEC Contract AT(30-1)-651, NYO 512, Columbia University, March 31, 1951.

3. Knudson, H. W. and L. White. "Development of Smoke Penetration Meters." Report P-2642, Naval Research Laboratories, September, 1954.

4. Thomas, J. W. and R. E. Yoder. "Aerosol Penetration Through a Lead Shot Column: A Method of Particle Size Estimation." A. M. A. Archives of Industrial Health, 13:550, 1955.

THORIUM MAXIMUM PERMISSIBLE AIR CONCENTRATIONS AND AIR SAMPLING PROBLEMS

J. W. Healy

Hanford Atomic Products Operation
General Electric Company
Richland, Washington

Thorium is not a completely new material in industrial or medical applications since it has been widely used in the manufacture of mantles for gas lamps and, in the form of thorium dioxide, as a contrast medium in radiography. Since interest in the material has increased in the past few years, a review of some of the possible radiological problems involved in increased handling was made.

MAXIMUM PERMISSIBLE CONCENTRATIONS

The metabolism of thorium is similar to that of plutonium,[1] with retention in bone of the same order of magnitude and with deposition in a similar pattern. Human data on the long term effects following administration of thorotrast are available but are not applicable to the establishment of MPC's, since the compound was administered intravenously as a colloid which deposited in the liver. Data available on thorium absorbed from the lung,[2] GI tract,[3] or intramuscular injection[4] indicate that the bulk of the thorium is deposited in bone.

Toxicity studies have shown that the chemical toxicity is low[5] although foreign body reactions may occur at the site of injection.

The maximum permissible body burden and the MPC in water given by the International Commission on Radiation Protection[6] were calculated with full release of all of the energy of the daughter products in the body and metabolism assumed, similar to that of plutonium. The MPC in air, however, was obtained at the Harriman conference[6] by comparison with the MPC in air for uranium. Comparison with the MPC of plutonium of 2×10^{-12} μc/cc, considering the same retention and deposition, would indicate an MPC of 3×10^{-13} μc/cc, if allowance is made for the 36 Mev kinetic energy of Th-232 and daughter alpha particles per disintegration as compared to the 5.15 Mev of plutonium. Calculation from the maximum permissible body burden of 0.01 μc for Th-232, assuming a 20 percent retention in the lung and a half-life of 4×10^4 days, results in an MPC in air of 1×10^{-13} μc/cc. In view of the present uncertainties in the constants involved, there is no significant difference between these values. The higher MPC of 3×10^{-13} μc/cc is recommended.

This MPC is based on soluble compounds. If it is assumed that "insoluble" thorium is eliminated from the lung to the bloodstream with a half-life of about 1 year, it can be shown that the bone will still be the limiting organ. Calculations on this basis over a period of 70 years indicate that the MPC for "insoluble" thorium compounds should be on the order of 3×10^{-13} μc/cc.

There are many uncertainties in this calculation. The retention in lung and rate of elimination from bone are unknown but are consistent with present assumptions used for the calculation of other isotopes. Estimation of the total retention in rats following exposure to aerosols of 0.8 to 1.4 microns mass median diameter over a period up to 20 weeks[2] indicated retentions of soluble ThF_4 of 10 to 20 percent of that inhaled, with 2/3 of the retained quantity in the bone. Insoluble

This paper is based on work performed for the AEC under Contract #W-31-109-Eng-52.

ThO_2 inhalations left 2 to 4 percent in the lung. Such values are not greatly different from the assumed retention of 10 to 20 percent, although the particle sizes and characteristics of the rat lung may well influence the results.

AIR SAMPLING RELATIONS

The measurement of thorium in air samples is made difficult by the possible presence of daughter products released from the operations. Since the MPC is calculated for the parent, Th-232, measurements must be designed to evaluate the quantity of this isotope and the excess of any of the daughters over the quantity in equilibrium with the parent. A change with time in the quantities of daughters present in a mixture following separation is caused by the relatively short half-lives of the intermediate members of the chain. The decay chain for Th-232 is given in Table 1.

TABLE 1

DECAY CHAIN - Th-232

Isotope	Half-life	Particle
Th-232	1.39×10^{10} Y	α
Ra-228($MsTh_1$)	6.7 Y	β^-
Ac-228($MsTh_2$)	6.13 H	β^-
Th-228(RdTh)	1.90 Y	α
Ra-224(ThX)	3.64 D	α
Tn-220	54.5 S	α
Po-216(ThA)	0.158 S	α
Pb-212(ThB)	10.6 H	β^-
Bi-212(ThC)	60.5 M	34% α 66% β^-
Po-212(ThC')	3×10^{-7} S	α
Tl-208(ThC'')	3.1 M	β^-

If the daughters are removed from this mixture during purification, only Th-232 and Th-228 remain. The 1.90 year half-life of Th-228, in comparison to the 6.7 year half-life of the Ra-228 intermediate, allows the quantity of Th-228 and daughter products to decrease until the Ra-228 has been produced in sufficient quantity from the Th-232 that its decay rate (and thus rate of production of Th-228) overbalances the decay of the Th-228. Thus the quantities of these later daughters and the rate of emission of alpha or beta particles pass through a minimum following separation and then increase to the equilibrium quantity. Figure 1 indicates the calculated rate of emission of alpha particles and beta particles for 1 microgram of thorium at various times following separation. Note that a subsequent separation at a later date will further distort this curve.

Since the quantity of daughter products associated with a given quantity of thorium will vary depending upon the previous history of the sample, the estimation of the quantity of thorium present by counting techniques is difficult. This difficulty is enhanced by the preferential release of daughter products during certain operations.

Figure 1

DISINTEGRATION RATE OF THORIUM FOLLOWING SEPARATION

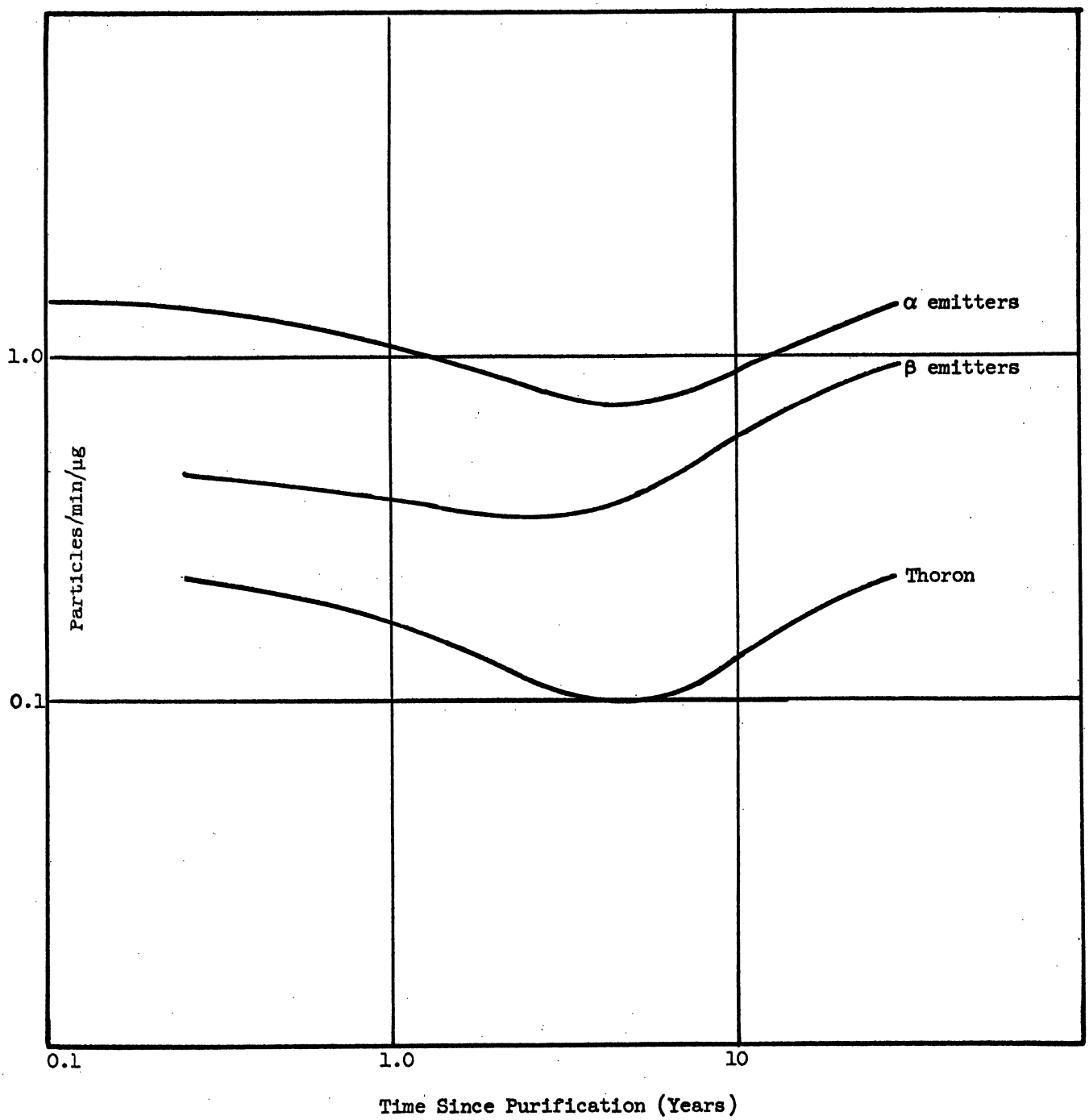

The estimation of the disintegration rate following any given situation must take into account the variations in possible concentration of each of the daughters as well as the build-up of each of the daughters from the parents previously collected. These calculations have been carried out with each daughter product assumed present in a quantity at least equal to that in radioactive equilibrium with the parent. The concentrations of interest, then, are the quantities in excess of the equilibrium. This method of calculation was chosen because the maximum permissible limits of the parents are derived with energy release assumed equal to that of the parent plus daughters. In such a mixture the quantities of concern are the excess over that in radioactive equilibrium.

The results of these calculations may be summarized in terms of the alpha particles and beta particles emitted for given collection and decay times. If the concentrations of the individual daughters, in units of disintegrations per minute per cc, are represented by Th-232, Ra-228, etc., and the collection rate through the sampler is R cc/minute, the number of alpha particles emitted per minute is

$$(1) \quad D/M_{\alpha} = R\left(\left[\text{Th-232} + 5\ (\text{Th-228})\right] T + A\ (\text{Ra-224}) + B\ (\text{Pb-212})\right)$$

where T is the time of collection and A and B are functions of the collection and decay times (Figure 2). These equations assume that the time of measurement is short enough so the Th-228 will not decay significantly, and that the short-lived products are in radioactive equilibrium with the long-lived parents. Thus the factor of 5 for the Th-228 includes the alpha particles from the Ra-224, Em-220, Po-216, Bi-212, and Po-212.

The rate of emission of beta particles may be calculated by the same technique.

$$(2) \quad D/M_{\beta} = R\left[(\text{Ra-229} + 2\text{Th-228})\ T + C(\text{Ra-228}) + D(\text{Ra-224}) + E(\text{Pb-212})\right]$$

Figure 3 illustrates the constants for various decay times and collection times of 15 and 60 minutes. It should be noted that the beta measurement is dependent on the Th-232 content only to the extent that the Th-228 is in equilibrium with its parent.

In practice, the beta measurement is made difficult by the variation in detection efficiency with the energy of the emitted particle. To account for this variation, additional terms must be added to the equation so that each component may be corrected for its efficiency.

$$(3) \quad (c/m)_{\beta} = R\left[(\beta_{\text{Ra-228}}T + \beta_{\text{Ac-228}}C)\text{Ra-228} + (\beta_{\text{Pb-212}} + \beta_{\text{Bi-212}})\text{Th-228}\right.$$
$$\left.(\beta_{\text{Pb-212}}F + \beta_{\text{Bi-212}}G)\text{Ra-224} + (\beta_{\text{Pb-212}}H + \beta_{\text{Bi-212}}J)\text{Pb-212}\right]$$

Figure 4 presents the coefficients required for the solution of this equation for a 1-hour collection period.

These calculations may be used to illustrate the types of decay curves which result from samples collected under various conditions. Figure 5 illustrates the alpha emitter decay rates expected for a mixture containing the maximum permissible concentrations for Th-232, Ra-228, Ra-224, and Pb-212. Figure 6 illustrates the curves expected for the measurement of the beta particles from the same mixture on Geiger counters with windows of 3 mg/cm^2 and 30 mg/cm^2 and 100 percent geometry.

An estimate of the quantities of the shorter-lived emitters may be made by the use of several measurements on the same sample and simultaneous solution of the equations. Thus from equation (1):

$$\text{R(Ra-224)} = \frac{D/M_2 - D/M_3 - \left[D/M_1 - D/M_2\right]\frac{B_2-B_3}{B_1-B_2}}{A_2-A_3 - (A_1-A_2)\left[\frac{B_2-B_3}{B_1-B_2}\right]}$$

Figure 2

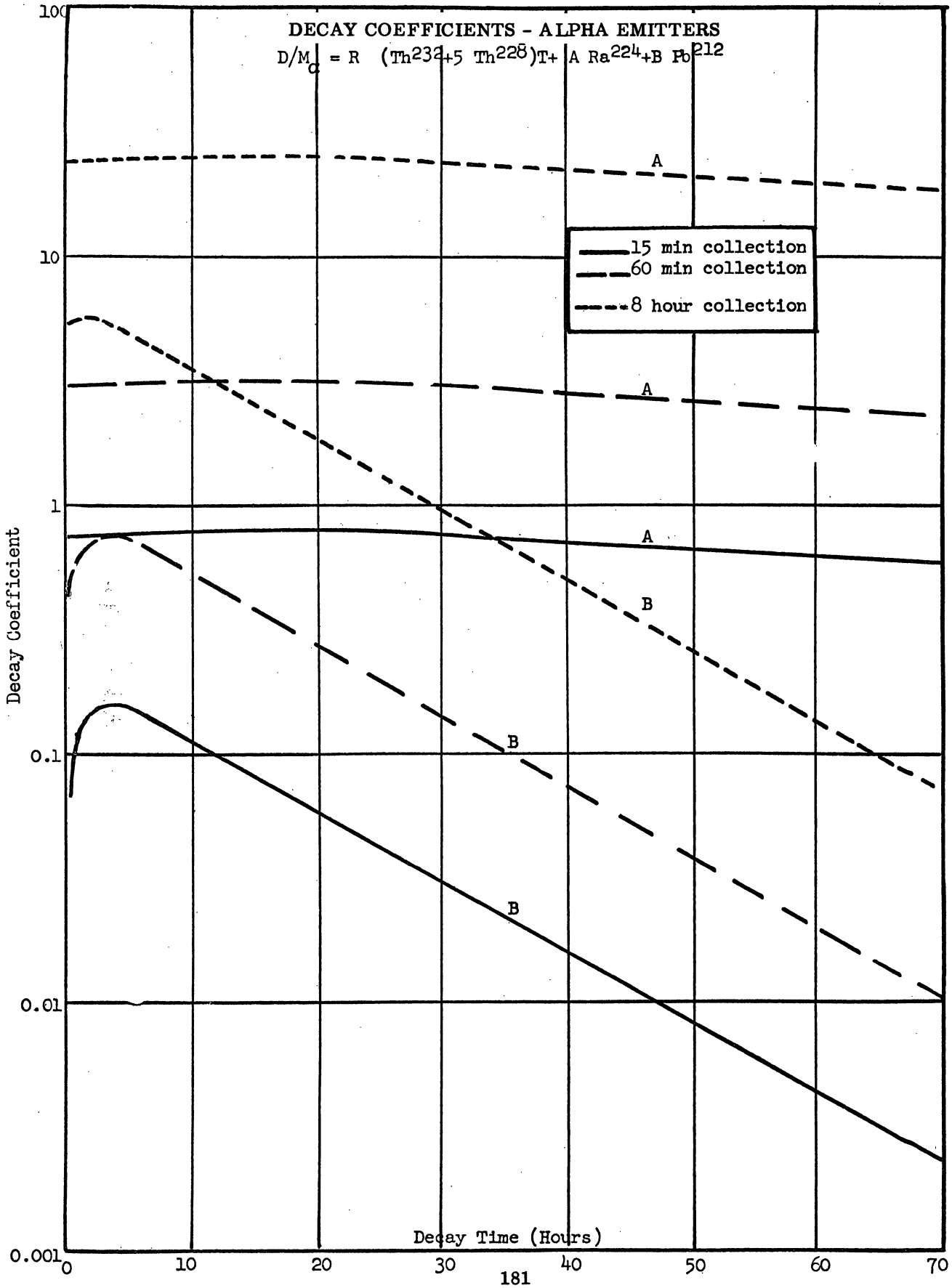
DECAY COEFFICIENTS - ALPHA EMITTERS
$D/M_\alpha = R\ (Th^{232}+5\ Th^{228})T + A\ Ra^{224}+B\ Pb^{212}$
15 min collection
60 min collection
8 hour collection
A
A
A
B
B
B
Decay Coefficient
Decay Time (Hours)
100
10
1
0.1
0.01
0.001
0
10
20
30
40
50
60
70

Figure 3

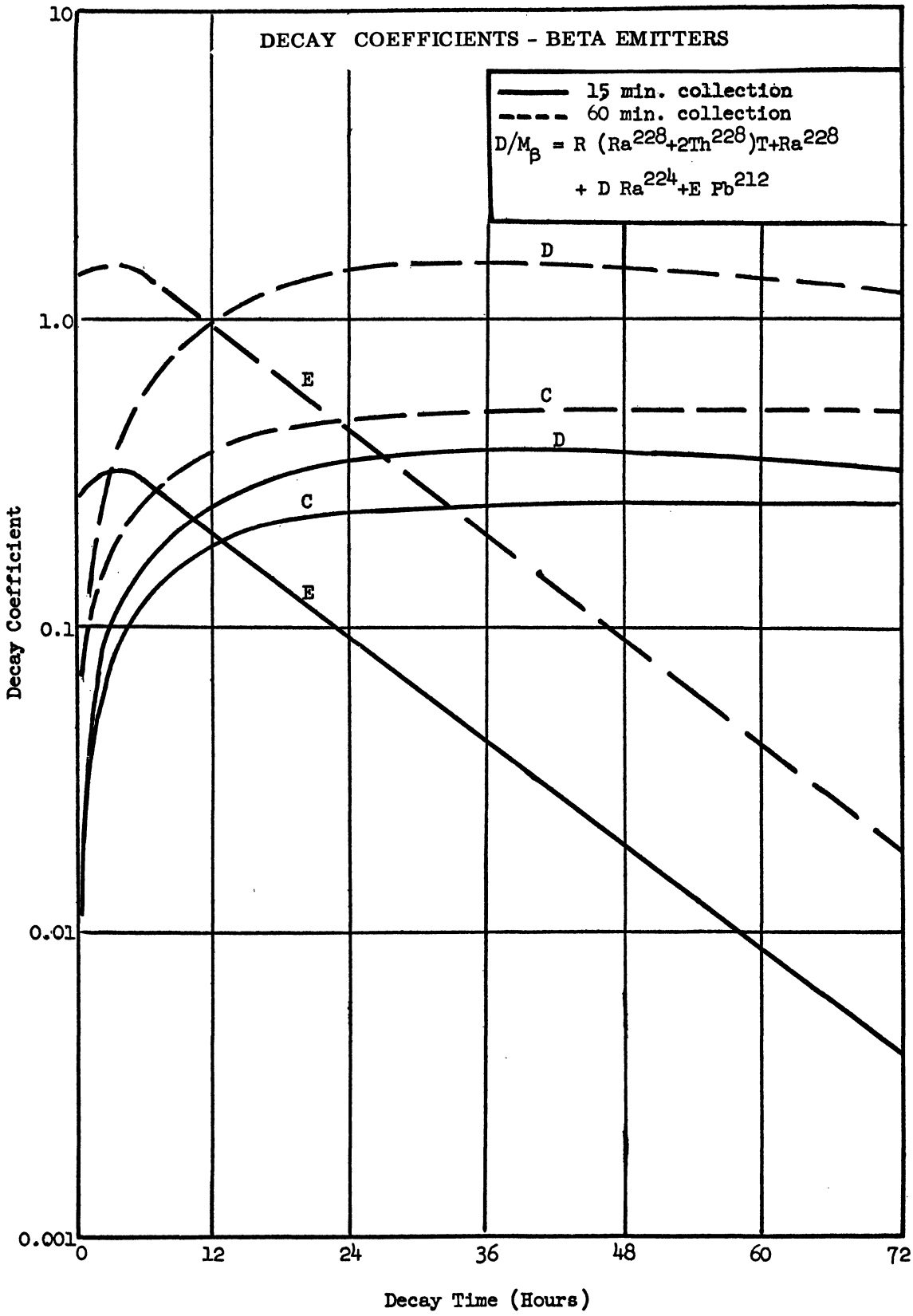
DECAY COEFFICIENTS - BETA EMITTERS
15 min. collection
60 min. collection
D/Mβ = R (Ra228+2Th228)T+Ra228
+ D Ra224+E Pb212
D
C
E
D
C
E
10
1.0
0.1
0.01
0.001
Decay Coefficient
0
12
24
36
48
60
72
Decay Time (Hours)

Figure 4

DECAY COEFFICIENTS - BETA EMITTERS

One-Hour Collection Time

$$C/M_\beta = R\ (\beta_{Ra228}T + \beta_{Ac228}C)Ra^{228} + (\beta_{Pb212} + \beta_{Bi212})Th^{228} + (\beta_{Pb212}F + \beta_{Bi212}G)Ra^{224} + (\beta_{Pb212}H + \beta_{Bi212}J)Pb^{212}$$

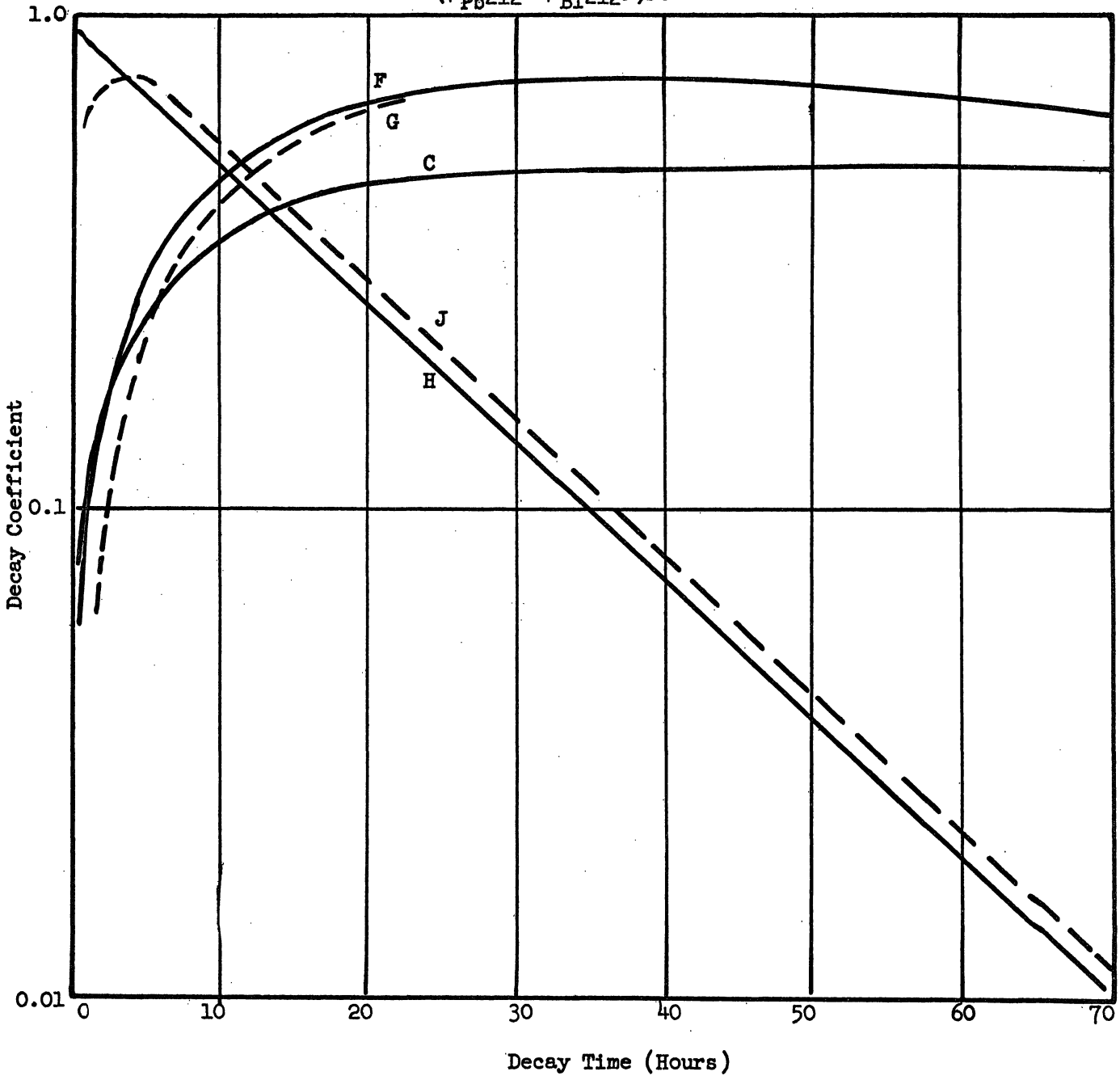

Figure 5

DECAY CURVES - ALPHA EMITTERS

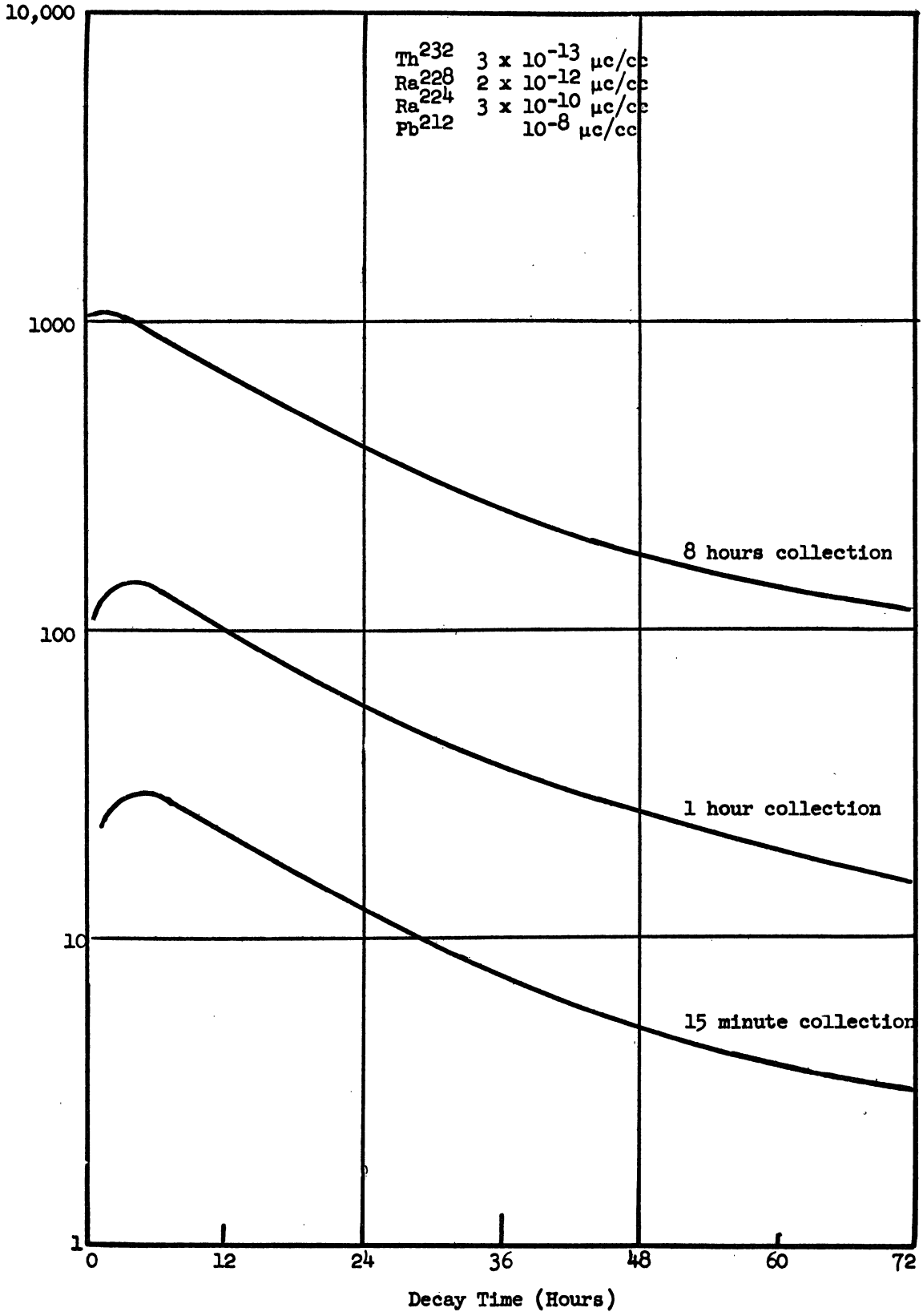

Figure 6

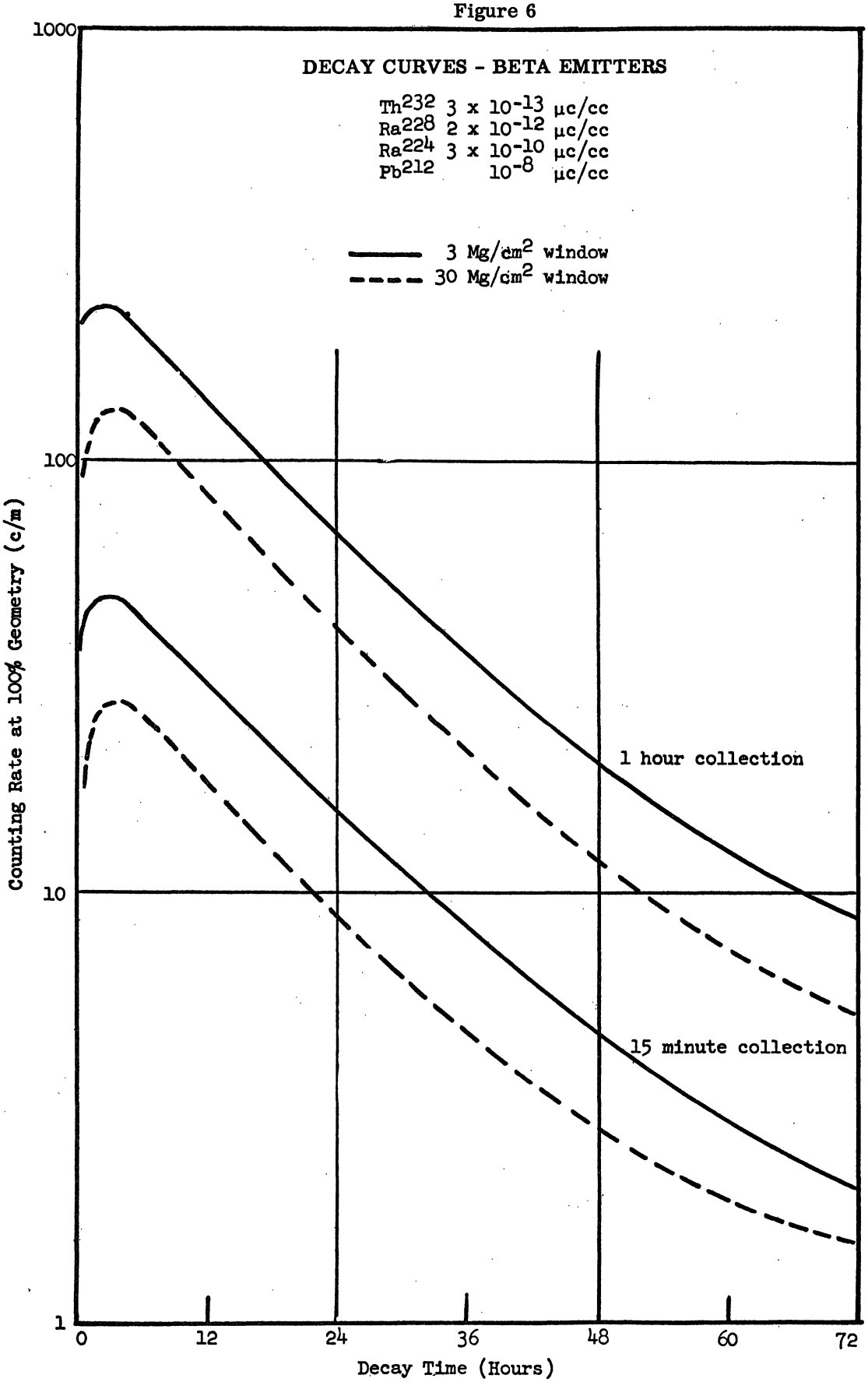
DECAY CURVES - BETA EMITTERS
Th232 3 x 10-13 µc/cc
Ra228 2 x 10-12 µc/cc
Ra224 3 x 10-10 µc/cc
Pb212 10-8 µc/cc
3 Mg/cm2 window
30 Mg/cm2 window
1 hour collection
15 minute collection
Counting Rate at 100% Geometry (c/m)
1000
100
10
1
0
12
24
36
48
60
72
Decay Time (Hours)

$$R(\text{Pb-212}) = \frac{D/M_2 - D/M_3 - \left[D/M_1 - D/M_2\right]\frac{A_2-A_3}{A_1-A_2}}{B_2-B_3 - (B_1-B_2)\left[\frac{A_2-A_3}{A_1-A_2}\right]}$$

where the subscripts refer to measurements at 3 different times. An estimate of the accuracy resulting for several assumed mixtures with a 1-hour collection time is given in Table 2.

TABLE 2

ESTIMATED ACCURACY OF SIMULTANEOUS SOLUTION
(Measurements at 1, 24, and 96 hours)

	Th-232 & Th-228	Ra-224	Pb-212
Assumed product of concentrations and collection rate	45	755	75, 500
Standard deviation			
1-minute measurements	540	280	880
10-minute measurements	160	85	270
Product of concentration and collection rate	45	76	755
Standard deviation			
1-minute measurements	85	43	110
10-minute measurements	27	14	36

In compilation of this table, only the counting errors were considered. The advantage of accurate measurements is self-evident.

From these considerations, it is apparent that unless the concentration of the daughters is low, counting measurements are of limited application to the measurement of thorium. They may be used to estimate the daughter concentrations, particularly Ra-228 and Pb-212. The estimation of Ra-228 is difficult, but may be accomplished by long-term measurements of both beta and alpha emitters, with the alpha measurement used to estimate the beta contribution from Th-228 for subtraction from the measurement of total beta emitters. Since this requires accurate calibrations of all counting equipment, a radiochemical separation of the Ra-228 may be desirable. The determination of Th-232 by counting methods is difficult and uncertain because of the variations in the quantity of Th-228 and the influence of the daughters. It would appear, then, that a sensitive chemical technique[7] or activation analyses[8] should be considered for the estimation of this material.

BIBLIOGRAPHY

1. Hamilton, J. G. AECD-2012, UCRL-67.
2. Maynard, E. A., W. L. Downs, and H. C. Hodge. AECD-2283, UR-13 n, February 28, 1949.
3. Lang, H., K. G. Scott, J. Crowley, and J. G. Hamilton. MDDC-648, August 23, 1946.
4. Ackerman, H., et al. AECD-2283, February 26, 1948.
5. McClinton, L. T. and J. Schubert. MDDC-1636, November 23, 1947.
6. International Commission on Radiological Protection. Br. Jour. Rad., Sup. No. 6, 1955.
7. Nielsen, J. M. Private Communication.
8. Leddicotte, G. W. and H. A. Mahlman. International Conference on the Peaceful Uses of Atomic Energy, Paper UN-117- 7-55.

INHALATION FROM URANIUM CONTAMINATED CLOTHING

J. C. Bailey, A. F. Becher, and H. F. Henry

Oak Ridge Gaseous Diffusion Plant
Union Carbide Nuclear Company
Oak Ridge, Tennessee

In order to determine realistic uranium contamination limits for clothing, a rather extensive series of tests was performed at the Oak Ridge Gaseous Diffusion Plant to evaluate the actual inhalation hazard associated with uranium contaminated clothing.

Throughout these tests only the front surfaces of the clothing were considered as sources of exposure, since surveys of contaminated coveralls from plant locations showed that (1) approximately 90 percent of the contaminating material is on these front surfaces, (2) in general this material is fairly well distributed over the front surfaces, and (3) the material on the back surfaces is confined primarily to the seat, where the probability of the material's being inhaled is obviously relatively small.

Coveralls were contaminated as uniformly as practicable over the front surfaces with varying amounts of uranium tetrafluoride powder; the powder was dusted onto the coveralls from a dust gun and was rubbed lightly into the fabric. The coveralls were then worn by personnel doing normal work in essentially uncontaminated locations. These individuals wore respirators. Each respirator was used for a 2-hour interval, and the amount of uranium that would have been inhaled was determined by alpha-activity analyses of the respirator filters. To calculate the air-borne concentration, the standard breathing rate of 10^7 cubic centimeters per 8-hour work day, as given in the National Bureau of Standards Handbook 52, was assumed.

From these data, a ratio between the air-borne activity level and the average front-surface coverall contamination was calculated.

The release of material from the test coveralls was compared with the release from coveralls contaminated during normal plant work. The first comparison involved having people perform a standard series of calisthenics while wearing the test coveralls contaminated with uranium tetrafluoride, then repeat the calisthenics while wearing coveralls which had been contaminated during plant work. Again, the air-borne activity level was determined from alpha-activity analyses of the respirator filters. The second comparison was made by shaking the different coveralls in front of an air sampler and comparing the amounts of radioactive material collected. The shake-test results, however, were not always consistent with the results of the calisthenics tests, and it appeared that the calisthenics gave a more valid basis for comparison.

From the calisthenics tests, it was found that the air-borne radioactive material from the coveralls contaminated during normal plant operations was lower by a factor of 2.3 than that from the coveralls contaminated to an equivalent level for these tests. Application of this factor to the inhalation results from the test coveralls indicated that, under plant conditions, the air-borne contamination caused by coverall contamination is given by the expression

$$\underset{(\text{dis/min/m}^3)}{\text{Air-borne Contamination}} = 0.244 \times \underset{(\text{dis/min/cm}^2)}{\text{Average Front-Surface Clothing Contamination}} \ (\pm 30 \text{ percent})$$

The limits of error indicated throughout this paper are the standard deviations of the means. On the basis of this expression, the average front-surface clothing contamination which would result in the inhalation of the maximum permissible air-borne concentration of 5.1×10^{-11} microcuries/cm^3, or 113 disintegrations/min/m^3 (40-hour work-week value), is 460 disintegrations/min/cm^2. With the 6 percent geometry found for Samson survey meters for detecting clothing contamination, this corresponds to an average Samson counting rate of about 2,800 counts/min/100 cm^2.

Since a determination of the average contamination on a suit of coveralls is time-consuming, it is not practicable to attempt to determine this average for each person checked in the plant. For a number of years, the maximum reading on any spot on the clothing of an individual has been recorded as a measure of his clothing contamination. These readings constitute a part of the records that are maintained to indicate contamination conditions in the plant. In general, the highest reading is about 3.5 (± 5 percent) times the average reading on the same coveralls. Thus, the air-borne contamination is related to the high-spot clothing contamination by the relation

$$\underset{(\text{dis/min/m}^3)}{\text{Air-borne Contamination}} = 0.0697 \times \underset{(\text{dis/min/cm}^2)}{\text{High-Spot Clothing Contamination}} \ (\pm 31 \text{ percent})$$

The maximum spot reading which might correspond to the inhalation of the maximum allowable air-borne concentration is thus 1,620 dis/min/cm^2, or 9,800 counts/min/100 cm^2. The Oak Ridge Gaseous Diffusion Plant uses a limit of 4,000 counts/min/100 cm^2 as the limit for clothing contamination.

Calisthenics tests also were conducted using uranium trioxide powder, uranyl fluoride powder, and uranyl fluoride solutions, the coveralls being used both while wet with the uranyl fluoride solution and after they had dried. All of these materials gave the same or lower air-borne contamination than uranium tetrafluoride powder, and cotton and Dynel coveralls also showed essentially the same results. This figure for air-borne contamination, therefore, is probably applicable to most uranium compounds.

With a 2-hour wearing period, about 40 percent of the contamination on the respirators was obtained during the first 5-minute interval in which the coveralls were put on, and about 24 percent was obtained when the coveralls were removed. Since it is assumed that after coveralls have become contaminated they will not be put back on when once removed, the results given include a reduction of 40 percent in the actual amounts of material collected to correct for this, but the contamination received when the coveralls were removed was considered to be a part of normal exposure associated with contaminated clothing and is included in the above values.

The contamination on the test coveralls was found to decrease rather rapidly during the wearing period, and dropped to about half the original value in 2 hours. The rate of decrease during the calisthenics tests was about the same for the coveralls from the plant as for the test coveralls, and a similar decrease during wearing might be expected for contamination received under plant conditions.

In an effort to determine the relationship between the amount of contamination on the clothing of individuals in a location and the degree of contamination within the location, survey results are reported in terms of both transferable contamination as obtained by smear tests, and total surface contamination as determined by direct instrument readings on the surfaces. The results discussed below are expressed in terms of the transferable contamination alone. A word about smear tests might therefore be in order.

It has been shown by Barry and Solon[1] of the A. E. C. New York Operations Office that the amount of material picked up on a smear test is a fairly consistent measure of transferable surface contamination. The method used here also has been found to be fairly insensitive to individual differences among the people taking the readings. A smear with a piece of paper towel about 10 cm

on each edge, and backed by the 4 fingers of 1 hand, is rubbed over approximately 100 cm^2 of the surface to be surveyed. Emerson[2] of the Y-12 Plant at Oak Ridge has made some preliminary comparisons of this method and one using a 1-inch diameter filter paper, and he found that the amount of material picked up by the larger papers was about 10 times that picked up by the smaller ones, although both were rubbed over about 100 cm^2 of surface area. Unfortunately, therefore, "transferable contamination" can mean different things, depending upon the smear method.

Survey data for a 1-year period indicates that the average high-spot clothing contamination is given by the expression

$$\text{Average High-Spot Clothing Contamination} = 28.3 \times (\text{Average Transferable Surface Contamination})^{1/2} \ (\pm 8 \text{ percent})$$

If this relationship is combined with the expression for air-borne activity from clothing contamination, the average air-borne activity which may be inhaled as a result of such clothing contamination is given by the expression

$$\text{Air-Borne Contamination from Clothing } \left(\frac{\text{dis/min}}{m^3}\right) = 1.97 \times (\text{Average Transferable Surface Contamination})^{1/2} \left(\frac{\text{dis/min}}{cm^2}\right) \ (\pm 32 \text{ percent})$$

On the basis of this expression, the surface contamination which would result in clothing contamination sufficient to cause the maximum allowable inhalation of uranium is calculated to be about 3,300 dis/min/cm^2.

When this figure is compared with estimates of the amount of transferable activity which might produce air-borne concentrations at the maximum allowable value by becoming air-borne directly from the surface, the direct transfer of contamination to the air is found to be a much more important health consideration than is clothing contamination. For example, Eisenbud, Blatz, and Barry[3] of the A. E. C. New York Operations Office concluded from their studies that about 15 dis/min/cm^2 of transferable contamination on surfaces might produce the maximum allowable air-borne concentration. Oak Ridge tests have indicated a corresponding surface contamination value of 60 dis/min/cm^2 to produce the MAC in air. Additional studies of air contamination in operating areas at the Oak Ridge Gaseous Diffusion Plant have indicated that this value is more probably between 120 and 360 dis/min/cm^2. The actual difference between these values and those of Eisenbud, Blatz, and Barry may not be as great as the figures seem to indicate, however, since they were using small filter papers and a different technique.

At the Oak Ridge Gaseous Diffusion Plant a limit of 0.5 dis/min/cm^2 is used for the "average" value on surfaces to which personnel are exposed, which corresponds to an average of 10 counts/min/cm^2. This is the point at which decontamination or minimal precautions take place, and at a value of 50 dis/min/cm^2, or a count of 1,000 counts/min/100 cm^2, respiratory protection and issued clothing are mandatory. The "average" values referred to are actually the readings on points exceeding 100 counts/min/100 cm^2 averaged over the work location involved, those readings below 100 counts/min/100 cm^2 being considered as zero.

These are not suggested as limits for general application, because in establishing limits at an installation, one must consider the relative importance of the different types of exposure, the administrative procedures involved, and even what the term "limit" is supposed to mean.

Issued clothing appears to provide no significant protection on the job. Issued clothing does permit an employee to remove the contaminated clothing after completion of a contaminated job, but the exposure from his clothing would be significant in relation to his direct inhalation exposure only if he had adequate respiratory protection while working. Thus, many jobs which require respiratory protection could be safely performed without protective clothing, and where protective clothing provides any significant protection, respiratory protection is, in essentially all cases, much more important.

BIBLIOGRAPHY

1. Barry, E. V. and L. R. Solon. "Radioactive Contamination Sampling by Smears and Adhesive Disks." Nucleonics, 11. No. 10:60, 1953.

2. Emerson, L. C. Union Carbide Nuclear Company, Y-12 Plant, Oak Ridge, Tennessee. Unpublished.

3. Eisenbud, M., H. Blatz, and E. V. Barry. "How Important is Surface Contamination?" Nucleonics, 12. No. 8:12, 1954.

A DEFINITION OF "SIGNIFICANT AMOUNT" TO BE APPLIED TO RADIOISOTOPE WORK

R. J. Magill

Radiation Laboratory
University of California
Berkeley, California

In many establishments, radioisotopes are used largely to implement work in one of the sciences. The isotopes used are beta and gamma emitters. Although a specific project may use as much as 2 curies of I-131 in a year, the isotope work is usually conducted in the regular space assigned to the individuals doing the job. Before a project of this size is started, suitable equipment for safe handling is installed and satisfactory techniques are worked out. Much more typical would be the use of 100 μc of C-14 per year with 10 μc in process at any one time. If there are a large number of these projects, they will be carried out in many departments and probably in several buildings. Operations of this nature are then characterized by a wide spread of radioactive materials, with a resultant low density. As a consequence, the possibility of a gross exposure will be very low, and the further chance that this gross exposure was received by a worker from another project, one on which he was not working, will be vanishingly small. This characteristic of wide dispersion is very evident at the University of California, where some 800 persons work with 24 curies of radioisotopes a year (not including sources) in 300 different laboratories on 7 campuses.

Most persons doing tracer work under these conditions do not have enough radioactive materials in process to create any health hazard. If all the material used in the tracer experiments were applied to 1 person in the group and could not produce radiation in any part of his body in excess of the allowable amount, it is quite obvious that the degree of hazard would be low. In many cases not only the isotope in process but the total in the laboratory, including that in stock, falls within this limit. It is also unusual in tracer work for all of the personnel on the project to handle the primary material. After the radioisotope has been dispersed in a liter of water or a rat, it is easy to see that the possibility of exposure to all of the isotope is decreased. Therefore, if all the radioactive material that could be ingested or inhaled during a given period were considered, and the resultant radiation to any portion of the body would not be higher than that from a maximum permissible body burden over the same period, this amount of material could not then be considered hazardous under these conditions.

Most legislative acts and authoritative sources of information concerning safe practices in working with radioactive materials suggest certain health protective measures such as physical examinations, blood counts, and personnel dosimetry for each person working with a "significant amount" of radioactivity. What amount is "significant" is considered rather generally in the N. C. R. P. Handbooks and is left undefined in most other sources. It would seem logical that this "significant amount" should not be less than the smallest quantity which could, under the conditions of its use, produce some hazard.

With a finite budget to cover all health and safety problems, it would seem that money could be spent better in other ways than on rather elaborate personal assessment measures for people engaged in sub-hazardous tracer operations. More elaborate periodic safety measures than a survey for technical contamination should then be applied when the "significant amount" is reached.

A finite value for the least amount of a given radioisotope that potentially could be hazardous can be computed for any given condition of use by considering 2 factors:

1. What proportion of a given experiment could be ingested or inhaled in case of an accident?

2. What is the largest amount of the material which would lead to no excessive radiation if this accident were to happen?

If the amount in item 1 does not exceed that in item 2, no potential hazard exists.

The amount of radioisotope which, if consumed in a period of time, would deliver the same amount of radiation to the "critical organ" over this period of time as the permissible body burden can be calculated by means of the equation

$$(1) \quad MPQ/T = \frac{0.69\ q \times T}{T_e \times F}$$

in which

MPQ/T = maximum permissible consumption in μc in period T
q = maximum permissible body burden
T_e = effective half-life
f = fraction of total dose reaching critical organ

Values for the terms of this expression may be found in the National Bureau of Standards Handbook No. 52.

Some typical values obtained for MPQ per month by this means are:

C-14	290 μc organic 3.6 mc inorganic
Na-24	540 μc
P-32	75 μc
S-35	1.4 mc
Sr-90	0.03 μc
I-131	4.1 μc

These values are often somewhat disparate from those suggested in NBS Handbook No. 42. In fact, the value for inorganic C-14 is considered high level there.

If the fraction taken up by the "critical organ" is small, the above method of computation yields some exceedingly high values. In the case of ingestion of Co-60, 0.4 percent of the cobalt reaches the liver, where it has a biological half-life of 8.4 days. Calculating the MPQ by equation (1) shows that 0.4 mc of Co-60 would have to be swallowed to give 0.3 r to the liver from this fraction. If equation C 15* from Recommendations of the International Commission on Radiological Protection, December, 1954 (British Journal of Radiology, Supplement No. 6, 1955) is solved for Co-60 in the lower GI tract, 7.9 μc gives 0.3 rep to this organ.

$$*C15 \quad (MPC)_W^{GI} = \frac{7.6 \times 10^{-7}\ m'\ G}{H\ f_w\ \Sigma E\ (RBE)}$$

in which

$(MPC)_W^{GI}$ = μc/ml in drinking water which will deliver 0.3 r/wk to a section of the GI tract when 2,200 ml of water at MPC are consumed per day.

m' = mass of contents of section of GI tract

$$G = \frac{0.693\ H}{\left(e^{-0.693\ \frac{h_0}{T_r}} - e^{-0.693\ \frac{h_1}{T_r}}\right) T_r}$$

H = time in section, days
f_w = fraction reaching critical organ
h_0 = time of arrival, days
h_1 = time of departure
T_r = half-life, radioactive

Values of

$G = 1$ (if T_r is >64d, $G = 1.00$ to 1.01)
$m' = 150$ (lower large intestine, if $T_r > 0.5$ day, the lower intestine is critical)
$H = 18/24$
$f_w = 0.8$
$\Sigma E = 0.37$ for Co-60

are given in the text.

$$(MPC)_W^{GI}\ \mu c/ml = \frac{7.6 \times 10^{-7} \times 150 \times 1}{0.75 \times 0.8 \times 0.37} = \frac{0.3 r/wk}{2,200\ ml/day \times 7\ days/wk}$$

$$= 7.9\ \mu c$$

In fact, the liver would receive about 0.3 mr from 0.4 mc of Co-60 passing through the GI tract. During the solution of equation C15, it was noted that if the physical half-life is more than 30 days and most of the material remains in the GI tract, the expression

$$(2)\quad MPQ/month \simeq \frac{12}{\Sigma(bE)}$$

can be used to approximate the number of μc which will deliver the maximum allowable radiation for 1 month to the GI tract.

Other chemical elements which go primarily from the GI tract to the blood but of which only a small fraction goes from the blood to the critical organs, listed in Handbook No. 52, require calculation on a basis of whole body radiation. Permissible amounts by inhalation have to be checked, of course, for radiation to the lungs. Before any relatively precise evaluation is applied, communication must be established to ensure that any changes in any project, and particularly any accident, will be reported to the Radiological Safety Officer. After the isotope used, the amount of it in process, and the conditions under which it is used have been considered, calculation will probably show (as it has at the University of California) that somewhat more than half of all persons doing tracer experiments are working with less than significant amounts of radioactive isotopes.

The meaning suggested here for the term "significant amount" of radioisotope is that amount of material which in the case of a total accident would involve as much irradiation to a critical organ over a finite period of time, say 1 month, as a permissible body burden. In case the biological half-life is long, therefore, the significant amount may be much less than 1 body burden. Sr-90, with a body burden of 1 μc and a significant amount or MPQ or 0.03 μc, demonstrates this point, which is usual with the alpha emitters.

FIELD RADIATION MONITORING RELATIVE TO EXPERIMENTAL REACTORS

P. Griffiths and E. D. Graham, Jr.

Health and Safety Division
U. S. Atomic Energy Commission
Idaho Falls, Idaho

At the National Reactor Testing Station, all radiation monitoring beyond each contractor's operational jurisdiction is performed by the A. E. C. Health and Safety Division. Because of the complex problems of a large site containing varied types of reactors and conducting a variety of experiments, monitoring necessarily is very diversified. In order to fulfill the Commission's obligation to the public from the standpoint of radiation control, and to provide regulatory standards among contractors, emphasis has been placed upon mobility of monitoring equipment and a positive communication system.

Routine reactor operation where a minimal hazard exists is covered by a network of fixed monitoring stations. These stations are located at points over the entire National Reactor Testing Station and its environs. Supplementing these stations, a complete ecological program for surface evaluation of radiation involvement is maintained.

In order to provide adequate immediate radiation monitoring controls during sensitive reactor experiments, mobile field monitoring units are utilized.

One type of monitoring vehicle in use for monitoring highways or streets, where speed is a factor, is a panel delivery truck equipped with a 2-way radio. The prime function of these units is to detect radiation quickly and to determine the extent of areas affected should there be a sudden release of air-borne radioactive material. In order to make this possible, a device consisting of 4 G. M. type tubes arranged end to end has been mounted on the front of these vehicles, as shown in Figure 1. The sensitivity obtained permits rapid evaluation over a large area.

Where the terrain precludes this type of monitoring, and where the collection of samples is desired, radio-equipped power wagons or pickup trucks are used. These vehicles have been fitted for complete monitoring and sampling function. In addition to standard field monitoring instruments and equipment, these units have electric generator plants to supply power for sample collectors and flood lights. Each unit is capable of collecting high-volume air samples, gas through liquid absorption, and particulates on millipore paper.

A new innovation which has proven extremely valuable in detecting air-borne radioactive materials is the "sky-scanner." Since its development by the Health and Safety Division, this instrument has been used to advantage in the remote monitoring of reactor experiments. The "sky-scanner" is a scintillation tube mounted in a shield which can be aimed at a point or automatically rotated, as shown in Figure 2. It can be mounted in a vehicle and operated in transit, or if preferred, it is possible to place it in a suitable location and transmit the record to a remote location by means of a simple extension wire.

Two house trailers have been converted to mobile laboratories. Each unit has a 2-way radio, constant air monitor, sample counter, and full back-up equipment for the monitoring teams. A microscope and microprojector for particle size determinations also are carried on one of these trailers. In addition, accomodation for off-shift and stand-by personnel has been provided in the

form of bunks, stoves, and rations. When a test is in progress these trailers are placed in readily accessible locations in order to provide service for monitoring teams in the field.

Throughout test operations, U. S. Weather Bureau personnel assigned to the National Reactor Testing Station make long-range forecasts and provide data to facilitate radiation monitoring.

The Health and Safety Division control station is located at the Central Facilities area where phone and radio liaison is maintained with the IDO management, experiment area, U. S. Weather Bureau, and all field monitoring units. Progress of the experiment, meteorological advice, and field monitoring data are relayed continuously to responsible personnel at the control station. They in turn coordinate the placing and movement of monitoring units, and keep management informed of developments. Should a radioactive release occur, initial detection can be made at the source by the operating group through the medium of fixed stack monitors, by the IDO scanners monitoring the stack, or by field survey teams.

Normally, 2 or 3 monitoring teams are located down-wind of experimental operations. Under the operating plan established, should a radioactive release occur, all sampling equipment is activated immediately, additional teams are dispatched from other duties, all branches of the Division are alerted, and necessary liaison is established with other contractors who might possibly be affected by the condition.

RADIOLOGICAL SAFETY ASPECTS OF THE SRE

M. F. Huntsinger

North American Aviation Company
Downey, California

The letters "SRE" refer to the Sodium Reactor Experiment, a power reactor feasibility study by Atomics International, a division of North American Aviation, Inc. Physically, the SRE is a liquid-sodium cooled, graphite moderated, 20 thermal megawatt reactor. Electrical generating equipment, being installed in cooperation with the Southern California Edison Company, will allow the SRE to serve as a 6 megawatt electrical power station for commercial electrical distribution. The first critical experiments will begin October first.

A major effort has been made by Atomics International's Health Physics Group to accomplish radiation hazard control by inherent design rather than only by establishing operational procedures after the fact. In the SRE design phases, our radiation engineering group attempted direct participation in the form of analytical studies of proposed systems. Valuable precedents were established during the SRE design which are now enabling heavy participation in other projects.

The reactor site is in the Simi Hills, which form the western boundary of the San Fernando Valley. The building is set among eroded sandstone boulders and is about 30 miles from the Los Angeles Civic Center. Because of the uneven terrain, the poor hydrological situation, and the nearness of high population density, simple release of radioactive effluents cannot be used as a disposal method.

The reactor proper is a cylindrical cavity below the building floor level filled with the fuel and moderator elements in a pool of liquid sodium (Figure 1). The primary sodium is circulated through a pump and heat exchanger system which transfers the heat to a secondary, nonradioactive, sodium system. The secondary sodium is cooled either by an air blast heat exchanger or the steam generating equipment. A complete auxiliary system, sufficient to transfer afterglow heat, is provided in case of main system failure. Above the floor level, fuel element and moderator element handling casks are supported by a 75-ton bridge crane. The fuel handling cask can deliver a fuel element to a fuel storage farm, to 1 of 3 fuel cleaning cells, or to a hot cell in the partial basement.

The bridge crane requires a high bay room which encloses the floor-level engagement plugs for the fuel manipulation cask (Figure 2). The hot cell area, control room, change rooms, and office areas are separately enclosed and ventilated. The air blast heat exchangers, steam generator, electrical apparatus, and other supporting systems are outside.

Uranium enriched to 2.78 atomic percent is arranged in 7-rod clusters to form the SRE fuel element. Each rod is composed of a dozen 6-inch uranium slugs stacked in a 10 mil stainless steel tube. Sodium-potassium alloy fills the clearance spaces to provide thermal conduction. The helium-filled expansion space will collect about 10 curies of gaseous activity during the fuel cycle. Radioiodine normally is expected to react with the NaK. Each fuel cluster is suspended in a coolant channel in the center of zirconium-clad, helium-soaked, graphite moderator elements.

The SRE top shield rotates on ball bearings which are normally immersed in a low melting-point alloy (Figure 3). When electrical heaters melt this alloy, the gas seal is maintained

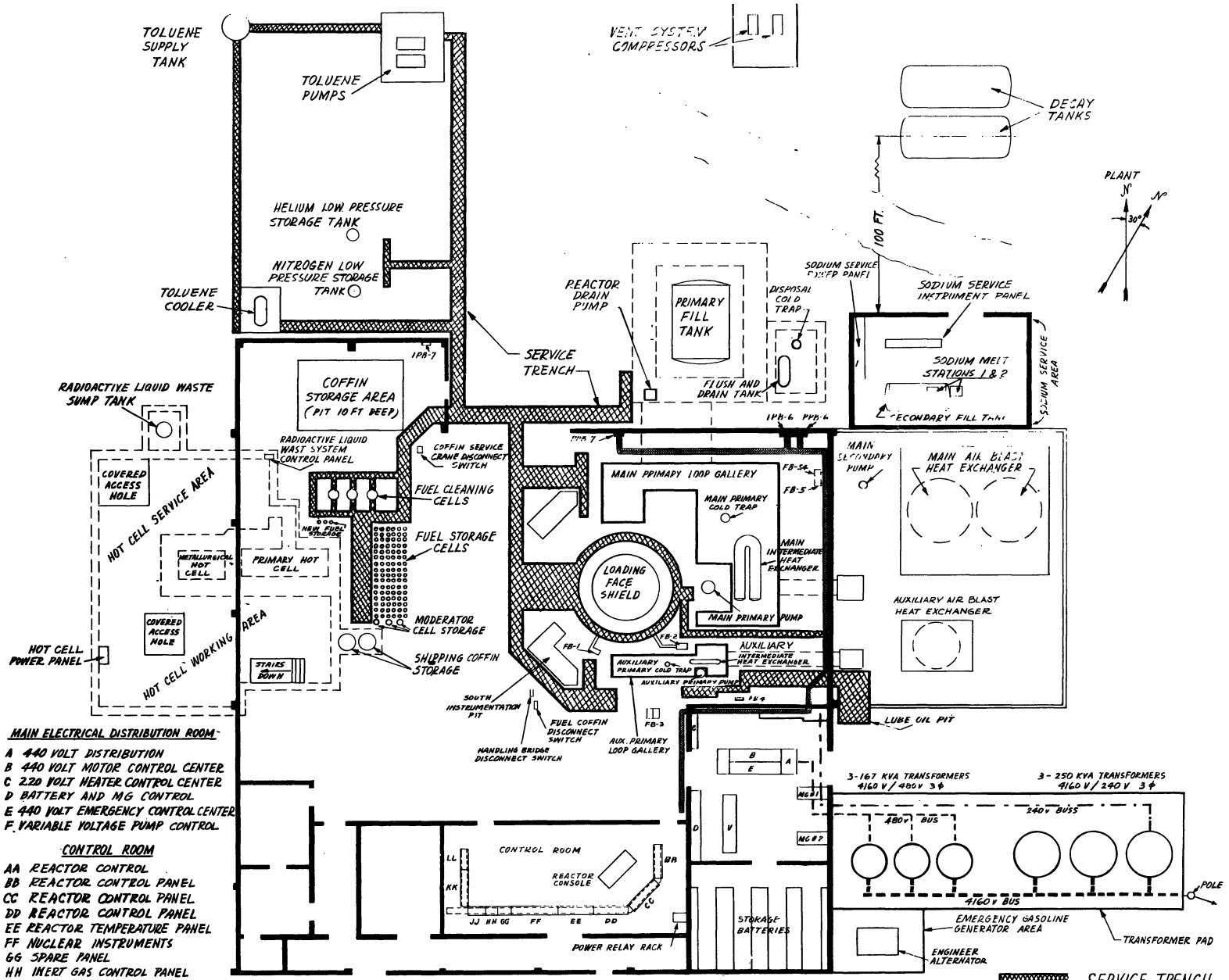

SRE REACTOR BUILDING ARRANGEMENT
(GROUND FLOOR)

Figure 2

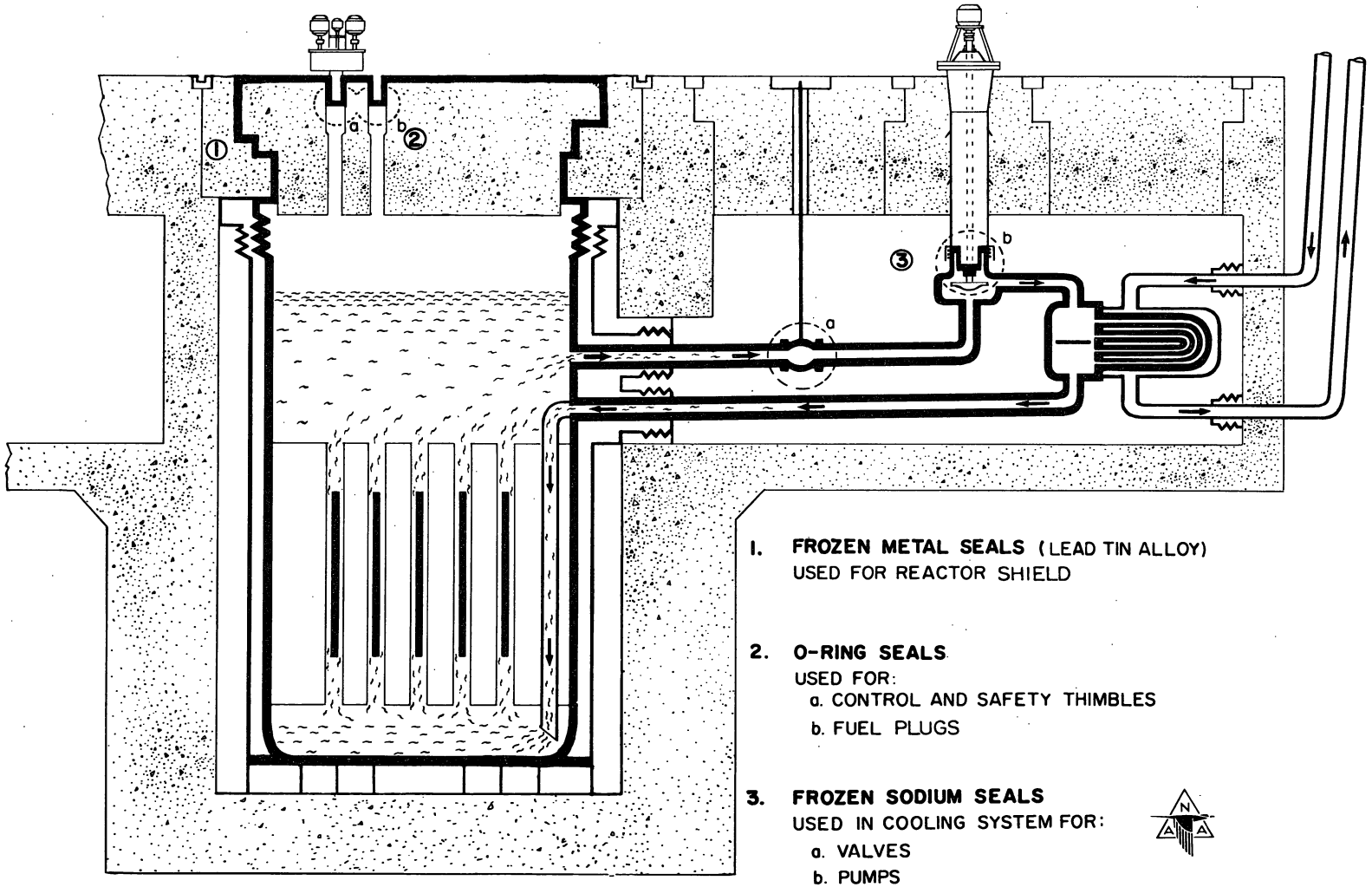

1. **FROZEN METAL SEALS** (LEAD TIN ALLOY)
   USED FOR REACTOR SHIELD

2. **O-RING SEALS**
   USED FOR:
   a. CONTROL AND SAFETY THIMBLES
   b. FUEL PLUGS

3. **FROZEN SODIUM SEALS**
   USED IN COOLING SYSTEM FOR:
   a. VALVES
   b. PUMPS

6-10-55

Figure 3

9693-5538

and the shield may be rotated to allow removal of fuel and moderator elements by the handling casks. The 925°F sodium and helium blanket gas is contained in a sealed system at 1.3 psig; the low pressure represents the major safety advantage of sodium graphite reactors. A secondary circulating tetralin cooling system provides shield cooling and is used to maintain movable frozen sodium seals for the sodium circulating pumps and valves. Exposure of the tetralin system to neutrons has been minimized; however, this coolant will represent a low-order contamination problem.

From the radiological safety standpoint, the chief disadvantage of sodium graphite reactors is represented by the chemical nature and induced radioactivity of sodium. The equilibrium sodium radioactivity for the SRE has been calculated to be 0.32 curie per cc. This is partially offset by the short half-life of Na-24 and the experimental evidence that the system sodium, with impurities and corrosion products, should decay by a factor of 10^6. The effect on this limit caused by rather severe fuel rod ruptures is shown in Figure 4. During fuel element removal, about 0.1 pound of sodium will adhere to the stainless steel surfaces. After most of the afterglow heat has decayed, this sodium must be removed prior to exposure of the fuel element to the air atmosphere in the hot cells.

The liquid waste system centers around this fuel cleaning operation (Figure 5). The fuel elements are simply immersed in water and the resulting liquid waste is stored in small hold-up tanks. Sampling of these tanks by the monitoring unit will allow prediction of decay characteristics. Ultimate disposal will be dumping at sea in conjuction with Atomics International's other programs. The large storage tanks will hold all of the expected effluent for 1-year operation.

The various inert atmosphere spaces in the SRE are all ultimately piped to a compressor system which stores the gas at 100 psig in 2 large underground storage tanks (Figure 6). The principal radioactive gases expected are A-41 from impurities in the helium blanket gas and Xe and Kr isotopes from possible fuel rod leaks or fuel rod dismantling in the hot cells. In addition, a very small amount of C-14 from the N-14(n, p)C-14 is expected. Helium from the reactor atmosphere pressure relief valve plus purge gases from the coffin, coffin interlock, and cleaning cells are directly connected to the compressor system.

The gases which are not likely to contain radioactive material are normally directly diluted with the building exhaust ventilation air and released at roof level (Figure 7). As this diagram shows, valves controlled by line monitors can direct these gases to the compressor and tank system. These monitors, which are simple ion chambers, will activate the valves when radioactivity corresponding to 0.1 MPC is detected in the building exhaust air. This point will be chosen with the worst possible situation concerning the chamber sensitivity, isotope MPC, and flow rates assumed. The storage or decay tanks again have a 1-year normal capacity; however, after sampling, the tanks will be emptied under controlled conditions into the building air exhaust. The stack monitor can override these controllers and automatically halt decay tank venting.

Because of the low gaseous radioactivity production expected, the SRE does not require a tall stack. Under these conditions, permissible gaseous activity release rates have been prescribed in terms of 0.1 the Handbook 52 permissible concentrations for Kr and Xe isotopes in the air exhaust itself. On a weekly basis, a short-duration release of 10 times this total activity is allowable under appropriate meteorological conditions (Figure 8). This could result in a 0.3 rem dose if one were immersed in an atmosphere of the exhaust air during the time of the release.

In addition to direct participation in the design phase of the Sodium Reactor Experiment, health physics personnel have written appropriate portions of the SRE operating manual. This reactor is to be operated on a 24-hour basis. Health physics monitors will be provided for each shift and a supervising engineer normally will be present during the daytime shift. Manipulations involving high radiation levels will not be scheduled for the off shifts. Environmental monitoring, which has already started, continuing meteorological and geological studies, and medical services will also form a part of the operational program.

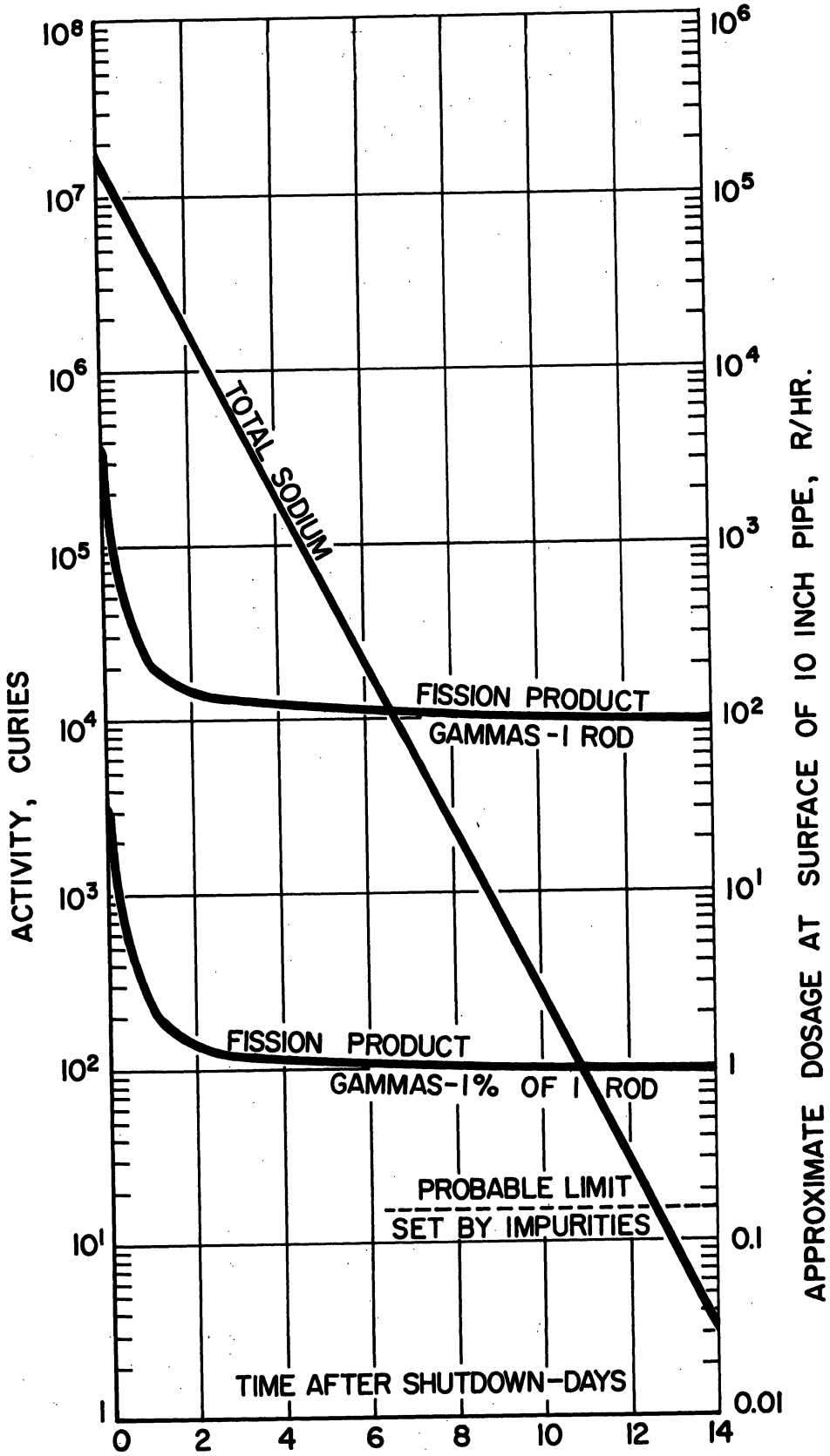

Figure 4

6-10-55 AE 31 - 5501

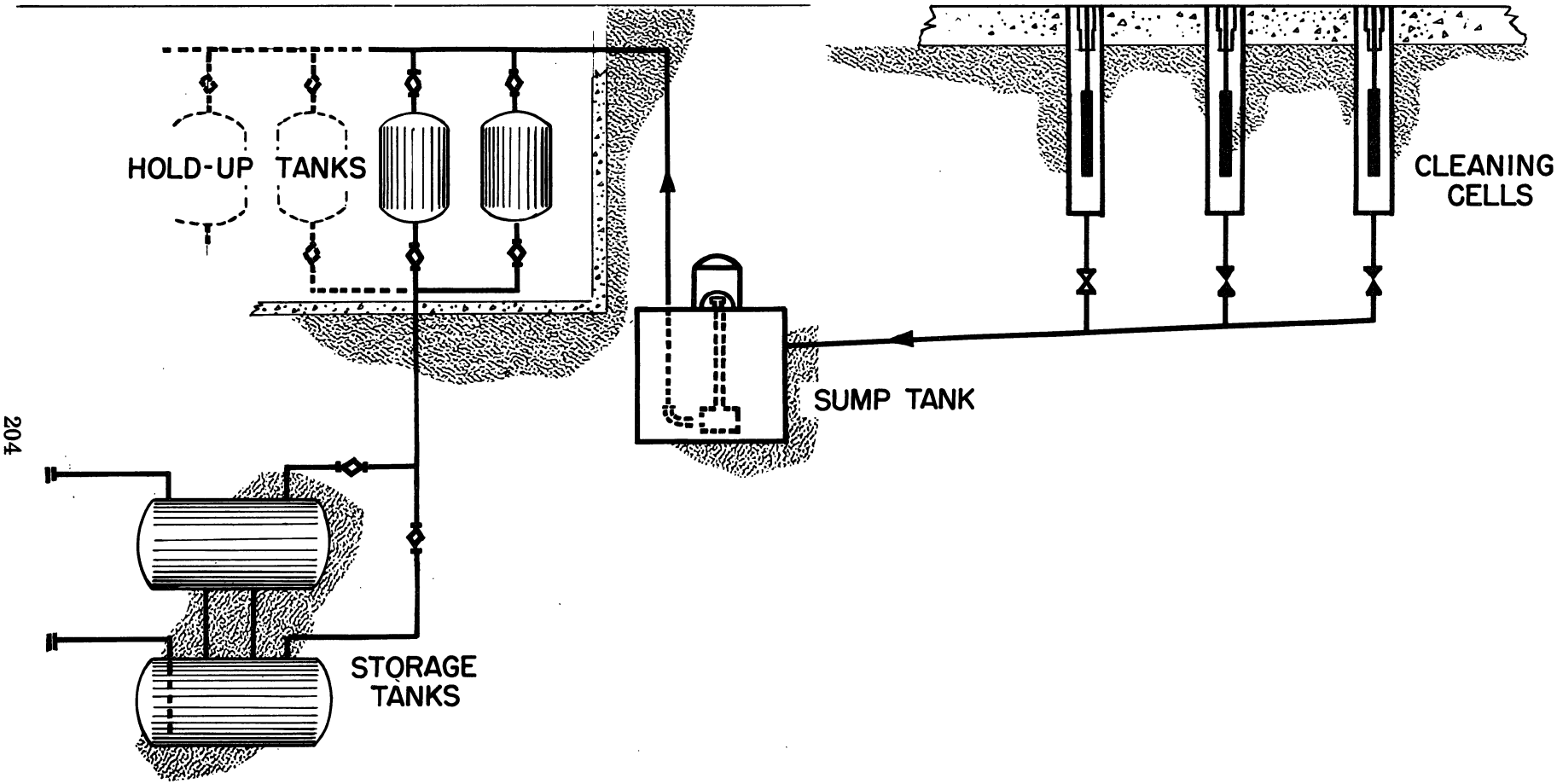

9693-5801
UNCLASSIFIED
1-28-55

Figure 5

GASEOUS WASTE DISPOSAL SYSTEM

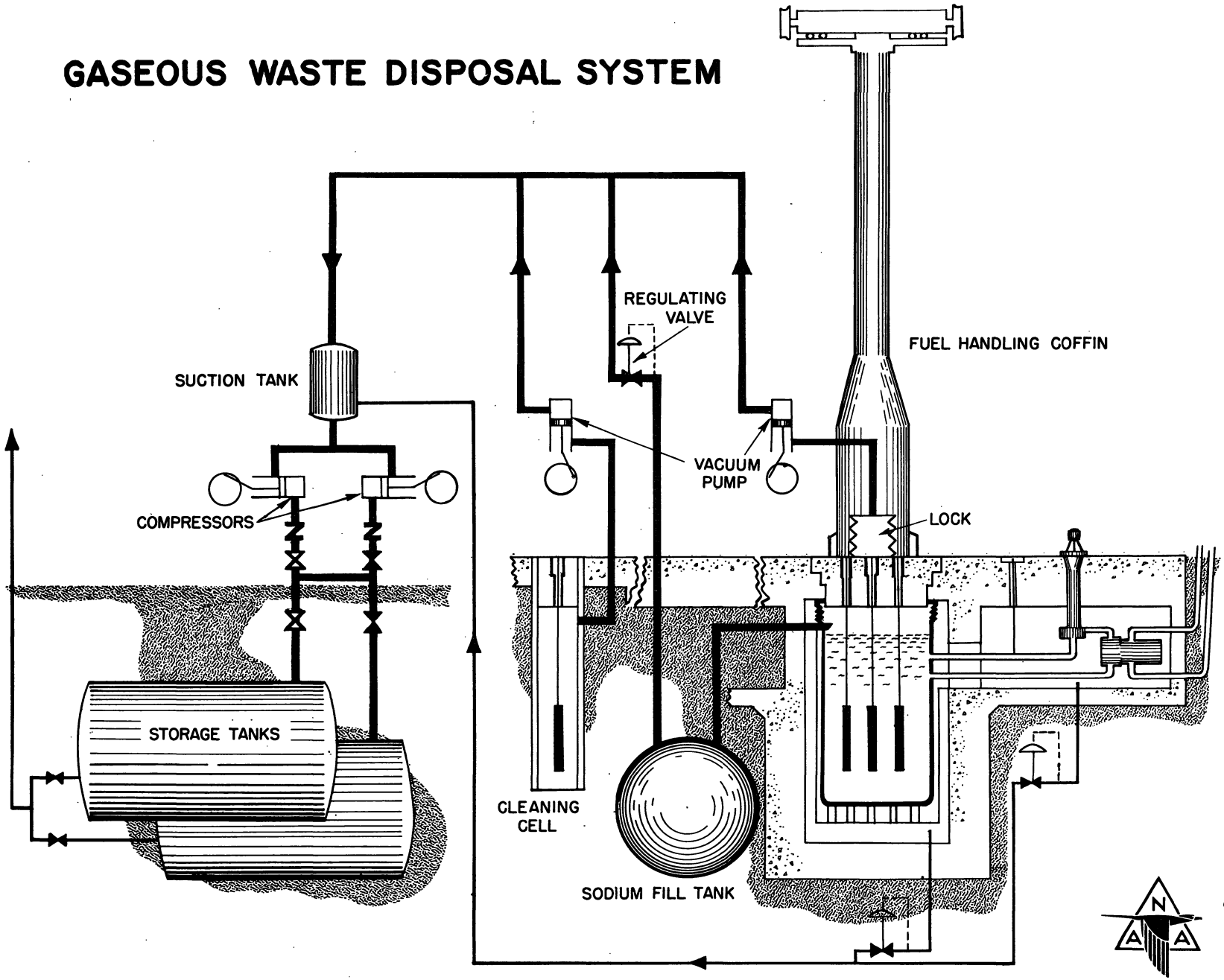

Figure 6

SRE RADIOACTIVE GAS VENT SYSTEM

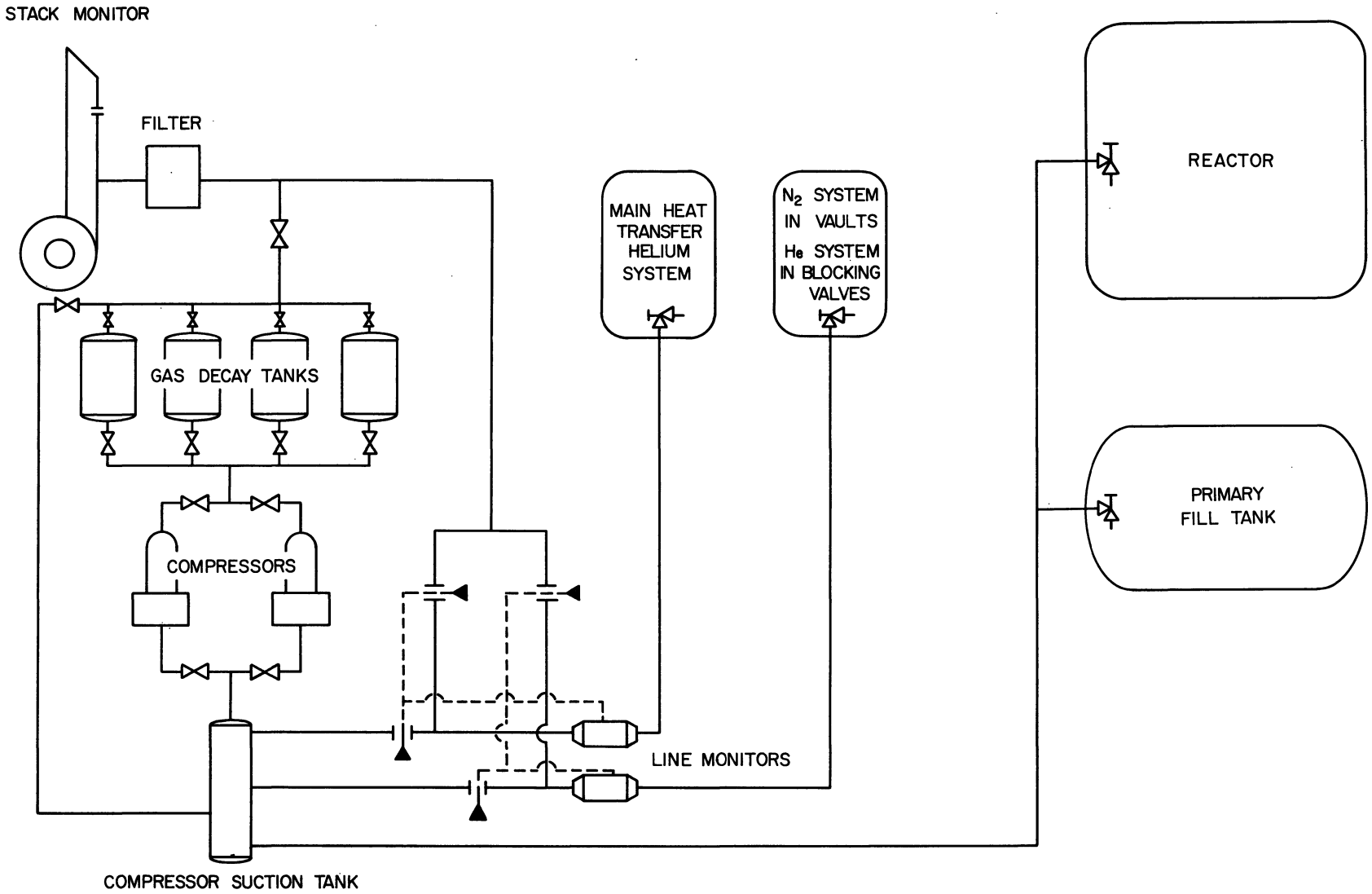

6-20-56

Figure 7

00-41195

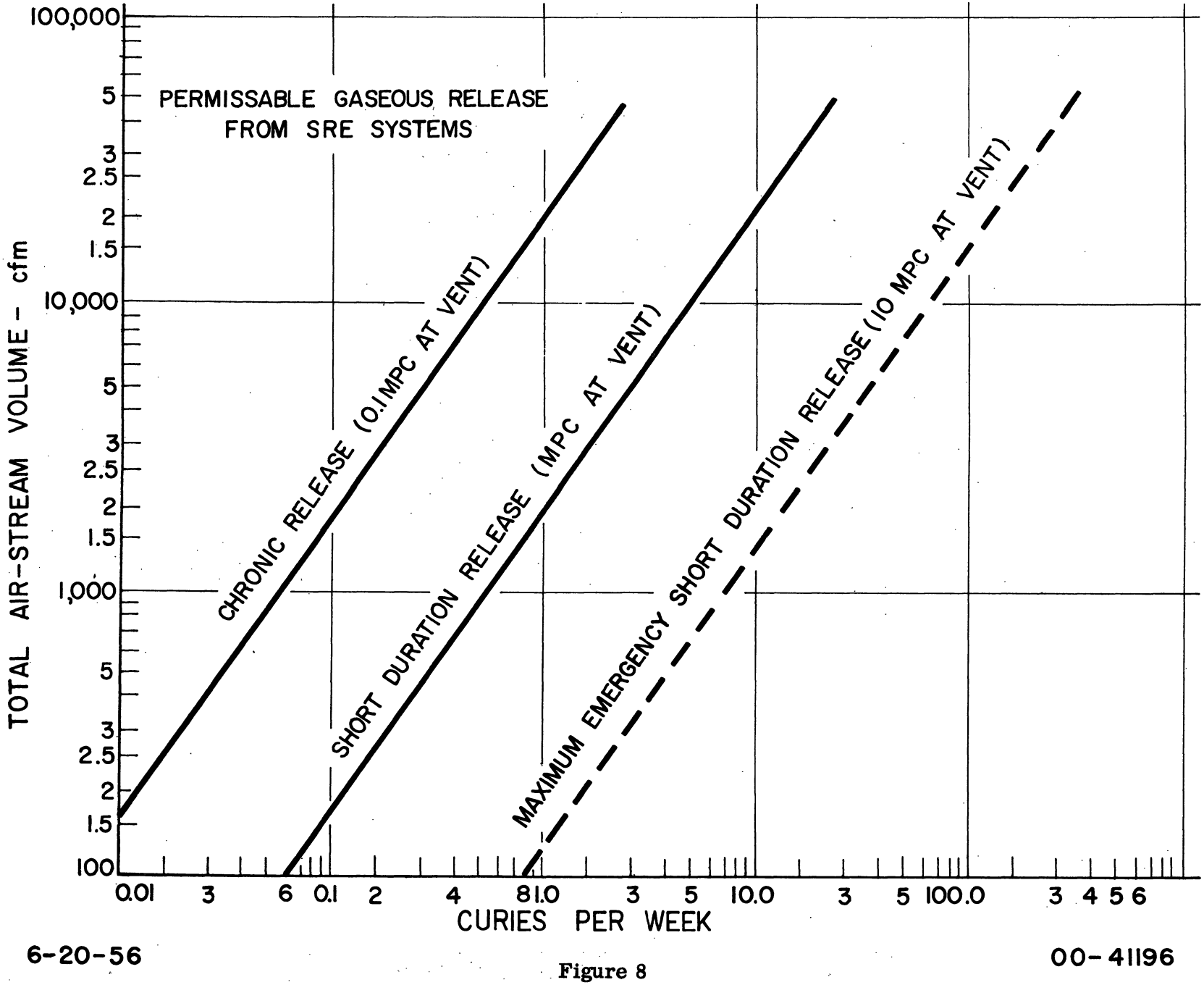
PERMISSABLE GASEOUS RELEASE
FROM SRE SYSTEMS
CHRONIC RELEASE (0.1 MPC AT VENT)
SHORT DURATION RELEASE (MPC AT VENT)
MAXIMUM EMERGENCY SHORT DURATION RELEASE (10 MPC AT VENT)
TOTAL AIR-STREAM VOLUME - cfm
100,000
5
3
2.5
2
1.5
10,000
5
3
2.5
2
1.5
1,000
5
3
2.5
2
1.5
100
0.01
3
6
0.1
2
4
8
1.0
3
5
10.0
3
5
100.0
3
4
5
6
CURIES PER WEEK
6-20-56
00-41196

Figure 8

Participation by radiation safety personnel in all phases of experiments involving high radiation levels has long been a basic health physics philosophy. It is our conviction that this same principle must be even more diligently applied to reactor power installation development.

OPTIMUM PARTICLE SIZE FOR PENETRATION THROUGH THE MILLIPORE FILTER

J. J. Fitzgerald and C. G. Detwiler

Knolls Atomic Power Laboratory
General Electric Company
Schenectady, New York

INTRODUCTION

The advantages of sampling water and air streams with molecular or membrane filters have been cited in many technical reports.[1] The Millipore Filter, a membrane type filter, is known to be highly efficient for collecting particles greater than approximately 0.1 micron in diameter.[2] Essentially all of the particulate material is collected on the surface of the Millipore Filter (within approximately 10 and 50 microns of the upstream surface of the type HA and AA filters, respectively). This filter medium is therefore suitable for direct radiation detection of alpha air-borne particulate material.

The shallow depth of penetration in the filter, and the high degree of transparency which can be obtained by impregnating the filter with immersion oil, make the Millipore Filter an exceptionally good medium for filter efficiency and particle size distribution studies. An additional advantage results from the possibility of detecting particles in the same medium in which they are collected without appreciably changing the particle size or the size distribution. A silica replication of the particle collection on the membrane filter can be made without significantly altering the particles, thus permitting an electronmicrography size count and an accurate analysis of particles with diameters down to 0.005 micron. The radioactive particle size distribution can be studied and distinguished from the non-radioactive particle size distribution by the use of Millipore Filter and autoradiographic stripping film.

Since optimum particle sizes for the penetration of material through several fibrous air sampling and air cleaning filter papers were observed,[3] it was desirable to determine the efficiency of the Millipore Filter for the collection of particulate material with particle sizes down to 0.005 micron and to investigate the possibility of an optimum particle size for total penetration. In this paper it will be demonstrated that (1) there is an optimum particle size for total penetration through the Millipore Filters, (2) the collection efficiency for particles greater than 0.1 micron in diameter is very high and relatively independent of the face velocity, and (3) the collection efficiency for particles with diameters less than 0.1 micron passes through a point of optimum penetration at approximately 0.02 micron and the absolute efficiency is dependent on the face velocity.

DISCUSSION OF EXPERIMENTAL PROCEDURE

An aerosol generator, based essentially on a design by K. E. Lauterbach[4] of the University of Rochester, was modified[5] for use with the KAPL particle collection efficiency testing apparatus. The aerosol generator operates on an atomizer principle and was used in these tests to generate liquid potassium permanganate. Although the particles are generated in the liquid phase, a portion of the droplets solidify while passing through the collection efficiency test unit.

The arrangement used to expose the test filters to the $KMnO_4$ aerosol is illustrated in Figure 1. The test aerosol is introduced to the system at the intake port (A). An impaction plate

Figure 1

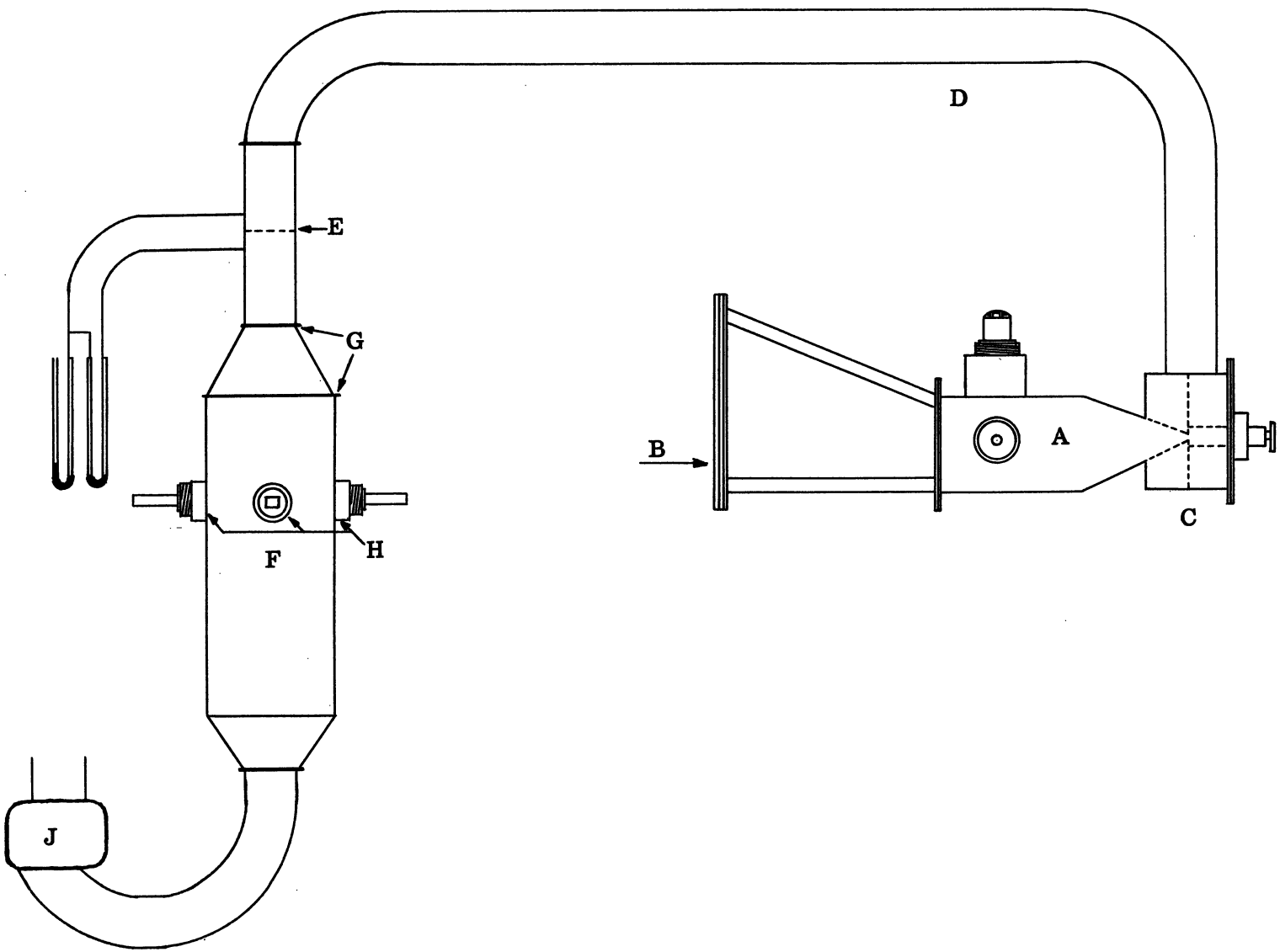

SCHEMATIC DIAGRAM OF TEST UNIT

(C) takes out particles exceeding 3 microns in diameter. The test aerosol passes through the duct (D) and smoothing vanes (G) to the aerosol chamber (F). Sampling ports (H) are located at 90° intervals around the circumference of the aerosol chamber.

Isokinetic sampling tubes, as shown in Figure 2, pass through 2 of the ports in the aerosol chamber. The filter to be tested is held between flanges in one of the isokinetic sampling tubes. The exhaust end of the sampling tube holding the test filter is connected in series with a type HA Millipore Filter. Another type HA Millipore Filter, mounted at the second port, samples the aerosol exposed to the test filter. The Millipore Filters sample essentially in parallel so that a direct comparison of the aerosol collection on the 2 filters yields an efficiency evaluation for the test filter. The efficiency is expressed as a function of face velocity of the air stream passing through the test filter with particle size as a parameter. The face velocity is varied by altering the cross-sectional area of the test filter while maintaining a constant flow rate.

The efficiency determinations for a filter medium do not necessitate complete knowledge of the absolute efficiency of the standard filter medium, such as the Millipore Filter, in order to make absolute efficiency studies. The efficiencies of the standard filters, for a given set of experimental conditions, should not vary significantly if satisfactory test filter efficiency information is to be provided. When determining the efficiency of a relatively high efficiency test filter medium, it is desirable that the standard filter medium should be very efficient. This requirement is necessary to provide a significant collection of the aerosol on the downstream side of the test filter when the maximum concentration of the test aerosol is generated.

DISCUSSION OF EXPERIMENTAL DATA

Both the type AA and type HA Millipore Filters were evaluated for particle collection efficiency throughout the particle size range of 0.005 to 2.1 microns. The studies were made at face velocities of 10, 20, and 40 cm/sec. The data are presented graphically in Figures 3 and 4.

The efficiency data for the Type AA Millipore Filter yield a family of curves which indicate an optimum particle size for penetration at the same particle size (approximately 0.02 micron in diameter) for each face velocity tested. Penetration appears to increase with face velocity for particles less than approximately 0.1 micron in diameter.

The points of maximum total particle penetration for the type HA Millipore Filter for the face velocities of 10, 20, and 40 cm/sec fall between 0.022 and 0.026 micron. The degree of particle penetration for each face velocity is similar for both the type AA and type HA Millipore Filter, although in general, the latter is a slightly more efficient filter within the limits of the tests.

The type AA Millipore Filter data for the 40 cm/sec face velocity test, in the particle size range of 0.01 to 0.03 micron, are not considered significant. However, the general trend of the data obtained in this particle size region suggests particle penetrations approaching 100 percent.

Within the stated face velocity limits and size limits of the tests, the type AA Millipore Filter particle collection efficiency exceeds 99 percent for particles greater than 0.1 micron in diameter. For particles less than 0.01 micron in diameter, the efficiency exceeds 40 percent. It is clear from the data that the efficiency was most consistent and was highest throughout the size range tested at the lower face velocities.

As a means of comparing the points of maximum total penetration for different filter media, the particle penetration curves from several past studies using $KMnO_4$ aerosol have been combined with the Millipore Filter curves, each for a face velocity of 10 cm/sec, in Figure 5. The fibrous type filter points of maximum penetration and the membrane type filter points of maximum penetration appear in separate groups, with the latter exhibiting the greater penetration. The maximum penetration occurs at approximately the same particle size for each of the filters with the exception of the Hollingsworth and Vose-70 filter media.

Figure 2

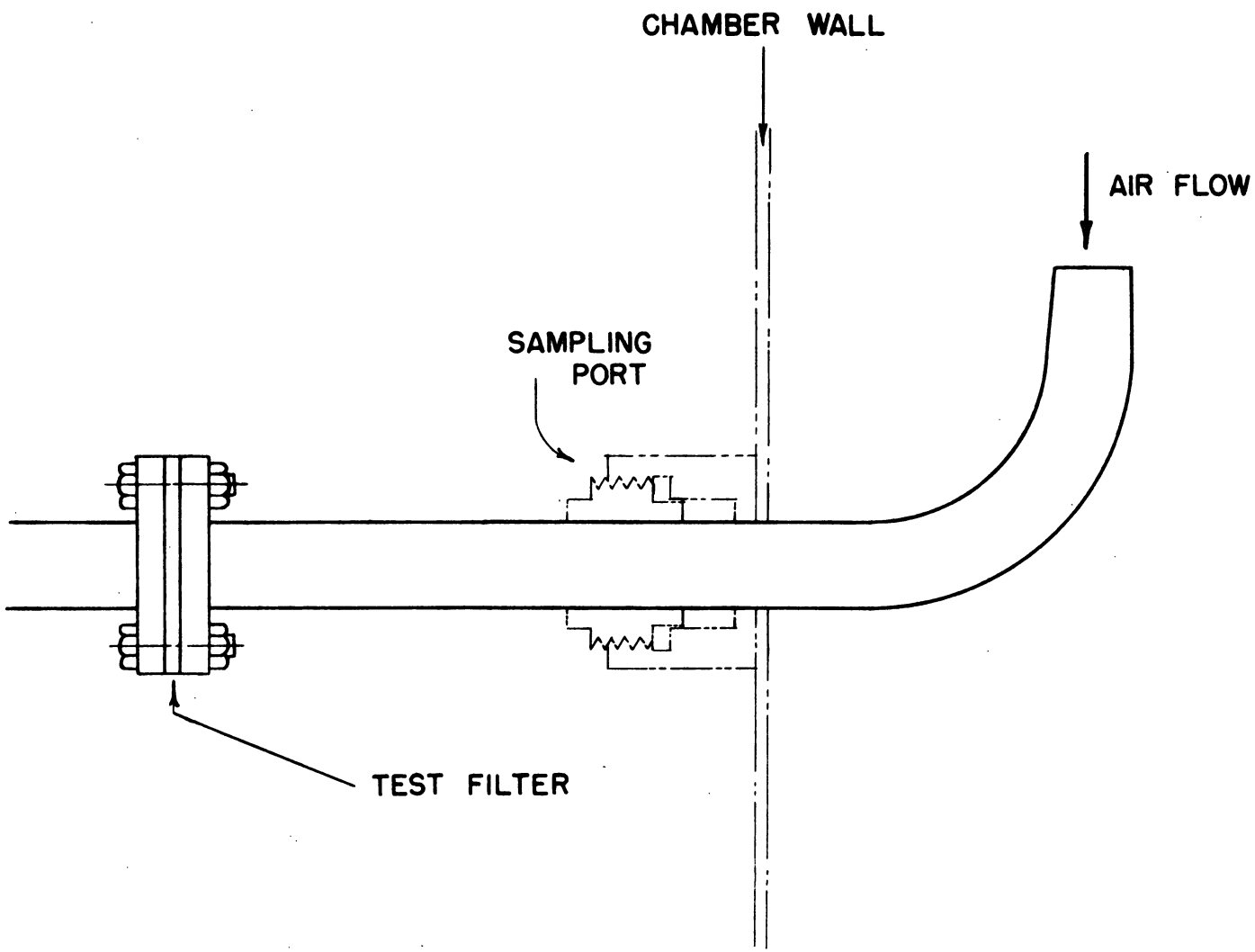

ISOKINETIC SAMPLING HEAD

Figure 3

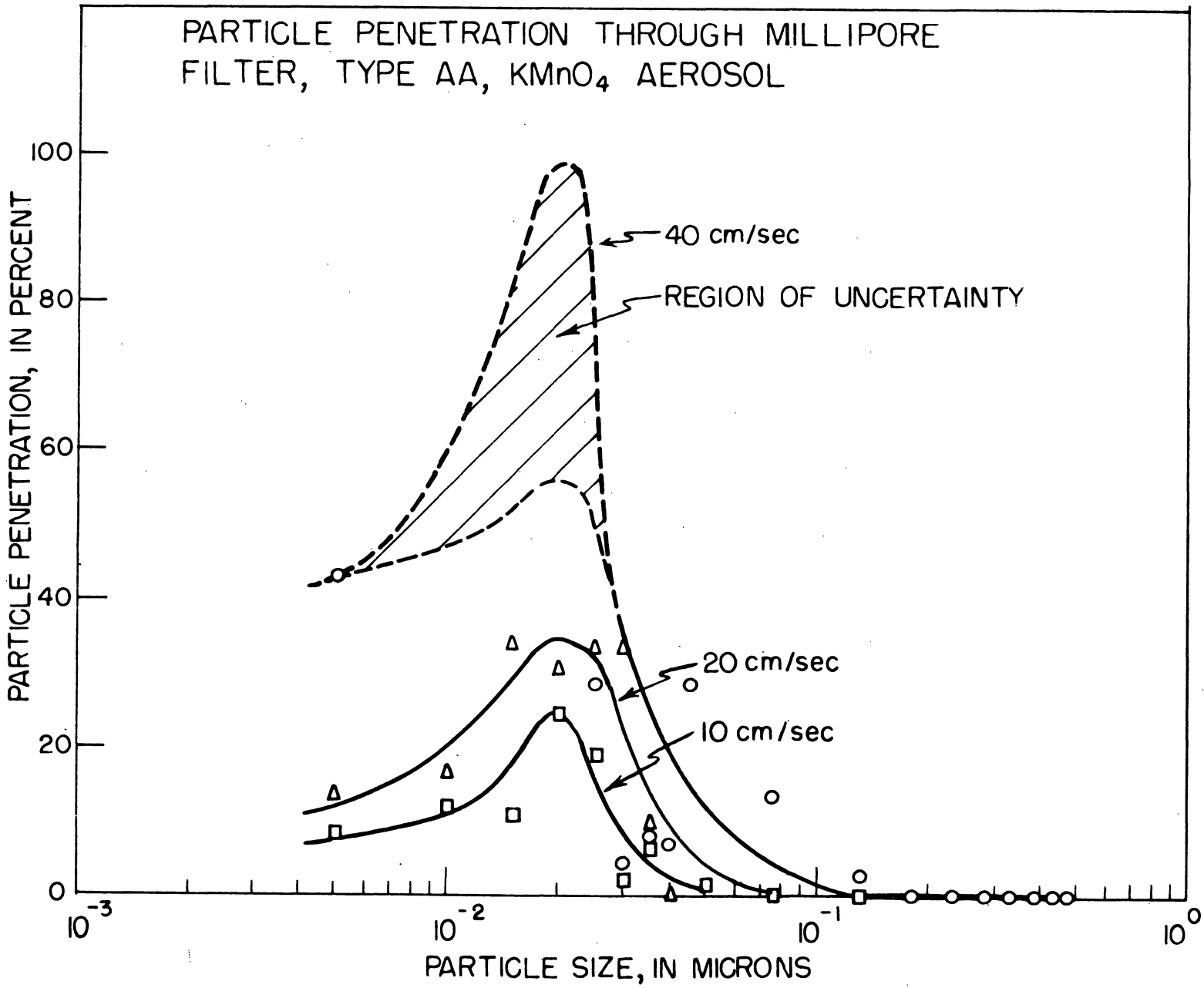
PARTICLE PENETRATION THROUGH MILLIPORE FILTER, TYPE AA, $KMnO_4$ AEROSOL
PARTICLE PENETRATION, IN PERCENT
100
80
60
40
20
0
40 cm/sec
REGION OF UNCERTAINTY
20 cm/sec
10 cm/sec
10^{-3}
10^{-2}
10^{-1}
10^{0}
PARTICLE SIZE, IN MICRONS

Figure 4

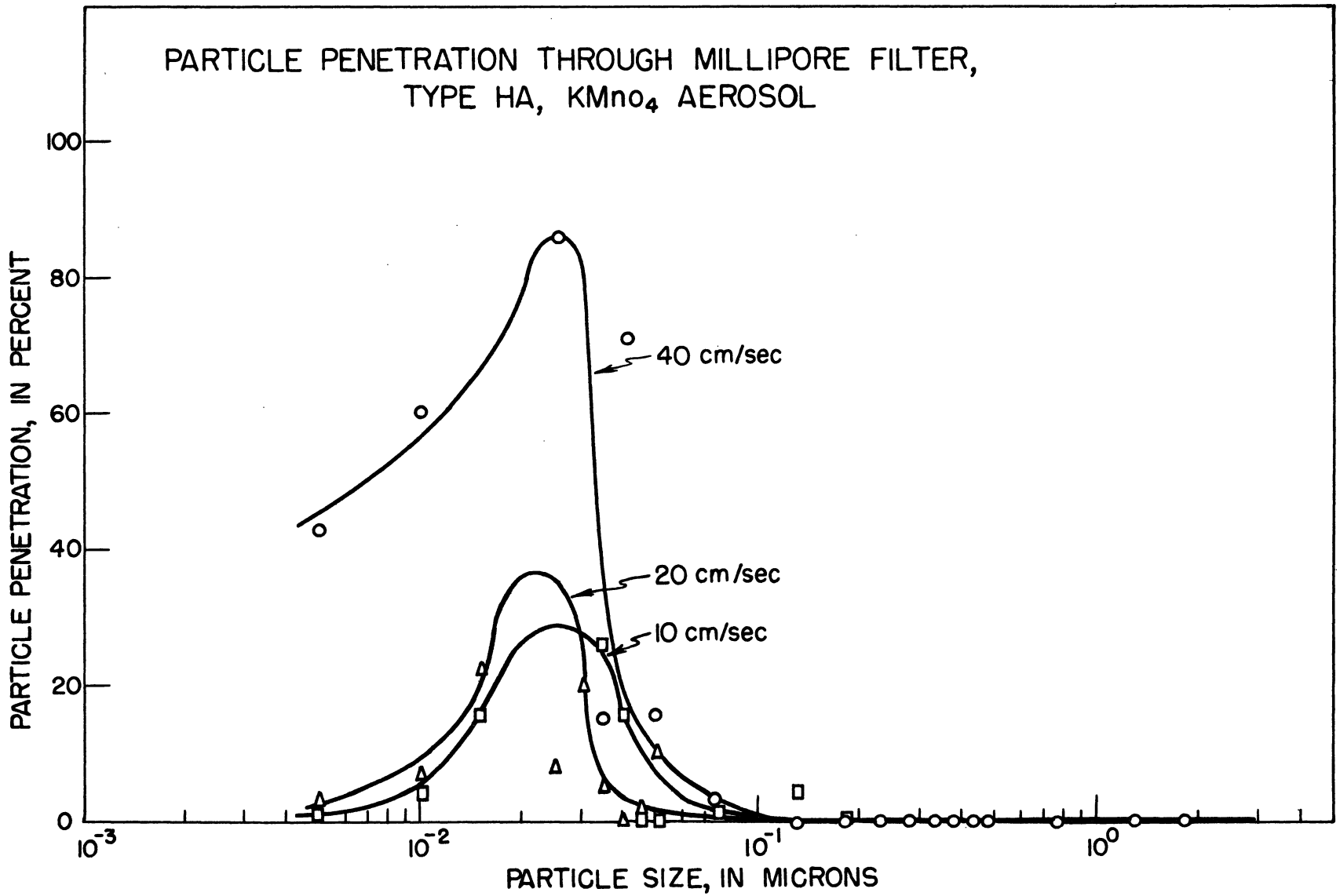
PARTICLE PENETRATION THROUGH MILLIPORE FILTER,
TYPE HA, KMno4 AEROSOL
PARTICLE PENETRATION, IN PERCENT
100
80
60
40
20
0
40 cm/sec
20 cm/sec
10 cm/sec
10-3
10-2
10-1
100
PARTICLE SIZE, IN MICRONS

Figure 5

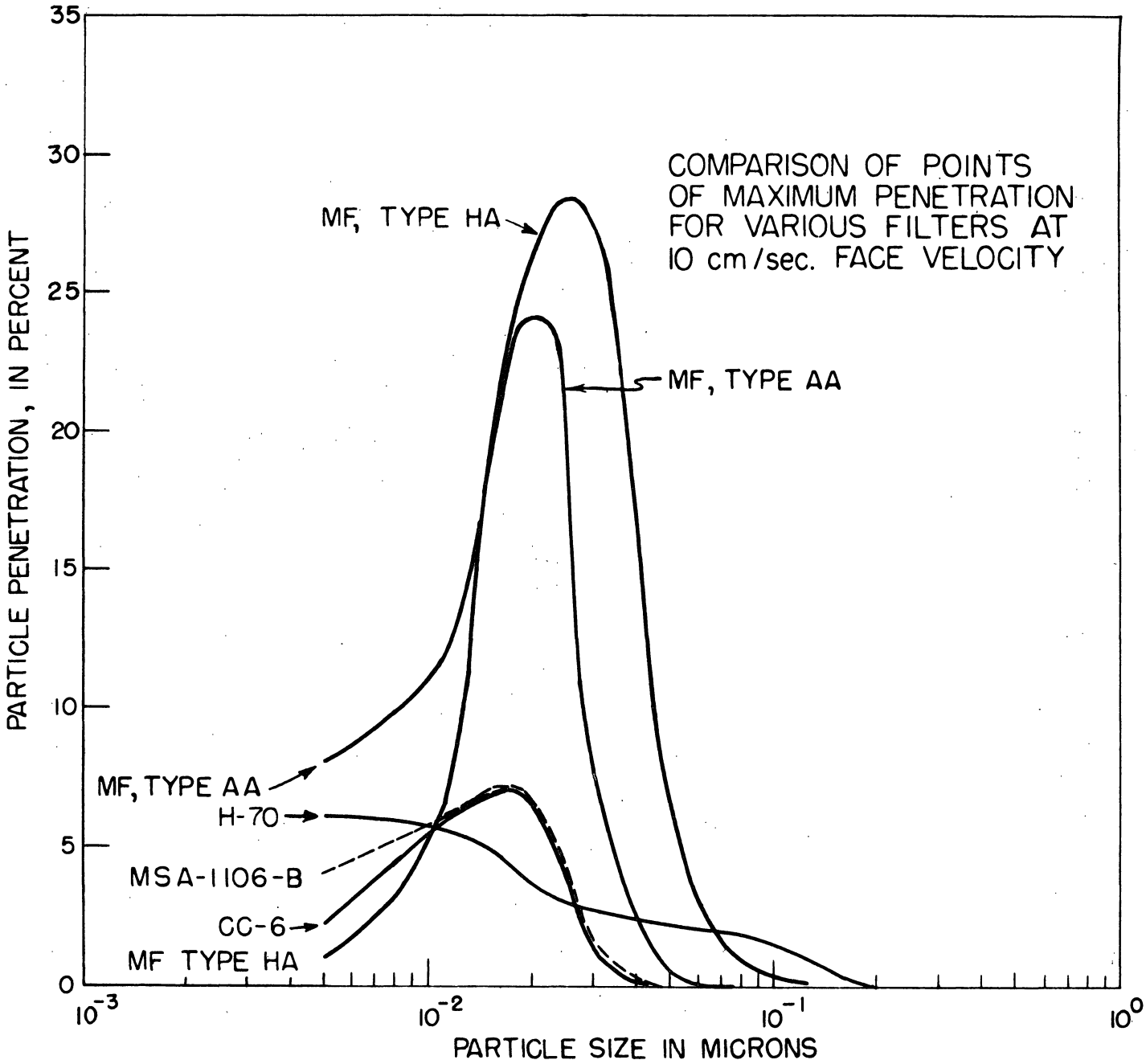
COMPARISON OF POINTS
OF MAXIMUM PENETRATION
FOR VARIOUS FILTERS AT
10 cm/sec. FACE VELOCITY
MF, TYPE HA
MF, TYPE AA
MF, TYPE AA
H-70
MSA-1106-B
CC-6
MF TYPE HA
PARTICLE PENETRATION, IN PERCENT
PARTICLE SIZE IN MICRONS
35
30
25
20
15
10
5
0
10^{-3}
10^{-2}
10^{-1}
10^{0}

CONCLUSION

The collection efficiency of the Millipore Filter is particle size dependent and varies with face velocity in the range of 10 to 40 cm/sec. A point of maximum total penetration of particulate material through the Millipore Filter with respect to particle size was observed.

Although the Millipore Filter has frequently been considered exempt of the above deviations from the ideal filter, it appears to have, in these respects, much the same characteristics as conventional fibrous type high efficiency filter media. The point of maximum penetration may or may not significantly distort size counts and size distribution studies, depending on the relative fraction of the aerosol which falls in the region of maximum total penetration. If a significant fraction of the aerosol falls within this size region, another filter medium should be substituted for the face velocity adjusted, if possible, so that the point of maximum total penetration lies in a different size region.

The point of maximum penetration does not affect the application of the Millipore Filter for use as the standard in filter efficiency studies if the efficiency is not too low. For instance, it would be preferable to avoid using the AA Millipore Filter at a face velocity of 40 cm/sec as a standard filter. This filter, however, is satisfactory for use as a standard at the other face velocities tested, since, as previously stated, the standard filter effectiveness is dependent upon the relative filter efficiency consistency rather than the absolute efficiency.

If the Millipore Filter is used for particle size distribution studies in the size region less that 0.1 micron, the effect of the efficiency variation with particle size and the point of maximum penetration must be considered and appropriate adjustments made to express the results adequately.

The Millipore Filter is an excellent filter medium for particle size distribution and filter efficiency studies because of (1) the shallow surface collection of particulate material, (2) the ease of rendering the medium transparent with immersion oil for light microscopic examination of the collected particulate material, and (3) the applicability of the silica replication technique for subsequent electron microscopic size count analyses. However, as with other high efficiency filters, there are certain limitations which must be recognized for optimum usefulness of the material.

BIBLIOGRAPHY

1. "Millipore Filters, Supplemental Technical Information Regarding Bacteriological and Other Analytical Procedures." Section VI, Bibliography (84 references), pp. 34 and 35. Millipore Filter Corporation, Watertown, Massachusetts.

2. Goetz, Alexander. "Application of Molecular Filter Membranes to the Analysis of Aerosols." Am. Jour. of Public Health, 43:155, February, 1953.

3. Fitzgerald, J. J. and C. G. Detwiler. "Collection Efficiency of Air Cleaning and Air Sampling Filter Media in the Particle Size Range of 0.005 to 0.1 Micron." KAPL-1463, December 9, 1955.

4. "Quarterly Technical Report, April-June 30, 1954." UR-348, The University of Rochester, August 26, 1954.

5. "Semiannual Progress Report of Radiological Development Activities in the Health Physics Unit, January-June, 1954." KAPL-1268, p. 14.

CURRENT SAFETY PROBLEMS AT THE COSMOTRON

M. R. Beebe

Health Physics Division
Brookhaven National Laboratory
Upton, New York

The Cosmotron is a proton-synchrotron which accelerates protons to 3 Bev, usually once every 5 seconds. Acceleration takes 1 second, after which there is a burst of radiation lasting from 1 to 100 milliseconds, depending upon rf turnoff time and target location. Normally, however, the radiation burst has a duration of between 30 and 50 milliseconds. A discussion of the special problems associated with radiation appearing in this manner and of instruments used to measure it can be found in a health physics report on the Cosmotron.[1]

Figure 1 shows the relative positions of the Cosmotron, its main shielding, and the balcony on which are located the control room, experimental laboratory, and health physics office. Experience has shown that such an arrangement is inadequate from a safety standpoint. Present beam intensities were not anticipated at the time of design of the machine, but undoubtedly more thought should have been given to future possibilities at that time. Beam intensities in the first year of operation were approximately 3 to 5 x 10^9 protons per acceleration pulse. Operation continued for about 4 hours per day. At present it is possible to accelerate up to 1 or 2 x 10^{11} protons per pulse with operation on a 24-hour a day, 5-day a week schedule. These increases in intensity and operation time have combined to produce the present problems for the health physicists.

INTERNAL BEAM OPERATION

The first aspect of the present radiation safety problem concerns high intensity operation with an internal beam only, the beam striking a target located usually in one of the straight sections. Figure 2 shows the results of a typical survey of radiation conditions during a recent high intensity target experiment. As can be seen, the radiation levels throughout were high. Such operation must of necessity be of limited duration in order to keep exposures to personnel below the maximum permissible 300 mrem per week. Experimenters usually do not need to remain in these areas for long periods. The main problem is to keep exposures to operations personnel below the permissible maximum. By using operators in shifts and by moving them to the rear of the control rooms, it is possible to operate at these levels for about 12 hours a week. Since lower intensity operation continues during the remainder of each week, it is necessary to schedule operators' working time in a manner similar to the scheduling of machine time for experiments.

EXTERNAL BEAM OPERATION

It is now possible, by means of an ejection magnet, to produce an external proton beam with the Cosmotron. In this beam, up to 60 percent of the circulating protons leave the Cosmotron at a point near the East Straight Section and follow a northerly course through the shielding and out across the landscape toward the northern boundary of the laboratory site.

Health physics aspects of external beam operation differ from those of internal beam operation because regions remote from the Cosmotron must be considered as well as the area near the Cosmotron. Measurement of radiation and control of access to these areas are somewhat difficult but none the less very interesting.

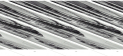

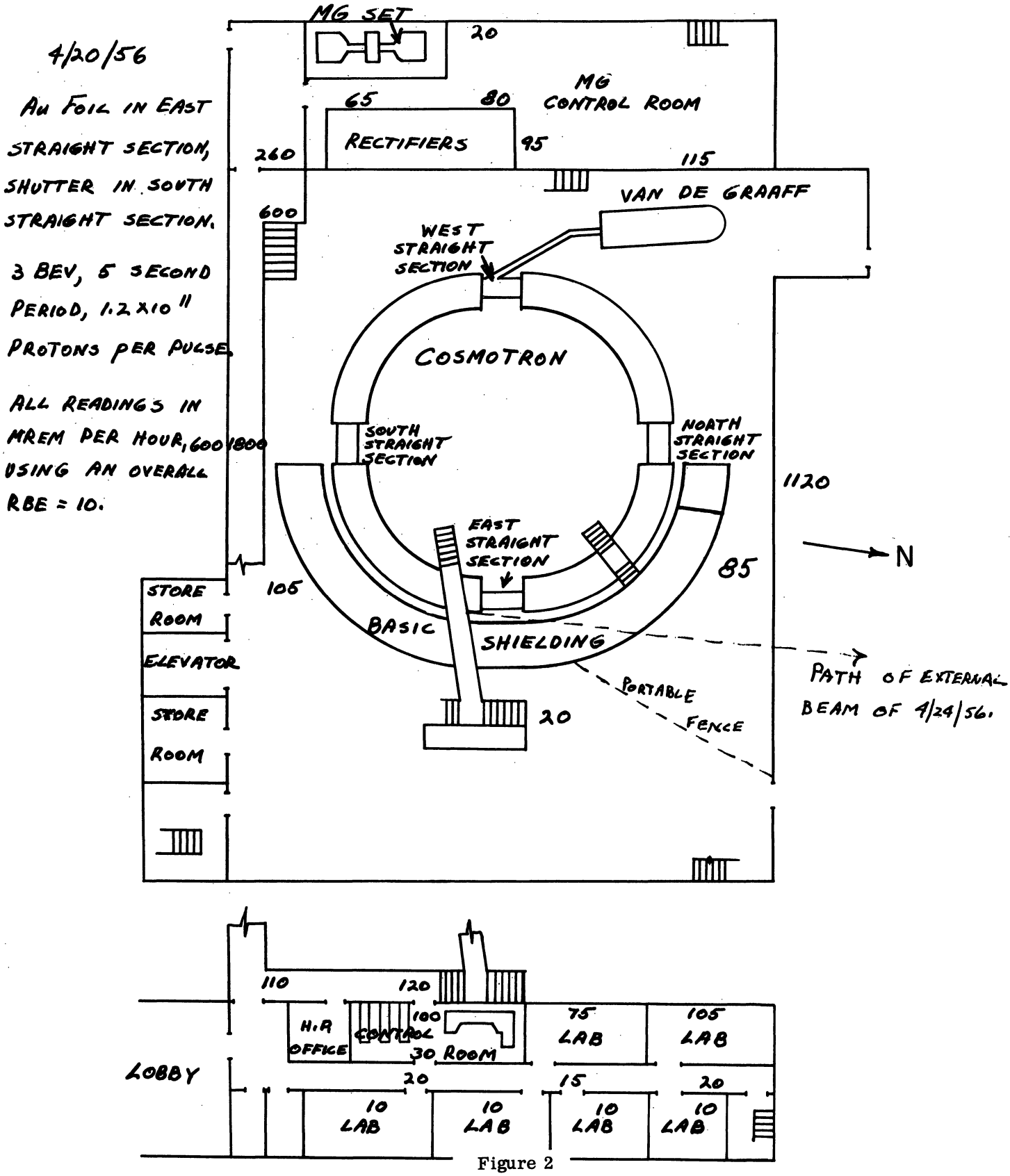
4/20/56
Au Foil in East straight section, shutter in South straight section.
3 BEV, 5 second period, 1.2 x 10 11 protons per pulse.
All readings in mrem per hour, 600 1800 using an overall RBE = 10.
MG SET
20
MG CONTROL ROOM
65
80
RECTIFIERS
95
260
115
VAN DE GRAAFF
600
WEST STRAIGHT SECTION
COSMOTRON
SOUTH STRAIGHT SECTION
NORTH STRAIGHT SECTION
1120
EAST STRAIGHT SECTION
N
85
105
STORE ROOM
ELEVATOR
STORE ROOM
BASIC SHIELDING
PORTABLE FENCE
PATH OF EXTERNAL BEAM OF 4/24/56.
20
110
120
100
H.P. OFFICE
CONTROL ROOM
30
75
LAB
105
LAB
LOBBY
20
15
20
10
LAB
10
LAB
10
LAB
10
LAB

Figure 2

Recently a complete study[2] was made of radiation conditions during an external beam run made expressly for this purpose. After correction for the difference in circulating beam intensity, radiation levels inside the Cosmotron building were approximately the same as those shown in Figure 2. The magnitude of the dose rate in the beam itself was about 1,600 rep per hour[3] at a point between the shielding and the focus of the beam, north of the building and about 50 feet from the outer wall of the shielding.

In order to prevent personnel from walking into such a high intensity beam, a fence was installed inside the Cosmotron building, as shown in Figure 2, and outside the Cosmotron building, as shown in Figure 3. To reduce the radiation intensity in the external beam to a reasonable figure, a large earthen beam catcher of approximately 40,000 cubic yards was erected at a point about 800 feet along the beam path from the Cosmotron building. The thickness of this catcher is equivalent to about 15 feet of heavy concrete of 300 pound per cubic foot density. Figure 4 shows the position of the catcher in relation to the Cosmotron building, the Test Shack, and the site of the new AGS accelerator.

In order to simulate worst possible scattering conditions, the thickness of Pb target at the focus which would produce the maximum amount of scattered radiation at a point on top of the beam catcher above the center line of the beam was determined. Figure 5 gives the results of this experiment.

Surveys were made of the Test Shack and surrounding areas inside the fence and of outlying areas as far away as the site boundary, both with and without the maximum scattering target at the focus. As a result of these surveys, some of the data for which appear in Figures 3, 6, and 7, the following conclusions were made:

1. Radiation levels in the Test Shack and rear yard are, with the exception of areas in and adjacent to the beam and in the east third of the Test Shack, about the same as with internal beam operation as shown in Figure 2. Under present conditions, the east third of the Test Shack is uninhabitable except for short periods of time and is closed off during operation.

2. The addition of the maximum scattering target at the focus raises levels in all areas but much less than was expected, being only a factor of 2 or less in most instances. Estimates by physicists at the Cosmotron ranged as high as a factor of 10 before this study. In the case of the outlying areas, the target in conjunction with the very high intensity beam raised levels significantly, but not so high that they could not be tolerated for occasional short periods of operation.

3. Most of the people interested in this study were relatively confident that the beam catcher would reduce the radiation behind it and at the edge of the site to a tolerable level. The data indicate that this is indeed the case. There were, however, misgivings as to the effect on radiation levels near the sides and front of the catcher resulting from scattering of the primary beam. Figure 3 shows that such scattering is so slight as not to be significant. The reason for such a small amount of back-scattered radiation is that the catcher acts as a sink. The 3 Bev protons which impinge on the surface undoubtedly penetrate well into the catcher before producing large numbers of secondaries. These secondaries, probably mostly star components of 50 to 100 Mev, suffer enough events so that few of them reach the surface to contribute significantly to the amount of radiation measured there.

4. There is little radiation scattered to the sides of the beam from the air through which the beam passes. Secondary radiation is caused primarily by the beam in passing through the shield and the various focussing and bending magnets. This conclusion is supported by the small increase shown to have resulted from the addition of the large Pb target at the focus.

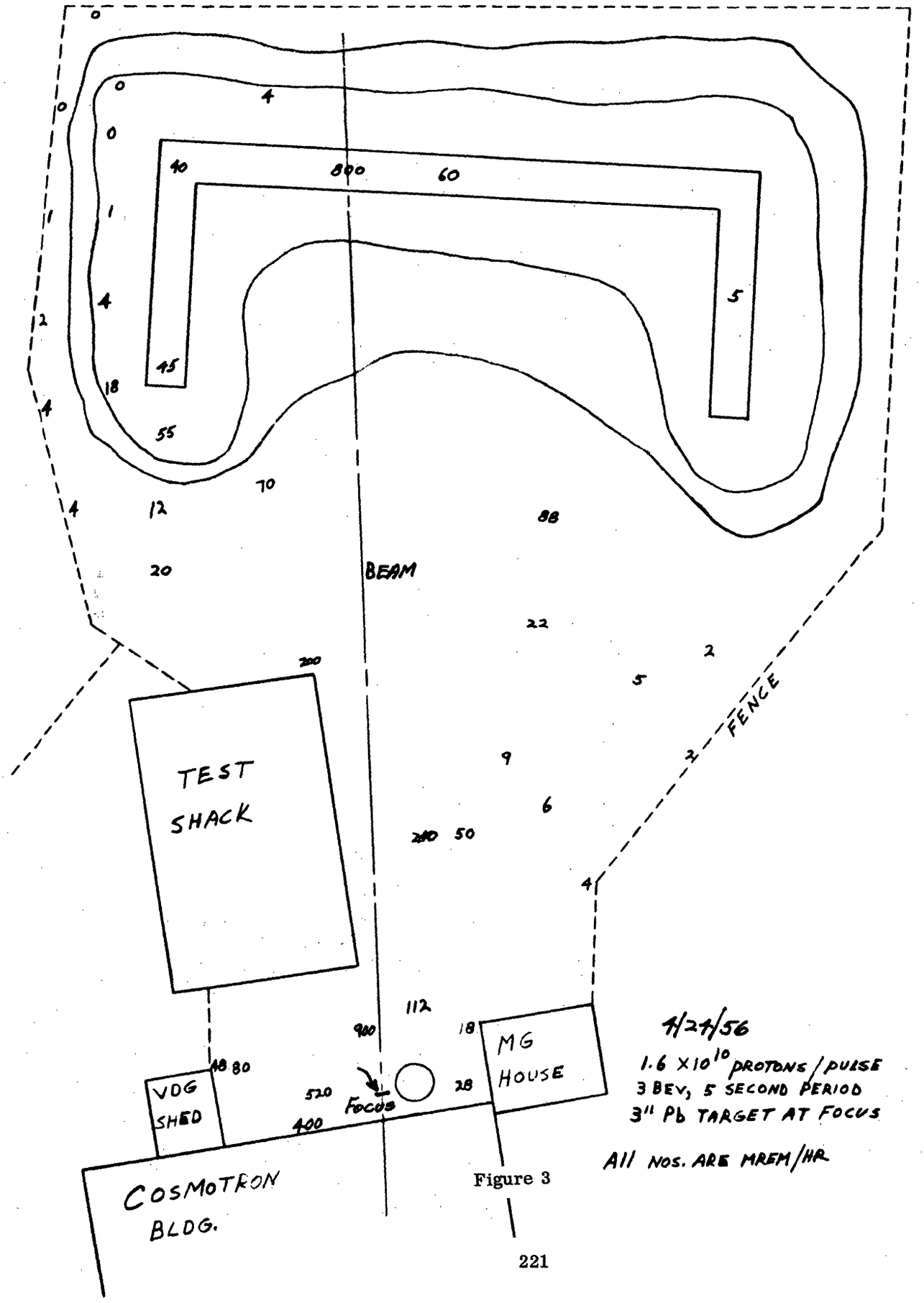
BEAM
TEST SHACK
VDG SHED
MG HOUSE
FOCUS
COSMOTRON BLDG.
FENCE
4/24/56
1.6 X 10^10 PROTONS / PULSE
3 BEV, 5 SECOND PERIOD
3" Pb TARGET AT FOCUS
ALL NOS. ARE MREM/HR

Figure 3

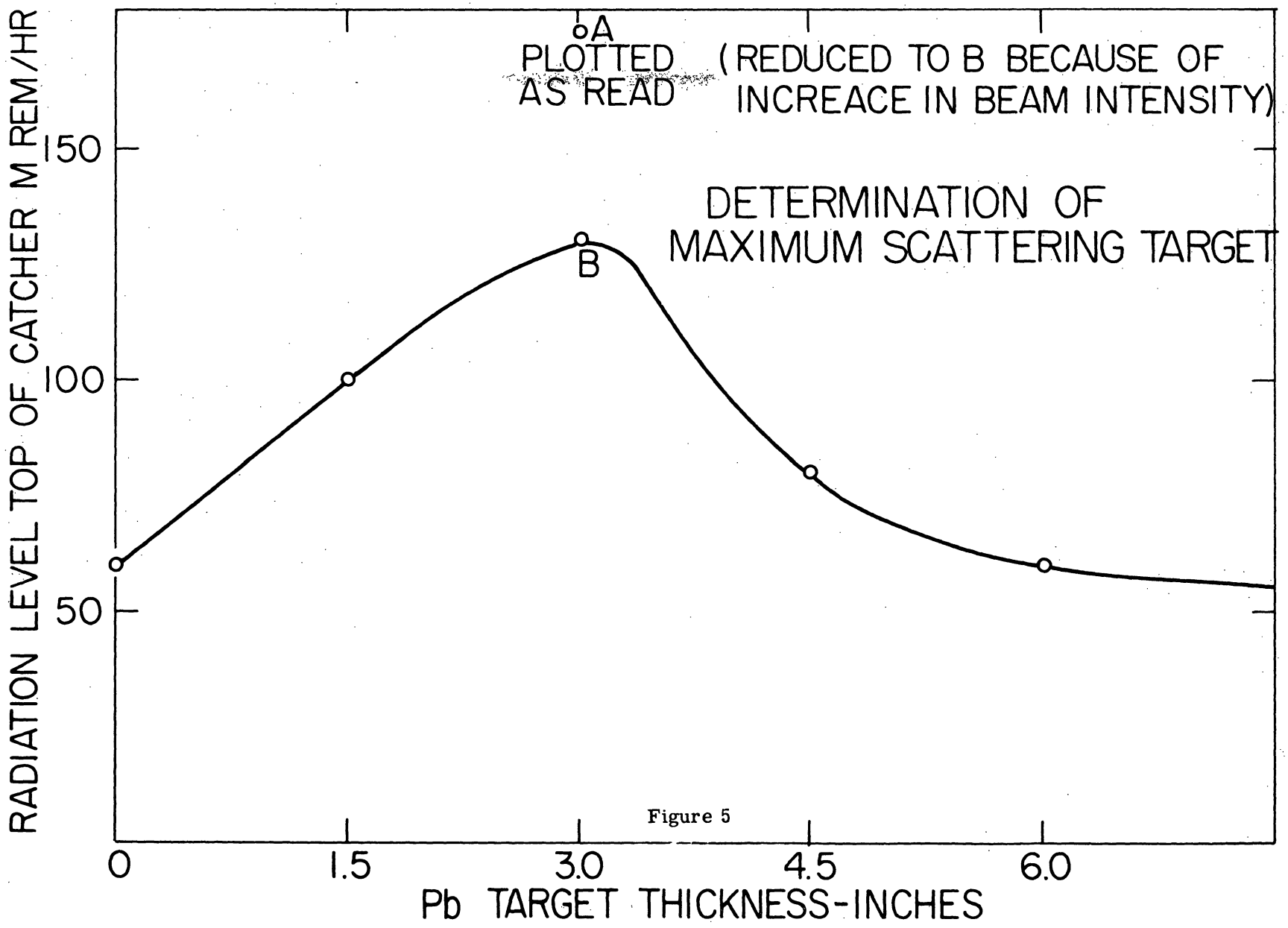
A
PLOTTED AS READ
(REDUCED TO B BECAUSE OF INCREACE IN BEAM INTENSITY)
DETERMINATION OF MAXIMUM SCATTERING TARGET
B
RADIATION LEVEL TOP OF CATCHER M REM/HR
150
100
50
0
1.5
3.0
4.5
6.0
Pb TARGET THICKNESS-INCHES

Figure 5

BROOKHAVEN NATIONAL LABORATORY

BY. ..... DATE ..... SUBJECT HEALTH PHYSICS SURVEY SHEET No ..... OF .....

CHKD. BY ..... DATE ..... JOB No. .....

DEPT. OR PROJECT .....

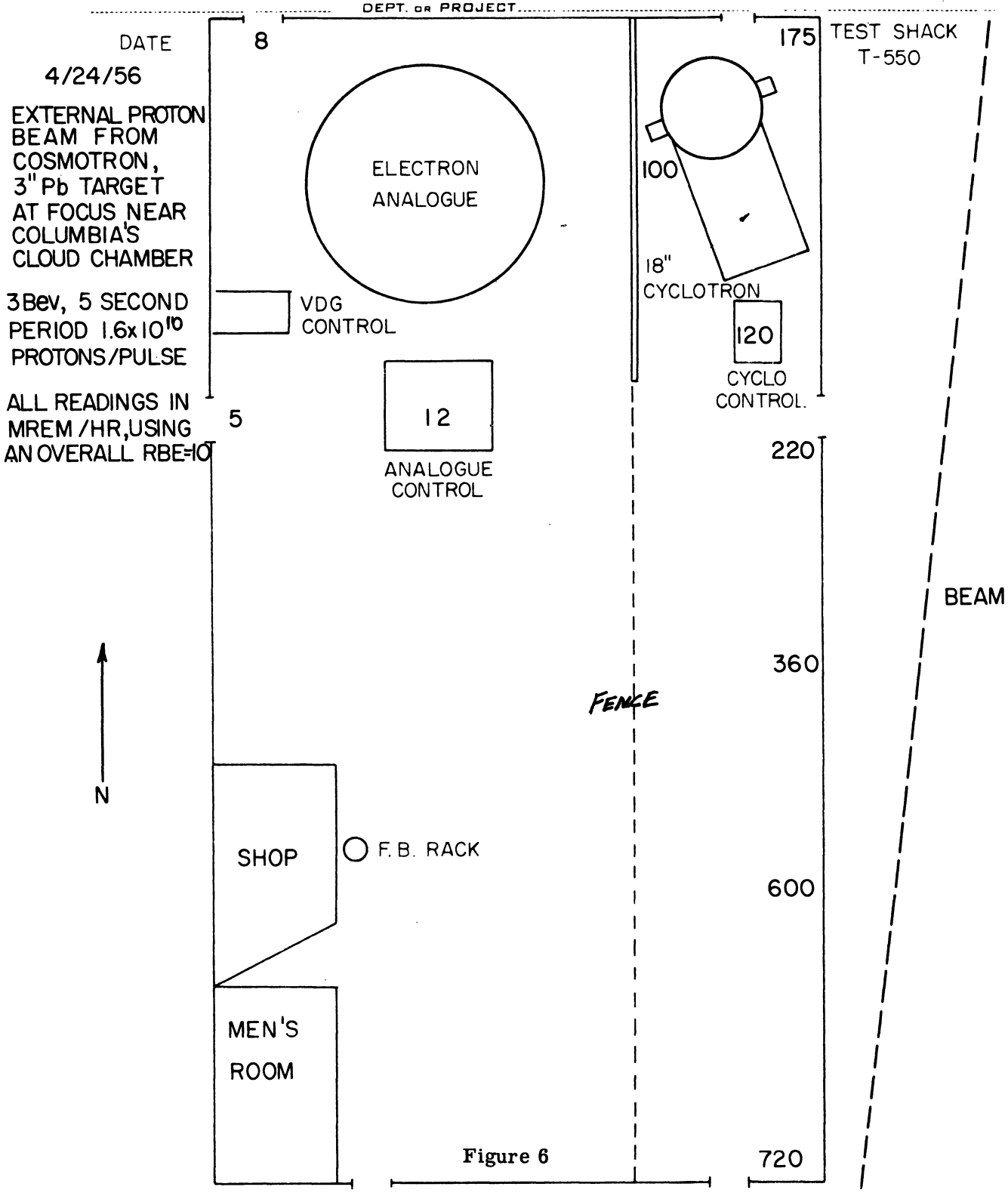

Figure 6

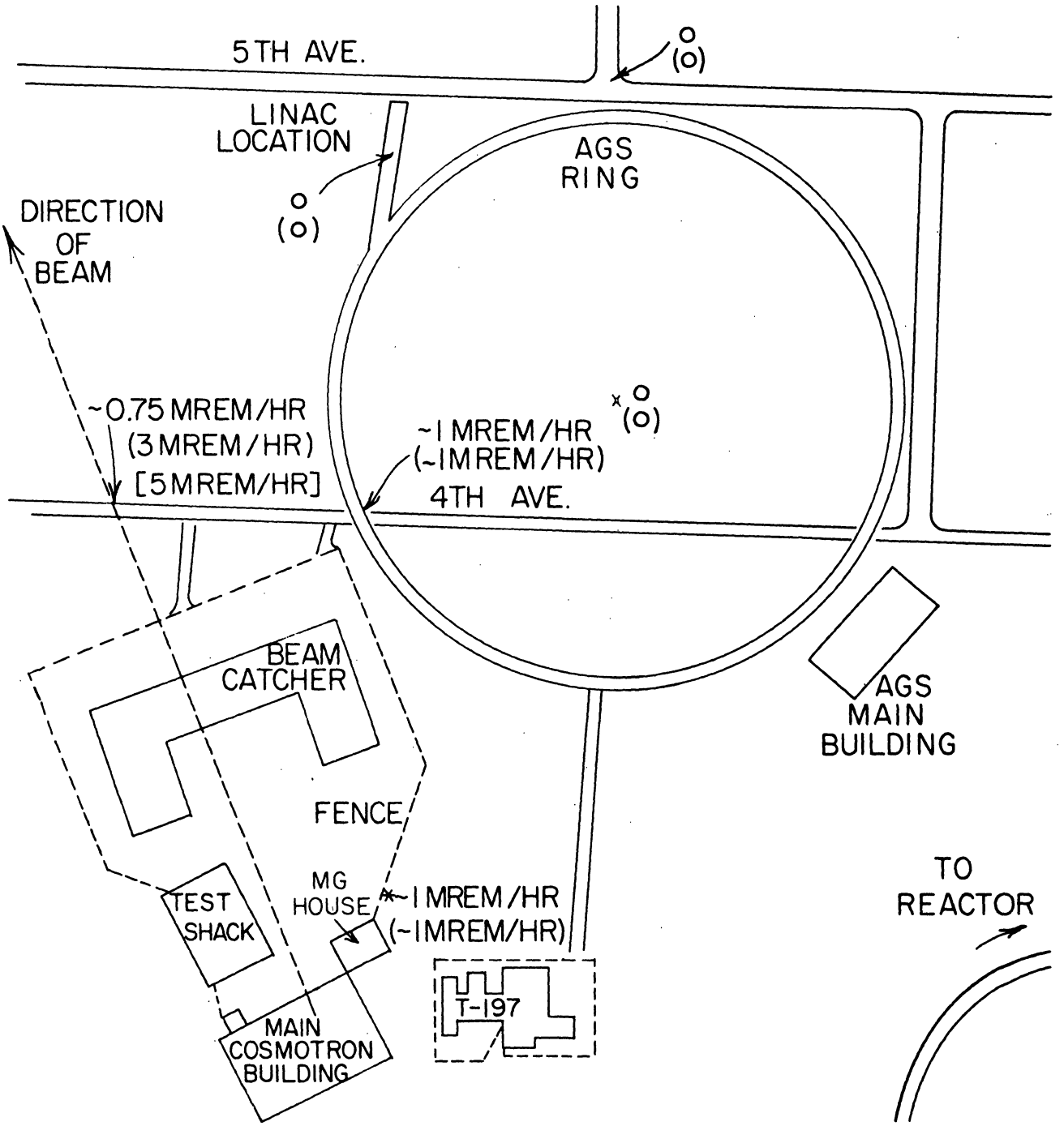

4/24/56 3 Bev, 5 SECOND PERIOD FOR ALL MEASUREMENTS.
CLEAR NOS. (1.6×10^{10} PROTONS/PULSE, NO TARGET)
(NO.) (1.6×10^{10} PROTONS/PULSE, 3" Pb TARGET AT FOCUS)
[NO.] (3.5 TO 4×10^{10} PROTONS/PULSE, 3" Pb TARGET AT FOCUS.)

Figure 7

FUTURE PROBLEMS AND PLANS

Experience has indicated that the present arrangement of shielding is inadequate. Plans are now being made to increase the beam intensity to 10^{12} protons circulating per pulse within a year, and to 10^{13} protons per pulse in 3 to 5 years. Obviously, the problem will then be magnified and could not be solved by the present scheme of piling local shielding where needed. Either the control rooms and experimental areas will have to be removed to remote locations, or an effective shielding arrangement will have to be made. It is not clear at this time which of these alternatives will be the one which is ultimately decided upon.

BIBLIOGRAPHY

1. Cowan, F. P. and J. Handloser. "Health Physics Program for the Brookhaven Cosmotron." BNL 264(T-43), November, 1953.

2. Beebe, M. "Cosmotron External Beam Survey." Memo to Health Physics File, April, 1956.

3. Handloser, J. "Cosmotron External Beam Dosimetry." Memo to Health Physics File, May, 1956.

LOADING AND HANDLING RADIOACTIVE TARGETS FOR ACCELERATOR BOMBARDMENT

M. D. Thaxter

Radiation Laboratory
University of California
Berkeley, California

At the Radiation Laboratory in Berkeley, radiation protection functions are performed by 2 groups. One, called Health Physics, attends to radiations which may be terminated by opening a switch - for example, from an accelerator. The other, called Health Chemistry, is concerned with the radiation from unstable matter - radioisotopes. The latter viewpoint will be considered here.

Radioisotopes arrive at the Laboratory from various sources. Whatever the origin, one or more accelerators may be employed for further bombardment. Thus, in addition to the use of the accelerators for nuclear physics studies, there are problems of handling both input and output radioactive materials as targets, which are subjected to subsequent mechanical and chemical manipulation.

A brief run-down of the 5 accelerators existing and the 1 now under construction at Berkeley may be in order, to delineate those which have posed certain problems.

1. A linear proton accelerator, known locally as the "Linac," accelerates protons to 32 Mev in a maximum beam intensity averaging 0.25 microampere. Targets are normally foils of non-radioactive aluminum, copper, etc. The largest radiation intensity found on the targets after bombardment has been about 100 mr/hr. It is used primarily by physicists to study the gamma rays produced during bombardment. This machine has not presented any notable radiation safety problems.

2. The synchrotron is an electron accelerator capable of producing pulses of electrons of 335 Mev. Normally the beam is used to bombard inactive targets. The consequent X-ray and gamma fluxes are studied. These targets are not worked up. No significant problems occur here.

3. The 184-inch synchrocyclotron, until recently the largest Berkeley machine, is so called because of the diameter of the magnet poles. This research tool has produced 350 Mev proton beams of 0.75 microampere average current, 195 Mev deuteron beams of 0.75 microampere average current, and 390 Mev alpha beams of 0.1 microampere average current. Starting this fall, the proton and deuteron beams are expected to be 728 and 475 Mev respectively. These beams may be deflected out of the vacuum, usually for physicists' studies. Most chemistry targets employ the internal beam and are foils or powders of both inactive and active materials, including transuranic substances. Targets of the latter are enclosed in double envelopes of welded 1 mil platinum. Some bombardments have resulted in "hot" targets, for example 100 r per hour at 3 to 4 feet. The new beam energies may add some problems. The beam characteristics have permitted simplified target assemblies, removable with 12-foot tongs to minimize exposure. This simplicity also has permitted use of a pneumatic tube system to transport targets automatically, from the cyclotron beam tank to the chemical laboratory some 100 yards away. This facility, called a "rabbit" target, has permitted

chemists, notably Dr. Meinke, now of the University of Michigan, to perform studies on targets containing isotopes of very short half-lives. With this equipment, Dr. Meinke was able to get targets in the counter within seconds of shut-off time.

The more active targets of the non-rabbit variety are promptly placed in a shielded container for transport via truck to the chemist. Subsequent handling is dependent on the nature of the isotopes bombarded and produced. Short half-life targets are usually dissolved behind hydrogenous or lead shields in fume hoods. Microcurie and larger quantities of long-lived emitters are worked up in Berkeley boxes, shielded or not as required.

4. The largest accelerator at Berkeley, the Bevatron, produces 6.2 Bev protons. A number of research stations are available for physicists' studies, many of which, such as the demonstration of the anti-proton, are special setups of but academic concern to the health chemist. Chemical targets are mounted in a so-called plunging target holder synchronized with the pulsed beam. These target assemblies, usually containing various metallic foils initially inactive, read a maximum of 1 r per hour at 10 inches after bombardment. Spallation reactions are the object of the chemists' studies. No important health problems have arisen.

5. Under construction is a heavy ion linear accelerator or "Hilac." This machine is scheduled to start up in September. It might be a productive tool for making elements beyond number 100, employing Neon-22 as the particle. The targets anticipated are curie and larger amounts of certain transuranics. Considering this fact, with beam currents up to 15 microamperes, thin protective foils and a 10.1 Mev particle energy expected, one may understand our concern about target burnup. Detailed solutions are not currently available for presentation.

6. For the nuclear chemist at Berkeley, the work horse accelerator has been the 60-inch cyclotron. It is capable of generating 12 Mev protons at 60 microamperes, 24 Mev deuterons at 150 microamperes, 48 Mev alphas at 75 microamperes, and a variety of heavy ion beams such as carbon, oxygen, nitrogen, and neon. It is the oldest accelerator at Berkeley. The skill of the designers and operators has, through several revisions, resulted in concentrated beams of high intensity and known position. This situation has demanded elaborate equipment to cool the target assembly, which is not usually required in the other accelerators. Without such cooling, tungsten foils melt in certain beams. Many target designs have been devised. A simple assembly as shown in Figure 1, a so-called "backing plate" target, is essentially a foil mounted on a plate in a collimator block. The back of the foil is cooled by a high velocity stream of water. When the foil involves fissionable material, it is possible for fission products to appear in the water, either because peroxides formed in the cooling water attack the metal, or because the beam actually knocks fission fragments out of the foil. Hence, the water must circulate in a closed system capable of being monitored. Another target, the so-called "micro" target, requires both water and air cooling, front and back, and a blanket of helium at 1/2-inch atmosphere adjacent to the last 1 mil platinum foil covering the transuranic material being bombarded. All of these media may become heavily contaminated should this foil rupture, therefore all are in sequestered or continuously cleaned systems. These systems are, further, sensed for pressure or flow rate changes and interlocked with quick acting valves and shut-offs on the cyclotron proper to protect it. The protective requirements result in considerable mechanical complexity, yet this complexity must not interfere seriously with the rapid transport of targets to the chemist who may be seeking short-lived material. Our solution to these contradictory specifications is (1) a list of procedural checks, (2) a target cart, and (3) associated Berkeley boxes.

The procedural checks involve, first, the original target preparation before it reaches the cyclotron building. This is a box job. Though it may contain many milligrams of very active material, its exterior envelope of thin platinum must be

contamination-free, able to withstand rapid air pressure changes, and survive a water leak test. Similar checks occur at the cyclotron test area after the envelope is assembled in the probe mechanism. During bombardment it is continuously monitored, as mentioned earlier. Following bombardment, when the target assembly may reach 50 r per hour at 3 feet, the envelope holder is visually checked and disengaged from the assembly under enclosure conditions on a cart. It contains the water, its pump, heat exchanger, flow rate control and adjustment, helium supply and exhaust bottle, pressure sensing mechanism, air supply and return lines and air filters, and a gloved box enclosure for disassembling the probe mechanism under contamination control conditions. A lead carrying case receives the envelope and its cooling block for transport to the chemist. The semifinal and final openings of the envelope are made in the lab in a box, where it may produce 2 r per hour through 1 inch of lead just prior to dissolution. During the target's transport to the chemist, the cooling water is sampled, plated, and counted. Swipes are made on target surfaces; area air samples are checked. A thorough survey of the immediate cyclotron environment is routine after bombarding transuranics. Any detection of loose activity is usually found in the cooling water. Since this is confined to the cart, decontamination of the latter is undertaken while a standby cart takes the successive targets.

In summary, while 5 carts have been contaminated and 2 spills have occurred, happily no cyclotrons have yet been lost. For the future, the ever-increasing target activities, heavier beams, and thinner foils make the job look even more challenging to the team of chemist, operator, designer, and health chemist involved in accelerator targets.

THRESHOLD DETECTORS FOR LOW LEVEL NEUTRON MEASUREMENT

J. F. O'Brien

Nuclear Division
The Glenn L. Martin Company
Baltimore, Maryland

A knowledge of neutron flux in discrete energy intervals resulting from any neutron-producing device is essential when a complete evaluation of neutron effects is to be made. It is often sufficient to be able to measure neutron flux density with detecting instruments whose neutron response and energy dependence are known for a few points over a large energy range, or to be able to relate detector response to tissue response. In many instances, however, especially where a difference in relative biological effectiveness caused by a large energy spread must be taken into account, a knowledge of neutron flux as a function of energy is essential. One method of obtaining such information is by the use of neutron threshold detectors.

A group of selected reactions and detectors have been investigated with special emphasis on various methods of improving detector sensitivity. The detectors investigated are listed in Table 1, together with descriptive and performance data. Values of minimum detectable flux were chosen arbitrarily so that the statistical uncertainty at the 90 percent confidence level is equal to the flux. This corresponds to a 95 percent probability that a measured flux of the stated minimum detectable value is greater than zero. Improvement in sensitivity has been accomplished in several ways. The methods used are best exemplified by an examination of the detectors themselves.

THE C-12(n, 2n)C-11 AND I-127(n, 2n)I-126 REACTIONS

A phosphor containing an element which is a threshold detector is best exemplified by a phototube used to count the positrons emitted in the decay of C-11 produced during previous neutron irradiation of an anthracene crystal mounted on the tube. The threshold for this reaction is 20 Mev, below which the cross section may be considered zero. The average cross section from 20 to about 100 Mev is 33 mb, with a peak of 78 mb at about 40 Mev. Efficiency was determined, by calibration with a known conversion line such as that resulting from the decay of Cs-137, to be 95 percent. This high efficiency is accounted for by the fact that all positrons emitted are seen by the counter; only a small portion being lost beneath the bias setting of the amplifier or at the surfaces of the crystal. The decay curves obtained after a number of exposures in various mixed fields of radiation at the Cosmotron all exhibited a half-life of 20 minutes. A 30-minute irradiation period suffices for the detection of a flux of 2.3 $n/cm^2/sec$. By irradiation and counting for longer periods of time, fluxes of the order of 1 $n/cm^2/sec$ may be detected. Some increase in sensitivity could be obtained by using a larger crystal, but corresponding increases in background which would result without the use of special shielding and anticoincidence techniques make this attractive only in extreme cases.

A NaI(Tl) crystal was used to improve the sensitivity for neutron detection in the range of 10 Mev and above. The I-126 produced decays with the emission of a number of beta particles and gamma rays but, since only 1 energizing particle in each chain is needed, counting easily may be done. The product nucleus has a comparatively long half-life of 13 days but, since the cross section for the reaction is quite large and the detector sensitivity is so high, the long half-life is not a great disadvantage. The use of this detector is somewhat complicated by the presence of 2 competing reactions, I-127(n,γ)I-128 with a 25-minute half-life, and Na-23(n,γ)Na-24 with a 14.9-hour half-life. For a correct evaluation of the induced activity caused by the reaction of

TABLE 1

DESCRIPTIVE AND PERFORMANCE DATA FOR THRESHOLD DETECTORS

Reaction used	*Threshold in Mev*	*Detector material*	*Induced activity*	*Half-life*	*Detector dimensions*	*Interfering reactions*	*Photo multiplier type*	*Irradiation time*	*Cooling time*	*Counting time*	*Min. detectable flux ($n/cm^2/sec$)*
$U^{238}(n,f)$	1.1	Uranium nitrate crystals	—	—	12.7 cm dia. thin coating	—	6364	30 min	—	30 min	6.6
$P^{31}(n,p)Si^{31}$	2.0	$NH_4H_2PO_4$ in "phoswich"	1.5 Mev beta	160 min	7.6 cm × 4.4 cm "phoswich"	Several	6363	180 min	30 min	30 min	200
$S^{32}(n,p)P^{32}$	2.0	Fused sulphur	1.7 Mev beta	14.5 days	10.2 cm dia. 0.32 cm thickness	none	6364	15 hrs	5 min	30 min	230
$Ag^{107}(n,2n)Ag^{106}$	9.6	Silver orthophosphate in "phoswich"	2.0 Mev positron	24.5 min	7.6 cm × 4.4 cm "phoswich"	$Ag^{107}(n,\gamma)Ag^{108}$ $P^{31}(n,p)Si^{31}$	6363	60 min	5 min	30 min	350
$I^{127}(n,2n)I^{126}$	10	NaI(Tl) crystal	0.87 Mev beta	13 days	3.8 cm dia. 2.68 cm thickness	$I^{127}(n,\gamma)I^{128}$ $Na^{23}(n,\gamma)Na^{24}$	6292	15 hrs	6 days	30 min	20
$C^{12}(n,2n)C^{11}$	20	Anthracene	0.97 Mev positron	20.3 min	7.62 cm dia. 1 cm thickness	$C^{12}(\gamma,n)C^{11}$ $C^{12}(p,pn)C^{11}$	6363	30 min	5 min	30 min	2.3
$Bi^{209}(n,f)$	50	Bismuth nitrate	—	—	16 cm dia. 38 cm high	—		—	—	—	—

interest, therefore, a decay curve must be plotted and the activity caused by the I-127(n, 2n)I-126 reaction extrapolated to zero cooling time. In general, it was found that a cooling period of about 6 days was required and that the I-126 activity was about 1 percent of the total activity measured shortly after the end of the irradiation period. Minimum detectable flux for irradiation periods less than 10 hours is about 500-700 $n/cm^2/sec$.

LARGE AREA COUNTING

The Sulfur Detector - The reaction S-32(n, p)P-32 with a threshold at about 2 Mev has been used previously in many investigations. One approach to sensitivity improvement lies in counting a large area, thin sample. In this case, 50 grams of sulfur were cast into the form of a disc 10 cm in diameter and 0.32 cm thick, shown in Figure 1. This was counted on an equal area anthracene chip mosaic bonded to the photocathode of a large phototube. The mosaic thickness varied from 1 1/2 mm at the center to 3 mm at the edges and was ground flat at the outer surface. The use of a thin scintillator resulted in a low background counting rate. The observed efficiency was determined as 5 percent, comparing the detector with the known neutron flux and spectrum of an Ra-Be source. The excitation function for the reaction was weighted against the Ra-Be neutron spectrum in order to obtain a properly weighted cross section for the efficiency determination. It was found that a greater improvement in sensitivity could be obtained by large area counting in the "phoswich," a term used to denote the phosphor sandwich.

The physical form of the "phoswich" is shown in Figure 2. It is fabricated from a large cylinder of plastic scintillator, such as p-terphenyl in polystyrene, which is grooved at right angles to its base. The grooves are filled with the material to be activated for counting. In the case of sulfur, slabs 0.125 inch thick and 1.5 inches long were cast in a mold by subjecting sulfur to a pressure of 30,000 pounds per square inch. These slabs were then inserted into the slots of the "phoswich." In the case of detectors utilizing other materials, the material to be activated was poured into the slots and the phoswich sealed with scotch tape. Detectors utilizing the Ag-107 (n, 2n)Ag-106 and P-31(n, p)Si-31 reactions with thresholds of 9.6 Mev and 2.0 Mev, respectively, were made as shown in Figure 2. Efficiencies were determined in the same way as for the sulfur disc detector. Possible interfering reactions in the phosphorous detector using $NH_4H_2PO_4$ are P-31(n, 2n)P-30, N-14(n, 2n)N-13, C-12(n, 2n)C-11 and P-31(n, α)Al-28. These are all of much shorter half-life than 170-minute Si-31, however, and hence are easily separated. Efficiencies of from 10 to 20 percent were found for the "phoswich," depending on detector material.

The characteristics of the "phoswich" are shown in Figure 3. It can be seen that the background plateau is quite steep. The slight flattening of the curve between 650 and 700 volts is because of all of the background pulses in the solid portion of scintillator at the base of the "phoswich" being counted. Since light pulses in the columns must be transmitted to the photocathode, there is some light loss. For example, a pulse from the top of the column which would have had enough amplitude, after being amplified, to pass the bias discriminator if it had been close to the photocathode, is not passed because its amplitude is diminished by losses in the column. Thus, as the tube voltage is increased, a larger number of light pulses occurring in the columns are passed by the discriminator, and the curve continues to rise until noise pulses from the photomultiplier begin to be passed. It follows that the efficiency of the detector should increase with increasing voltage until a saturation point is reached where all of the pulses are counted. The characteristics shown are those of the $NH_4H_2PO_4$ "phoswich" and are typical of other "phoswich" detectors.

The color of the detector material used in the "phoswich" has an effect on the characteristics since it acts as either a light reflector or a light absorber. The efficiency of a "phoswich" containing red phosphorous is lower by a factor of 7 than the efficiency of the "phoswich" containing $NH_4H_2PO_4$, a white powder.

The Uranium Detector - A sensitive threshold detector was obtained by utilizing the 1.1 Mev threshold for the fission of U-238 by fast neutrons. A thin layer, consisting of equal parts of uranium nitrate and ZnS(Ag) mixed with Zapon was painted on the photocathode of a 2-inch phototube. Pulses caused by the uranium alpha particles were biased out and fission pulses counted

Figure 2

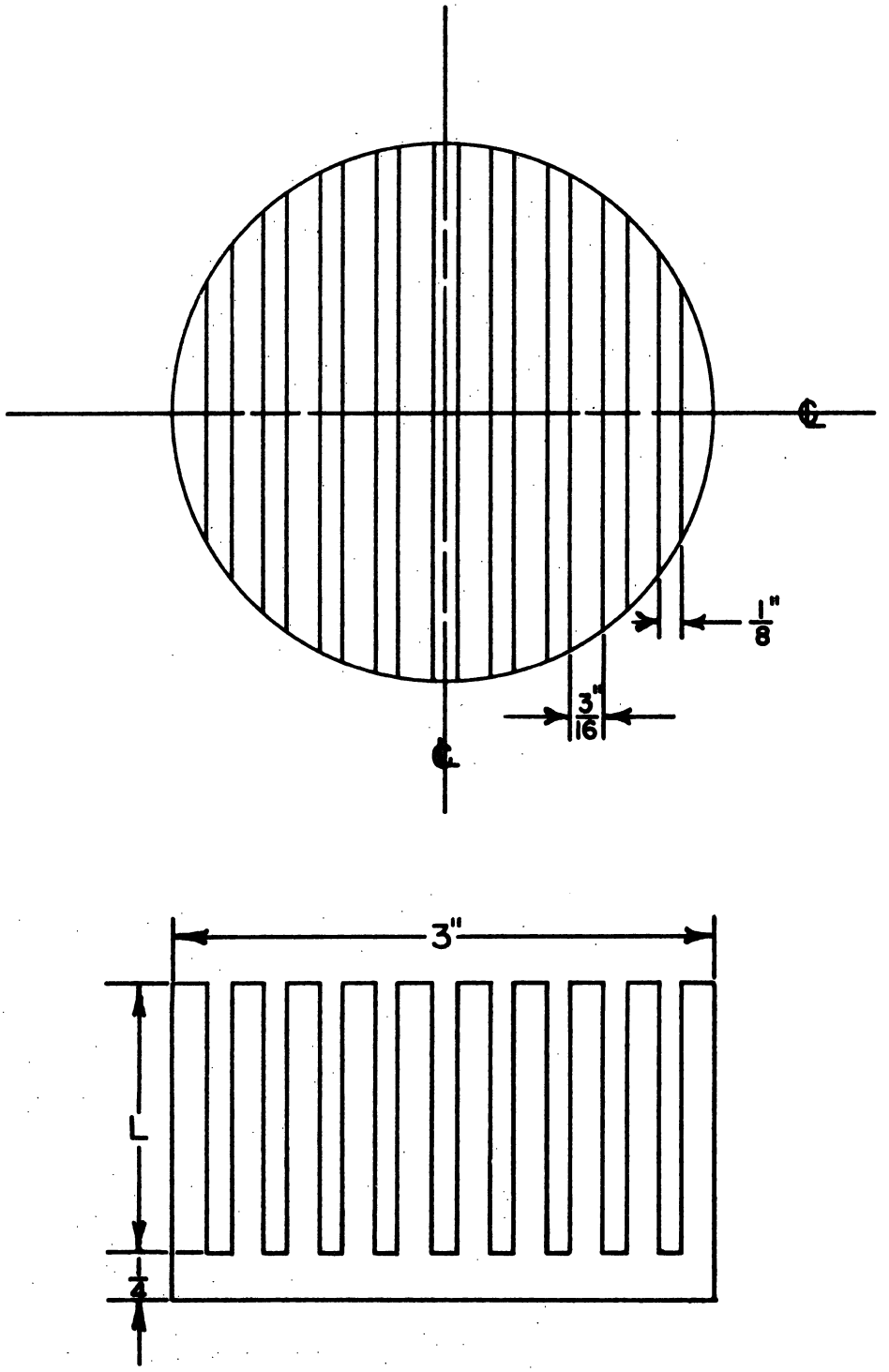

THE PHOSWICH

Figure 3

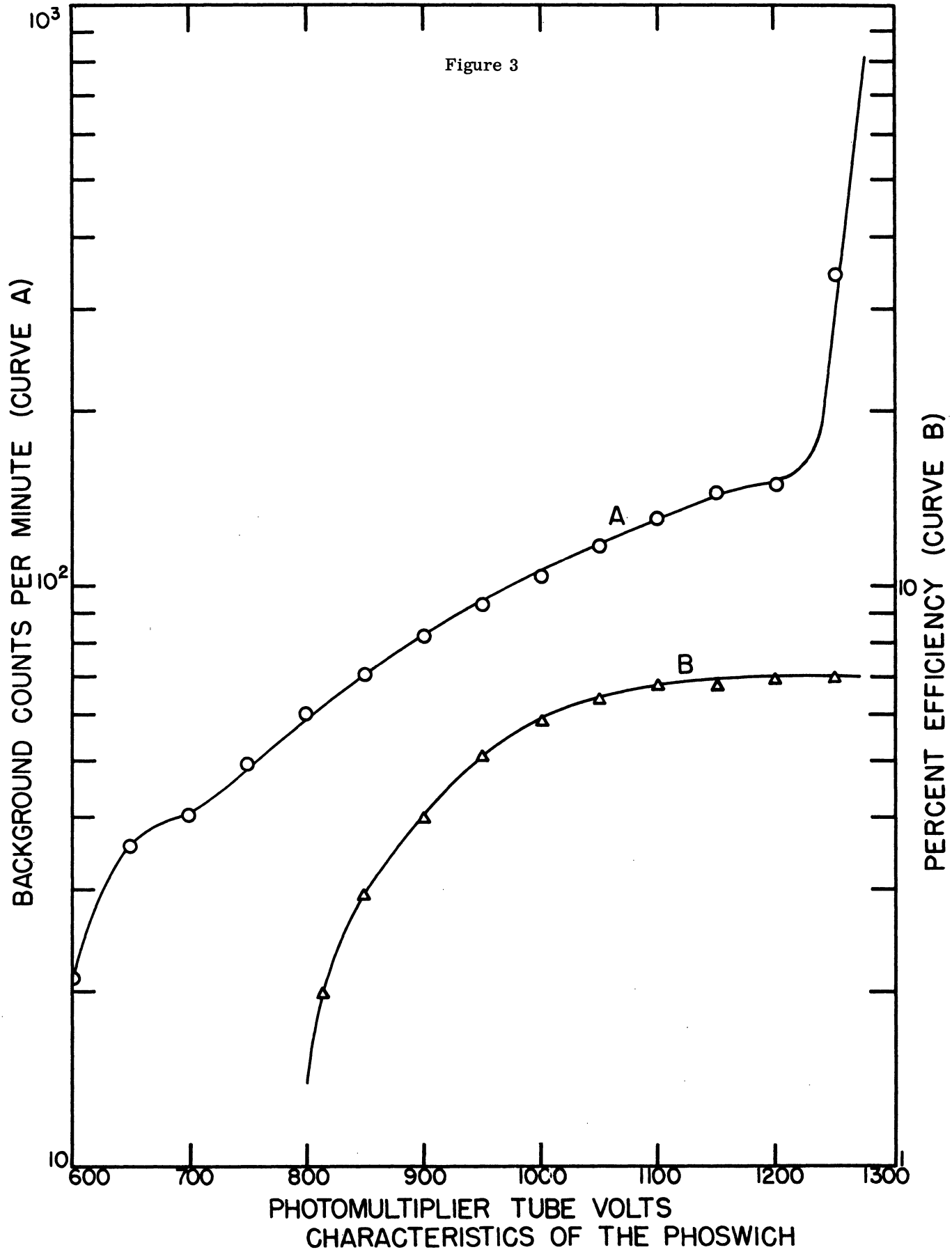
BACKGROUND COUNTS PER MINUTE (CURVE A)
PERCENT EFFICIENCY (CURVE B)
10^3
10^2
10
1
A
B
600
700
800
900
1000
1100
1200
1300
PHOTOMULTIPLIER TUBE VOLTS
CHARACTERISTICS OF THE PHOSWICH

while the detector was being irradiated. Calibration with Ra-Be neutrons gave an efficiency of 0.001 percent. Because of the inherently low background, the detector is quite sensitive despite the low efficiency.

The Bismuth Detectors - Bismuth fission has been used in a number of instances in monitoring and measuring ultra-fast neutron fluxes. The fission threshold is about 50 Mev with a cross section of about 30 mb for neutrons of mean energy 90 Mev. For low flux measurements it is desirable to have as much bismuth as possible exposed. A large chamber utilizing a number of parallel plates coated with bismuth nitrate was constructed and is shown in Figure 4. This chamber is described by De Juren.[1] Using an efficiency figure of 10 percent, the counting rate is 0.04 count per minute normalized to a neutron flux of 1 n/cm^2/sec. Since a very low background can be obtained, flux levels of a few neutrons per cm^2/sec can be detected by counting for an hour.

In order to improve the efficiency of the bismuth detector, a scintillator solution as described by Kallmann and Furst[2] was used. The scintillator material, 3 grams of γ-napthylphenyloxazole per liter of solvent consisting of 70 percent zylene, 24 percent napthalene and 6 percent triphenylbismuthene by weight, was used in a 12-liter cylindrical tank with two 5-inch phototubes at each end. The solution contained 1,340 grams of bismuth in a geometry such that a high percentage of bismuth fissions can be detected. A scintillation efficiency of 50 percent or better should result for fission pulses. The resulting counting rate should be 70 counts per minute normalized to 1 neutron/cm^2/sec.

MEASUREMENTS WITH THE DETECTORS

A series of measurements have been made at the Brookhaven National Laboratory Cosmotron. Several assumptions were made in approximating the neutron spectrum. First, it was assumed that the cross section rises to a peak value and does not decrease with further increasing energy. This is actually the case for most of the (n, p) reactions used. A better approximation to the spectrum may be obtained if the shapes of the excitation functions of the detectors are taken into account. In order to do this, the number of neutrons in equal energy intervals, from the first approximation to the integral neutron distribution, are weighted against the excitation functions of the reactions utilized, and weighted cross sections are obtained. The weighted cross sections are used to calculate a weighted integral neutron distribution, from which the differential spectrum is obtained.

The solid curve shown in Figure 5 was obtained in the exposure of the listed detectors close to the basic shield at the Cosmotron. The dashed line is the weighted distribution from which the neutron spectrum shown in Figure 6 was obtained.

BIBLIOGRAPHY

1. De Juren, J. "Low Capacity Giant Fission Counter." UCRL-1090, University of California Radiation Laboratory, February, 1951.

2. Furst, M. and H. Kallmann. "Enhancement of Flourescence in Solutions Under High-Energy Irradiation." Phys. Rev. 97:583, 1955.

Figure 5

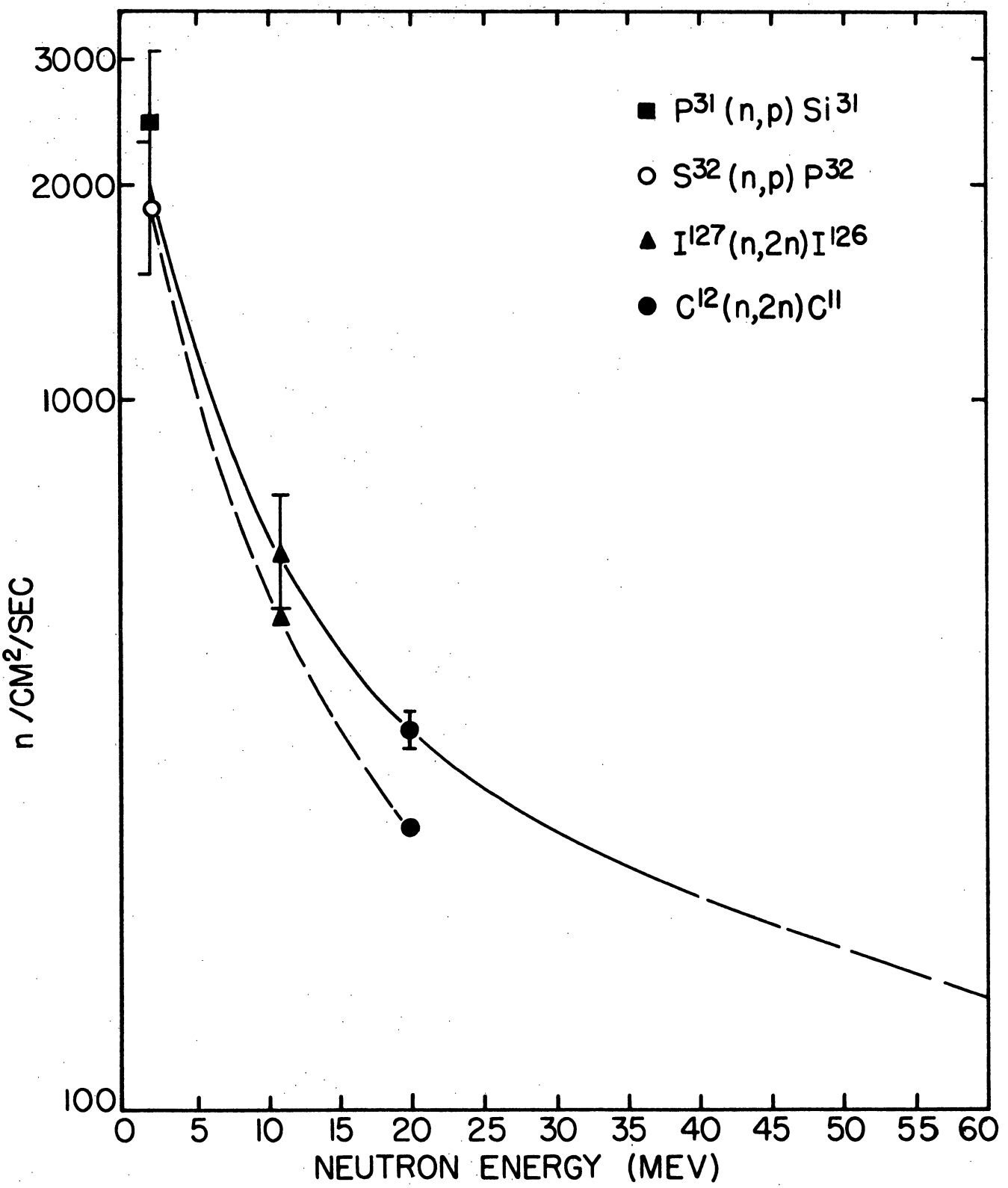

INTEGRAL NEUTRON DISTRIBUTION-BASIC SHIELD

Figure 6

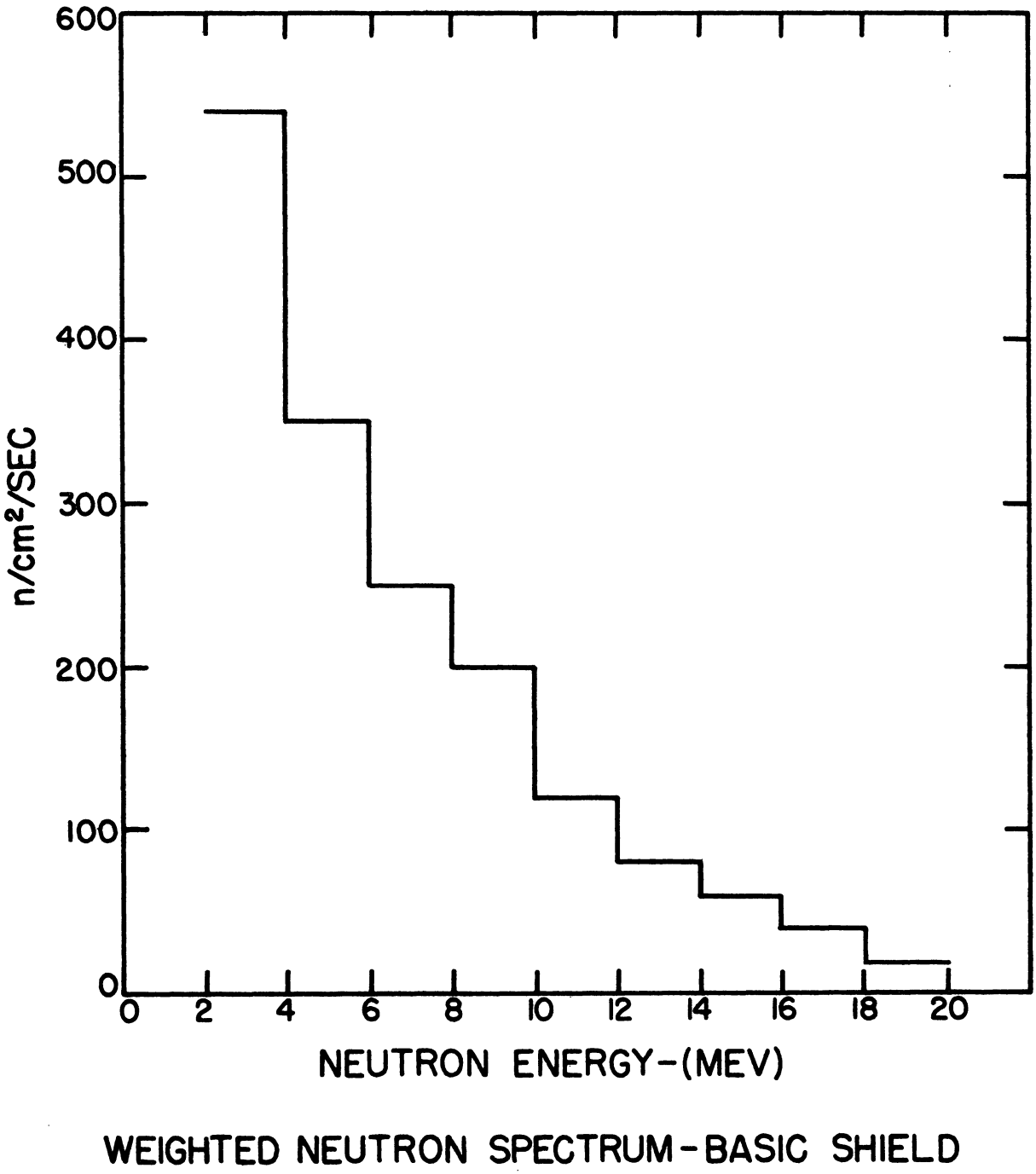

WEIGHTED NEUTRON SPECTRUM-BASIC SHIELD

ABSTRACT

THE MICHIGAN MEMORIAL PHOENIX LABORATORY AND OTHER FACILITIES OF INTEREST TO HEALTH PHYSICISTS

A. H. Emmons

Michigan Memorial Phoenix Project
University of Michigan
Ann Arbor, Michigan

A paper which described in detail the radiation research facilities of the Phoenix Laboratory on the North Campus of the University of Michigan was presented, together with 15 slides. These facilities include hot cells, radiochemistry laboratories, biological laboratories, and a 1-megawatt swimming pool reactor. Health physics criteria, as related to both design and operation of these facilities, were enumerated.

The author concluded his paper by introducing each of the 7 health physicists employed by the University.

ABSTRACT

MEASUREMENT OF THE SCATTER COMPONENT FROM A KILOCURIE COBALT-60 SOURCE

L. R. Solon, K. O'Brien, and H. Di Giovanni

Health and Safety Laboratory
U. S. Atomic Energy Commission
New York, New York

In order to evaluate the scatter contribution to the dose rate from a distributed source over an extended plane, an experiment was performed at the Biology Gamma Field of Brookhaven National Laboratory using approximately 2 kilocuries of cobalt-60 as a point source and a Failla-Rossi tissue equivalent ionization chamber as the detector. Corroborative measurements of dose rate were made with a graphite-walled carbon dioxide filled ionization chamber designed by H. Di Giovanni and built by the Instruments Branch of the Health and Safety Laboratory.

The point source measurements were numerically integrated over the plane to obtain the relative contribution of scatter to the total radiation.

ABSTRACT

A STUDY OF THE CHARACTERISTICS OF A FILM DOSIMETER USING THE RADIATION FROM Am-241 IN ALUMINUM SLUGS

G. Wilcox and J. Minkler

Radiation Laboratory
University of California
Livermore, California

This paper reports a study of film response to radiation from Am-241 contained in aluminum cylinders 4 inches long by 5/8 inch outside diameter. The walls of the containers were 1/16 inch thick. Dupont type 558 dosimeter film packets, containing sensitive film #508 and insensitive film #1290, were exposed in the standard UCRL film badge.

Scattering effects were minimized by suspending slugs and film in the center of a 15 by 15 foot room, halfway between ceiling and floor, using thin strands of wire. Appropriate critical distances and time were used for each exposure.

Step wedges of Al, Cu, Pb, and Lucite were affixed to the surface of the film packet with collodion. These provided a continuum of densities on the film in individual areas large enough to be read accurately on the densitometer. In this manner, the slope of an absorption curve could be established from data on a single film, ensuring uniformity of exposure time and distance factors for that run.

A calibration curve, relating density to dose, was run using the Norelco X-ray unit set at 100 Kvp ($\bar{E}$ = 49.9 Kv) and using Landsverk dosimeters to measure dose. This curve was used to estimate the dose received from the Am-241 under conditions of interest.

Examination of the film response curve for a fixed dose as the energy is varied indicates that while the response is changing in the region used in these measurements, the general change should not be more than 30 percent.

ABSTRACT

DECONTAMINATION OF RADIOACTIVITY FROM NON-FERROUS METALS BY REMELTING

P. B. Klevin and W. B. Harris

Health and Safety Laboratory
U. S. Atomic Energy Commission
New York, New York

Studies have been made on the extent of decontamination derived from resmelting stainless steel, copper, nickel, and aluminum that have been contaminated with uranium. This surface contaminated scrap metal showed negligible residual uranium after remelting in the case of stainless steel, copper, and nickel, while the aluminum still contained high concentrations. In the case of those metals which decontaminated satisfactorily, all of the original contamination was found to reside in the slag. No health hazard is involved in the operation.

ABSTRACT

MEASUREMENTS OF RADIOACTIVE GASES

R. L. Koontz

North American Aviation Company
Downey, California

Radioactive gas measurements have been made with ionization chambers and immersed GM detectors, on low activity fission gases from the Atomics International-Low Power Water Boiler Neutron Source. The non-availability of proper calibrating sources made it necessary to evaluate the response of these chambers by theoretical determinations of efficiency. Attempts then were made to verify the theories by experimentation.

The fission gases to be measured are removed from the core of the WBNS by flushing He into the uranyl nitrate solution, and collecting the mixture of He-WBNS gas in a 34.4 liter aircraft oxygen cylinder. The resulting gas consists mostly of He carrier because only a small volume of active gases is produced.

The results represent only 1 experiment based on the theoretical assumptions presented but seem to give reasonable agreement for activity values.

ABSTRACT

RADIATION FALLOUT

C. P. Malone

Research Laboratory
General Electric Company
Schenectady, New York

During recent months, measurements of radioactive fallout in the Schenectady area have been made in the Research Laboratory's Radiation Protection Office. Published measurements made in Chicago over the same period indicate certain similarities between the fallout in the 2 cities. A long-term increase in the background radiation level of the order of 10 percent seems indicated by the data. While it appears at this time that an increase of this magnitude in the general level can be expected to have no detectable deleterious effect upon human physiology, the question of whether it can harm future generations by small genetic damage to large segments of the population has not yet been answered with authority.

UNIVERSITY OF MICHIGAN

October 25, 1956

ENCYCLOPEDIA OF INSTRUMENTATION FOR INDUSTRIAL HYGIENE, University of Michigan, Institute of Industrial Health and School of Public Health, 1956. Technical Editors: C. D. Yaffe, A. D. Hosey, and D. H. Byers. Price $30.00. pp. 1243 plus xvii, 9 x 12 in. with 1400 illustrations, charts, and diagrams.

Authorities who have examined this monumental treatise on instrumentation have been unanimous in their evaluation of this work as a most useful tool that will prove invaluable to workers concerned with all phases of measurements in the areas covered in the 7 sections of the book. These sections cover 500 instruments, produced by 60 manufacturers, for measuring air contaminants in occupied spaces; for use in laboratories; for air pollution and meteorology; for air velocity and metering; for sound and vibration; for ionizing radiations; and for ultra violet, visible and infrared energy.

Each section includes:

1. A comprehensive review of instrumentation in that area, including progress, problems, possibilities, limitations, and needs not met by instruments now available.

2. Technical papers devoted to special problems or types of instruments used.

3. Descriptions of available instruments used for determination in this field, including name or identification of the instrument; name of the manufacturer; intended and special uses and adaptations; operating principle; physical description; performance data, such as sampling rate, range, sensitivity; interferences, limitations and safety hazards; price; operating instructions; calibration instructions; maintenance instructions; photographs, line drawings or wiring diagrams; bibliography.

Many of the instruments described, in addition to their use in determinations concerned with industrial hygiene, are employed extensively by diverse research organizations, teaching units, and in the conduct and control of industrial operations.

This large volume is well constructed, with a durable buckram cover and easy-to-read type. Its unusually large number of illustrations and diagrams are of sufficient size to visualize fine detail. A detailed index and a 36-page appendix of pertinent tables and charts are included.

This Encyclopedia brings together in one place a fund of specific information on instruments within the scope of the book. The content will be useful to everyone employing instrumentation, regardless of his field of interest. It has special value as a text and reference book for teaching the principles of instrumentation.

The Encyclopedia is a non-profit publication, produced through the combined efforts of personnel of the University with its financial support, the services of manufacturers' research directors and designers in supplying information on their instruments, authorities in the several areas of instrumentation, and a staff of experts assigned by the U. S. Public Health Service to assemble and edit the contents of the book.

THE PROBLEM OF RADIATION

Radiation has become one of the major health problems of our times. Moreover, it is evident that, because of the development of peacetime uses of atomic power, it will become an even greater problem in the future.

It is important, therefore, that both public officials and those in industry who are concerned in any way with this problem should understand the basic principles of radiation. They should know also the actual and potential dangers to the health and welfare of the general public arising out of the use of atomic power, as well as the dangers to those working in occupations involving contact with radiation or radioactive materials. They should be acquainted with the problems of handling radioactive materials and disposing of radioactive wastes, the safeguards which should be taken in connection with these activities, and the limitations of present knowledge on these matters.

Because of the need on the part of health and other public officials for general knowledge on radiation, the School of Public Health of the University of Michigan, working in collaboration with various other interested agencies, offered three courses concerned with radiation and radioactivity designed to apply available information to their needs, and has compiled the material presented at these courses into the following publications:

RADIOLOGICAL HEALTH. 1951. 140 pp., 101 illustrations. Price $3.00. A vast source of coordinated information, sorted out from the great mass of knowledge available through a multitude of sources, interpreted by masters of the subject and made available between two covers. Radiation is explained, its benign and malignant aspects are covered, and preventive measures and control procedures are outlined. A valuable aid for public officials, including health officers, civil defense authorities, industrial hygienists, and users of X-ray and radioactive materials.

RADIOACTIVE LIQUID WASTES - PART I. 1956. 90 pp., 45 illustrations. Price $3.00. The first 70 pages with 35 charts explain radiation in simple terms that can be understood without prior knowledge of radiation. It is a PRIMER on radiation. The remainder of the book is devoted to community effects of radioactive liquid wastes and implications for community planning.

RADIOACTIVE LIQUID WASTES - PART II. 1957 (to be published). Will cover fundamental concepts of instruments used in sampling, measurement, surveys, and control, together with survey and control programs. Price $3.00.

In order to facilitate the widespread dissemination of information on this vital subject, the University is offering these books for sale at the following special prices:

Set of three	$5.50
Any two in combination	$4.00
Any one, if buyer has already purchased one of the other books	$2.00

PUBLICATION ORDER BLANK

Send Orders to: University of Michigan Publications Distribution Service, 412 Maynard Street, Ann Arbor, Michigan.

No of Copies	Title of Publication

Books should be sent to: _____
Name

Address City State

PUBLICATION ORDER BLANK

Send Order to: University of Michigan Publications Distribution Service, 412 Maynard Street, Ann Arbor, Michigan.

No. of Copies	Title of Publication

Books should be sent to: _____
Name

Address City State